ROLE OF AMP-PROTEIN KINASE (AMPK) IN REGULATION OF PERIVASCULAR ADIPOSE TISSUE (PVAT) FUNCTION.

Tarek Ali Mohamed Almabrouk

MSc, MBChB

Submitted in fulfilment of the requirements of the degree of Doctor of Philosophy in the Institute of Cardiovascular and Medical Sciences,
University of Glasgow

Institute of Cardiovascular and Medical Sciences
College of Medical, Veterinary and Life Sciences
University of Glasgow

Author's Declaration

I declare that this thesis has been written solely by me with the research entirely generated by myself with the exception of the Western blots to study AMPK activation in adipose tissue and VSMCs and the PVAT confocal experiments. These were done in collaboration with Dr. Azizah Ugsman, Mr Omar Katwan and Alex Riddel. The research was carried out principally in the Institute of Cardiovascular and Medical Sciences at the University of Glasgow, under the supervision of Dr. Simon Kennedy and Dr.Ian Salt.

T A. Almabrouk, 2016

Acknowledgments

First and foremost I would like to thank my supervisors, Dr. Simon Kennedy and Dr. Ian Salt for all their support, guidance, advice and the opportunities I've had over the period of my PhD. I would also like to acknowledge the Libyan Government and my university for their support and funding of this project.

There are many people whose help over the years has been invaluable and greatly appreciated, at the Universities of Glasgow. I would like to thank all the members of the Kennedy and Salt groups past and present for helping me with just about everything. A special thanks goes to Dr. Marie-Ann Ewart who has supported me in my first steps in this project over the last few years.

A special thanks to my family. Words cannot express how grateful I am to my mother and for all of the sacrifices that you've made on my behalf. Your prayer for me was what sustained me thus far. I would also like to thank all of my friends who supported me during my PhD study. At the end I would like to express appreciation to my beloved wife who was always my support in the moments of difficulty and for her advice and encouragement. I couldn't have achieved it without you.

List of Contents

List of Figures

List of Tables

List of Publications

T.A.M. Almabrouk, M.A. Ewart, I.P. Salt and S. Kennedy (2014) Perivascular fat, AMP-activated protein kinase and vascular diseases. *British Journal of Pharmacology,* 171**,** 595-617.

T.A. Almabrouk, A.B. Ugusman, O. Katwan, I.P. Salt and S. Kennedy (2016) Deletion of AMPKα1 attenuates the anticontractile effect of perivascular adipose tissue (PVAT) and reduces adiponectin release. *British Journal of Pharmacology*, DOI:10.1111/bph.13633.

Abstracts:

T.A. Almabrouk, M.A. Ewart, I.P. Salt and S. Kennedy (2014) Regulation of vascular AMPK-activated protein kinase by Perivascular adipose tissue and its role in the regulation of vascular function. Scottish Cardiovascular Forum, Aberdeen (Oral communication).

T.A. Almabrouk, M.A. Ewart, I.P. Salt and S. Kennedy (2015) Effect of perivascular adipose tissue on vascular function mediated via AMPK Scottish Cardiovascular Forum, Edinburgh (Poster).

T.A. Almabrouk, M.A. Ewart, I.P. Salt and S. Kennedy (2015) AMP-activated protein kinase is critical for perivascular adipose tissue function. Maastricht AMPK meeting, Maasticht, Holand (Poster).

T.A. Almabrouk, I.P. Salt and S. Kennedy (2015) Role of AMPK in the anticontractile effect of the perivascular adipose tissue. British Pharmacology Society Meeting (Pharmacology 2015), London. pA_2 online, 13(3), 271P.

O. Katwan, **T.A.M. Almabrouk,** S. Kennedy and I.P. Salt (2016) The role of AMP-activated protein kinase in perivascular adipose tissue modulates vascular function. British Pharmacology Society Meeting (Pharmacological aspects of microvascular cell-cell signalling and CVS disease 2016), Oxford.

T.A.M. Almabrouk, A. Riddell, A.B. Ugusman, I.P. Salt and S. Kennedy (2016) AMPKα1 knockout mice have dysfunctional perivascular adipose tissue (PVAT) and impaired vascular function. American Heart Association meeting, New Orleans, Louisiana, USA. (Accepted for poster presentation).

A.B. Ugusman, **T.A. M. Almabrouk** and S. Kennedy (2016) Modulation of aortic perivascular adipose tissue function by peroxynitrite. British Pharmacology Society Meeting (Pharmacology 2016) (Accepted for poster presentation).

List of Abbreviations and definitions

PAI-1	Plasminogen Activator Inhibitor type-1
A769662	6,7-Dihydro-4-hydroxy-3-(2′-hydroxy[1,1′-biphenyl]-4-yl)-6-oxo-thieno[2,3-b]pyridine-5-carbonitrile
ADMA	Asymmetric Dimethylarginine
ADAMTS	Disintegrin and Metalloproteinase with Thrombospondin Motifs
ADRF	Adipocyte-Derived Relaxing Factor
AdipoR1	Adiponectin Receptor 1
ACC	Acetyl-CoA carboxylase
AMPK	AMP-Activated Protein Kinase
AICAR	5-Aminoimidazole-4-Carboxamide 1-β-D-Ribonucleoside
AIS	Autoinhibitory Sequence
ASC	C-terminal Sequence
BAT	Brown Adipose Tissue
BH4	Tetrahydrobiopterin
BMI	Body mass index
C/EBP	CCAAT/Enhancer-Binding Protein
cAd	Collagenous Domain
CAD	Coronary Artery Disease
CaMKKβ	Calcium/Calmodulin-dependent Protein Kinase Kinase β
CBM	Carbohydrate-Binding Module
CD68	Cluster of Differentiation 68
cGMP	Cyclic Guanosine Monophosphate
CBS	Cystathionine-β-Synthase
CideA	Cell Death-Inducing DFFA-like Effector A
CPT1	Carnitine Palmitoyltransferase 1
CSE	Cystathionine-Gamma-lyase Enzyme
CTRPs	C1q/TNF-Related Proteins
CVD	Cardiovascular Diseases
DHE	Dihydroethidium
Dio2	Deiodinase Iodothyronine Type I
ECM	Extracellular Matrix
eNOS	Endothelial NO Synthase
ERK1/2	Extracellular signal–Regulated Kinases 1/2
FMN	Flavin Mononucleotide
FAD	Flavin Adenine Dinucleotide
FATP-1	Fatty Acid Transport Protein 1

FFAs	Free Fatty Acids
FABP4	Fatty Acid Binding Protein 4
gAd	Globular Domain
GLUT	Glucose Transporter
GPCR	G-Protein-Coupled Receptor
GAPDH	Glycerol 3-Phosphate Dehydrogenase 1
GTP	Guanosine Triphosphate
H_2O_2	Hydrogen Peroxide
H_2S	Hydrogen Sulphide
HAECs	Human Aortic Endothelial Cells
HFD	High Fat Diet
HMG-CoA reductase	3-Hydroxy-3-Methyl-Glutaryl-Coenzyme A reductase
HMW	High-Molecular-Weight
ICAM-1	Intercellular Adhesion Molecule 1
IL-6	Interleukin 6
iNOS	Inducible NO synthase
IRS-1	Insulin Receptor Substrate 1
KCD	N-terminal Kinase Katalytic Domain
LKB1	Liver Kinase B1
MCP-1	Monocyte Chemoattractant Protein 1
MO25	Mouse Protein 25
mTOR	Mammalian Target for Rapamycin
NADPH	Nicotinamide Adenine Dinucleotide Phosphate
NMN	Nicotinamide Mononucleotide
NAMPT	Nicotinamide Phosphoribosyltransferase
nNOS	Neuronal NO synthase
NFk-B p65	Nuclear Factor-kappa B p65
$O_2^{\cdot -}$	Superoxide
PDGF-BB	Platelet-Derived Growth Factor BB
PI3K	Phosphatidylinositol-3-kinase
PKB	Protein kinase B
PPARγ	Peroxisome Proliferator-Activated Receptor γ
Prdm16	PR Domain Containing 16
PVAT	Perivascular Adipose Tissue
RORα	Retinoic acid-related Orphan Receptor α
S6K	Protein S6 Kinase
SAT	Subcutaneous Adipose Tissue

STRAD	STE20-Related Adaptor Protein
SVF	Stromal Vascular Fraction
T2DM	Type 2 Ddiabetes Mmellitus
TAK1	Transforming Growth Factor beta-Activated Kinase 1
THP-1	Human acute monocytic leukemia cell line
ROS	Reactive Oxygen Species
TNFα	Tumor Necrosis Factor α
TSC2	Tuberous Sclerosis Complex 2
TZDs	Thiazolidinediones
UCP-1	Uncoupling Protein 1
VSMCs	Visceral Adipose Tissue
VCAM-1	Vascular Cell Adhesion Molecule 1
VEGF-A	Vascular Endothelial Growth Factor A
WAT	White Adipose Tissue
ZMP	5-aminoimidazole-4-carboxamide-1-β-D-furanosyl 5′-monophosphate
β-SID	β subunit interacting domain

Abstract

This thesis, entitled: 'Role of AMP-protein kinase (AMPK) in regulation of perivascular adipose tissue (PVAT) function', has been submitted by author Tarek Ali Mohamed Almabrouk for a degree of Doctor of Philosophy (PhD) in the College of Medical, Veterinary and Life Sciences at the University of Glasgow, October 2016.

Apart from the cerebral circulation, all vasculature is surrounded by layers of adipose tissue known as perivascular adipose tissue (PVAT). In health, PVAT can function as an endocrine organ to produce a wide range of adipocytokines which can attenuate vascular contraction. The exact mechanism of this anti-contractile effect is still ill-defined, although much evidence suggests that PVAT-released adipocytokines may activate K^+ channels on VSMCs or eNOS on endothelial layer possibly via AMP-activated protein kinase (AMPK). However, obesity results in oxidative stress and inflammation of the PVAT leading to abnormal adipocytokine release and PVAT dysfunction. AMPK is a serine/threonine kinase with many potential physiological functions, including regulation of energy heamostasis. AMPK is expressed in the three layers of the blood vessel: smooth muscle (VSM), the endothelium and PVAT and it is known that activation of AMPK leads to vascular dilatation via both endothelium- and non-endothelium-dependent mechanisms. Although it is known that AMPK can modulate VSM and endothelial function, it is unknown whether AMPK can influence the anti-contractile activity of PVAT. Therefore, this project aimed to investigate the mechanism of the anticontractile effect of PVAT by determining the functions of AMPK within adipocytes, as well as to assess the importance of vascular AMPK to the PVAT anti-contractile function.

Experiments were conducted using wild type (WT) and global AMPKα1 knockout (KO) mice aortae. The phenotypic features of the PVAT were assessed by both histological, immunohistochemical and immunofluorescent methods. Secretory function of the PVAT was tested using an immunoblotting array and ELISA, whereas the anti-contractile effect of PVAT was studied using wire myography. Immunoblotting methods were used to test AMPK activity in the PVAT and VSMCs.

Aortic rings from WT and KO mice were denuded of endothelium and mounted on a wire myograph in the presence and absence of PVAT. The responses to an AMPK activator (AICAR) and the AMPK-independent vasodilator cromakalim were subsequently assessed. Relaxation responses to AICAR or cromakalim in the Sv129 (wild type) mouse were

significantly enhanced in the presence of endogenous attached or unattached PVAT, an effect that was absent in vessels from KO mice. Furthermore, enhanced relaxation was observed in vessels from KO mice incubated with PVAT from Sv129 mice, whereas PVAT from KO mice had no effect on relaxation of vessels from Sv129 mice. Furthermore, conditioned medium (CM) transfer experiments demonstrated the presence of an anticontractile factor released from PVAT that was absent in KO mice. Adiponectin secretion was reduced in PVAT from KO mice and PVAT-enhanced relaxation was attenuated in the presence of adiponectin blocking peptide. Adipokine array and ELISA demonstrated that adiponectin release is significantly reduced in the KO conditioned media in comparison with wild type CM. Globular adiponectin restores the relaxation response in both wild type aortae without PVAT and in KO aortae with and without PVAT.

High fat diet (HFD) fed mice showed a reduction in the relaxation response to cromakalim in wild type vessels with intact PVAT in comparison with animals fed a normal chow diet (ND). HFD animals had increased inflammatory infiltrates in the PVAT which were associated with reduced AMPK activity and adiponectin release in comparison with ND fed WT mice. In KO mice, AMPK activity was also reduced and increased inflammatory infiltration was observed in both ND and HFD mice.

In conclusion, the current project demonstrates that AMPKα1 has a critical role in maintaining PVAT's anti-contractile effect; likely mediated through altered adiponectin secretion or sensitivity, and through protection of PVAT against inflammation. Marked reduction in AMPK activity in WT PVAT, accompanied with the reduction in the release of adiponectin in HFD and KO animal may explain the impaired vascular function observed in obesity.

Chapter 1

General Introduction

1.1 Obesity and Cardiovascular disease

Obesity has been recognized as one of the major global health issues by the World Health Organization (WHO) and its incidence is rapidly rising in both industrialised and developing nations (Antipatis and Gill, 2001). The WHO has estimated that more than 1.9 billion adults in the world are overweight (body mass index (BMI) > 25.0 kg/m²); of which at least 600 million are obese (BMI >30.0 kg/m²) (World Health Organisation, 2014). Obesity is associated with increased risk of insulin resistance, type 2 diabetes mellitus (T2DM), hypertension, coronary artery disease (CAD), myocardial infarction (MI) and sudden death, congestive heart failure and stroke (reviewed in Almabrouk et al., 2014).The extent of this epidemic stresses the need for developing an approach for obesity management and a better understanding of the mechanism which links obesity and cardiovascular disease.

Many studies have demonstrated that the regional distribution of adipose tissue in the body determines both the obesity phenotype and its complications. For instance, intra-abdominal and visceral fat depots have been associated with a higher risk of development of cardiometabolic disease and mortality linked with obesity (Fox et al., 2007, Gesta et al., 2007). One of these regional fat depots is perivascular adipose tissue (PVAT) which is now proposed to be a link between obesity and metabolic syndrome development and diabetes as a result of the adverse effect which PVAT exerts on the vasculature in disease states. In health PVAT releases a range of adipokines such as adiponectin which are capable of modulation of metabolism and local vascular tone. However, in disease states, there is an alteration in adipokine release which results in vascular malfunction and development of metabolic syndrome. Furthermore, the elevated levels of inflammatory cytokines such TNFα in obesity may disrupt the interaction between PVAT and the vascular wall (Yudkin et al., 2005).

AMP activated protein kinase (AMPK) regulates adipocyte metabolism, adipose biology and vascular function and as such AMPK activation is an attractive therapeutic target for metabolic disorders such as T2DM and the vascular complications associated with obesity and T2DM. Recent studies have identified AMPK as a potential regulator of PVAT and also a target of PVAT action in the blood vessel (Almabrouk et al., 2014). The studies described in this thesis will focus on the vasoactive properties of perivascular adipose tissue as mediated by adipokines and also the role of AMPK in the regulation of vascular function and metabolism.

1.2 Anatomy of cardiovascular system

The cardiovascular system is composed of the heart and its associated blood vessels. The role of the blood vessels is to transport blood containing oxygen and nutrients from the heart via systemic circulation to the rest of the body before returning the blood back to heart and delivering it to the lung via the pulmonary circulation. Based on their physiological function, blood vessels can be divided into five types: arteries, arterioles, capillaries, venules and veins. The arteries transport blood away from the heart and progressively branch from muscular arteries to smaller arterioles and eventually to capillaries (site of substance exchange). Capillaries then coalesce to form bigger venules which progressively increase in size to form the large veins which return the blood back to the heart.

The wall of all blood vessels except capillaries is composed of three layers: tunica intima, a layer of endothelial cells; media, the middle smooth muscle layer and adventitia. The adventitia consists of two layers: adventitia compacta, a layer of mainly fibroblasts and perivascular adipose tissue (PVAT) which surrounds most blood vessels. The wall of the capillaries consists of a single layer of endothelial cells on a basement membrane, which facilitates substance exchange between blood and tissue. Figure 1-1 illustrates the basic strucure of the blood vessel wall including PVAT.

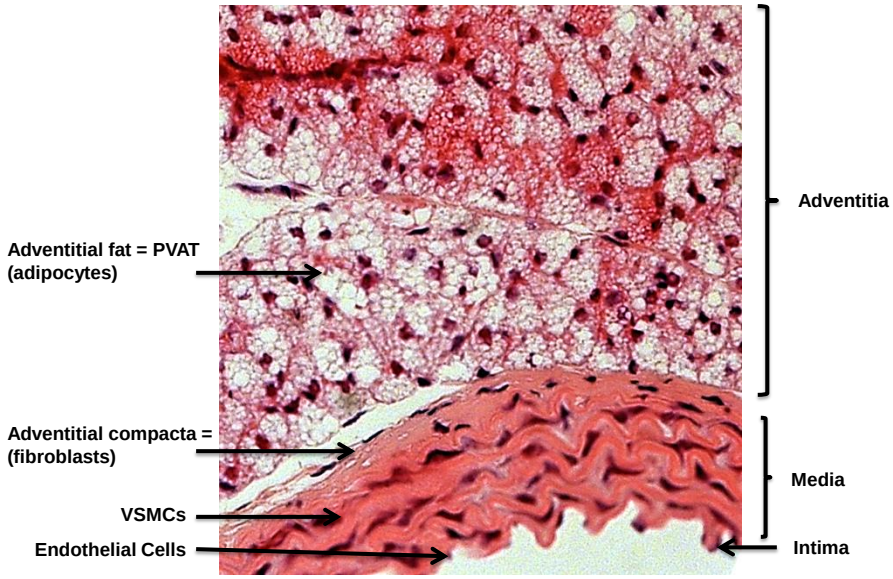

Figure 1-1 Structure of the blood vessel.

Representative H&E stained mouse aorta showing the structure of the wall of blood vessels. The blood vessel wall is composed of three layers: tunica intima (endothelium), tunica media (VSMCs layer) and adventitia which includes PVAT. PVAT contains adipocytes, vasa vasorum and other cells (macrophages, adipocyte stem/progenitor cells, lymphocytes, fibroblasts, etc respectively).

1.2.1 Endothelium

The vascular endothelium is a monolayer of cells that line the lumen of all vascular beds and mechanically and metabolically separates the vascular wall from the circulating blood and its components (Lerman and Zeiher, 2005). The role of the endothelium in the regulation of vascular function gained prominence in 1980 when Furchgott & Zawadski discovered that the relaxant effect of acetylcholine was lost in denuded vessels (Furchgott and Zawadzki, 1980). Furthermore, the endothelium is now known to release many bioactive substances which are involved in control of vascular function including regulation of vascular tone, proliferation, inflammation, platelet function and angiogenesis (Deanfield et al., 2007).

1.2.2 Vascular smooth muscle layer

This layer is composed principally of smooth (involuntary) muscle cells and elastic fibres arranged in roughly spiral layers. Arteries in comparison with veins tend to have a thicker medial layer. Smaller arteries and arterioles are termed resistance vessels which are important in the regulation of blood flow through changes in peripheral vascular resistance. Several mechanisms are involved in the regulation of vascular tone such as myogenic mechanisms, endothelium-derived factors, sympathetic adrenergic stimulation and hormones. Vasoconstriction and vasodilation is a function of myocytes and occurs in response to transmural pressure or stretch. Based on the demand of the tissue, perfusion is controlled by constriction or dilation of arteries which controls the blood flow to the tissue (Schubert and Mulvany, 1999).

1.2.3 Adventitia (Perivascular adipose tissue)

PVAT is a regional adipose tissue surrounding most of vasculature. PVAT is present throughout the body and has been shown to have a local effect on blood vessels (Almabrouk et al., 2014). The structure and function of the perivascular adipose tissue will be discussed in detail in section 1.4.

1.3 Adipose tissue (General Features)

All adipose tissue is composed of mature adipocytes containing lipid droplets, T lymphocytes, macrophages, collagen fibres, fibroblasts, preadipocytes, blood vessels and nerves. According to the size of the lipid vacuoles and the number of mitochondria,

adipose tissue is divided into two categories: brown adipose tissue (BAT) and white adipose tissue (WAT). Morphologically, WAT is composed of adipocytes with more than 90% of their volume occupied by a single spherical lipid droplet separated from the cytoplasm by a non-membranous barrier containing functionally active proteins such as perilipin (Greenberg et al., 1991). WAT is also characterised by adipocytes containing a variable number of thin elongated mitochondria with short, randomly arranged cristae (Cinti, 2011). BAT differs from WAT essentially in the characteristics of the adipocytes, vascularity and rich nor-adrenergic innervation. Adipocytes in BAT have multiple lipid vacuoles and a larger number of mitochondria. The mitochondria in brown adipocytes have a spherical or oval shape and are rich in laminar cristae with a characteristic marker protein called uncoupling protein 1 (UCP-1), responsible for their thermogenic activity (Cinti, 2011). The presence of a large number of mitochondria and rich vascularity is responsible for the brown colour of BAT.

The distribution of WAT and BAT are to a large extent different depending on genetic background, age, gender, and environmental status (temperature, diet, exercise) (Cinti, 2011). In small mammals both types of adipose tissue are located in subcutaneous and trunk depots surrounded by connective tissue capsules (Cinti, 2005). In small rodent adipose tissue (mice and rats), most of the intrascapular area is considered the classical BAT depot, whereas the posterior subcutaneous depot is mostly WAT. Mediastinal adipose tissues are largely BAT, especially in mice, whereas omental and mesenteric adipose are predominantly white. Depots including perirenal, periovarian and perivesical adipose tissue contain equal amounts of brown and white adipocytes. In males, the epididymal adipose depot is composed only of white adipocytes (Cinti, 2011).

In the human body, BAT can be found in the trunk fat depot and that is likely due to differences in the thermogenic needs in comparison with small mammals which are based on different surface/volume ratio. WAT in humans is confined to subcutaneous with increased accumulation in mammary and gluteofemoral areas in female (Cinti, 2011). Furthermore, adipose tissue in humans and rodents has the same cellular composition, including distinct blood and nerve supply density in both WAT and BAT (Zingaretti et al., 2009).

1.4 Perivascular adipose tissue (PVAT)

PVAT differs from other fat depots due to the following specific features:

PVAT is situated outside of the blood vessels and adventitia. It surrounds the adventitia, although no clear barrier separates the two and PVAT surrounds most systemic blood vessels, with the exception of cerebral blood vessels (Gao, 2007). In relation to the type of adipose tissue, PVAT is composed of either white adipose tissue, brown adipose tissue or both, depending on the type of the blood vessel. PVAT may be composed of WAT such as rodent mesenteric PVAT or mixed in aortic PVAT (Gao, 2007). Mixed aortic PVAT displays the morphological and gene expression features of BAT (Fitzgibbons et al., 2011), with its characteristic multilocular adipocytes and expression of UCP-1 while mesenteric PVAT contains white adipocytes that are lacking UCP-1 and are less vascularised (Cinti, 2011).

PVAT also differs from other adipose tissue in its secretory profile. Mouse aortic PVAT releases less adiponectin, leptin and resistin compared with subcutaneous adipose tissue (SAT) and visceral adipose tissue (VAT). Furthermore, regions of PVAT display a similar pattern of adipose tissue markers as BAT which includes CIDEA, UCP-1, Dio2, and Prdm16 (Fitzgibbons et al., 2011). PVAT expresses lower levels of lipid oxidation genes such as PPARγ, C/EBP, and FABP4 and lipid synthesis genes such as fatty acid synthase, glycerol 3-phosphate dehydrogenase 1 (GPDH), lipoprotein lipase, hormone-sensitive lipoprotein lipase, adipose triglyceride lipase, and perilipin (associated with the lipid droplet) in comparison with SAT and VAT (Chatterjee et al., 2009). Moreover, PVAT is different from other depots in the expression of immune and inflammatory genes. PVAT produces higher levels of interleukins (IL)-6, IL-8 and monocyte chemoattractant protein 1 (MCP-1) (Chatterjee et al., 2009). However, a study by Fitzgibbons *et al* reported that PVAT showed lower expression levels of chemokines, T-cell receptor and macrophage markers (CD68 and F4/80) (Fitzgibbons et al., 2011).

Depending on the vascular bed, there are differences in the profile of secretion and gene expression of proteins in PVAT. For example, the expression of renin–angiotensin system components by mesenteric and aortic PVAT in Wistar Kyoto (WKY) rats is characterised by higher angiotensin AT1a- and AT2 - receptor, chymase, and angiotensin II expression, and lower prorenin-receptor expression in mesenteric compared with aortic PVAT (Galvez-Prieto et al., 2008).

Adipocytes are the most abundant cell type in PVAT. Along with adipocytes, PVAT contains a stromal vascular fraction (SVF) which includes fibroblasts, mesenchymal stem cells, lymphocytes, macrophages and endothelial cells that line the vasa vasorum. The SVF has been suggested to be involved in the vasocrine function of the PVAT and also in disease states by enhancing the infiltration of inflammatory cells such as macrophages (Szasz et al., 2013). The extracellular matrix (ECM) of PVAT consists of collagen, laminin and fibronectin fibres along with ECM-processing enzymes, such as the matrix metalloproteinases, tissue inhibitors of metalloproteinases, and proteins from the disintegrin and metalloproteinase with thrombospondin motifs (ADAMTS) family (Mariman and Wang, 2010). PVAT consists also of nerve fibres which are predominantly sympathetic. There is apparently no parasympathetic innervation of WAT (Giordano et al., 2004, Giordano et al., 2006).

1.4.1 PVAT function

Adipose tissue was once considered to be a connective tissue with a traditional supporting structure involved in lipid storage (WAT) and nonshivering thermogensis (BAT). PVAT was also considered to act as scaffolding of nearby blood vessels and was removed during vascular function assessment because it was thought to impair diffusion of exogenous substances. However, accumulating evidence has led to the wide acceptance that adipose tissue including PVAT is not only a supporting structure but an important endocrine organ. It can release many bioactive molecules with various metabolic and vascular functions.

In addition to its contribution to metabolism via release of free fatty acids (FFAs)/nonesterified fatty acids by lipolysis, adipose tissue secretes bioactive proteins that are collectively termed adipocytokines and have endocrine, autocrine and paracrine actions. They are termed adipocytokines because of their adipocyte origin and cytokine-like effects. PVAT-released adipocytokines participate in the control of vascular function under normal physiological conditions (reviewed in Almabrouk et al., 2014).

An extensive range of adipocytokines have since been identified and shown to have a wide spectrum of haemodynamic, metabolic and immunological effects (Trayhurn and Wood, 2004, Trayhurn, 2005). Adipocytokines can be classified according to their effect on cytokine levels as either pro-inflammatory, such as leptin, or anti-inflammatory, such as adiponectin and adrenomedullin. As emerging vascular modulators, adipocytokines including adiponectin, omentin, nesfatin, vaspin and chemerin have been proposed to play

a role in the regulation of cardiovascular function (Table 1-1). The classification of some adipokines, such as resistin, can be somewhat blurred since it can be expressed by other cell types such as macrophages and participate in inflammation throughout the body (Jamaluddin et al., 2012). Others such as visfatin, originally considered as adipocytokines, may actually be produced in greater quantities by the stromal vascular tissue within PVAT (Stastny et al., 2012). Nevertheless, studies seem to indicate that generation of visfatin is elevated in obesity and metabolic syndrome and so it is likely to be an important pro-inflammatory mediator in cardiometabolic disease.

In addition to release of adipocytokines, adipocytes in PVAT also produce classical cytokines and chemokines including IL-6, IL-8, CCL2 (MCP-1) and plasminogen-activator inhibitor-1 (Thalmann and Meier, 2007, Rajsheker et al., 2010). Furthermore, inflammatory cells such as macrophages and T lymphocytes, fibroblasts and capillary endothelial cells, which are normally found in PVAT or attracted in response to inflammatory chemokines released by adipocytes, have also been demonstrated to contribute to the secretory profile of adipose tissue (reviewed in Szasz and Webb, 2012).

In addition to classical adipocytokines, PVAT can also produce angiotensin peptides, which, along with angiotensinogen, angiotensin-converting enzymes and receptors, are part of the renin–angiotensin–aldosterone system (Lu et al., 2010). PVAT also releases reactive oxygen species (ROS), including superoxide ($O_2^{\cdot -}$) (Gao et al., 2006), H_2O_2 (Gao et al., 2007) and gaseous molecules such as H_2S (Schleifenbaum et al., 2010). In denuded vessels, generation of H_2O_2 induces relaxation via activation of soluble guanyle cyclase sGC (Gao et al., 2007), whereas an enzyme present in PVAT, cystathionine γ-lyase, can generate H_2S. The H_2S induces relaxation by opening voltage-gated potassium channels in the vascular smooth muscle cells (VSMCs) to cause hyperpolarization (Schleifenbaum et al., 2010). In contrast, superoxide and angiotensin can potentiate vasoconstriction to electrical field stimulation *in vitro* (Gao et al., 2006, Lu et al., 2010). Another adipocytokine, apelin, has been found to induce NO-dependent vasorelaxation of peripheral and splanchnic human arteries both *in vitro* and *in vivo* (Salcedo et al., 2007, Japp et al., 2008). Table 1-1 illustrates the adipocytokines with known vascular effects and the mechanism of dysregulation.

Table 1-1 List of Adipocytokines released by PVAT

Adipokines/ Cytokines	Physiological effect	Effect on vasculature	Associated disease	PVAT dysfunction
Leptin	Proatherogenic Proinflammatory	Direct vasodilator, ↑VSMC proliferation/migration, ↑Vascular permeability , ↑TNF-α, IL-6, IL-12, ROS Indirect vasoconstrictor	Obesity, Hypertension, Atherosclerosis, Insulin resistance	↑in obesity ↓hypertension ↑atherosclerosis
Adiponectin	Antiinflammatory Anti-atherogenic	Direct vasodilator , ↓ VSMC proliferation/migration ↓ IFN-γ, IL-6, NF-κB, TNF-α phagocytosis, endothelial adhesion molecules, ↑IL-10, IL-1RA	Obesity Hypertension Atherosclerosis Insulin resistance T2DM	↓obesity diabetes ↓Atherosclerosis
Resistin	Proatherogenic	↑VSMC proliferation /migration, ↑Endothelial adhesion molecule,↑TNF-α, IL-6,NF-kB	Atherosclerosis Insulin resistance T2DM	↑Endothelial injury
Visfatin	Proatherogenic Proinflammatory	↑VSMC proliferation /migration, vasodilatation ↑TNF- α, IL-6, IL-8, ↓Apoptosis	Atherosclerosis Insulin resistance T2DM	↑atherosclerosis
Omentin	Antiatherogenic Antiinflammatory	↑eNOS, ↓ NF-κB	Atherosclerosis Metabolic syndrome	↓atherosclerosis, obesity and metabolic syndrome
Chemerin	Antiatherogenic Antiinflammatory	↓TNF-α-induced VCAM-1 expression and ↓Monocyte adhesion	Atherosclerosis	↓ atherosclerosis
Nefastin	Contractile	Impair NO donor and SNP vasodilatation	Hypertension Obesity	↑hypertension and obesity
Vaspin	Antiinflammatory Antiatherogenic	↓SMC migration	Atherosclerosis T2DM, Obesity	↑atherosclerosis, obesity and diabetes milletus
Apelin	Anticontractile Angiogenic	↑ Glucose utilization in skeletal muscle Antagonize the effect of Ang II,↑NO production	Obesity,Insulin resistance	↑obesity and insulin resistance and heart failure
Interleukins IL-1, IL-6, IL-8, CCL2	Proinflammatory	↑Endothelial proliferation	Atherosclerosis	↑atherosclerosis
HGF	Proinflammatory	↑Endothelial proliferation, ↑Cytokines release from SMCs	Obesity	↑obesity
TNF-α	Pro-inflammatory	Vasodilator, ↑ROS, ↑ Endothelial dysfunction	Obesity, Hypertension, Atherosclerosis, T2DM	↑ obesity, hypertension, atherosclerosis and T2DM

PVAT-derived factors with influence on vascular function and related cardiometabolic disorders. HGF, hepatic growth factor; NF-κB, nuclear factor kappa-light-chain enhancer of activated beta cells; PVAT, perivascular adipose tissue; ROS, reactive oxygen species.

1.4.1.1 Adiponectin

Adiponectin is a small protein of 30 kDa made of 247 amino acids. It consists of four domains: an amino-terminal signal sequence, a variable region, a collagenous domain (cAd), and a carboxy-terminal globular domain (gAd) (Figure 1-2) (Scherer et al., 1995). The collagenous domain is responsible for formation of high order complexs. These complexes have been identified as the high-molecular-weight (HMW) form (12–36 mer), low molecular weight (LMW) form (hexamer), and trimeric form (trimer). The essential mediator for formation of higher order complexes is a cysteine residue in the collagenous domain (Schraw et al., 2008). Based on its amino acid sequence and subunit domain structure, adiponectin is similar to C1q, which is a member of complement-related proteins. Furthermore, the globular domain of adiponectin has been found to be similar to the TNF-α family of proteins. C1q and TNFα are prototypical members of a growing family of paralogues known as C1q/TNF-related proteins (‘CTRPs’) (Davis and Scherer, 2008).

In general, adiponectin exists in two isoforms: full length and/or a smaller globular fragment (Kadowaki and Yamauchi, 2005, Kadowaki et al., 2006). Their mechanisms and extent of action of are still elusive. Adiponectin acts via two receptors, Adipo-R1 and Adipo-R2 (Yamauchi et al., 2003). Both receptors are composed of seven transmembrane domains although structurally and functionally they are distinct from G-protein-coupled receptors (GPCR) because the amino (*N*)-terminus of Adipo-R1 and Adipo-R2 is intracellular, and the C terminus is extracellular. The full length form acts via the R2 receptor and the globular form via R1 (Yamauchi et al., 2003). There is an additional cell surface molecule, referred to as T-cadherin which has been identified (Hug et al., 2004) and although it binds adiponectin, it is not considered to be a signalling receptor because it has no intracellular signalling domain (Denzel et al., 2010).

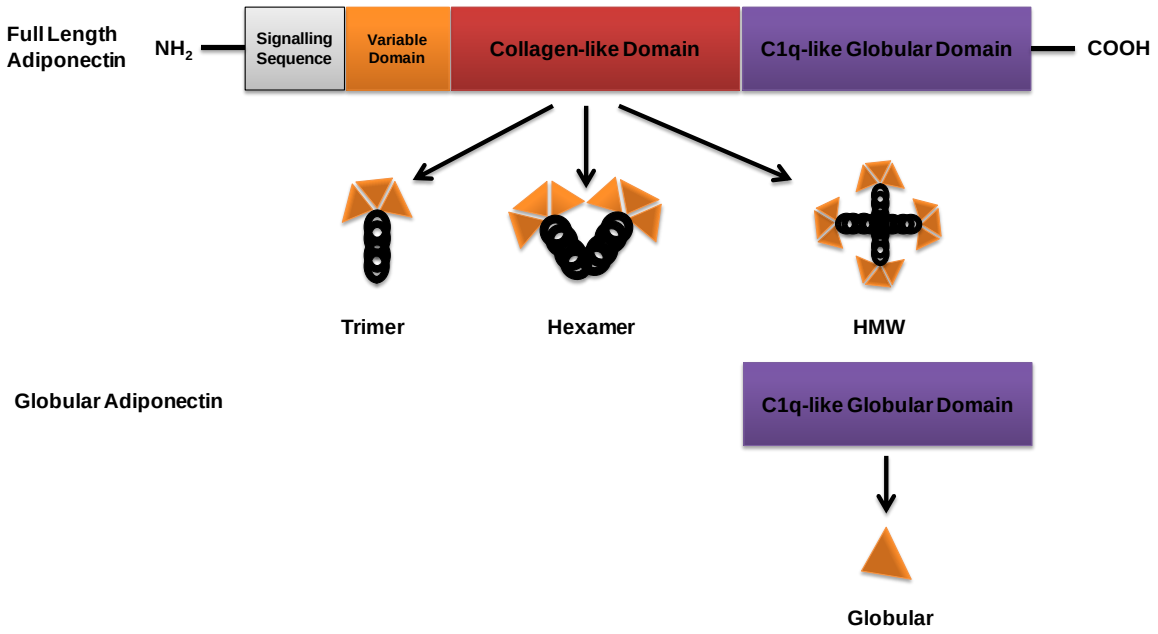

Figure 1-2 Structure of Adiponectin.

Full-length adiponectin is composed of 247 amino acids, including a collagen-like domain at the N-terminus and a C1q-like globular domain at the C-terminus. Full-length adiponectin combines via the collagen domain and forms higher order complexs including trimers and hexamers, and a high-molecular-weight (HMW) form. A smaller form of adiponectin composed of the globular domain also exists as globular adiponectin (adapted from Okamoto et al., 2006).

Adiponectin is produced exclusively by adipose tissue. It forms 0.01–0.05% of plasma protein (usual range, 2–20 μg/ml). Adiponectin is a very stable protein in the circulation, with minimal degradation (36 hours) (Pischon et al., 2003). It has very short half-life (~45-75 minutes) (Halberg et al., 2009) because it is cleared rapidly. The primary site of adiponectin clearance is the liver and although adiponectin is rapidly cleared, its plasma levels remain relatively constant (Halberg et al., 2009). The circulating adiponectin can bind pancreatic beta cells, vascular smooth muscle cells and some cell types in the heart and kidney where it elicits its effects (Turer and Scherer, 2012).

Adiponectin concentration within plasma is affected by many factors including gender, pregnancy, and diseases (Combs et al., 2003). In general, females have more adiponectin than males and this level is increased during pregnancy (Combs et al., 2003). Decreased plasma adiponectin levels are observed in patients with diabetes, metabolic syndrome, coronary artery disease, and hypertension (Arita et al., 1999, Yamauchi et al., 2001, Chow et al., 2007, Kumada et al., 2003, Ouchi et al., 2003, Salmenniemi et al., 2004). High plasma levels of adiponectin have been reported to suppress development of atherosclerosis in apolipoprotein E-deficient mice by reducing vascular smooth muscle cell proliferation and migration. The mechanism involved has been suggested to be a direct

binding to platelet-derived growth factor (PDGF)-BB and inhibiting growth factor-stimulated ERK signalling in vascular smooth muscle (Arita et al., 2002). In addition, adiponectin knockout mice are susceptible to development of diet-induced insulin resistance. This is likely through high TNFα expression decreasing muscle FATP-1 mRNA and IRS-1 mediated insulin signalling, predisposing to diet-induced insulin resistance (Maeda et al., 2002). High adiponectin concentration in the circulation is also associated with decreased risk of type 2 diabetes, and this is independent of abdominal fat deposition, suggesting a significant protective function of adiponectin against the development of type 2 diabetes (Yamamoto et al., 2014). Furthermore, adiponectin has been reported to protect against cardiovascular diseases via inhibition of pro-inflammatory and hypertrophic responses, and stimulation of endothelial cell responses. These effects of adiponectin are mainly attributed to the modulation of signalling molecules, including AMP-activated protein kinase (AMPK) (reviewed in Shibata et al., 2009). Adiponectin also prevents development of atherosclerosis by regulating the main signalling pathways involved in the genesis of atherosclerosis. These involve PI3K-Akt, eNOS and AMPK (Shimada, et al. 2004). Adiponectin appears to suppress monocyte adhesion to the vascular endothelium and promotes angiogenesis by stimulating crosstalk between Akt and AMPK in endothelial cells (Ouchi, et al. 1999).

Adiponectin is also involved in regulation of vascular reactivity and thus is important in blood pressure regulation. It induces vascular dilatation via two distinct mechanisms (Figure 1-3): an endothelium-dependent mechanism via increased production of NO via increased AMPK and endothelial nitric oxide synthase (eNOS) activity (Chen et al., 2003, Cheng et al., 2007), and an endothelium-independent pathway by activation of potassium channels at the level of vascular smooth muscle cells (Lynch et al., 2013). Adiponectin stimulates production of NO in endothelial cells *via* a phosphatidylinositol-3-kinase (PI3K) pathway involving phosphorylation of eNOS at Ser1179 by AMPK (Chen et al., 2003). The importance of adiponectin in regulation of blood pressure was confirmed in adiponectin knockout mice which developed elevated blood pressure (Ouchi et al., 2003, Ouchi et al., 2006).

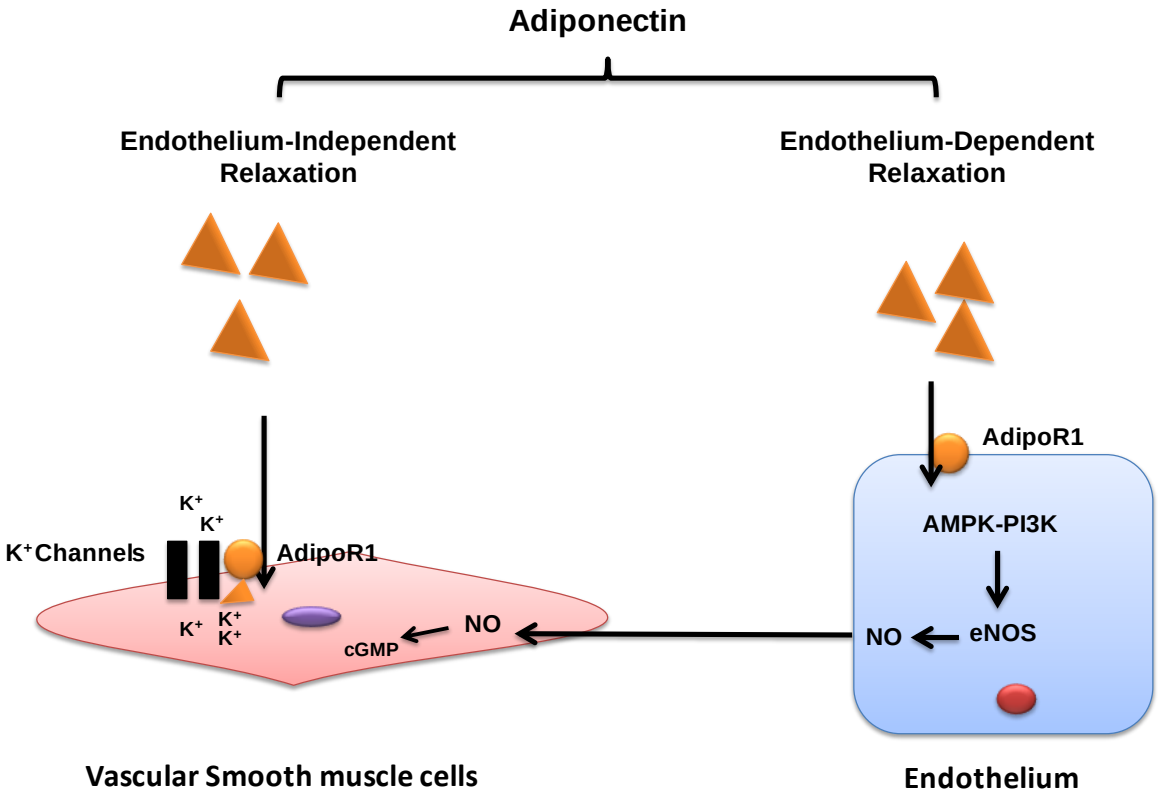

Figure 1-3 Mechanism of adiponectin-induced vascular relaxation.

1.4.1.2 Nitric Oxide (NO)

In 1980, Furchgott and Zawadzki proposed that vascular endothelium is essential to induce relaxation to acetylcholine *in vitro* using segments of rabbit aorta. Removal of the endothelial layer prevented relaxation to acetylcholine but the relaxation in response to glyceryl trinitrate was preserved (Furchgott and Zawadzki, 1980). This response was found to be due to an endogenous mediator termed endothelium-derived relaxing factor (EDRF) (Furchgott and Zawadzki, 1980) and which was later identified to be the gas nitric oxide (NO) (Ignarro et al., 1987, Palmer et al., 1987). NO is synthesized by conversion of the amino acid L-arginine to NO and L-citrulline via NO synthase enzyme (NOS) (Palmer et al., 1988). There are three NOS isoforms: neuronal isoform (nNOS) localized predominantly in the central and peripheral nerves but has also been detected in non-neuronal cells, including myocytes, epithelial cells, mast cells, and neutrophils (Asano et al., 1994, Forstermann et al., 1998, Nakane et al., 1993, Wallerath et al., 1997) which produces NO to act as a neuronal messenger, inducible isoform (iNOS) initially identified in cytokine-induced macrophages, is now recognized as expressed in macrophages, neutrophils, platelets, and VSMCs, as well as in other nonvascular cells such as skeletal muscle and the hippocampus. Endothelial NOS (eNOS) isoform is largely expressed in

endothelial cells. However, it can be found in other cells including cardiac myocytes, platelets, certain brain neurons, and human placenta syncytio-trophoblasts and in LLC-PK_1 kidney tubular epithelium (Forstermann and Sessa, 2012).

Activation of NOS requires binding to cofactors and dimerization. NOS binds to the cofactors flavin mononucleotide (FMN), flavin adenine dinucleotide (FAD), and tetrahydrobiopterin (BH4). BH4 along with L- arginine,,heme, nicotinamide adenine dinucleotide phosphate (NADPH) and molecular oxygen all act as cosubstrates which allows the NOS to dimerise and become activated. In the case of eNOS and nNOS, the dimer formed is in an inactive state in the absence of Ca^{2+} and is stimulated by elevated cytosolic Ca^{2+}-calmodulin. In contrast to eNOS and nNOS, iNOS dimers are active at basal intracellular Ca^{2+} concentrations (reviewed in Liu and Huang, 2008). The enzyme function can also be regulated by phosphorylation which enables Ca^{2+} -independent activation of eNOS in endothelial cells by fluid shear stress. Shear stress stimulates a pathway involving PI3K and the serine/threonine kinase Akt, which phosphorylates eNOS. This phosphorylation directly increases eNOS activity at resting [Ca^{2+}] (Fisslthaler et al., 2000). The synthesised NO diffuses through biological membranes into the underlying smooth muscle where it stimulates guanylyl cyclase to produce cGMP from guanosine triphosphate (GTP), stimulating vasorelaxation (Jin and Loscalzo, 2010).

1.5 Mechanism of vascular myocyte contraction

Vascular smooth muscle contraction is initiated by an increased concentration of intracellular Ca^{2+} mediated via opening of voltage-gated Ca^{2+} channels. Influx of Ca^{2+} causes myocyte membrane depolarisation and initiation of contraction. The intracellular Ca^{2+} interact with calmodulin which activates myosin light chain kinase (MLCK) and phosphorylation of myosin light chain (MLC), leading to smooth muscle contraction (Webb, 2003). Elevation of cytosolic Ca^{2+} can also be mediated by activating phospholipase C, leading to formation of inositol 1,4,5-trisphosphate (IP3) to cause Ca^{2+} release from the intracellular stores (sarcoplasmic reticulum) through IP3 receptors. Myocyte relaxation commences when cytosolic Ca^{2+} concentration is diminished. Reduction of intracellular Ca^{2+} leads to activation of MLC phosphatase, causing removal of the phosphate on the MLC kinase. Three subunits of MLC phosphatase has been identified; catalytic subunit, variable subunit, and a myosin-binding subunit. Phosphorylation of myosin-binding subunit abolishes the activity of MLC phosphatase, causing the light chain of myosin to remain phosphorylated, sustaining contraction. The

activity of MLC phosphatase is also regulated by small G protein RhoA and Rho kinase, the downstream target. MLC phosphatase is phosphorylated by Rho kinase, thereby inhibiting its activity and promoting the contraction via keeping MLC in the phosphorylated state (Webb, 2003).

The increase of cytosolic Ca^{2+} concentration activates Ca^{2+} removal mechanisms to restore myocyte equilibrium. Ca^{2+} removal mechanisms involve Ca^{2+} uptake into the sarcoplasmic reticulum and through the plasma membrane via Ca, Mg-ATPase dependent mechanism. Ca^{2+} removal is also mediated via Na^{+}/Ca^{2+} exchangers located on the plasma membrane which use the Na^{+} electrochemical gradient to remove intracellular Ca^{2+} ion (Webb, 2003).

1.6 Mechanism of VSMCs relaxation and the role of K^{+} channels.

Vascular smooth muscle relaxation occurs in response to contractile stimuli removal or as a result of direct stimulation by a mediator or of a receptor or ion channel that triggers inhibition of the contractile response. The principle of VSMCs relaxation is alleviation of the contractile response by reducing the intracellular Ca^{2+} concentration. Reduction in cytosolic Ca^{2+} reverses the calcium-calmodulin-dependent contraction mechanisms. Induction of relaxation is mediated by stimulation of MLC dephosphorylation by MLC phosphatase and inhibition of MLC kinase.

In general, contraction in VSMCs is connected to membrane potential. Depolarisation of the cell membrane is associated with opening of L-type voltage-dependent Ca^{2+} channels, influx of Ca^{2+} and cell contraction. However, hyperpolarisation reduces L-type Ca^{2+} channel opening and the cell remains relaxed. Hyperpolarisation of the myocyte membrane is mediated by opening of K^{+} channels in the cell membrane allowing K^{+} efflux. 4 types of K^{+} channels have been identified: Ca^{2+}-activated (K_{Ca}), voltage dependent (K_v), ATP-sensitive (K_{ATP}) and inward rectifying (K_{ir}) channels. This section will discuss some types of K^{+} channels.

1.6.1 Ca^{2+}-activated K^{+} channels (BK_{Ca} channels)

This class of K^{+} channels are activated by an increase in intracellular Ca^{2+} concentration. This family include 3 subfamilies: large-conductance K_{ca} (Big; BK_{Ca}), intermediate-conductance (IK_{Ca}) and small-conductance (SK_{Ca}). SK_{Ca} and IK_{Ca} are voltage-independent channels activated by an increase in intracellular Ca^{2+}. Their Ca^{2+} sensitivity is due to their

association with calmodulin (Xia et al., 1998, Fanger et al., 1999). Both SK_{Ca} and IK_{Ca} are thought to be essential for endothelium-dependent myocyte hyperpolarisation (Coleman et al., 2004).

Large-conductance Ca^{2+}-activated K^+ channels are the most common characterised type of K_{Ca} in VSMCs. It is activated in response to changes in intracellular Ca^{2+} and membrane depolarisation (Nelson and Quayle, 1995). It composed of a pore-forming α-subunit and a regulatory β-subunit (Tanaka et al., 1997). The α subunit comprises of seven transmembrane domains (S0-S6), including a voltage sensor (S4) and four hydrophobic domains located on the cytoplasmic surface. The S0 domain is a ubiquitous feature for the BK_{Ca} channels and facilitates the interaction with, and channel modulation by β subunits. The cytoplasmic tail (the C-terminus) has regulatory domains including regulator of conductance for K^+ 1 (RCK1), RCK2 and a Ca^{2+} bowel (in RCK2) (Wei et al., 1994). There are four β subunit isoforms (β1-4). Each isoform consists of two transmembrane domains which may be linked to α-subunits. The β1 subunit is the most common isoform expressed in VSMCs (Ko et al., 2008). Overall, the function of the β subunit is to increase sensitivity of the channel to Ca^{2+}, channel kinetics and pharmacological properties (Hanner et al., 1997, Meera et al., 1996). Activation of BK_{Ca} leads to K^+ efflux and hyperpolarisation of the cell membrane which reverses pressure- or chemical-induced depolarization and vasoconstriction (Ko et al., 2008).

1.6.2 Voltage-gated K^+ channels (K_v)

K_v channels include 12 subfamilies (K_v1-12) (reviewed in Gutman et al., 2005). They are expressed in vascular smooth muscle cells (Caterson et al., 2004). Activation of K_v channels leads to opening of the channel and K^+ efflux in response to membrane depolarisation. This will result in repolarisation which causes the membrane potential to return to resting membrane potential. Membrane depolarisation in VSMCs has been reported to be associated with opening of L-type Ca^{2+} channels and Ca^{2+} influx resulted in contraction. Therefore, K_v channels act as a switch to maintain resting vascular tone by limiting membrane depolarisation (Nelson and Quayle, 1995, Sobey, 2001). They are composed from pore forming α-subunits and have cytoplasmic N- and C- termini formed from six transmembrane domains (S1–S6) with an S4 acting as the voltage-sensing transmembrane domain (Korovkina and England, 2002). The α subunit is linked with ancillary β subunits which define the properties of the channel (Bahring et al., 2001). It is worth noting that α subunits are characterised by heteromultimerization which mean that α

subunits from different subfamilies can form functional channels with varying properties (McKeown et al., 2008). Depending on their voltage-dependence and pharmacological data, K_v channels expressed in VSMCs have been classified into two basic groups including rapidly activating/inactivating such as K_v4.2 and 4.3 and slowly activating; the delayed rectifiers such as K_v7.

K_v7 channels have five subtypes: K_v 7.1-7.5 and are encoded by KCNQ1-5 genes; thus they are sometimes termed KCNQ channels and have various tissue localisations. K_v 7.1, 7.4 and 7.5 have been demonstrated in VSMCs of rat aortic and mesenteric artery (Brueggemann et al., 2007, Mackie et al., 2008). They conduct a current that is slowly activating with a threshold -60 mV and is non-inactivating. Their activation threshold maintains the opening state of the channel during resting membrane potential, allowing conduction of the resting K^+ current in vascular myocytes (Xiong et al., 2008).

1.6.3 ATP-sensitive K^+ channels (K_{ATP})

K_{ATP} channels were initially chracterised in cardiac muscle and since then have been reported in many cells types including vascular smooth muscle (Nelson and Quayle, 1995). The single-channel conductances demonstrated for K_{ATP} channels in VSMCs are varied. However, it can be classified into two main categories: small/medium conductances and large conductances (Quayle et al., 1997). They are hetero-octameric complexes composed from 4 pore-forming Kir6 subunits and 4 regulatory sulphonylurea receptors (SUR) (reviewed in Cole and ClÉMent-Chomienne, 2003). The pore-forming subunits include two subtypes, Kir6.1 and Kir6.2 (Teramoto et al., 2006) with two transmembrane domains connected by an ion selectivity loop (Nichols, 2006). The sulfonylurea receptors (SUR) are an atypical ABC protein that binds to Kir6 subunits to form functional K_{ATP} channels. They belong to the ATP-binding cassette protein family. There are three isoforms of SUR (SUR1, SUR2A, and SUR2B). SURs have no role in pore-forming, but are important for surface expression of K_{ATP} and nucleotide-dependent activation of the K_{ATP} channel (Hill et al., 2003).

The K_{ATP} channel is activated in response to a decrease in the intracellular ATP/ADP ratio, causing K^+ efflux from the cell, cell membrane hyperpolarization, and electrical activity suppression. The K_{ATP} channel can be inhibited by ATP (in the absence of Mg^{2+}) by binding directly to Kir6 in a binding pocket located at the internal surface of the NH_2- and COOH- ends (Hund and Mohler, 2011). In VSMCs, the current induced as a result of K_{ATP}

opening is both time and voltage-independent and can be inhibited by sulphonylurea compounds such as glibenclamide. The channel conductance in vascular myocytes via K_{ATP} is relatively small (20-50 pS) (Ko et al., 2008). Native K_{ATP} channels in VSMCs most likely have Kir6.1/SUR2B or Kir6.2/SUR2B with the Kir6.1/SUR2B being the predominant molecular entity (Koh et al., 1998, Cinti, 2005). However, it is worth noting that two different K_{ATP} channels may exist in the same type vessel. For example, it has been reported that both a small conductance and activated by nucleotide diphosphate and a larger conductance (50 pS) and inhibited by ATP are expressed in rat portal vein (Bolton and Imaizumi, 1996). Therefore, it is plausible to think that more than one type of K_{ATP} channels exists in the blood vessels.

1.7 Mechanism of anticontractile effect of the PVAT

Previously, vascular reactivity experiments were usually conducted in vessels with no attached PVAT. This practice was based on the traditional belief that PVAT only acted as scaffolding of the adjacent blood vessels. Additionally, PVAT was also removed as its presence was thought to affect reactivity either by impairing diffusion of the agents or metabolising some pharmacological agents added to the organ bath (reviewed in Oriowo, 2015). However, in early 90s, the first evidence emerged suggesting modulation of vascular smooth muscle tone by PVAT was provided by Soltis and Cassis (Soltis and Cassis, 1991). They demonstrated that the presence of PVAT significantly attenuated noradrenaline-induced contraction of the rat aorta in comparison with vessels in which PVAT was removed. This effect was explained by uptake of noradrenaline into adrenergic nerves in the fat tissue, since PVAT had no effect on phenylephrine and KCl contractions (Soltis and Cassis, 1991). Lohn and co-workers confirmed the anticontractile effect of the PVAT on 5-HT and angiotensin II (Lohn et al., 2002). This finding would suggest that the anticontractile effect is not due to uptake into noradrenaline containing nerve fibres since angiotensin II is not a substrate for the uptake mechanism. Lhon *et al* suggested that the anticontactile effect of the PVAT is due to a transferable factor which is adipocyte-derived and they were the first to coin the term (ADRF) (Lohn et al., 2002). These early findings have been supported in many subsequent studies in different vascular beds and with different agonists (Verlohren et al., 2004, Dubrovska et al., 2004, Fesus et al., 2007, Gao et al., 2006, Gao et al., 2007, Lu et al., 2011b). PVAT released factors induce the anticontractile effect via modulation of vascular function either at the level of the endothelium or vascular smooth muscle layer by targeting certain effectors or receptors.

Therefore, the function of ADRFs can be classified into two main categories which will be discussed in the following section.

1.7.1 Endothelium-dependent mechanism of PVAT action

PVAT was reported to attenuate the contraction of rat thoracic aorta induced by phenylephrine (Gao et al., 2007). In this study, conditioned medium from donor PVAT-intact rat aorta induced relaxation in endothelium-intact vessels. Removal of the PVAT from the donor or the endothelium from recipient aortic rings led to loss of the relaxant effect of the PVAT. In the same study, transfer of conditioned medium from intact PVAT vessels to segments with denuded endothelium did not enhance the relaxation response of the vessels. These findings indicated that the PVAT is a source of transferable factors and its effect is dependent on the endothelium. This effect was proposed to be mediated via PVAT generated NO and subsequent activation of calcium-dependent K^+channel activation in VSMC (Gao, 2007). Adipokines in the conditioned medium have therefore been proposed to underlie these actions of PVAT.

Leptin is an adipokine released by adipose tissues including PVAT and is involved in regulation of appetite and energy metabolism. It also has vasoactive properties (Figure 1-2) mediating both vasodilatation (Vecchione et al., 2002) and vasoconstriction (Cooke and Oka, 2002). The vasodilation is reported to be mediated by activation of the AMPK signalling pathway, resulting in eNOS activation via Ser1177 phosphorylation (Vecchione et al., 2002).

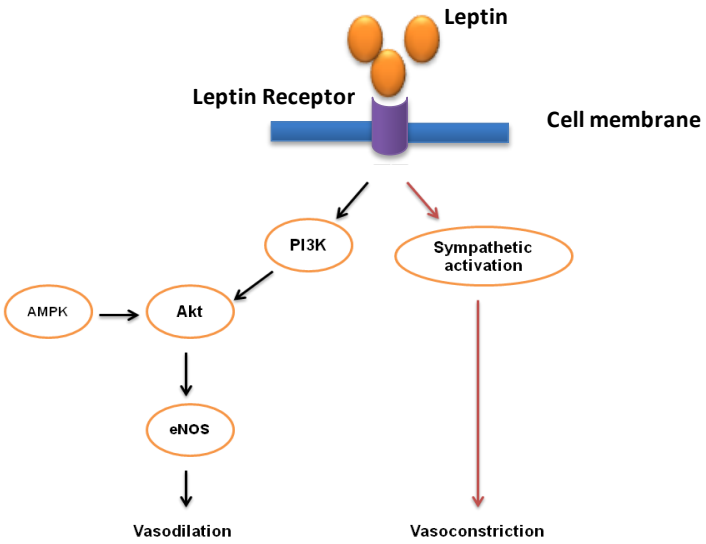

Figure 1-4 Mechanism of leptin induced vasodilation and vasoconstriction.

Adiponectin is another important cardioprotective adipokine (Antoniades et al., 2009) that can also induce vascular relaxation via endothelium dependent mechanisms. It enhances production of NO from endothelial cells by increasing phosphorylation of eNOS at ser1177 with involvement of PI3K-Akt and AMPK (Chen et al., 2003). This effect is mediated through binding to adiponectin type 2 receptor (rather than type1) or T-cadherin (Greenstein et al., 2009), and also binding of heat shock protein HSP90 (Xi et al., 2005) in which APPL1 acts as an immediate downstream modulator of adiponectin receptors 1 and 2 (Cheng et al., 2007). In human endothelial cells, adiponectin reduced TNF-α-induced production of asymmetric dimethylarginine (ADMA), an L-arginine analogue that inhibits NO formation and impairs vascular function (Eid et al., 2007).

Other adipokines that have been reported to influence endothelium-mediated vascular tone include omentin, visfatin and hydrogen peroxide (H_2O_2), Omentin is reported to induce endothelium-dependent vascular relaxation via eNOS phosphorylation and stimulated NO synthesis (Yamawaki et al., 2010) while visfatin, has been reported to activate Akt and cGMP-dependent protein kinase (Yamawaki et al., 2009) and H_2O_2 induces endothelium-dependent vasodilation through COX-1-mediated release of PGE_2 (Thengchaisri and Kuo, 2003).

1.7.2 Endothelium-independent mechanism of PVAT action

In addition to being produced by vascular smooth muscle and heart tissue (Zhao et al., 2001, Zhao and Wang, 2002), H_2S is also generated by PVAT from cysteine by cystathionine-gamma-lyase enzyme (CSE) (Fang et al., 2009). H_2S induces a dose-dependent vascular relaxation in both rat aorta and mesenteric arterioles that is not dependent on nitric oxide but is calcium-dependent (Zhao and Wang, 2002, Zhao et al., 2001). The mechanism of relaxation is thought to be due to opening of ATP-sensitive potassium channel (K_{ATP} channel) and enhancing K^+efflux (Zhao et al., 2001) since Fang and co-workers demonstrated that the anticontractile effect of endogenous H_2S from PVAT was abolished by blocking the K_{ATP} channel (Fang et al., 2009).

PVAT has also been found to significantly attenuate vascular responsiveness of mesenteric arteries to several agonists, including serotonin, phenylephrine, and endothelin I. The mechanism of this anticontractile effect is reported to be mediated by activation of voltage-dependent, delayed-rectifier K (Kv) channels that hyperpolarize the vascular smooth muscle cell membrane (Verlohren et al., 2004).

In 2007, Gao *et al* suggested that perivascular adipose tissue releases transferable factor(s) that can induce vascular relaxation both via endothelium-dependent and endothelium-independent mechanisms. The endothelium-independent mechanism was suggested to be due to release of H_2O_2 with subsequent activation of soluble guanylate cyclase (sGC) (Gao et al., 2007). Hydrogen peroxide was also demonstrated to induce NO-independent vascular relaxation via activation of K_{Ca} channels (Thengchaisri and Kuo, 2003, Hattori et al., 2003). Furthermore, H_2O_2 has been reported to induce relaxation through activating voltage-dependent K^+ channels (Iida and Katusic, 2000, Gao et al., 2003) and independent of phospholipase A_2, cyclooxygenase, lipoxygenase, cytochrome P450 monooxygenase, adenylate or guanylate cyclase (Gao et al., 2003) or ATP-dependent K^+ channels (Gao et al., 2003).

1.8 PVAT involvement in cell proliferation and migration

In addition to its role in regulation of vascular reactivity, PVAT has been proposed to be involved in development of atherosclerosis via its effect on vascular smooth muscle proliferation and migration (Engeli, 2005). It has long been known that endothelium and VSMC layers are the major contributors to the development of atherosclerotic lesions (Rudijanto, 2007, Davignon and Ganz, 2004). Furthermore, adventitia with its fibroblasts is involved in vascular remodelling and constriction of the external lamina by the accumulation of α smooth muscle-containing myofibroblasts in the injured area of the blood vessels (Scott et al., 1996, Wilcox and Scott, 1996). Furthermore, macrophage infiltration associated with plaque neovascularisation (Maiellaro and Taylor, 2007) and the profound inflammation of adventitia following balloon angioplasty of porcine coronary arteries is further evidence supporting the involvement of other layers of vasculature rather than just the endothelium and VSMCs (Sartore et al., 2001, Okamoto et al., 2001). The inflammatory response to arterial angioplasty has been demonstrated in the PVAT surrounding the treated arterial segment (Okamoto et al., 2001). These results suggest a potential role for PVAT in vascular remodelling and proliferation. However, the current view regarding the role of PVAT in atherosclerosis is that PVAT may have opposing effects; proatherosclerotic and antiatherosclerotic (Almabrouk et al., 2014).

1.8.1 Pro-Atherosclerotic Properties of PVAT

The major mechanism that promotes development of atherosclerosis is the inflammatory response in which PVAT may play a role via the recruitment and proliferation of

adventitial myofibroblasts (Okamoto et al., 2001). There are also many changes in PVAT which have been observed in response to endothelial injury. Wire or balloon injury to the lumen of mouse and rat vessels significantly increased the expression of pro-inflammatory adipocytokines and reduced adiponectin, an effect that was absent in TNF-α knockout (KO) mice and which could be replicated by TNF-α application to the perivascular area of the vessel. Furthermore, TNF-α KO mice had reduced neointimal formation, reinforcing the potential importance of PVAT-derived inflammatory mediators in vascular remodelling (Takaoka et al., 2010). Another study showed that the adipokine C1q/TNF-related protein-9 attenuates neointima formation in the wire-injured obese mouse femoral artery (Uemura et al., 2013).

Inflammatory responses in PVAT have also been demonstrated to occur not only due to injury but also as a response to high fat feeding (Chatterjee et al., 2009). The proinflammatory phenotype found in murine PVAT in response to high fat feeding is characterised by the markedly reduced secretion of anti-inflammatory adiponectin with increased secretion of the proinflammatory cytokines IL-6, IL-8, and the chemokine MCP-1 in coronary perivascular adipocytes (Chatterjee et al., 2009, Henrichot et al., 2005). These findings suggest that PVAT has strong chemotactic activity which is mainly mediated via the secretion of chemokines IL-8 and MCP-1. These factors are likely to contribute to the infiltration of macrophages and T cells at the interface between human PVAT and the adventitia of atherosclerotic plaques in the aorta (Henrichot et al., 2005). Another study investigated the relationship between development of atherosclerosis and pro-inflammatory PVAT by transplantation of visceral fat to the mid-perivascular area of the carotid artery in apolipoprotein-E-deficient mice (Ohman et al., 2011). Transplant of visceral WAT (inflammatory fat with a higher macrophage content) stimulated development of atherosclerotic lesions in the carotid artery accompanied by an increased level of serum MCP-1 (also called CCL2) and enhanced endothelial dysfunction. Such a detrimental effect was not seen with transplantation of subcutaneous fat and could be ameliorated by an antibody to P-selectin glycoprotein ligand (Ohman et al., 2011). This important study demonstrates that the pro-inflammatory and pro-atherogenic properties of adipose tissue in the hypercholersterolaemic state can have an adverse influence on vascular function and plaque formation.

PVAT may mediate cell growth and proliferation via release of bioactive adipokines. In addition to its function as a vasodilator, leptin has been reported to induce VSMCs growth and proliferation (Oda et al., 2001, Huang et al., 2010, Shan et al., 2008). Leptin regulates

VSMCs proliferation and migration by stimulating phosphorylation and activation of mitogen-activated protein (MAP) kinases, and also increased phosphatidylinositol (PI) 3-kinase activity (Oda et al., 2001). High levels of serum leptin are observed in obese and diabetic patients and have been found to be associated with enhanced neointimal formation following femoral artery injury in both wild type and leptin-deficient mice treated with exogenous leptin and this was due to activation of the key regulator of protein and amino acid metabolism, mammalian target for rapamycin (mTOR) (Shan et al., 2008). Leptin also can stimulate VSMCs proliferation via increased phosphorylation of extracellular signal-regulated kinase 1/2 (ERK1/2), and nuclear factor (NF)-kappa Bp65 (Huang et al., 2010).

Visfatin has been identified as nicotinamide phosphoribosyltransferase (NAMPT) and is involved in the synthesis of nicotinamide mononucleotide (NMN) from nicotinamide (Wang et al., 2009a, Wang et al., 2011a). In comparison with subcutaneous fat, visfatin is mainly expressed in and secreted from visceral fat. The circulating visfatin level is correlated with obesity and its associated abnormalities (Fukuhara et al., 2005, Wang et al., 2010a, Stastny et al., 2012). Visfatin has been also reported to be expressed in and released from aortic PVAT (Wang et al., 2009a). The expression of visfatin in rat thoracic aorta PVAT is higher in comparison with subcutaneous and visceral adipose tissue. Similar findings have been reported in adipose tissue samples derived from monkeys (Wang et al., 2009a). Furthermore, visfatin has also been identified in conditioned medium from PVAT, demonstrating that this protein can be secreted by PVAT (Wang et al., 2009a). Visfatin has no effect on VSMC contraction (Wang et al., 2009a), however, PVAT-derived visfatin has been found to be a VSMC growth factor. PVAT-conditioned medium induces VSMC growth and proliferation which is inhibited by visfatin-specific neutralising antibodies. Application of exogenous visfatin enhances VSMC proliferation and this effect was abolished after co-incubation with FK866, a selective inhibitor of NAMPT activity (Wang et al., 2009a). In the same study, visfatin stimulated VSMC proliferation in a dose- and time-dependent manner mediated via extracellular signal-regulated kinase (ERK) 1/2 signalling pathways (Wang et al., 2009a) and also attenuated VSMC apoptosis induced by H_2O_2. The knockdown of insulin receptors abolished insulin-induced Akt phosphorylation and VSMC proliferation but had no effect on the response to visfatin while the visfatin product NMN also stimulated proliferative signalling pathways and cell proliferation (Wang et al., 2009a). Visfatin also exhibits pro-inflammatory effects, stimulating iNOS and activation of the key proinflammatory transcription factor, NF-κB (Romacho et al., 2009).

Epicardial adipose tissue thickness was reported to be associated with elevated plasma visfatin levels and local visfatin expression in CAD patients (Cheng et al., 2008) while increased visfatin expression has been detected in the PVAT of aortic and coronary vessels with atherosclerosis (Spiroglou et al., 2010).

1.8.2 Anti-atherosclerotic properties of PVAT

As well as the important role inflammation in atherosclerosis development, impaired energy metabolism in the blood vessels is also linked with atherogensis (Mayr et al., 2005). Temperature has long been recognized to influence energy metabolism, and one of the main roles of BAT is to provide adaptive thermogenesis via uncoupling of respiratory chain by UCP1 (Brown et al., 2014). BAT is involved in the regulation of energy expenditure in humans, and since some adipocytes within PVAT possess the morphological features of BAT, it might be anticipated that the fat surrounding the blood vessels can control the local energy metabolism of the vessel wall. Studies have shown that PVAT can generate heat, which helps in maintaining intravascular temperature and correlates with increased activity of metabolic enzymes in mice housed at 16°C (Chang et al., 2012). In this study, development of atherosclerotic plaques in the mice was attenuated and serum triglyceride concentrations decreased markedly. Peroxisome proliferator-activated receptor γ (PPAR-γ) is a key regulator of white and brown adipocyte differentiation (Siersbaek et al., 2010) and in mice lacking smooth muscle PPARγ, an absence of PVAT was found, which caused endothelial dysfunction and temperature loss (Chang et al., 2012).

It is well known that obesity-induced inflammation in periadventitial adipose tissue is associated with upregulation of inflammatory adipocytokines and downregulation of the antiinflammatory adipocytokine adiponectin (Takaoka et al., 2009). These changes were associated with enhanced neointima formation after endovascular injury. Endothelial injury induces adhesion and migration of leukocytes, macrophages, and bone marrow–derived progenitor cells into the vessel wall (Sata et al., 2000). Furthermore, pro-inflammatory cytokines have a fundamental role in mediating the initiation and progression of vascular lesion formation (Serrano et al., 1997, Libby, 2002). Takaoka *et al* provide direct evidence that PVAT may protect against neointimal formation after angioplasty in lean mice and that inflammatory changes in the periadventitial fat may have a direct role in the pathogenesis of vascular disease accelerated by obesity. They also suggested that adiponectin released from PVAT may play a protective role in neointima formation of the

adjacent artery after vascular injury in lean mice (Takaoka et al., 2009). In this study, PVAT removal enhanced neointimal hyperplasia following endovascular injury in the femoral artery. Transplantation of subcutaneous fat from a normal mouse to surround the injured artery significantly reduced neointimal formation. In line with the previous findings, the protective effect of exogenous adipose tissue was lost when transplanted subcutaneous adipose tissue was derived from obese mice. This is likely related to phenotypic changes in adipose tissue associated with obesity. These changes include reduced production of anti-inflammatory adiponectin and increased pro-inflammatory adipokines; IL-6, MCP-1, tumour necrosis factor-α (TNF-α) and plasminogen activator inhibitor type-1 (PAI-1) in subcutaneous adipose tissue-conditioned medium from obese mice compared with that from normal mice (Takaoka et al., 2010). In the same study, the conditioned medium derived from the subcutaneous adipose tissue of normal mice attenuated VSMC proliferation stimulated by platelet-derived growth factor (PDGF)-BB (Takaoka et al., 2010). On the other hand, the conditioned medium from obese mice increased VSMC proliferation, which was attenuated by pretreatment with anti-TNF-α antibodies. Furthermore, the conditioned medium of adiponectin-deficient subcutaneous adipose tissue enhanced VSMC proliferation. These findings reveal that TNF-α secreted from adipose tissue increases VSMC growth, and that adiponectin secreted from adipose tissue inhibited VSMC growth in response to PDGF-BB stimulation (Takaoka et al., 2010).

Further experiments revealed that adiponectin suppressed endothelial cell proliferation induced by a low dose of oxidized low density lipoprotein (Motoshima et al., 2004). Interestingly, exogenous adiponectin suppressed PDGF-BB-induced VSMC proliferation via AMPK activation (Igata et al., 2005). The AMPK pathway is central to many of the effects of adiponectin including: inhibiting the expression and activity of iNOS, secretion of adventitial infective factors, division, proliferation and translation of adventitial fibroblasts, change of adventitial fibroblasts to myofibroblasts, and oxidative/nitrative stress which reduces atherosclerotic plaque area and stabilizes the plaque (Cai et al., 2008). In the next part of the introduction, I will focus on AMPK and its role in the function of PVAT.

1.9 AMP-activated protein Kinase (AMPK)

1.9.1 Background

AMPK is a metabolic stress-sensing protein kinase that is involved in regulation of metabolism in response to energy requirements; phosphorylating key regulatory enzymes in different metabolic pathways as well as regulating gene expression (Kemp et al., 2003). AMPK was identified by ATP-dependent inhibitory activity observed during preparation of rat liver acetyl-CoA carboxylase (ACC) (Jeong et al., 2007) and purification of 3-hydroxy-3-methylglutaryl coenzyme A from rat liver microsomes (Maenhaut and Van de Voorde, 2011). Later, both enzymes were found to be activated by AMP (Yeh et al., 1980, Ferrer et al., 1985). Carling *et al* found that ACC and the HMG-reductase kinases were identical and the name of AMPK was adopted (Greif et al., 2009). AMPK monitors cellular energy status by sensing increases in the ratios of AMP/ATP and ADP/ATP (Hardie, 2011). Therefore, a reduction in ATP/AMP ratio leads to activation of AMPK which acts to inhibit anabolic pathways such as fatty acid, triglyceride and cholesterol synthesis, protein synthesis and transcription and stimulate catabolic pathways including glycolysis and fatty acid oxidation (Kemp et al., 2003).

In this section I will review the role of AMPK in physiological and pathophysiological function with particular emphasis on its role in the regulation of vascular function.

1.9.2 AMPK structure

AMPK is heterotrimeric serine-threonine protein kinase. The complex is composed of one catalytic α subunit, and two regulatory subunits (βand γ). There are multiple subunit isoforms in mammals (α1, α2, β1, β2, γ1, γ2 and γ3), which enables the formation of 12 different heterotrimer combinations that are thought to possess distinct subcellular localization and signalling mechanisms (Hardie, 2007). Figure 1.2 illustrates the domain organizations of α, β and γ subunits of AMPK.

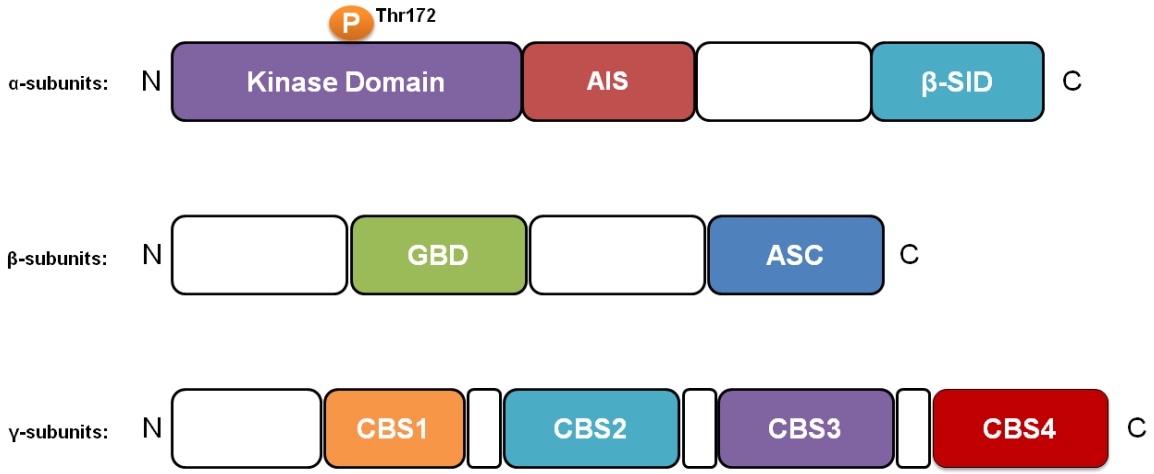

Figure 1-5 Structure of AMPK.

The figure shows the components of the AMPK subunits. The catalytic α-subunit can be phosphorylated at Thr^{172}. The β-subunit contains a glycogen-binding domain (GBD). The γ-subunits contain four nucleotide-binding modules (CBS domains) capable of co-operatively binding to AMP, ADP and ATP. AIS; autoinhibitory sequence, β-SID; β subunit interacting domain (adapted from Ewart and Kennedy, 2011).

The α subunit (α1: 550 residues) is composed of an N-terminal kinase catalytic domain (KCD), followed by an autoinhibitory sequence (AIS) and complex-forming C-terminal domain (β-SID) which are separated by a region of predicted high flexibility. The β subunits act as targeting scaffolds that influence subcellular localization. Mammalian β1 consists of an N-terminal (~70 residue) sequence, followed by an internal carbohydrate-binding module (CBM) related to the N-isoamylase domain subfamily and glycogen-branching enzyme. The highly conserved C-terminal sequence (ASC) has been reported by genetic and structural studies to act as a tethering domain for both α and γ AMPK subunits. Each γ subunit comprises of four cystathionine-β-synthase (CBS) sequence repeats which are small motifs found in tandem pairs called Bateman domains. The CBS sequences act as structural elements which are required for binding the regulatory nucleotides AMP and ATP. In comparison with γ1, the γ2 and γ3 subunits have large extensions to the N-terminus prior to their canonical pair of Bateman domains (reviewed in Oakhill et al., 2009).

1.9.3 Activation of AMPK

1.9.3.1 Allosteric AMPK activation

AMPK is a primary sensor of cellular energy change that responds to stresses that cause increases in the AMP:ATP ratio. Metabolic stresses including hypoxia, nutrient

deprivation, heat shock and metabolic poisoning, have been reported to activate AMPK (Salt et al., 1998, Hardie, 1999). Reduction in the cellular ATP sensed by a rise in AMP or ADP will increase AMPK activity by 10 fold. Binding of AMPK to AMP or ADP induces a conformational change that results in α-subunit Thr172 phosphorylation, as well as inhibition of Thr172 dephosphorylation by protein phosphatases (Hardie et al., 2011). AMP has been shown to support allosteric activation of AMPK that has already been phosphorylated on Thr172 of the α-subunit (Corton et al., 1995).

1.9.3.2 Activation by upstream Kinases

In addition to the allosteric activation due to changes in ATP/AMP ratio, AMPK can be activated at Thr127 on the catalytic α subunit by upstream kinases. Two major AMPK kinases have been identified and they are liver kinase B1 (LKB1) (Woods et al., 2003a) and Ca^{2+}/calmodulin-dependent protein kinase kinase β (CaMKKβ) (Figure 1-3) (Hawley et al., 2005).

LKB1 is the major Thr172 kinase that regulates mammalian AMPK and is the most thoroughly investigated (also referred to as serine/threonine kinase 11). LKB1 was originally identified as a tumour suppressor gene (Hemminki et al., 1998), which is mutated in Peutz Jeghers syndrome. This syndrome is characterised by the development of hamartomas (benign intestinal polyps) and development of high risk malignant cancers in other organs within the body (Hardie, 2005). Inactive LKB1 is located within the nucleus. However, when LKB1 is activated, it translocates to the cytoplasm forming a heterotrimeric complex with two supporting subunits, STE20-related adaptor protein (STRAD), and scaffolding mouse 25 protein (MO25) (van Veelen et al., 2011). STRAD functions as a blocker of the nuclear re-localization of LKB1 and Mo25 stabilizes LKB1-STRAD-Mo25 complex. LKB1 is constitutively active and it has been suggested that the phosphorylation of AMPK by LKB1 is upregulated by physiological and pathological metabolic stress that affects the ATP/AMP ratio such as hypoxia, hypoglycaemia, ischaemia and exercise (Hawley et al., 2003). LKB1 phosphorylates AMPK on its α-Thr172 residue, resulting in at least a 100-fold increase in AMPK activity (Hardie, 2011). Binding of AMP to AMPK stimulates LKB1-dependent phosphorylation of Thr-172 through inhibition of dephosphorylation by causing a conformational change which makes the AMPK complex a less desirable substrate for protein phosphatases and produces a large effect on kinase activity by allosterically activating the phosphorylated form of AMPK (Viollet et al., 2010). In addition, LKB1 has also been identified as being essential

for the phosphorylation and activation of 13 other AMPK-related kinases (Lizcano et al., 2004). However, their physiological functions have not yet been thoroughly defined and they do not appear to be regulated by metabolic stress (Lizcano et al., 2004).

Although LKB1 was considered to be the major kinase responsible for activation of AMPK via an AMP-dependent mechanism, activation of AMPK via phosphorylation at Thr172 has been identified in cells lacking LKB1 (Woods et al., 2005, Hawley et al., 2005). CaMKKs, as the name implies, were originally thought of as acting upstream of Ca^{2+}/calmodulin-dependent protein kinases, however they were also found to activate AMPK *in vitro* as early as 1995 (Hawley et al., 1995). Unlike LKB1, CaMKKs are tissue restricted and are mainly expressed in neurons, T cells and endothelial cells (Anderson et al., 2008, Tamas et al., 2006, Stahmann et al., 2006). CaMKKβ rather than CaMKKα phosphorylates and activates AMPK in response to increased levels of calcium influx into the cell (Hawley et al., 2005, Woods et al., 2005). In human endothelial cells, thrombin activates AMPK via an increase in Ca^{2+} and activation of CaMKKβ (Stahmann et al., 2006). In the same type of cells, VEGF-B activates AMPK in a CaMKK-dependent manner and AMPK activitation is required for proliferation in response to either VEGF-A or VEGF-B and migration in response to VEGF-A (Reihill et al., 2011).

TGF-β-activated kinase 1 (TAK1), was also proposed as an upstream kinase for AMPK based on a genetic screen for mammalian kinases. TAK1 was shown to activate the yeast orthologue of AMPK, Snf1 protein kinase, *in vivo* and *in vitro* and co-expression of TAK1 and its binding partner TAB1 in HeLa cells stimulated phosphorylation of AMPK-Thr172 (Momcilovic et al., 2006). Mice carrying a cardiac-specific dominant negative mutation for TAK1 had signs of the Wolff–Parkinson–White syndrome, which is similar to those associated with mutations in human AMPKγ2 (Xie et al., 2006). Moreover, TAK1-deficient MEFs exhibit reduced AMPK activation by oligomycin, metformin and 5-aminoimidazole-4-carboxamide 1-β-D-ribonucleoside (AICAR), leading the authors to propose that TAK1 has a pivotal role in the regulation of LKB1/AMPK signalling axis, an essential pathway in the regulation of cell metabolism (Xie et al., 2006). Despite this, no recent studies have further corroborated the action of TAK1 as an AMPK Thr172 kinase.

1.9.3.3 Physiological modulators of AMPK

AMPK is activated by metabolic stresses that inhibit catabolic generation of ATP such as glucose deprivation, hypoxia, ischaemia, and treatment with metabolic poisons or increases

ATP demand or consumption such as muscle contraction, thereby increasing cellular ADP:ATP (Oakhill et al., 2010, Oakhill et al., 2011) and AMP:ATP ratios (Hardie, 2007).

1.9.3.4 Pharmacological modulators of AMPK

In addition to physiological activation of AMPK by increases in the cellular AMP/ATP ratio (Ewart and Kennedy, 2011, Hardie, 2007), many pharmacological AMPK activators have been identified (Figure 1-4).

Metformin is a commonly used medication in the treatment of type 2 diabetes that reduces hyperglycaemia (Kirpichnikov et al., 2002). Metformin is a biguanide that activates AMPK in intact cells and *in vivo* (Musi and Goodyear, 2002). Activation of AMPK by metformin is dependent on its uptake by organic cation transporter 1 (Shu et al., 2007), and recent studies have shown that metformin stimulates AMPK activity by increasing AMP levels (Hawley et al., 2010). Others have suggested that ROS and reactive nitrogen species are also involved in the activation of AMPK by metformin (Zou et al., 2004, Fujita et al., 2010). However, many studies have revealed that metformin can induce anti-gluconeogenic actions in an AMPK-independent manner via a decrease in hepatic energy state (Foretz et al., 2010), although it remains possible that AMPK activation underlies other effects of metformin.

In the vasculature, metformin-induced AMPK activation has been reported to up-regulate eNOS phosphorylation to increase NO bioavailability (Calvert et al., 2008, Zhang et al., 2011) and reduce SMC proliferation, migration and inflammatory responses (Kim and Choi, 2012). In cardiac tissue, metformin-induced AMPK activity sustains energy balance, cardiomyocyte function and myocardial viability (Cha et al., 2010, Fu et al., 2011). The reported cardioprotective effect is principally achieved by the reduction of hypertrophic cell growth and endoplasmic reticulum (ER) stress (Dong et al., 2010).

Thiazolidinediones (TZDs) are another class of anti-diabetic drugs, including rosiglitazone, troglitazone and pioglitazone, which have been used to counteract insulin resistance in patients with T2DM by increasing the sensitivity of peripheral tissues to insulin (Krishan et al., 2015). They act by binding to PPARγ, which promotes the synthesis of glucose transporters and proteins regulating lipid metabolism, leading to storage of lipids in adipocytes rather than hepatocytes and muscle, protecting against lipotoxicity-driven insulin resistance (Semple et al., 2006, Burns and Vanden Heuvel, 2007). PPARγ receptors are nuclear hormone receptors that are expressed widely not only in adipose tissue but also

in skeletal muscle (Hevener et al., 2003), liver (Gavrilova et al., 2003) and macrophages (Hevener et al., 2003).

TZDs exert pleiotropic effects in a manner similar to statins, and some of these effects are observed acutely and do not require gene transcription. The acute effects of TZDs have been proposed to be via activation of AMPK in adipose tissue, skeletal muscle and liver (LeBrasseur et al., 2006). The mechanism of AMPK activation is reported to be due to an increase in intracellular AMP/ATP ratio (Fryer et al., 2002). Similar to metformin and phenformin, TZDs have been demonstrated to act as inhibitors of complex 1 of the respiratory chain (Brunmair et al., 2004); thus, an increase in the AMP/ATP ratio may be the mechanism for AMPK activation in response to these drugs. Notably, this effect was reported to be independent of PPARγ (Guh et al., 2010). TZDs can also activate AMPK by stimulating adiponectin release from adipose tissue (Yamauchi et al., 2002) and this effect may be important in PVAT. Both rosiglitazone and pioglitazone have been reported to have beneficial anti-atherosclerotic and anti-inflammatory effects (Stocker et al., 2007), as well as an additional beneficial influence on endothelium via AMPK-dependent and PPAR-γ-independent mechanisms (Polikandriotis et al., 2005, Ceolotto et al., 2007). It has been also shown that rosiglitazone can stimulate NO synthesis in human endothelial cells via AMPK-mediated eNOS Ser1177 phosphorylation (Boyle et al., 2008). However, it should be noted that TZD use is associated with the risk of fluid retention which may exacerbate heart failure (Hannan et al., 2003). There is also a concern that rosiglitazone is associated with additional cardiovascular (MI and stroke) risk in patients with T2DM (Azimova et al., 2014).

Statins are HMG-CoA reductase inhibitors used in the treatment of metabolic syndrome and hypercholesterolaemia. Besides their cholesterol-lowering effects, statins have also been reported to activate AMPK in human and bovine endothelial cells (Sun et al., 2006). Sun et al. also reported that while atorvastatin and lovastatin rapidly stimulate AMPK and eNOS in mouse myocardium and endothelial cells, they do not alter the cellular AMP/ATP ratio, suggesting a different pathway of AMPK activation (Sun et al., 2006, Goirand et al., 2007). Two days of treatment with fluvastatin (at a concentration of 20 mM) has also been reported to stimulate eNOS and AMPK in human iliac endothelial cells. This effect was blocked by an eNOS inhibitor, implying that AMPK up-regulation was dependent on NO synthesis (Xenos et al., 2005). In another study conducted in rat aorta, simvastatin up-regulated both AMPK and the upstream kinase LKB1. They also reported that this activation of AMPK was dependent on PKCζ-mediated phosphorylation of LKB1 (Choi et

al., 2008). However, another study using HeLa cells expressing mutant LKB1 reported that phosphorylation of Ser431 on LKB1 was not required for AMPK up-regulation (Fogarty and Hardie, 2009). In addition to the beneficial effects of statins on endothelial function, which are likely due to eNOS up-regulation (Laufs et al., 2002, Laufs et al., 2000), statins exert anti-inflammatory (Cahoon and Crouch, 2007) and anti-atherogenic effects (Nissen et al., 2005). These observations all indicate that AMPK activation might be important in the pleiotropic effects of statins on cardiovascular protection.

6,7-Dihydro-4-hydroxy-3-(2′-hydroxy[1,1′-biphenyl]-4-yl)-6-oxo-thieno[2,3-b]pyridine-5-carbonitrile (A769662) is a member of the thienopyridone family that activates AMPK both allosterically and by inhibiting dephosphorylation of the kinase at Thr172 (Cool et al., 2006). A769662 is dependent on the β-subunit carbohydrate-binding module and γ subunit (Guh et al., 2010) of AMPK and, notably, exclusively activates trimers containing the β1 subunit (Scott et al., 2008). In *in vitro* studies, A769662 has been shown to stimulate phosphorylation of acetyl-CoA carboxylase (ACC) independently of the upstream kinases LKB1 and CaMKK (Cool et al., 2006, Goransson et al., 2007). In cell-free assays, it has no direct effect on the ability of LKB1 or CaMKK to phosphorylate AMPK. The mechanism of AMPK activation by A769662 is thought to be distinct from that of AMP, as A769662 can still activate an AMP-insensitive AMPK containing a mutation in the γ subunit. In addition, A769662 activation of AMPK was inhibited by a mutation in the β1 AMPK subunit (Ser108 to Ala), which is an auto-phosphorylation site within the glycogen-binding domain; however, the same mutation only partially reduced AMPK activation by AMP (Cool et al., 2006, Sanders et al., 2007). A769662 stimulates AMPK directly in partially purified rat liver and suppresses fatty acid synthesis in primary rat hepatocytes. Short-term treatment of normal Sprague-Dawley rats with A769662 has been shown to reduce liver malonyl-CoA levels and the respiratory exchange ratio of CO_2 production to O_2 consumption, indicating an increased rate of whole-body fatty acid oxidation (Cool et al., 2006). Treatment with A769662 reduced plasma glucose, weight gain, and both plasma and liver triacylglycerol (triglyceride) levels in leptin-deficient ob/ob mice (Cool et al., 2006).

Another potent activator that binds to the same binding site of A769662 which has been identified to be a cleft located between the N-lobe of the kinase domain on the α subunit and the carbohydrate-binding module on the β-subunit (Calabrese et al., 2014) is 991 (also known as ex229). Discovered via high-throughput screens, 991, like A769662, shows

some selectivity for β1 complexes although it will activate β2 complexes at higher concentrations (Grahame Hardie, 2016).

Another widely used AMPK activator is AICAR, also known as acadesine. AICAR is a pro-drug and analogue of adenosine that enters cells and stimulates AMPK, following its phosphorylation to its active nucleotide ZMP (5-aminoimidazole-4-carboxamide-1-β-D-furanosyl 5′-monophosphate), which mimics AMP (Merrill et al., 1997). AICAR has been tested in human studies of ischaemic heart disease due its ability to block adenosine reuptake by cardiac cells, promoting stimulation of adenosine membrane receptors. In 1997, treatment with AICAR before and during surgery was shown to alleviate early cardiac death, MI and combined adverse cardiovascular consequences, although whether the effects were via AMPK was not investigated at that time (Mangano, 1997). AICAR has been demonstrated to reverse many aspects of the metabolic syndrome in animal models such as the ob/ob mouse, the fa/fa rat and high fat-fed rat (Buhl et al., 2002, Iglesias et al., 2002), and also in human subjects (Cuthbertson et al., 2007). AICAR has also been reported to stimulate release of adiponectin and inhibit release of cytokines such as TNF-α and IL-6, which have been implicated in the development of obesity-induced insulin resistance (Kern et al., 2001, Lihn et al., 2004). AICAR is not suitable for clinical use because of its short half-life, requirement for i.v. infusion and variable effectiveness. AICAR has also been reported to cause bradycardia and hypoglycaemia when administered intravenously (Young et al., 2005).

In addition to galegine, several natural products derived from plants have been reported to activate AMPK. These include resveratrol from red grapes, ginsenoside from *Panax ginseng*, berberine from *Coptis chinensis*, epigallocatechin gallate from green tea, theaflavin from black tea and hispidulin from snow lotus (Hwang et al., 2009, Lin et al., 2010). The role of these compounds in the activation of the AMPK was reasoned with the results that berberine can inhibit the respiratory chain (Turner et al., 2008) and resveratrol can inhibit the F1 ATP synthase (Gledhill et al., 2007), and thus they activate AMPK indirectly. By inhibiting mitochondrial ATP production and thus increasing cellular AMP: ATP and/or ADP: ATP ratios, they activate AMPK in a similar manner to the biguanides. Supporting this, AMPK activation by resveratrol, berberine, and quercetin was abolished in cells expressing the AMP/ADP-insensitive AMPK mutant (Hawley et al., 2010).

Dorsomorphin (compound C) is an inhibitor of AMPK activity. Compound C binds the ATP-binding site of the AMPK kinase domain although it is poorly selective, inhibiting

several other protein kinases more effectively that AMPK. Despite this, compound C has been used to inhibit AMPK activity in muscle cells, several tumor cell types, and in angiogenesis studies *in vivo* (Nagata et al., 2003, Baumann et al., 2007, Dowling et al., 2007, Isakovic et al., 2007).

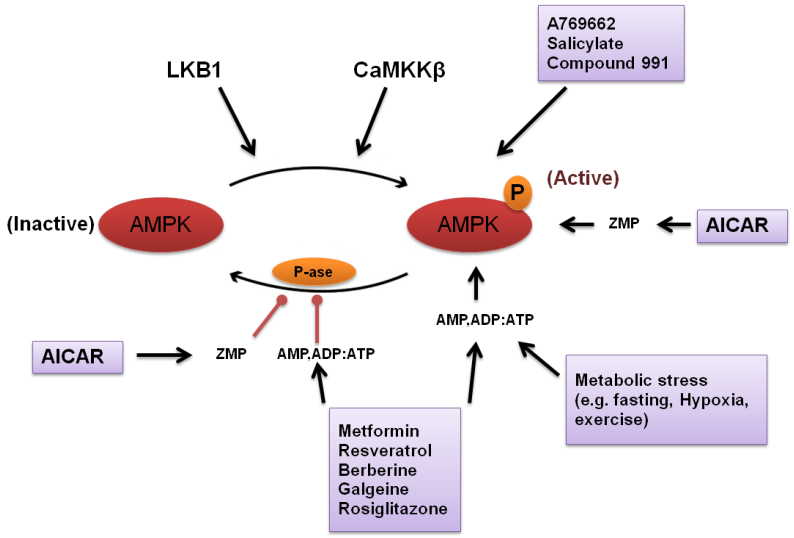

Figure 1-6 Activation of AMPK.

AMPK is activated by phosphorylation of the α catalytic subunit at Thr172 by LKB1 or CaMKKβ. Increased AMP or ADP/ATP ratio bind to the regulatory γ subunit, allosterically activating AMPK and inhibiting dephosphorylation of Thr172 by protein phosphatase (P-ase). Neither LKB1 nor CaMKKβ are regulated directly by adenine ATP, AMP or ADP. Increased intracellular Ca^{2+} stimulates CaMKKβ-mediated AMPK activation. The antidiabetic drugs metformin and rosiglitazone (a TZD) increase AMP/ATP or ADP/ATP concentrations, thereby activating AMPK. Resveratrol, galgeine and berberine also activate AMPK by this mechanism. AICAR is phosphorylated to the nucleotide ZMP, which mimics AMP. A769662, salicylate and compound 991 are reported to activate AMPK complexes containing the β1 subunit

1.10 Downstream targets of AMPK

Once activated, AMPK directly activates a number of downstream effectors that control energy metabolism and growth, or induce changes in gene expression that will result in long-term effects on metabolic function (reviewed in Kahn et al., 2005). In general, AMPK up-regulates catabolic pathways (e.g., glucose uptake in muscle, glycolysis, fatty acid oxidation and mitochondrial biogenesis) and down-regulates anabolic pathways (e.g., fatty acid, triglyceride, cholesterol, glucose (via gluconeogenesis) and glycogen synthesis) to maintain energy balance within the cells (reviewed in Kahn et al., 2005). Figure 1-5 summarises the most well know downstream protein targets of AMPK.

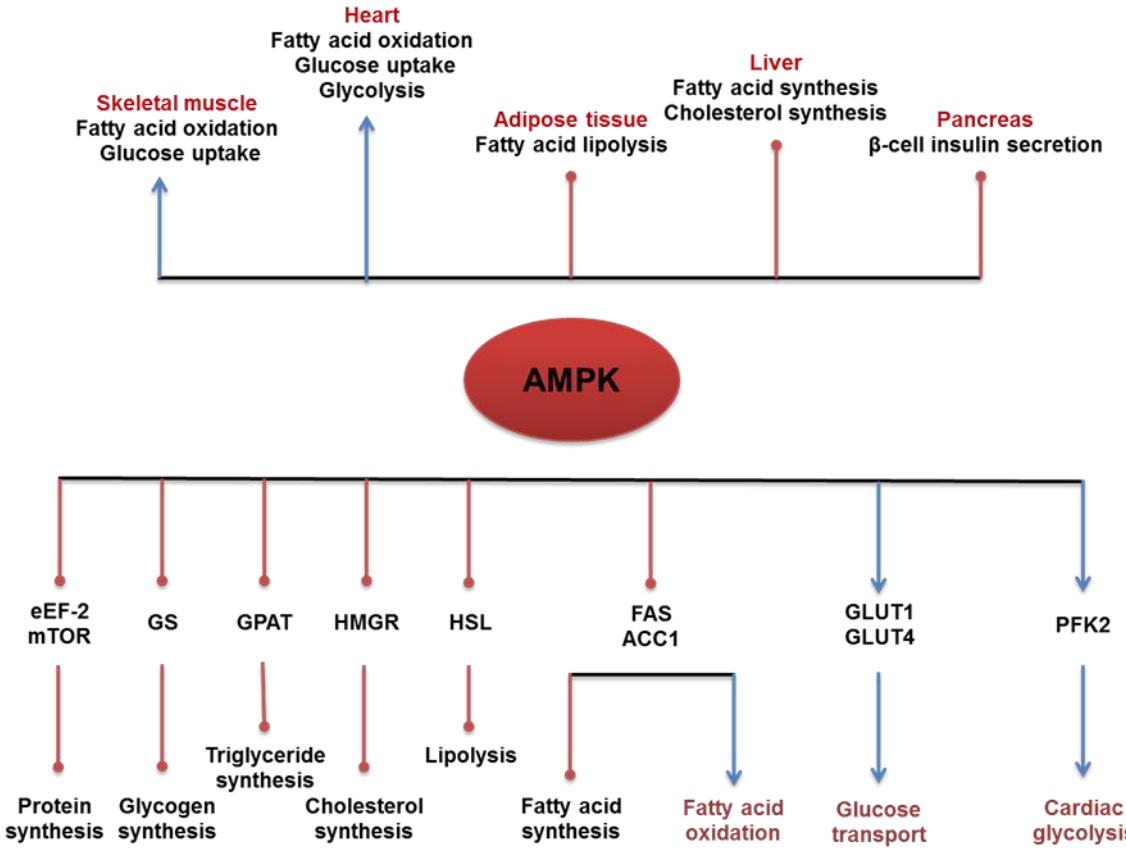

Figure 1-7 Demonstration of some downstream target proteins of AMPK involved in regulation of metabolism.

Target proteins and processes activated by AMPK activation are shown in Blue arrow, and those inhibited by AMPK activation are shown in red arrow. Abbreviations: ACC1, 1 (α) of acetyl-CoA carboxylase; eEF2, elongation factor-2; FAS, fatty acid synthase; GLUT1/4, glucose transporters; GS, glycogen synthase; HMGR, 3-hydroxy-3-methyl-CoA reductase; HSL, hormone-sensitive lipase; mTOR, mammalian target of rapamycin; GPAT, glycerol-3-phosphate acyltransferase; PFK-2, 6-phosphofructo-2-kinase.

1.11 Role of AMPK in peripheral tissue

AMPK has a well-defined regulatory role in lipid metabolism. Activation of AMPK phosphorylates and inactivates ACC and HMGR, as well as reducing expression of fatty acid synthase (FAS). The net effect is a reduction in fatty acid and cholesterol synthesis (Kahn et al., 2005). In the liver, inactivation of ACC1 results in increased fatty acid transport and subsequent oxidation. In skeletal muscle, activated AMPK stimulates fatty acid oxidation by decreasing malonyl-CoA levels through the inhibition of ACC. This leads to an increase in carnitine palmitoyltransferase 1 (CPT1) activity and the subsequent activation of fatty acid oxidation (Kahn et al., 2005). AMPK has been suggested to inhibit lipolysis in adipocytes (Daval et al., 2005, Corton et al., 1995), thereby reducing the plasma level of fatty acids. Furthermore, AMPK activation stimulates and upregulates the

peripheral muscle expression of PPAR-γ coactivator-1α (PGC1α), which enhances mitochondrial biogenesis (Terada et al., 2002).

AMPK is also involved in the regulation of glucose homeostasis. Activation of AMPK in skeletal muscle up regulates hexokinase II expression (Holmes et al., 1999). It also increases glucose uptake via cell membrane translocation of the glucose transporter GLUT4 and the stimulation of GLUT4 gene expression (Derave et al., 2000, Wright et al., 2005). AMPK inhibits hepatic gluconeogenesis by repressing the transcription of phosphoenolpyruvate carboxykinase (PEPCK) and glucose-6-phosphatase (G6Pase) (Lochhead et al., 2000). Furthermore, AMPK activation decreases glycogen synthesis via phosphorylation and inhibition of glycogen synthase (Wojtaszewski et al., 2002).

Hypothalamic AMPK is also involved in regulation of peripheral tissue metabolism, indicating that AMPK is a crucial enzyme in regulation of the interaction between peripheral and central energy production. In a study by Perrin *et al*, intraventricular AICAR administration increased both insulin-mediated and non-insulin-mediated glycogen synthesis (Perrin et al., 2004), which implies a role for hypothalamic AMPK in muscle glycogen synthesis. The same study showed that AMPK is also involved in increasing muscle glycogen synthesis and this effect was blocked by the co-administration of glucose (Perrin et al., 2004). Activation of hypothalamic AMPK by central adiponectin administration decreases energy expenditure, possibly by a reducing the expression of UCP-1 in BAT (Kubota et al., 2007). On the other hand, central α-lipoic acid inhibits hypothalamic AMPK activity, thus increasing UCP-1 expression and energy expenditure in BAT (Kim et al., 2004). Central ghrelin treatment has been shown to increase glucose utilisation rate of white and brown adipose tissues (Theander-Carrillo et al., 2006). Ghrelin has been shown to abolish, at least in part the effects of central leptin treatment on fat weight, plasma glucose and insulin, the effects in which AMPK involved (Minokoshi et al., 2004).

1.12 Vascular effects of AMPK

1.12.1 Role of AMPK in the vascular endothelium

Both α subunit isoforms of AMPK are expressed in endothelium (Fisslthaler and Fleming, 2009), yet the total cellular activity of AMPK complexes containing α1 is higher than those containing α2 (Morrow et al., 2003). Despite this, it has been shown that mice lacking the α2 AMPK subunit isoforms have endothelial dysfunction characterised by excessive ROS

generation (Wang et al., 2010b). The α2 subunit isoform of AMPK is critical in maintaining endothelial cells in a normal, non-atherogenic phenotype as it is considered to be a physiological suppressor of NAD(P)H oxidase; the marker of oxidative stress and generation of ROS (Wang et al., 2010b). However, the role of the α1 subunit in endothelial cells has also been examined (Liu et al., 2010) and it was found that AMPK-mediated suppression of NF-κB, glucose deprivation and hypoxia-stimulated endothelial cell apoptosis was lost in mice lacking AMPKα1, suggesting that AMPKα1 is essential for AMPK to promote cell survival by NF-κB-mediated expression of anti-apoptotic proteins (Liu et al., 2010). AMPK activation has also been shown to alleviate endoplasmic reticulum stress (Dong et al., 2010).

AMPK enhances release of NO from vascular endothelium. Activated endothelial AMPK phosphorylates eNOS at Ser1177, thereby enhancing NO production in human aortic endothelial cells (HAECs) (Morrow et al., 2003). AMPK activation may also stimulate eNOS association with heat shock protein 90 (Hsp90), which stimulates NO synthesis (Wang et al., 2009c, Davis et al., 2006). NO release leads to vasodilation in both conduit (Wang et al., 2009c) and resistance vessels (Bradley et al., 2010). Shear stress, statins and adiponectin have been found to increase NO bioavailability in the endothelial cells by activation of AMPK which phosphorylates eNOS at Ser1177 and also Ser663/635 (Chen et al., 2009). In the absence of Ca^{2+}/calmodulin, AMPK phosphorylates eNOS at the inhibitory Thr495 site, *in vitro*, reducing the activity of eNOS (Chen et al., 1999). In addition the phosphodiesterase inhibitor cilostazol which activates AMPK via altering [AMP:ATP] ratio has been demonstrated to enhance NO production and restore endothelial function in diabetic rats (Suzuki et al., 2008).

The lesions of atherosclerosis usually start with endothelial dysfunction and inflammatory cell adhesion events (Ross, 1999) and AMPK has been implicated in both of these events. In HUVECs, activated AMPK has been found to abolish TNFα stimulated leukocyte adhesion and migration via an NO-dependent mechanism associated with reduced MCP-1 secretion and an NO-independent mechanism by decreasing the expression of adhesion molecule E-selectin (Ewart et al., 2008). Similarly, activation of AMPK by berberine significantly reduces monocyte (THP-1) adhesion to HUVECs by reducing the expression of the adhesion molecules ICAM-1 and VCAM-1 (Wang et al., 2009b). AICAR has been found to reduce leukocyte rolling and adhesion by both eNOS-dependent and -independent mechanisms. In those experiments, administration of AICAR 30 min prior to induction of ischaemic perfusion in mesenteric artery injury reduced inflammatory cell adhesion

independent of eNOS, whereas administration of AICAR 24 hours before induction of ischaemic perfusion injury abolished leukocyte adhesion in an eNOS-dependent manner (Gaskin et al., 2007). In addition, the statin fluvastatin has been reported to upregulate eNOS and AMPK and reduce adhesion molecule expression in cultured human iliac artery endothelial cells (Xenos et al., 2005).

AMPK has been shown to control vascular redox balance in endothelial cells. Increased oxidant stress and/or defective antioxidant function are involved in endothelial dysfunction in atherosclerosis and following vascular injury caused by balloon angioplasty or stenting (Siersbaek et al., 2010). Activating AMPK in endothelial cells increases the expression of manganese superoxide dismutase (Kukidome et al., 2006) and reduces NF-κB-mediated transcription (Hattori et al., 2008). AMPK activating agents such as rosiglitazone and AICAR inhibit ROS generation in endothelial cells exposed to oxidant stress via increased glucose concentration (Ceolotto et al., 2007). Moreover, activated AMPK enhances uncoupling of protein-2 expression which supresses ROS formation and nitration of prostacyclin synthase (Xie et al., 2008).

AMPK is also implicated in angiogenesis. Vascular Endothelial Growth Factor (VEGF), the key regulator of angiogenesis, induces differentiation, survival, migration, proliferation and vascular permeability (Ferrara et al., 2003). It does so via increasing NO synthesis via an AMPK-dependent mechanism (Reihill et al., 2007).

1.12.2 Role of AMPK in vascular smooth muscle cells

Many studies have provided evidence that AMPK is important in regulation of vascular smooth muscle function and its dysfunction leads to development of vascular disease such as hypertension and atherosclerosis.

Both catalytic α isoforms are expressed in VSMCs, although the ratio of α subunits differs according to the type of the vessel (Rubin et al., 2005). Activation of AMPK in vascular smooth muscle using AICAR induces vascular relaxation in an endothelial- and eNOS-independent mechanism mediated by AMPKα1 rather than AMPKα2 (Goirand et al., 2007). AMPK has been also found to attenuate vascular smooth muscle contraction induced by phenylephrine via phosphorylating and inactivating myosin light chain kinase (MLCK) (Horman et al., 2008). Moreover, acetylcholine induces endothelial independent vascular relaxation by stimulating AMPK-LKB1 dependent mechanism. Activation of

AMPK by LKB1 inhibits myosin light chain kinase and decreases phosphorylation of myosin light chain which might attenuate vasoconstriction (Lee and Choi, 2013).

AMPK is also implicated in inhibition of VSMCs proliferation. This effect appears to be mediated by many different signalling mechanisms including regulation of the cell cycle and inhibition of protein synthesis, de novo fatty acid and cholesterol synthesis (reviewed in Motoshima et al., 2006). AMPK activation can induce G1 cell cycle arrest by upregulation of p53-p21 which inhibits VSMCs proliferation (Igata et al., 2005). Retinoic acid-related orphan receptor alpha (RORα) is implicated in reducing progression of atherosclerosis. RORα abolishes VSMCs proliferation through AMPK-induced mTOR suppression and ribosomal protein S6 kinase (S6K), thus alleviating VSMC proliferation (Kim et al., 2014). Vascular calcification is a complication associated with type 2 diabetes, peripheral and coronary artery disease and occurs due to disturbed osteoblastic differentiation (Snell-Bergeon et al., 2013). Activation of AMPK by adiponectin has been found to attenuate vascular calcification via AMPK-TSC2-mTOR-S6K1 signalling pathway. Furthermore, metformin activated AMPK supresses vascular calcification by AMPK-eNOS-NO pathway in rat aortic VSMCs (Zhan et al., 2014, Cao et al., 2013). Activation of AMPK abolishes VSMCs proliferation via direct inhibition of IGF-I (Ning and Clemmons, 2010). AMPK stimulates the phosphorylation of IRS-1 Ser794 which leads to reduced IRS-1 tyrosine phosphorylation and the association of the p85α subunit of PI3K with IRS-1 in response to IGF-I. The net effect will be diminished protein synthesis due to reduced phosphorylation of Akt at Ser473 (Ning and Clemmons, 2010).

1.13 Cross talk between PVAT and vascular layers and role of AMPK

PVAT, via its release of adipokines, may therefore affect vascular function via activation of AMPK in both endothelium and VSM layers. AMPK-stimulating adipokines, such as adiponectin, are potentially the principal mediators of the modulatory effect of PVAT on blood vessels. Adiponectin release is markedly reduced in obese PVAT and this has been reported to lead to inhibited vasorelaxation. Adiponectin receptor antagonism and the AMPK inhibitor compound C have been reported to attenuate vascular relaxation, whereas globular adiponectin failed to induce vascular relaxation in AMPKα2-deficient mice (Meijer et al., 2013). Furthermore, activation of adipocyte β3-adrenoceptors has been reported to stimulate release of a substance, assumed to be adiponectin that indirectly opens myocyte BK_{Ca} channels. This effect was reported to involve AMPK since it could be

mimicked by the AMPK activator, A-769662, and blocked by compound C (Weston et al., 2013). The indirect activation BK_{Ca} by AMPK was demonstrated by blocking adipocyte-dependent myocyte hyperpolarization induced by BK_{Ca} channel opener, NS1619 with glibenclamide and clotrimazole (Weston et al., 2013). PVAT has also been reported to induce vasodilatation in muscle resistance arteries by increasing secretion of adiponectin and activation of AMPK α2 in the blood vessels. Furthermore, this study reported that in obese *db*/*db* mice, PVAT mass increased dramatically in the muscle and was associated with loss of insulin-mediated vasodilation. Notably, the lack of insulin-induced vascular reactivity could be restored by JNK inhibition (Meijer et al., 2013). Figure 1-8 illustrates the mechanisms by which PVAT may induce vascular relaxation in both endothelium and VSMC layers.

It has been suggested that adiponectin exerts beneficial effects via activation of AMPK and suppression of iNOS expression in the vascular adventitia (Cai et al., 2008). The same group tested the effects of adiponectin on adventitial fibroblast transition and migration. They reported that adiponectin induced AMPK phosphorylation and reduced the migration of fibroblasts, the expression of iNOS and the peroxynitrite marker nitrotyrosine in response to LPS treatment (Cai et al., 2010).

Although this thesis focuses on the adiponectin as a potential PVAT derived adipocytokines, there are many others such as leptin, apelin and resitin and some gasiuos molecules such as H_2O_2, NO and H_2S are ivolved in regulation of vascular function. Figure 1-8 illustrates the mechanisms by which theses factors modulates vascular function.

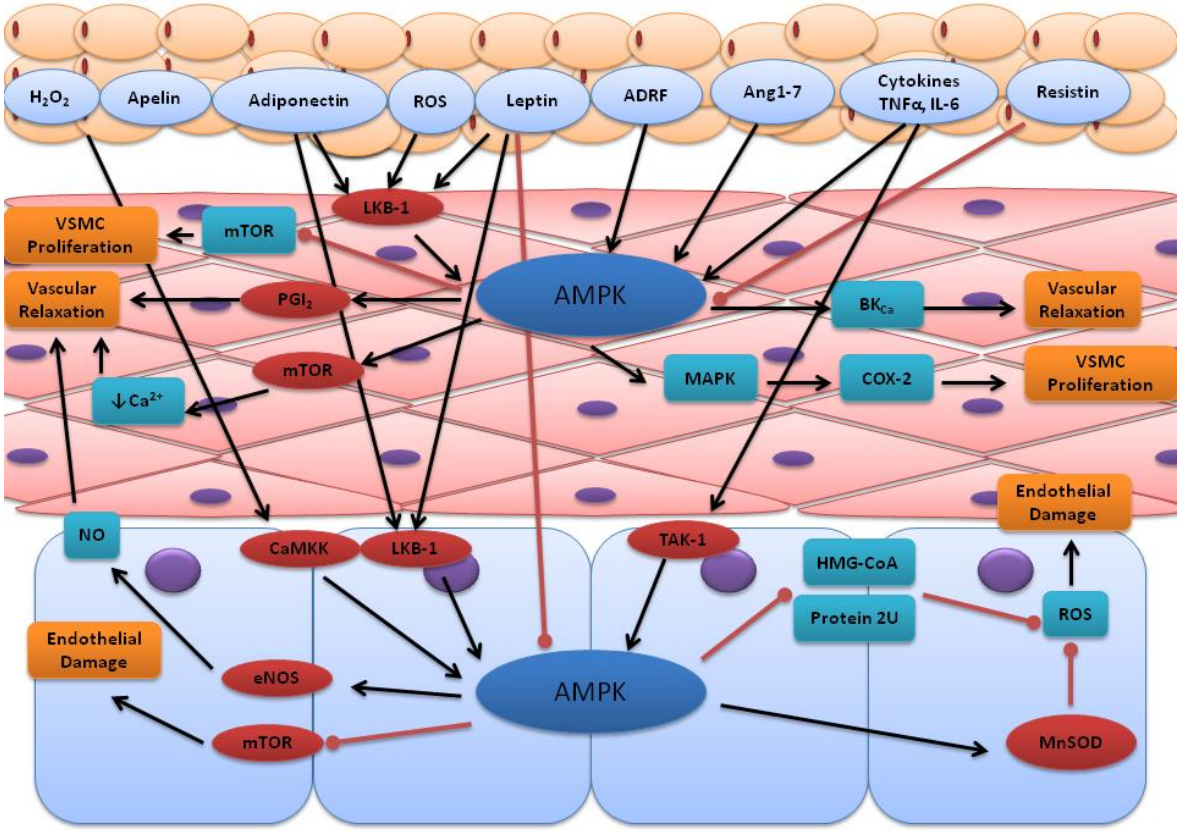

Figure 1-8 schematic presentation of how PVAT modulates the function of AMPK in both endothelium and vascular smooth muscle and how these affect vascular function.

PVAT is a highly active organ secreting various adipokines and cytokines implicating in the regulation of vascular contractility via modulation of AMPK activity. ADRF, adipose tissue-derived relaxation factor; Ang1-7, angiotensin 1–7; BKCa, calcium-dependent big potassium channel; CAMKK, calcium/calmodulin-dependent protein kinase kinase; eNOS, endothelial NOS; HMG-COA, 3-hydroxy-3-methylglutaryl-coenzyme A; LKB, liver kinase B; MAPK, mitogen-activated protein kinases; MnSOD, manganese superoxide dismutase; mTOR, mammalian target of rapamycin; PGI2, prostacyclin; ROS, reactive oxygen species; TAK1, transforming growth factor β-activated kinase (Almabrouk et al., 2014).

Activation of AMP-activated protein kinase (AMPK) phosphorylates tuberous sclerosis complex 2 (TSC2) which in turn inhibits of mTOR activity and limits protein synthesis (Inoki et al., 2003). Ma *et al* discovered that PVAT can induce vascular dysfunction via dysregulation of the AMPK/mTOR pathway in diet-induced obese rats, with mesenteric arterial rings incubated with periaortic fat from HFD rats showing reduced endothelium-dependent relaxation and down-regulation of AMPK and eNOS in the aorta with a concurrent up-regulation of mTOR. This effect was absent in periaortic fat from rats on a chow diet. In the same study, co-culture of vascular SMCs with periaortic adipocytes from HFD animals also reduced AMPK phosphorylation and increased mTOR phosphorylation (Ma et al., 2010).

Cytokines generated from the PVAT (Figure 1-7) may induce vascular dysfunction indirectly via up-regulation of iNOS. 3T3 L1 adipocytes incubated with TNF-α showed a 200-fold increase in iNOS gene expression (Digby et al., 2010). Furthermore, FFAs released by adipocytes increase iNOS expression and vascular dysfunction, as human vascular SMCs stimulated with a combination of conditioned media from adipocytes and oleic acid induced not only iNOS up-regulation and NO formation but also a proliferative response (Lamers et al., 2011). Activation of AMPK in adipose tissue has been found to suppress iNOS expression and NO production in cytokine (TNF-α, IFN-γ) treated adipocytes (Pilon et al., 2004, Centeno-Baez et al., 2011).

1.14 Role of AMPK in perivascular adipose tissue

AMPK is expressed in the three layers of the blood vessel: the endothelium, smooth muscle and PVAT and is known to induce vasodilatation by both endothelium and non-endothelium dependent mechanisms. Furthermore, it is well known that AMPK exerts an anti-proliferative effect at the level of the endothelium and VSM. Although it is known that AMPK can modulate VSM and endothelial function, it is unknown whether AMPK can modulate the anti-contractile and anti-proliferative effects of PVAT, despite the expression of AMPK in endothelium, VSM and in perivascular adipocyte.

At the start of these studies, the role of AMPK in PVAT function had not been examined. The studies described in this thesis test the hypothesis that AMPK in PVAT modulates the activity of vascular smooth muscle cells, and that this may underlie PVAT-mediated changes in vascular function and vessel remodelling in CVD (s).

1.15 Hypothesis and Aims

Perivascular adipose tissue (PVAT) surrounds most blood vessels and secretes numerous active substances, including adiponectin which produce a net anticontractile effect in healthy PVAT. The anticontractile mechanism of PVAT is still unclear, although it is generally proposed that PVAT can induce vascular relaxation via both endothelium and non-endothelium dependent mechanism. Although it is known that AMPK can modulate VSM and endothelial function, it is unknown whether AMPK can modulate the anti-contractile effects of PVAT. Obesity is an independent risk factor for cardiovascular disease and is associated with altered arterial contractility. It is known that AMPK activity

in PVAT is reduced with obesity; however it is unknown whether the effects of AMPK on arterial contractility are modulated by obesity.

Therefore, the hypothesis of this thesis is that AMPK expressed in the PVAT is essential in regulation of anti-contractile effect of the PVAT and that AMPK acts as a protective mechanism in case of HFD-induced obesity. Therefore, this study aimed to:

i. Investigate the morphological features of PVAT in wild type mice and mice lacking AMPKα1.

ii. Investigate the mechanism responsible for the anticontractile effects of PVAT, specifically:

- The involvement of AMPK in the anticontractile effect of PVAT.
- To investigate the role of PVAT-derived adiponectin in mediating the anticontractile effects of PVAT.

iii. To determine the role of AMPK in regulation of redox state of PVAT, specifically:

- To characterise any differences in ROS and RNS expression between wild type and AMPKα1 KO PVAT.
- To define the role of AMPK in the NO-dependent anticontractile effect of PVAT.

iv. To determine the effect of high fat diet on the function of the PVAT and AMPK, specifically:

- To characterise the effect of high fat diet on the anticontractile effect of PVAT.
- To determine the role of AMPK in high fat diet-induceed inflammatory response of PVAT.
- To determine the whether wire-induced injury could affect AMPK function in the PVAT and thus the antiprolefertive response in mice carotid artery.

Chapter 2

Materials and Methods

Materials

2.1 Animals

Wild type (Sv129) mice were originally purchased from Harlan Laboratories (Oxon, UK). AMPKα1 knockout mice were kindly supplied by Benoit Viollet (Institut Cochin, Paris, France) the generation of which has been described previously (Jorgensen et al., 2004). Mice were housed at the Central Research Facility at the University of Glasgow and maintained on 12 hour cycles of light and dark and at ambient temperature. Mice were fed a standard chow diet unless otherwise stated and allowed free access to both food and water. All experiments were conducted in accordance with the United Kingdom Animals (Scientific Procedure) Act of 1986. Where appropriate all experimentation was performed under the project licences, 60/4114 and 70/8572, held by Dr Simon Kennedy (University of Glasgow, U.K.).

2.2 Chemical and Reagents

All chemicals were supplied by Sigma-Aldrich (Poole, UK) unless otherwise stated. All cell culture reagents were obtained from Gibco (Paisley, U.K.) unless otherwise stated. All Western blot materials were supplied by Life Technologies (Paisley, U.K.) unless otherwise stated. High-fat diet (Western RD) was purchased from SDS (SDS diets, U.K). The composition of the diet is illustrated in Table 2-1.

Table 2-1 Composition of the high-fat diet (HFD).

Specification	% (W/W)	Kcal/g	% kcl
Crude fat	21.4	1.93	42
Crude Protein	17.5	0.70	15
Crude Fibre	3.5	/	/
Ash	4.1	/	/
Carbhydrate	50.0	2.00	43
Total AFE		4.63	100

Methods

2.3 Genotyping

The genotype of all wild type (Sv129) and AMPKα1 knockout mice was confirmed prior to inclusion in all studies. Genotypes were confirmed by reverse transcription polymerase chain reaction (RT-PCR) using the Go Taq amplification system (Promega, Southampton, U.K.), following DNA extraction from ear clips and immunofluorescence staining of the targeted sequence. Details of the technique are outlined below.

2.3.1 DNA Extraction

Ear notches from mice were obtained by staff from the Central Research Facility at 8 weeks of age when animals were numbered. Samples were stored at -20^{o}C until DNA was ready to be extracted using DNAreleasy (Anachem, Luton, UK). 10 µl of DNAreleasy was added to each ear notch and PCR was performed as follows: 75°C for 5min, 96°C for 2min and then kept at 20°C (until needed). 90µl of nuclease free dH_2O was then added to the samples. Genotyping was performed by RT-PCR using the Go Taq amplification system (Promega, Southampton, UK) as per the manufacturer's instructions, with reaction mixture details given in Table 1-1.

Table 2-2 RT-PCR reaction mixture for genotyping

Reaction Mixture
TAQ(GO) HOT START GREEN MASTERMIX (Promega, Southampton, UK) which contains dNTPs, MgCl and load dye.
FORWARD primer for both wild type and knockout sequence
REVERSE primer for both wild type and knockout sequence
Prepared DNA samples

2.3.2 Polymerase Chain Reaction for AMPKα1 Wild type (WT) and AMPKα1 Knockout (KO)

Details of the primers and their sequences, annealing temperatures and electrophoresis bands are showed in Table 2-2. All PCR cycles were subject to a hot-start 95 °C for 5min (enzyme activation), followed by 40 cycles of 95°C for 30 seconds (DNA denaturation), 58°C for 40 seconds and 72°C for 1min (primer binding). Samples were subjected to 72°C for 10 min (primer extension) and then 4°C where they were stored until visualised. Samples were electrophoresed on a 2% (w/v) agarose/TAE (242g TRIS, 18.6g EDTA, pH 8) gel and visualized with ethidium bromide (final concentration 0.1% (v/v)) using the

Alpha Innotech digital imaging system (San Leandro, CA, USA). The wild type and knockout animals were identified by the presence or absence of a targeted sequence in comparison with a 100 bp ladder (Promega, UK) run at the same time as shown in Figure 2-1.

Table 2-3 list of DNA primers for genotyping

Target	Primer	Type	Sequence (50´ -30´)	Annealing temp. (°C)	Molecular weight (bp)	Reaction product
AMPKα1	wild-type	Forward primer	AGCCGACTTTGGTAAAGGATG	62.9	6200	WT
		Reverse primer	CCCACTTTCCATTTTCTCCA	63.7	5917	
	knockout	Forward primer	GGGCTGCAGGAATTCGATATCAAGC	72.7	7731	KO
		Reverse primer	CCTTCCTGAAATGACTTCTG	58.9	6043	

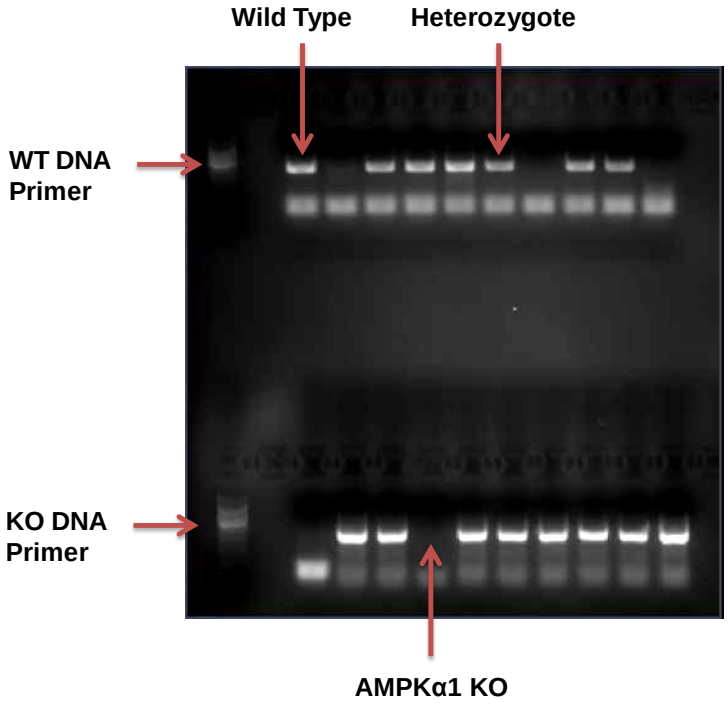

Figure 2-1 AMPK colony genotyping.

Gel electrophoresis of amplified PCR products from ear notches taken from mice. A 100 bp DNA ladder is shown on the left. The upper half of the agarose gel shows DNA products from PCR reactions using primers specific to WT alleles (normal gene). The lower half of the agarose gel shows DNA products from PCR reactions using primers specific to KO alleles (gene construct). Examples of WT, KO and heterozgote genotypes are indicated.

2.4 Histology

2.4.1 Sample Preparation and Fixation

Thoracic aortae were dissected from the both AMPKα1 knockout and S129 control mice and divided into four rings. Two aortic rings per mouse were freed of PVAT and any connective tissue and the remaining aortic rings had PVAT left intact. All were fixed in 10% acetic zinc formalin (Cell Path Ltd, UK) overnight. Tissues were processed through a gradient of ethanol solutions prior to Histoclear (a xylene substitute, Thermo Scientific, Loughborough, U.K.) with the terminal step into paraffin wax. Aortic ring processing was performed using a Citadel 1000 tissue processor (Thermo Shandon, Runcorn, U.K.). The sequence and the time of incubation is summarised in table 2-3.

Paraffin-embedded wire-injured carotid arteries produced by a previous study in our laboratory were utilised in the current research. Endothelial wire injury was performed by Marie-Ann Ewart. Briefly, mice were anesthetized and endothelial injury of the left common carotid artery was performed with flexible nylon wire introduced through the left external carotid artery. The endothelium was damaged by passing the wire through the lumen of the artery several times (Grassia et al., 2010). Right carotid artery was spared and used as a control for the experiment in both strains of mice. A week after wire injury, mice were sacrificed and carotid arteries with surrounding PVAT were dissected and processed as previously described.

Table 2-4 Sequence for processing samples for histological analysis

Solution	Length of incubation of sample
70 % (v/v) ethanol	15 minutes
85% (v/v) ethanol	15 minutes
90% (v/v) ethanol	25 minutes
100% (v/v) ethanol	25 minutes
100% (v/v) ethanol	15 minutes
100% (v/v) ethanol	15 minutes
100% (v/v) ethanol	15 minutes
Histoclear	30 minutes
Histoclear	30 minutes
Paraffin wax	30 minutes
Paraffin wax	30 minutes

2.4.2 Haematoxylin and Eosin staining

Haematoxylin and eosin (H&E) stain the nucleus and cytoplasm of cells respectively and were used to compare the gross histology of the perivascular adipose tissue around the aorta between WT and KO. Paraffin was removed from the cut sections by immersion in xylene and slides were rehydrated through an ethanol gradient of 100 % (v/v), followed by 90 % (v/v) and 70 % (v/v) ethanol for 5 minutes each and washed in running water for a further 5 minutes. Sections were then stained with Harris haematoxylin (Raymond A Lamb Ltd, Eastbourne, U.K.) for 4 minutes and washed in running water before being placed in acid alcohol (1 % v/v HCl in ethanol) for 30 seconds. Slides were washed in water for 1 minute, placed in 1 % (v/v) eosin (Raymond A Lamb Ltd, Eastbourne, UK) for 2 minutes before a further 5 minute wash in deionised water. Sections were then dehydrated by successive immersion in 70 % (v/v), 90 % (v/v) and 100 % (v/v) ethanol followed by 10 minutes in Histoclear (National diagnostic, Hessle Hull, UK). Finally, cover slips were fixed over the section using DPX mounting medium (BIOS Europe, Lancashire, U.K.). Nuclei appeared blue/purple whereas cytoplasm was stained pink/orange. Sections were photographed using AxioVision microscope software (Zeiss, Germany) and analysed with Image J computer software.

2.4.3 Immunohistochemistry

The following steps were adopted as a general protocol for immunohistochemical staining for each of the antibodies unless otherwise stated:

2.4.3.1 Antigen Retrieval

Paraffin was removed from the cut sections using xylene and rehydrated through an ethanol gradient of 100 % (v/v), followed by 90 % (v/v) and 70 % (v/v) ethanol for 5 minutes each and washed in running water. Heat-induced antigen retrieval was then performed with the sections incubated in 10 mM sodium citrate buffer (Tri-sodium citrate 2.94g, 0.05% Tween20, pH 6.0) and heated to 95-100 °C for 10 minutes in a microwave oven. Antigen retrieval was not required for MAC-2 immunostaining. Sections were then allowed to cool to room temperature over 20 minutes in order to minimise epitope refolding then placed under running tap water for 10 minutes.

2.4.3.2 Blocking of Endogenous Peroxidases

Endogenous peroxidase activity was blocked by incubation in 3 % (v/v) H_2O_2 in methanol for 20 minutes. Following this, sections were washed in running water for 10 minutes.

2.4.3.3 Blocking of nonspecific binding

Tissue sections were encircled using a Dako pen (Dako, Glostrup, Denmark) and incubated with 2.5 % (v/v) normal horse blocking serum from ImmPRESS REAGENT KIT (Vector, USA) in a humidified chamber for 1 hour at room temperature. For staining using anti-Mac 2 antibodies, blocking buffer was composed of phosphate buffered saline (PBS) supplemented with 0.05% (v/v) Tween20 and 20 % (v/v) normal rat serum since this was the species in which the secondary antibody was raised.

2.4.3.4 Primary and Secondary Antibody Incubation

The arterial sections were then incubated overnight with the primary antibody diluted in 1 % (w/v) BSA in PBS (Sigma Aldrich, Poole, U.K.) in a humidified chamber. A summary of the primary antibodies used along with dilutions and lengths of incubation are found in Table 2-4. A blank and negative control was carried out for each experiment using 1 % (w/v) BSA in PBS and rabbit IgG diluted in 1 % (w/v) BSA in PBS respectively.

Following this, sections were washed twice in Tris buffred saline with tween 20 (Tris base 3.03g, NaCl 8g, Tween20, 0.1% (v/v)) (TBS-T) for 15 minutes and incubated with ImmPRESS™ anti-rabbit Ig antibodies (Vector Laboratories, Peterborough, U.K.) for 1 hour in a humidified chamber at room temperature. The exception from this protocol was sections stained for phosphorylated and total AMPK. These sections were incubated with a biotinylated secondary antibody followed by treatment with streptavidin-peroxidase solution using the Histostain®-*Plus* Bulk kit (Life Technologies, Paisley, U.K.), both for 10 minutes at room temperature to improve the signal.

Table 2-5 Primary and Secondary antibodies for Immunohistochemistry

Primary Antibody	Supplier	Species & clonality	Dilution	IgG control	Secondary antibody	Dilution	Blocking serum
AMPKα	Abcam #ab131512	Rabbit polyclonal IgG	1:100	rabbit IgG Vector Labs (I-1000)	Biotinylated anti-rabbit Ig antibody Histostain®-*Plus* Bulk kit	#	Blocking Solution Ready-to-use Histostain®-*Plus* Bulk kit
Phospho AMPKα	Cell Signalling Technology #2535	Rabbit polyclonal IgG	1:100	rabbit IgG Vector Labs (I-1000)	Biotinylated anti-rabbit Ig antibody Histostain®-*Plus* Bulk kit	#	Blocking Solution Ready-to-use Histostain®-*Plus* Bulk kit
UCP1	Abcam #ab10983	Rabbit polyclonal IgG	1:500	rabbit IgG Vector Labs (I-1000)	ImmPRESS™ anti-rabbit Ig antibody	#	2.5 % (v/v) normal horse serum
Mac2	Cedarlane #CL8942AP	Rat Monoclonal IgG	1:5000	Rat IgG2a Pharmingen BD (559073)	Rabbit anti-rat Vector Labs (BA-4000)	1:200	Normal Rabbit Serum Vector Labs (S-5000)

Abbreviation: UCP1, Uncoupled protein 1; DFFA-like effector; Mac2, Galectin-3. (# = Ready to use).

2.4.3.5 Antibody Complex detection

To remove excess unbound secondary antibody, all sections were next washed twice in PBS-T for 15 minutes each. Then, sections were incubated with DAB chromagen solution (3,3-diaminobenzidine and hydrogen peroxidase solution, Vector Laboratories, Peterborough, U.K.) for immunoperoxidase staining for 2 to 5 minutes. Positive staining is indicated with the appearance of a dark brown colour. The reaction was stopped by washing the sections in water. Sections were then counterstained with haematoxylin to visualise the nucleus of the cells by incubation for 4 minutes followed by washing in warm water for 5 minutes to "blue" the nuclei. Finally, the sections were dehydrated in an ethanol gradient: 70 %, 90 % and 100 % (v/v) ethanol followed by 10 minutes in Histoclear. The sections were then mounted with coverslips using DPX mounting medium. Staining was visualised using a light microscope and positive immunostaining was seen as a brown/dark brown colour with nuclei appearing blue/purple. Sections were photographed using AxioVision microscope software (Zeiss, Germany).

2.5 Functional studies (wire myography)

2.5.1 Preparation of the vessels

Both AMPKα1 knockout and Sv129 control mice were sacrificed by cervical dislocation and the aortae were collected in oxygenated physiological Krebs-Henseleit buffer solution with the following composition (in mM): 118 mM NaCl, 4.7 mM KCl, 1.2 mM $MgSO_4$, 25 mM $NaHCO_3$, 1.03 mM KH_2PO_4, 11 mM glucose and 2.5 mM $CaCl_2$, PH 7.4. Paired

aortic arterial rings (1-2 mm long), one with PVAT intact (PVAT+) and the other with PVAT removed (PVAT-) (Figure 2-3), were prepared from each artery and for both strains of mouse. The intimal layer of the artery was removed by gently rubbing the vessel with the back of forceps to remove and eliminate the action of the endothelium in the response. The vessels were then mounted on two stainless steel pins in a four-channel small vessel wire myograph (Danish Myo Technology, Aarhus, Denmark), with one of the wires connected to a force transducer and the other to an adjustable arm. Vessels were incubated at 37 °C in Krebs-Henseleit buffer and gassed continuously with 95% O_2, 5 % CO_2. The artery segments were equilibrated for at least 30 minutes at resting tension. A predetermined optimum tension of 1 g was then applied to the artery for a further 30 minutes. Chart™ 5 Pro software (ADInstruments, Chalgrove, U.K.) was used to record and measure vessel responses to different reagents. At the beginning of each experiment, the arterial rings were challenged with two additions of 40 mM KCl (Ward et al., 2011) with washout in between at intervals of 30 minutes to establish the viability of the segments and also to sensitise the vessel before other pharmacological agents were added.

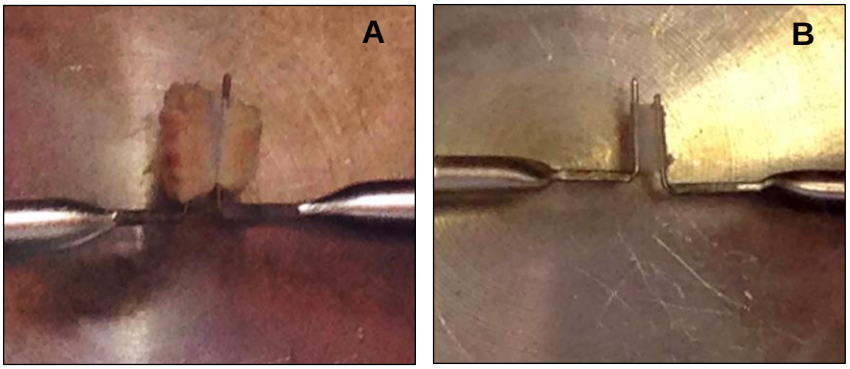

Figure 2-2 Representative pictures of mouse aortic artery mounted in the small vessel wire myograph.

Segments (2 mm) of vessel were mounted on two pins with one connected to a force transducer and a computer to record the changes in vessels tone of the mounted arteries. The other wire was connected to an adjustable jaw for the application of the desired tension on the vessel. (A) Thoracic aorta with intact PVAT (B) Thoracic aorta with PVAT removed.

2.5.2 Cumulative Dose response curve

After the vessels had been sensitised, they were pre-constricted with the thromboxane A_2 mimetic, 9,11-dideoxy-11α,9α-epoxymethanoprostaglandin $F_2α$ (U46619, Sigma-Aldrich, Poole, U.K.) at a concentration of $3x10^{-8}$ M. The absence of endothelium was confirmed by the absence of a relaxation response to acetylcholine (10^{-5} M) in pre-contracted rings.

Cumulative concentration-response curves to the AMPK activator AICAR (Toronto research chemicals, Canada) were performed by addition of AICAR in increasing concentrations from $1x10^{-4}$ M to $2x10^{-3}$ M at 10 minute intervals. Cumulative concentration-response curves to the K^+ channel opener cromakalim (Sigma-Aldrich, Poole, UK) were also constructed by addition of increasing concentrations from $1x10^{-9}$ to $1x10^{-6}$ at 10 minute intervals and the nitric oxide donor sodium nitroprusside (Sigma-Aldrich, Poole, UK) between $1x10^{-9}$ and $1x10^{-6}$ at 5 minute intervals, which acts directly on VSMCs (Schultz et al., 1977). Data were expressed as a percentage of loss in the vascular tone induced by U46619.

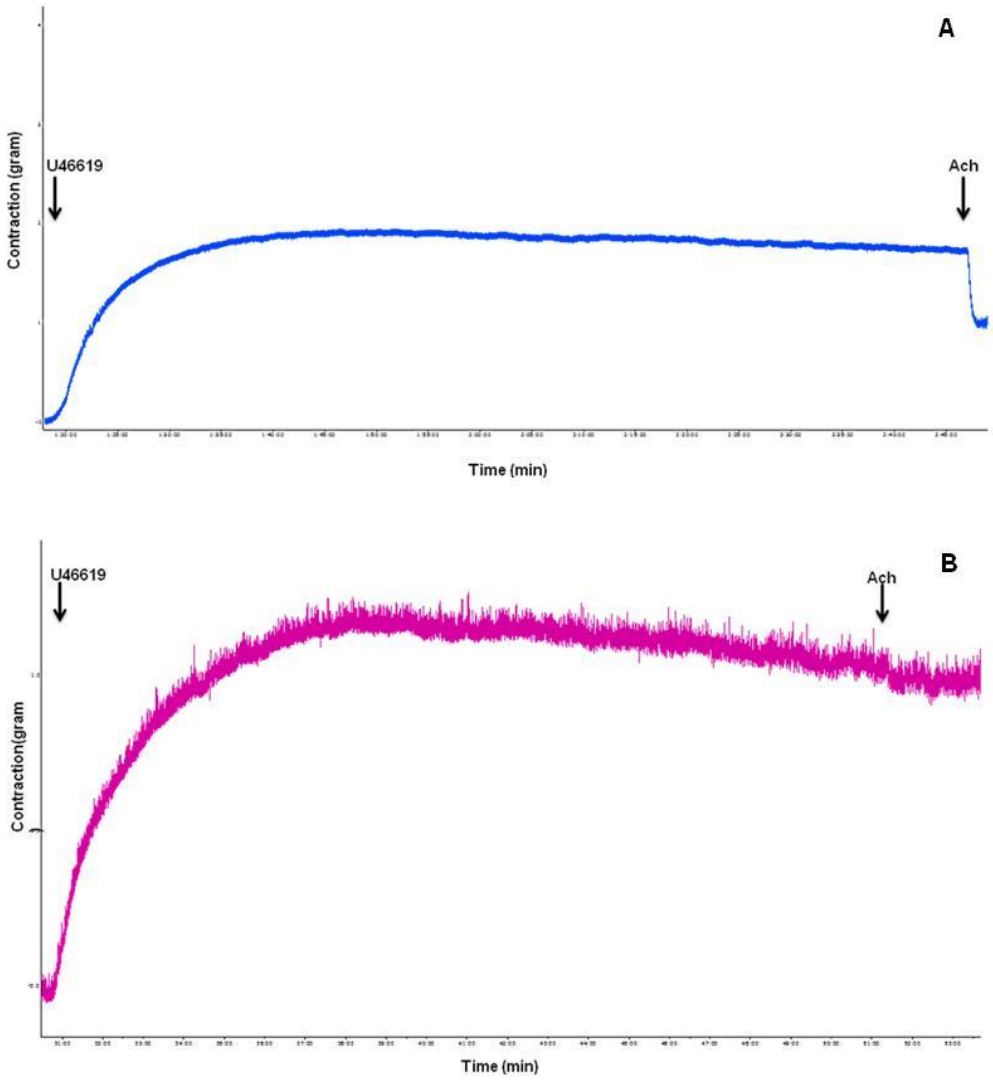

Figure 2-3 Representative force myograph traces showing isometric tension (g) plotted against time in mouse thoracic aorta rings.

(A)Represents a trace showing presence of intact endothelium demonstrated by a relaxation induced by 10^{-5} M acetylcholine. (B) Represents a trace showing absence of endothelium demonstrated by a lack of relaxation to acetylcholine.

2.5.3 PVAT releases bioactive molecules

To test the endocrine activity of the PVAT, PVAT was carefully dissected from both the thoracic aorta of wild type and AMPKα1 knockout mice. Once dissected, thoracic aortae devoid from PVAT were mounted in the wire myography and contracted to U46619. Dissected PVAT were then added to the myography chamber containing the vessels from which the PVAT had been dissected and then the dose response curve was constructed as previously described.

2.5.4 PVAT transfer experiment

To examine the ability of PVAT from mouse thoracic aorta to modify vascular tone, PVAT was carefully dissected and weighed. The isolated wild type PVAT was then transferred to the chamber containing AMPKα1 knockout thoracic aorta without PVAT and *vice versa* as shown in figure 2-4. After the equilibration and stabilization time both preparations were simultaneously contracted with U46619 and relaxed to cromakalim.

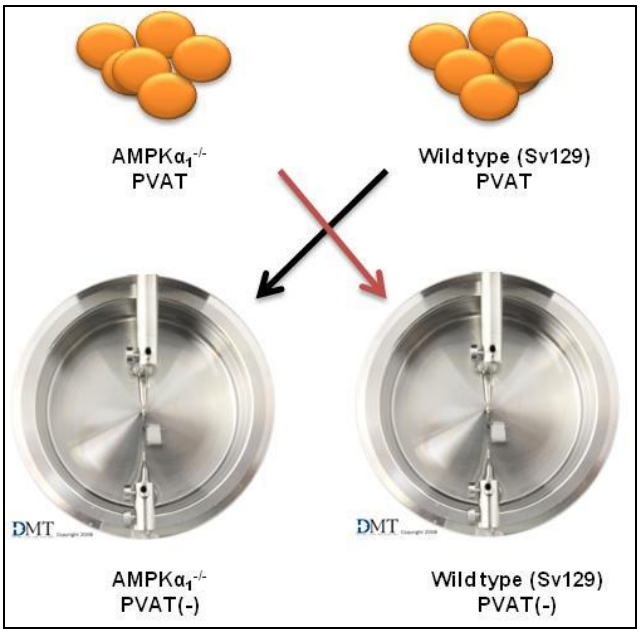

Figure 2-4 PVAT transfer experiment.

The figure illustrates a study protocol in which isolated wild type PVAT is transferred to AMPKα1 knockout arteries devoid of PVAT and *vice versa*.

2.5.5 Bioassay Experiment (Conditioned Media)

To examine the paracrine function of the PVAT, bioassay experiments using conditioned media were carried out. In these experiments, PVAT from wild type mice was used to

produce conditioned media and this was added to PVAT− rings without endothelium. The same procedure was applied to the AMPKα1 knockout vessels. The conditioned media was prepared as following: PVAT from both mouse strains was carefully dissected and weighed. The dissected samples were then incubated in warm Krebs' solution at 37 ˚C for one hour. The conditioned medium was transferred to the recipient chamber containing the vessels lacking PVAT. After equilibration and stabilization, aortic rings were successively contracted with U46619 and relaxed to cromakalim. At the end of every experiment, the conditioned media from both mouse strains was collected and stored at -80˚C to be used for further studies.

2.5.6 Effect of adiponectin on vascular relaxation

To test whether adiponectin is a potential PVAT-derived vasodilator, adiponectin blocking peptide against adiponectin receptor 1 (AdipoR1) (GeneTex, U.K.) (5µg/ml) was added to preconstricted vessels with and without PVAT. The response to exogenously applied globular adiponectin (1µg/ml) (Enzo Life Sciences Ltd, U.K.) was also assessed in arteries prior to contracting the arteries with U46619. Prior to application, globular adiponectin was diluted in sterile water containing 1% bovine serum albumin (BSA) which acts as carrier protein.

2.6 Secretory function investigation

Two methods were used to define the difference in secretory profile of PVAT from wild type and AMPKα1 knockout mice, described below:

2.6.1 Mouse Adipokine Array (Proteome Profiler)

The release of adipokines was assessed using a commercial adipokine array (ARY-013, R&D systems, Minneapolis, MN). The proteome profiler adipokine array is able to detect 38 adipokines in duplicates that are captured on nitrocellulose membranes (Figure 2.5), with the manufacturer's protocol summarised below.

2.6.1.1 Preparation of tissue lysates

Thoracic aorta PVAT from both wild type and AMPKα1 deficient mice was dissected, snap frozen and stored at -80˚C until use. PVAT was pulverised in liquid nitrogen using a mortar and pestle into a fine powder and re-suspended in ice-cold lysis buffer which consists of cell extraction buffer (Invitrogen, CA), supplemented with 1mM of protease

inhibitor cocktail (Sigma Aldrich, U.K.), 1mM phenylmethylsulfonyl fluoride (PMSF) and 1mM dithiothreitol (DTT) (Sigma Aldrich, U.K.). Lysate samples were transferred into ice-cold centrifuge tubes and stored at -80°C until use.

2.6.1.2 Protein concentration estimation

PVAT lysates, aortae were centrifuged at 8000 rpm for 10 minutes in a Pico 17 Thermo Scientific Heraeus bench-top centrifuge (Fisher Scientific, Loughborough, U.K.). Supernatants were transferred to fresh ice-cold microcentrifuge tubes. Standard dilutions of bovine serum albumin (BSA) ranging from 0.1 mg/ml to 1mg/ml were used to generate a standard protein curve with distilled water as a blank. Protein samples from VSMCs and aortic PVAT were diluted in distilled water at a ratio of 5:1. Each sample (10 µl) and standards were added in triplicate to a 96 well plate followed by 100 µl DC™ Protein Assay Reagent (Bio-Rad Laboratories Ltd, Herts, UK). Absorbance was read at 595 nm using a FLUOstar OPTIMA microplate reader (BMG Labtech, Germany). The mean absorbance from each sample was generated in triplicate and the protein concentration was determined by comparison with the BSA standard curve.

2.6.1.3 Array procedure

Adipokine expression profiling was performed using an Adipokine proteome profiler, following the protocol provided by the manufacturer. In summary, membranes were blocked with a blocking buffer, and then 1 ml of pooled samples from PVAT and conditioned medium were incubated with a cocktail of biotinylated detection antibodies and incubated at 4°C overnight with the membranes. Membranes were washed with washing buffer. The membranes were then incubated with 2 ml of horseradish peroxidase–conjugated streptavidin at room temperature for 30 min and the presence of adipokines was detected by chemiluminescence. The resultant film images were scanned with a densitometer and converted to densitometric units using Quantity One software (Bio-Rad Laboratories, Hercules, CA, USA). Data were analysed according to recommendations from R&D Systems. Data were imported into an Excel spreadsheet and normalized against an internal control, and final values were calculated and analysed via Graphpad Prism. Two arrays for each group, making a total of 4 independent arrays were analysed. The data presented represents the average of the four arrays over the two groups.

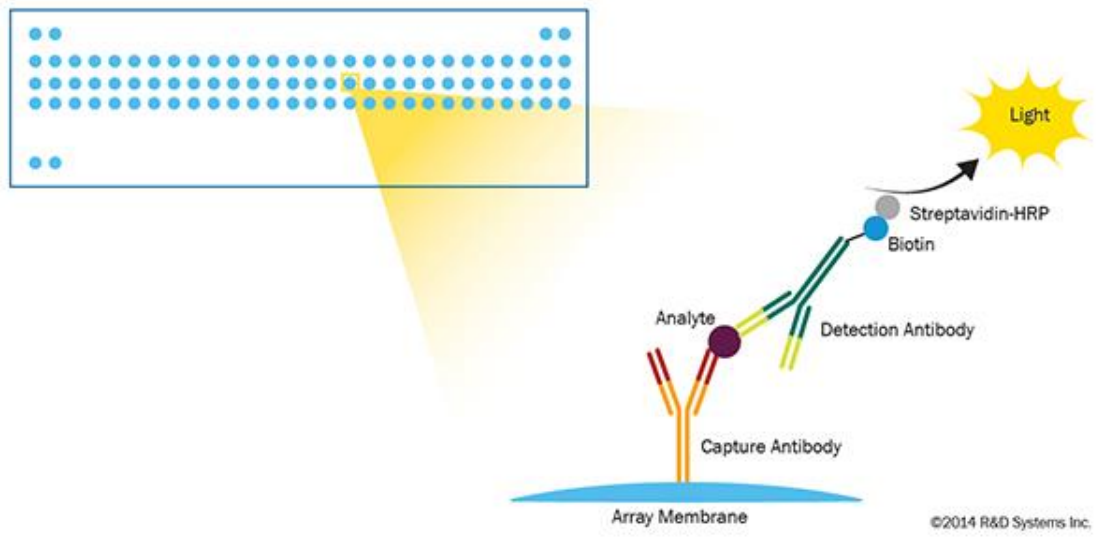

Figure 2-5 Proteome Profiler Array Assay Principle.

Capture adipocytokines antibodies have been spotted in duplicate on nitrocellulose membranes. Tissue lysates and conditioned media are diluted and mixed with a cocktail of biotinylated detection antibodies. The sample/antibody mixture is then incubated with the array over night. Any cytokine/detection antibody complex present is bound by its cognate immobilized capture antibody on the membrane. Streptavidin-Horseradish Peroxidase and chemiluminescent detection reagents are added. The produced signal is in proportion to the amount of adipocytokine present in the samples. Chemiluminescence detected is treated as a Western blot (Finkel et al., 2014).

2.6.2 Adiponectin ELISA

Adiponectin concentration was determined using a mouse adiponectin/Acrp30 Quantikine ELISA Kit (MRP300, R&D systems, Minneapolis, MN), designed to measure full-length mouse adiponectin concentrations.

Samples of PVAT and conditioned media were prepared and protein concentration in the samples was estimated using the method described in section 2.6.1.2. Following the protocol provided by the vendor, the adiponectin concentration in the sample was determined. Briefly, 50 µl of assay diluent was added to each well in the microplate. Standard, PVAT lysate or conditioned media (50 µl) was then added to each well. The plate was then sealed and incubated at room temperature for 3 hours. After incubation, each well was aspirated and washed. Adiponectin antibody conjugate (100µl) was added, covered, and then incubated for 1hour at room temperature. Substrate solution (100 µl) was added and incubated at room temperature for 30 minutes away from light. Addition of 100 µl of stop solution to each well resulted in the development of a yellow colour which indicates presence of the target protein. The absorbance of the ELISA plate at 450 nm was determined within 30 minutes with a wavelength correction set to 540 nm or 570 nm using

a FLUOstar OPTIMA microplate reader (BMG Labtech, Germany). The mean absorbance from each sample was generated in duplicate and the protein concentration was determined by comparison with the standard curve.

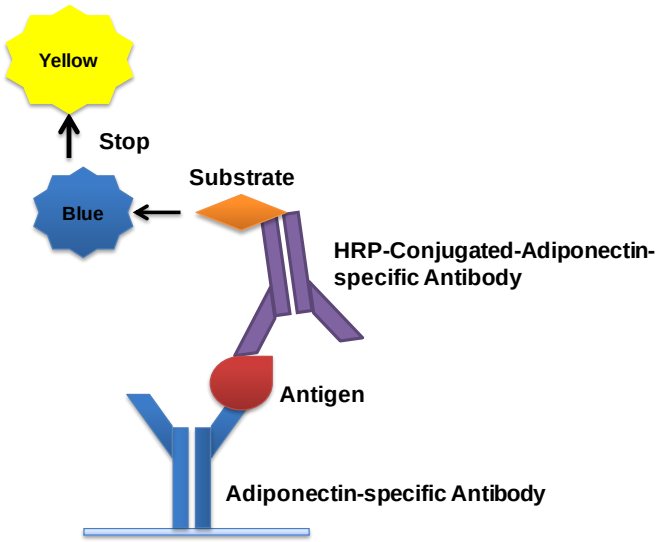

Figure 2-6 Principle of Adiponectin ELISA.

Uses a capture antibody and enzyme-linked (HRP) detection antibody to measure adiponectin concentration in CM.

2.7 AMPK activity determination

2.7.1 Vascular smooth muscle cell (VSMC) culture

As a general rule, tissue culture was performed in sterile conditions in a biological safety class II vertical laminar flow cabinet. Tissue explants from experimental animals (see details in 2.7.1) were used as the source of material and cells were cultured at 37°C in an atmosphere of 5 % (v/v) CO_2 and 95 % (v/v) air.

Wistar Kyoto rat-derived VSMCs were supplied by Dr Augusto Montezano (Institute of Cardiovascular & Medical Sciences, University of Glasgow). VSMCs were maintained in Dulbecco's modified Eagle medium (DMEM) (Gibco®-Life technologies, U.K.) supplemented with 10% fetal bovine serum (FBS) (Invitrogen, U.K.) and pencillin/ streptomycin antibiotic combination (Sigma Aldrich, U.K.) and used for experiments at passage 4 to 5. Before each experiment, medium was discarded and cells were washed with PBS and incubated in serum-free medium for 2 hours.

2.7.1.1 Treatment of VSMCs

Cells were incubated with AICAR (10^{-2}-10^{-3}M) or cromakalim (10^{-8}-10^{-6}M) for 45 minutes. Medium was removed and 200µl of lysis buffer added into each well of a 6-well plate. Cell lysates were then scraped and transferred to microcentrifuge tubes. Lysates were incubated on ice for 30 minutes and then centrifuged at 8000 rpm for 10 minutes. Supernatants were collected and stored at -80℃ prior to use.

2.7.2 3T3-L1 adipocytes cell culture

Preadipocytes were maintained as fibroblasts (American Type Culture Collection, Manassas, USA) (passage 2-12) in DMEM supplemented with 10% (v/v) fetal bovine serum and 100 U/ml (v/v) penicillin and streptomycin. Cells were incubated at 37°C in a humidified atmosphere of 10% (v/v) CO_2 and the media was replaced every 48 h.

2.7.2.1 3T3-L1 differentiation protocol

To differentiate 3T3-L1 fibroblasts into adipocytes, fibroblasts were grown to 70-80% confluent in DMEM containing 10% (v/v) FBS, 100 U/ml penicillin and 100 µg/ml streptomycin. At 48 hr post-confluence, cell medium was aspirated and replaced with differentiation medium consisting of DMEM containing 10% (v/v) FBS, 0.25 µM dexamethasone (Sigma-Aldrich Ltd, Gillingham, Dorset, UK), 0.5 mM 3-isobutyl-1-methylxanthine (IBMX) (Sigma-Aldrich Ltd, Gillingham, Dorset, UK), 5 µM troglitazone (Tocris Bioscience, Bristol, UK) and 1 µg/ml insulin. After 72 hour, this medium was changed with DMEM containing 10% (v/v) FCS, 5 µM troglitazone and 1 µg/ml insulin. The cells were incubated in this medium for three days before the medium was aspirated and replaced with DMEM containing 10% (v/v) FBS, in which the cells were then maintained. At 8-12 days post-induction of differentiation, cells were used for experimentation.

2.7.2.2 Treatment of differentiated 3T3-L1

Over a time course of 10 min and 30 min, 3T3-L1 were incubated with AICAR (2mM) alone, AICAR (2mM) + cromakalim (200µM) and cromakalim (200µM) alone. Medium was removed and 200µl of lysis buffer added into each well of a 6-well plate. Cell lysates were then scraped and transferred to microcentrifuge tubes. Lysates were incubated on ice for 30 minutes and then centrifuged at 8000 rpm for 10 minutes. Supernatants were collected and stored at -80℃ prior to use.

2.7.3 Western blotting

Sodium dodecyl sulphate polyacrylamide gel electrophoresis (SDS PAGE) and immunoblotting were conducted using a Novex® NuPAGE® gel electrophoresis system (Life Technologies, Paisley, U.K.), using the procedure described in the following sections.

2.7.3.1 Preparation of the tissue lysates

The full description of preparation of samples homogenate was discussed in detail in elsewhere (2.5.1.1).

2.7.3.2 SDS PAGE

Prior to protein loading, prepared protein samples were mixed with 7.5 µl of DTT and 12.5 µl of NuPAGE® LDS sample buffer as a load dye, to a total volume of 50 µl and heated at 70°C for 10 mins. Samples (10 µg) were then loaded on NuPAGE® Novex® 4-12 % Bis-Tris mini gels (1.0 mm thick, 10 or 12 wells) with 10 µl Novex® sharp pre-stained protein standards in one lane. Gels were resolved for approximately 45 minutes in NuPAGE® MOPS SDS running buffer at 200V until the dye front reaches the bottom of the gel. At this stage, gel running was stopped and proteins were transferred onto a nitrocellulose membrane (Thermo scientific, Germany) at 30 V for 90 min in NuPAGE® transfer buffer containing 10 % (v/v) methanol.

2.7.3.3 Immunoblotting

Once the transfer of protein was complete, the nitrocellulose membranes were blocked for 1 hour in 5 % (w/v) milk powder (Marvel) prepared in Tris-buffered saline (20mM Tris 3.03g, 137mM NaCl 8g, PH 7.4) containing 0.1% (v/v) Tween-20 (TBST) at room temperature with continuous shaking. Membranes were then rinsed in TBST and incubated with primary antibody overnight at 4°C in 50% (v/v) TBS, 50% (v/v) Odyssey®-Block (LI-COR, USA). Membranes were then washed in TBST and incubated for 2 hours at room temperature with IRDye® 800CW Donkey anti-Rabbit IgG antibodies (Li-COR, USA) diluted in the same way as the primary antibody. Membranes were then washed in TBST prior to visualisation of immunolabelled bands using an Odyssey Sa Infrared Imaging System (LI-COR, USA) linked with Odyssey Sa Infrared Imaging System software (LI-COR, USA). A summary of the primary and secondary antibodies used along with dilutions are presented in Table 2-5.

Table 2-6 Summary of antibodies and dilutions used for immunoblotting

Epitope	Molecular weight	Host Species	Dilution	Secondary antibody dilution	Manufacturer and product number
AMPKα	62kDa	Rabbit	1:1000	1:5000	Cell Signalling Technology #2603
Phospho-AMPKα (Thr172)	62kDa	Rabbit	1:1000	1:5000	Cell Signalling Technology #2535
ACC	280kDa	Rabbit	1:1000	1:5000	Cell Signalling Technology #3676
Phospho-ACC (Ser79)	280kDa	Rabbit	1:1000	1:5000	Cell Signalling Technology #3661
AMPKα1	62kDa	Human	1:1000	1:5000	Abcam Ab110036
AMPKα2	62kDa	Sheep	1:1000	1:5000	A generous gift from Prof. D.G. Hardie, University of Dundee, Dundee, UK. (Woods et al., 1996)
eNOS (1177)	140kDa	Mouse	1:1000	1:5000	BD Transduction Laboratories™ #612392
Phospho-eNOS (1177)	140kDa	Rabbit	1:1000	1:5000	Cell Signalling Technology #9571
UCP1	32kDa	Rabbit	1:1000	1:5000	Abcam #ab10983
GAPDH	37kDa	Rabbit	1:2000	1:5000	Thermoscientific #PA1-988

Primary and secondary antibodies were diluted in a mixture of 50% TBST and 50 % Odyssey® (TBS) (LI-COR, USA) incubated at 4 °C overnight and at room temperature for 2 hours respectively. IRDye® 800CW Donkey anti-Rabbit and Donkey anti-sheep IgG (Li-COR, USA) was used secondary antibody.

2.7.4 PathScan® Intracellular Signalling Array Kit (Fluorescent Readout)

The effect of CM and adiponectin on AMPK activity on VSMCs, an Intracellular Signalling Array Kit (Cell Signalling Technology, U.K.) was used. The PathScan Intracellular Signalling Array is a slide based antibody which allows simultaneous detection of 18 important and well-characterized signaling molecules when phosphorylated. Following the protocol provided by the manufacturer.

2.7.4.1 Preparation of the samples

VSMCs were incubated with globular adiponectin (1µg/ml) and (100 ng/ml), WT CM (1ml) and KO CM (1ml). Untreated VSMCs were used as control for the current

experiment. Medium was removed and lysis buffer added into each well of a 6-well plate. Lysates were incubated on ice for 30 minutes and then centrifuged at maximum speed at 4℃ for 15 minutes. Supernatants were collected and stored at -80℃ prior to use.

2.7.4.2 Assay Procedure

Following manufacturer's protocol, the glass slides were blocked with a blocking buffer for 15 min and 75 µl diluted lysate (1mg/ml) added to each well and covered with sealing tape and incubated for 2 hours at room temperature over orbital shaker. Slides were then washed 4x5 min using washing buffer provided in the kit. Detection antibody cocktail was then added to each well and covered with sealing tape and incubated for 1 hour at room temperature on an orbital shaker. After that, slides were washed again using array wash buffer 4x5 min and incubated with DyLight 680™-linked streptavidin for 30 min away from the light. Following this, slides washed once for 10 second using deionised water and left to dry completely. Images of slides were captured using visualised using the LI-COR Odyssey® SA system. The intensity of each spot was calculated using ImageJ software. Data were imported into an Excel spreadsheet and normalized against an internal control, and final values were calculated and analysed via Graphpad Prism.

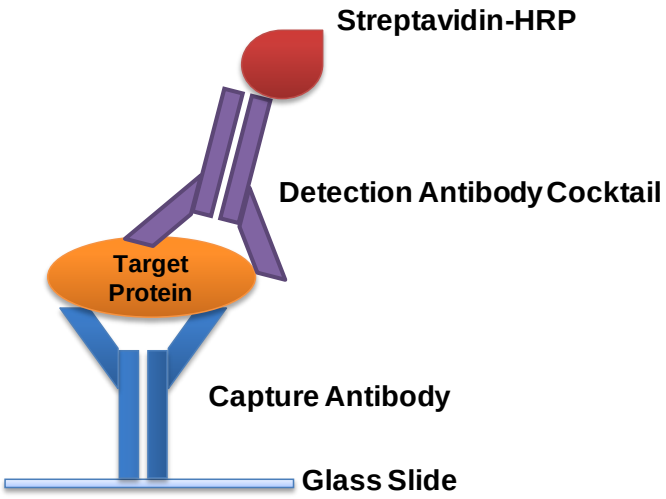

Figure 2-7 The PathScan Intracellular Signalling Array reaction.

Capture antibodies have been spotted in duplicate on glass slide. Blocking buffer was added to the slide. The sample is then incubated with the array over for 2 hour. Any activated signalling molecule present is bound by its cognate immobilized capture antibody on the slide. Detection antibody cocktail will bound to target protein-antibody complex. Streptavidin-Horseradish Peroxidase was added. The produced signal is in proportion to the amount of activated signalling molecule present in the samples.

2.7.5 Quantification of expression of protein

The relative expression of the protein of interest was determined using ImageJ software (version 1.47). The housekeeping protein, glyceraldehyde-3-phosphate dehydrogenase (GAPDH) was used as a protein loading control. Therefore, data were expressed as a ratio of protein of interest to the loading control or as a ratio of phosphorylated to the total amount of target protein present in the sample.

2.8 Determination of superoxide and nitric oxide availability

2.8.1 Preparation of the PVAT samples

For the detection of nitric oxide and superoxide, segments of aortic PVAT samples were was stabilised in Krebs' Henseleit buffer (118 mM NaCl, 4.7 mM KCl, 1.2 mM $MgSO_4$, 25 mM KH_2PO_4, 11 mM glucose and 2.5 mM $CaCl_2$) (KH) at 37°C for 30 minutes and incubated with dyes designed to detect the species of interest as described in 2.9.2 and 2.9.3.

2.8.2 Detection of superoxide

Dihydroethidium (DHE) was used to assess superoxide levels. DHE is oxidised by $O_2^{\cdot-}$ in the cytosol to form the fluorescent product oxyethidium (Zhao et al., 2003). Once prepared, segments were incubated with 10^{-5} M DHE for 30 minutes at 37°C in the dark and then washed (2 x 15 min) in KH at 37°C. Negative controls were incubated with 15 U/mL of superoxide dismutase (SOD) during exposure to DHE. Segments were fixed by immersion in acetic zinc formalin for 1 hour at room temperature, mounted on slides and visualised by confocal fluorescence microscopy, using the 488 argon line for excitation and 570 nm long-pass filter for detection. Data from 5 Kalman-averaged scans were collected using LaserSharp 2000 software (BioRad, UK) using set, tissue specific values of laser intensity, brightness and contrast, and the 20 X oil objective without zoom. The mean fluorescence intensity of each image was quantified using ImageJ software.

2.8.3 Detection of Nitric oxide

To assess NO production by PVAT, 4,5-diaminofluorescein diacetate (DAF- 2DA) was used. DAF-2DA is hydrolysed by cellular esterases to form 4,5-diaminofluorescein (DAF-2) which subsequently reacts with cellular NO to form fluorescent triazolofluorescein

(Broillet et al., 2001). The preparation of sample was described in the previous section. PVAT samples were incubated in 10 μM DAF-2DA for 30 minutes. 0.1 mM Nω-nitro-L-Arginine (L-NNA) and 15 U/L SOD were used also as negative and positive controls respectively. After fixation, samples were incubated in 1 μM SYTO 61 fluorescent nucleic acid stain (Thermo Fisher Scientific, U.K.) for 1 hour prior to mounting and confocal microscopy examination. DAF-2DA fluorescence was detected using the 488 nm argon line for excitation and 530 +/-30 nm filter for detection. Fluorescence from SYTO 61, detected using the 637 nm laser diode and 660 nm long pass filter, was used to aid image collection.

2.9 Statistical analysis

All results are expressed as mean ± standard error of the mean (SEM) where n represents the number of experiments performed or number of mice used. Data were analysed with GraphPad Prism 5.0 software (California, U.S.A.). When comparing three or more data groups, One-way ANOVA (analysis of variance) tests followed by Bonferroni post-hoc tests were used. When comparing two or more data groups (contraction data), two-way ANOVA (analysis of variance) tests followed by Newman–Keuls post hoc test was used. In all cases, a p value of less than 0.05 was considered statistically significant.

Chapter 3

Characterisation of the role of AMPKα1 in modulating PVAT function

3.1 Introduction

Perivascular adipose tissue (PVAT) which surrounds most arteries is now recognized as a major regulator of vascular tone. PVAT acts as an active endocrine organ producing a range of adipokines, inflammatory cytokines and other factors which influence vascular tone (Dubrovska et al., 2004, Gao, 2007, Malinowski et al., 2008, Weston et al., 2013). PVAT can induce vasodilatation via release of vasodilatory molecules such as adipocyte-derived relaxing factor (ADRF) (Lohn et al., 2002, Verlohren et al., 2004, Galvez et al., 2006), leptin (Vecchione et al., 2002), adiponectin (Fesus et al., 2007, Chen et al., 2003), angiotensin 1–7 (Ang 1-7) (Lee et al., 2009a), hydrogen peroxide (Gao et al., 2007), nitric oxide (NO) (Gil-Ortega et al., 2010) and hydrogen sulphide (H_2S) (Fang et al., 2009). In addition to vasodilatory factors, PVAT can release vasoconstrictor factors such as angiotensin II (Ang II) (Galvez-Prieto et al., 2008) and superoxide anion (Gao et al., 2006). PVAT is composed of brown adipocytes, white adipocytes or both depending on the vascular bed (Gao, 2007, Fitzgibbons et al., 2011, Cinti, 2011). While all PVAT types have anticontractile properties (Lohn et al., 2002, Greenstein et al., 2009), the mechanism(s) by which this occurs remains uncertain.

The anti-contractile effect of PVAT is proposed to be due to the release of an as yet undefined PVAT-derived relaxing factor(s) that are proposed to act via different pathways. These pathways are reported to include gated potassium (K) channels including the adenosine triphosphate (ATP) activated potassium channels (K_{ATP}) (Dubrovska et al., 2004), the voltage-gated (K_V) (Verlohren et al., 2004) and large conductance calcium-activated potassium channels (BK_{Ca}) (Lynch et al., 2013). Gao and co-workers demonstrated that PVAT exerts its anti-contractile effects in rat aortic vessels through two distinct mechanisms: (1) by releasing a transferable relaxing factor which induces endothelium-dependent relaxation through NO release and subsequent K_{Ca} channel activation, and (2) by an endothelium-independent mechanism involving H_2O_2 and subsequent activation of sGC in vascular smooth muscle (Gao et al., 2007).

AMP-activated protein kinase (AMPK) is now considered as a potential modulator of vascular function. Although recognized primarily as a cellular energy gauge and modulator of cellular metabolism (Hardie et al., 2003), the identification of its expression in vascular tissue and of its ability to respond to cellular energy state (Chen et al., 1999, Fleming et al., 2005, Evans et al., 2005), hormonal changes (Cheng et al., 2007, Chen et al., 2003, Nagata et al., 2004), and drugs (Thors et al., 2004, Levine et al., 2007, Bilodeau-Goeseels et al.,

2011, Ford et al., 2012) demonstrates an important role for AMPK in the regulation of vascular tone. Many studies have shown that activated endothelial AMPK enhances phosphorylation and activation of endothelial nitric oxide (NO) synthase (eNOS) at Ser^{1177} (Chen et al., 2003, Morrow et al., 2003, Davis et al., 2006) and Ser633 (Chen et al., 2009) to increase NO availability and vascular relaxation (Chen et al., 2003, Morrow et al., 2003, Davis et al., 2006). In addition, the role of AMPK in endothelium-independent relaxation has been demonstrated in many vascular beds including porcine, mouse, and rat conduit arteries in response to AMPK activators such as hypoxia (Rubin et al., 2005), 5-aminoimidazole-4-carboxamide 1-β-D-ribofuranoside (AICAR) (Goirand et al., 2007), and metformin (Majithiya and Balaraman, 2006). Furthermore AMPK activation has been documented to directly regulate myosin light-chain kinase (MLCK) leading to reduced sensitivity to intracellular calcium and induction of vascular relaxation (Horman et al., 2008). Collectively, these findings suggest that AMPK may modulate vascular tone via both endothelium-dependent and -independent mechanisms.

AMPK is expressed in the three layers of the blood vessel: the endothelium, smooth muscle (VSM), and perivascular adipose tissue (PVAT) (Ewart and Kennedy, 2011) and is known to induce vasodilatation by both endothelium-dependent and -independent mechanisms. Although it is known that AMPK can modulate VSM and endothelial function, it is unknown whether AMPK can modulate the anti-contractile effect of PVAT. Therefore, the hypothesis of the current study is that AMPK can act as switch which modulates the releasing profile of the PVAT to control vascular contractility.

3.2 Aims of the study

- To investigate the morphological features of aortic and mesenteric PVAT in normal mice and mice with a global knockout of the AMPKα1 subunit.

- To investigate whether there is any functional difference between PVAT of normal mice and AMPKα1 knockout mice.

3.3 Methods and Results

3.3.1 Morphology of the PVAT

To test the effect of AMPKα1 subunit deletion on the morphological features of the PVAT, haematoxylin and eosin-stained sections of PVAT, BAT and WAT from wild type (WT)

and AMPKα1 Knockout (KO) mice were examined. Thoracic arteries with intact PVAT were excised immediately and placed in 10% zinc formalin overnight. Arteries were processed through a gradient of alcohols to Histoclear and embedded vertically in paraffin wax before being cut into 5 μm sections. To compare the morphology of aortic PVAT with other fat depots, mesenteric PVAT, subscapular brown adipose tissue (BAT) and epididymal white adipose tissue (WAT) were also fixed and sectioned. H&E staining and immunohistochemical staining with anti-UCP-1 antibody was performed and sections were visualised under a microscope. There was no obvious difference in adipose tissue composition (Figure 3-1), whereby thoracic PVAT (E&F) appeared very similar to BAT (A&B), with round nuclei, and small, multilocular lipid droplets, whereas mesenteric PVAT (I&J) was very similar to WAT (B&D), with large single lipid vacuoles and marginal nucleus. Abdominal PVAT (F&G) showed features of both BAT and WAT in WT and KO (Figure 3-1).

Immunohistochemical staining of the BAT marker uncoupling protein-1 (UCP-1) (Figure 3-2) confirmed the results of H&E staining. The Intensity of UCP-1 staining was similar in adipose tissue depots including PVAT from WT and KO animals. Thoracic PVAT (Figure 3-2 E&F) from both strains of animal exhibited relatively the same distribution of UCP-1 in the BAT (Figure 3-2 A&B). The intensity of UCP-1 staining in the mesenteric PVAT (Figure 3-2 I&J) was very low regardless of AMPKα1 subunit deletion, likely due to the predominance of WAT in this depot (Figure 3-2 C&D). Abdominal aortic PVAT in both mouse strains showed similar distribution of both BAT and WAT as assessed by UCP-1 staining (Figure 3-2 G&H).

Next, UCP-1 levels were studied in PVAT and compared to that found in BAT (intrascapular area) and WAT (epididymal) from both WT and KO mice by immunoblotting. Quantitative analysis showed that PVAT shares a similar protein expression pattern with BAT, which includes high levels of UCP-1 (Figure 3-2) relative to the glycolytic protein GAPDH, regardless of AMPK deletion. These data indicate that thoracic PVAT has a similar phenotype to BAT, but is clearly different from WAT, suggesting that PVAT might have a similar function to BAT. Abdominal aorta showed no marked difference compared to thoracic PVAT. In contrast to these virtually identical protein levels between thoracic PVAT and BAT, mesenteric PVAT exhibited a similar phenotype to WAT.

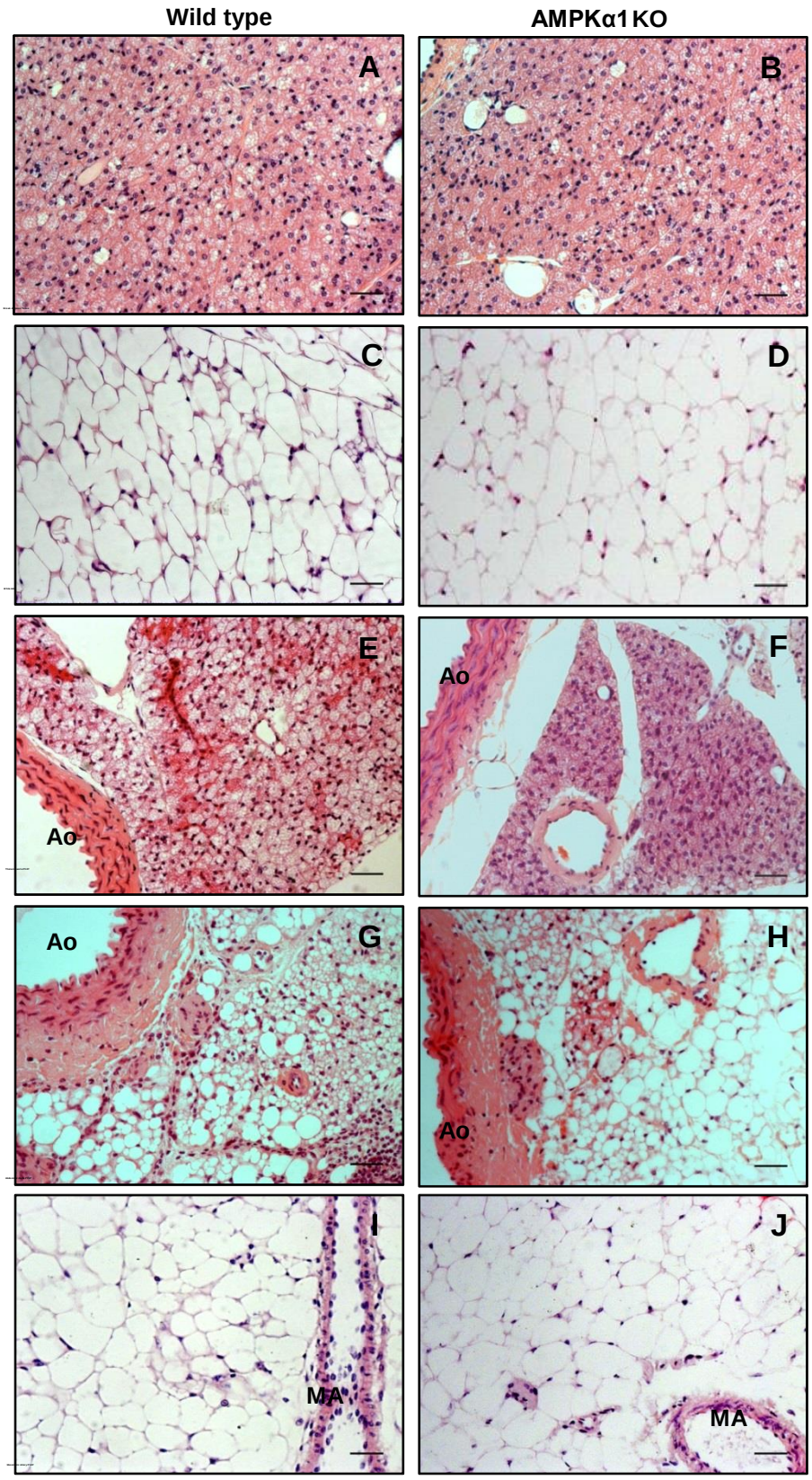

Figure 3-1 Effect of AMPKα1 deletion on the morphology of PVAT.

Representative H&E stained sections harvested from subscapular brown adipose tissue (BAT) (A&B), epididymal white adipose tissue (WAT) (C&D), thoracic perivascular adipose tissue (PVAT) (E&F), abdominal PVAT (G&H), and mesenteric PVAT (I&J) in wild type and AMPKα1 knockout mice. Nuclei appear blue/purple whereas cytoplasm is stained pink. Abbreviation: BAT; brown adipose tissue, WAT; white adipose tissue, Ao; aorta, MA; mesenteric artery. Scale bar; 20 μm,

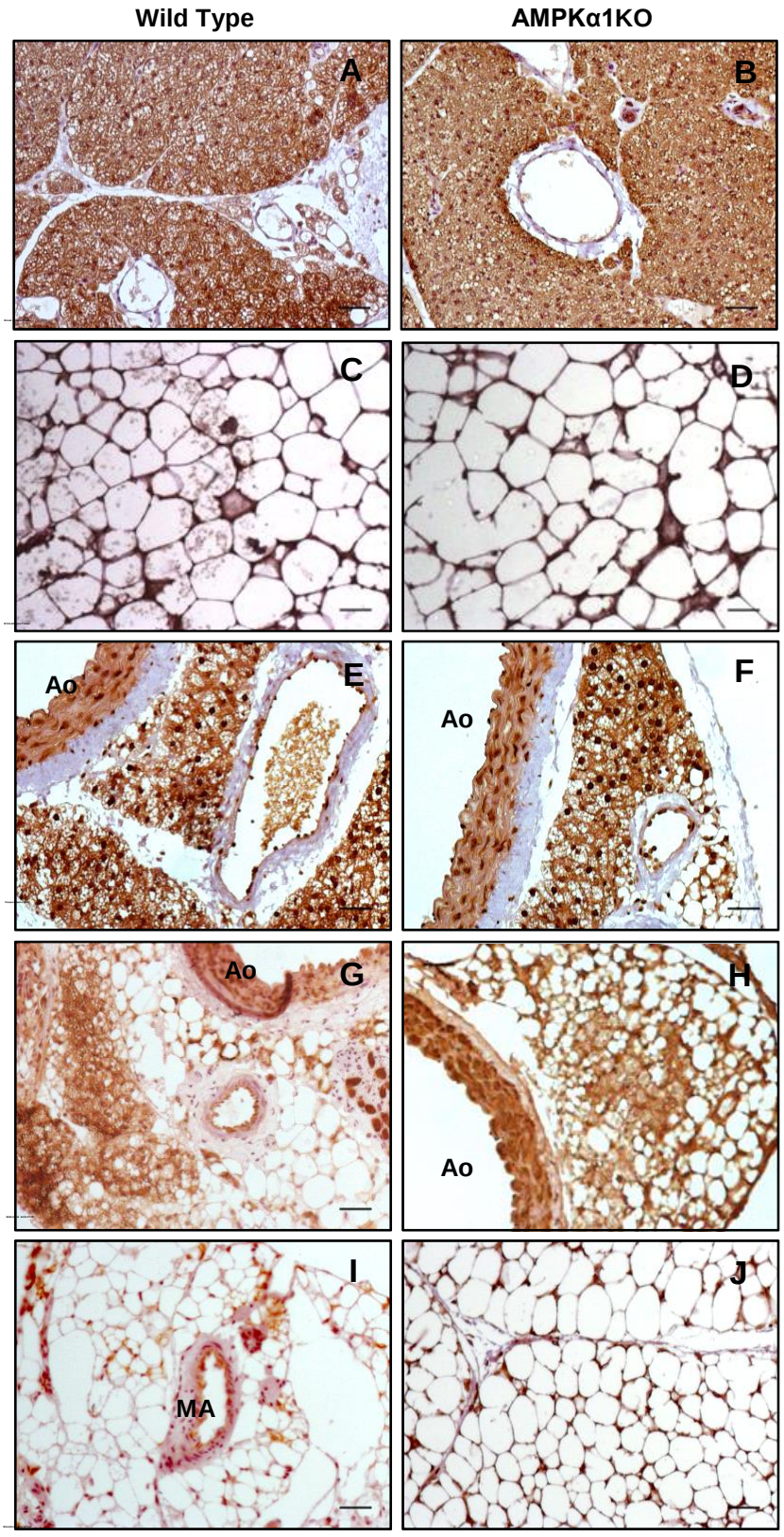

Figure 3-2 Immunohistochemical analysis of UCP-1 levels in PVAT in comparison with BAT and WAT for both wild type and AMPKα1 knockout mice.

Representative histological sections of brown adipose tissue (BAT) (A&B), white adipose tissue (WAT) (C&D), thoracic PVAT (E&F), Abdominal (G&H) and Mesenteric PVAT (I&J) stained with anti UCP-1 and counterstained with haematoxylin. Positive immunoreactivity for UCP-1 is indicated by brown colour. Scale bar 20 μm

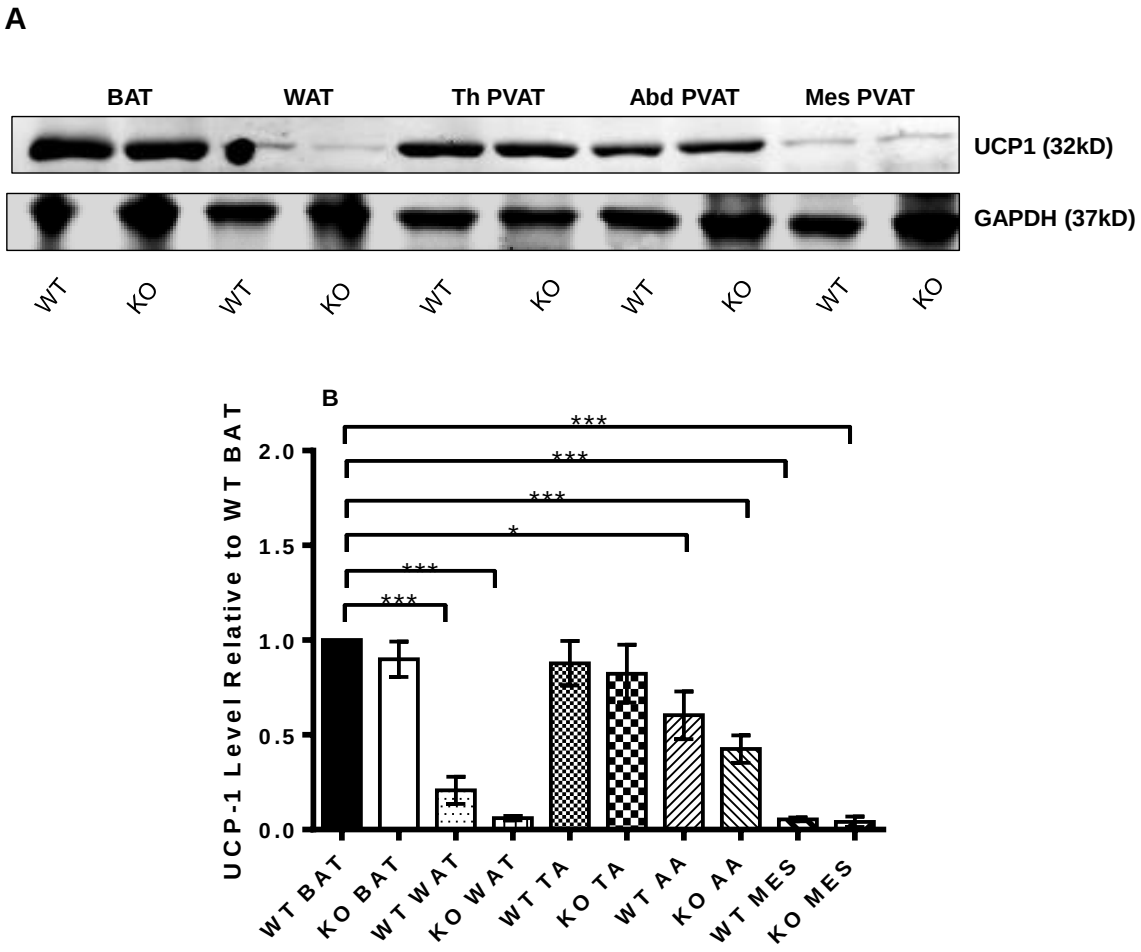

Figure 3-3 UCP-1 levels in different PVAT depots.

Tissue lysates (n= 3) were prepared from WT and KO BAT, WAT, thoracic PVAT (TA), abdominal PVAT (AA) and mesenteric PVAT (MES). UCP-1 level is presented as a ratio of the density of the GAPDH band to adjust for protein loading. Western blotting was performed in BAT (brown adipose tissue); WAT (white adipose tissue); TA (thoracic aorta PVAT); AA (abdominal aorta PVAT); MES (mesenteric artery PVAT) from WT and KO. Blot shown are representative ***p<0.001 vs WT BAT; *p<0.05 vs WT BAT; ***p<0.001 vs WT BAT; ***p<0.001 vs WT BAT.

3.3.2 AMPK expression and activity

As AMPKα1 is one of two AMPKα subunit isoforms, the effect of AMPKα1 deletion on the total AMPKα and phospho-AMPKα Thr172 levels in PVAT was examined by immunohistochemistry and immunoblotting. There was reduced intensity of both total AMPKα and phospho-AMPKα Thr172 staining in AMPKα1 knockout thoracic aorta in both the PVAT and the medial vascular smooth muscle region (Figures 3-4 and 3-5). Immunoblot analysis further demonstrated that AMPK activity, reflected by the levels of phospho-AMPKα Thr172 (pAMPKα) and the AMPK substrate phospho-ACC Ser79

(pACC), was significantly reduced in AMPK-α_1 knockout mice in comparison with wild type (Figure 3-6).

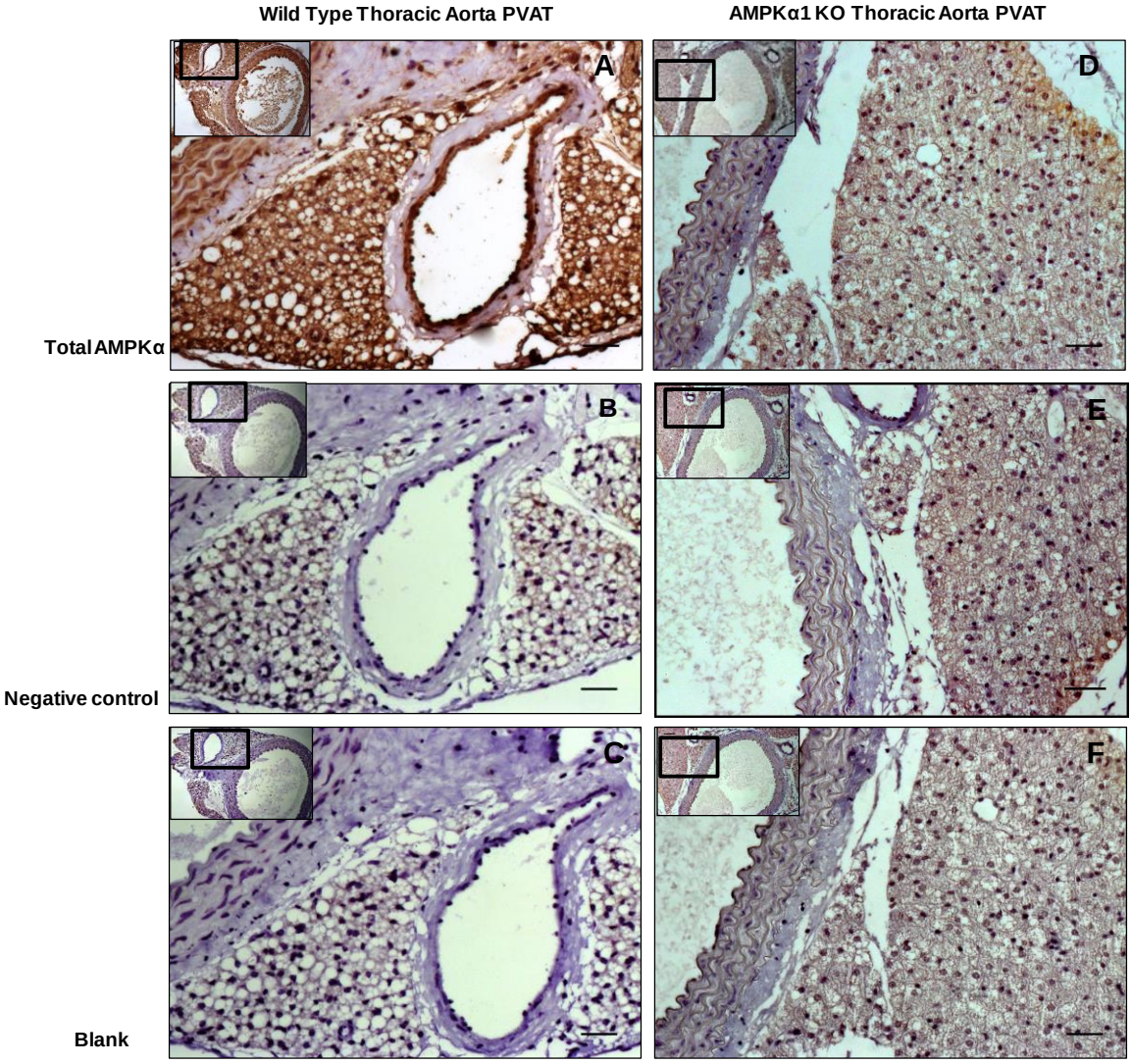

Figure 3-4 Total AMPKα levels in wild type and AMPKα1 knockout mouse thoracic aorta with intact PVAT.

Representative histological sections of thoracic aorta with intact PVAT from WT and KO mice stained with anti-AMPKα antibodies and counterstained with haematoxylin. (A, D) Positive staining is indicated by brown colour. (B, E) Negative control represents aortic rings with anti-AMPKα primary antibodies only; (C, F) Blank (untreated) represents aortic rings without treatment. Scale bar 20μm.

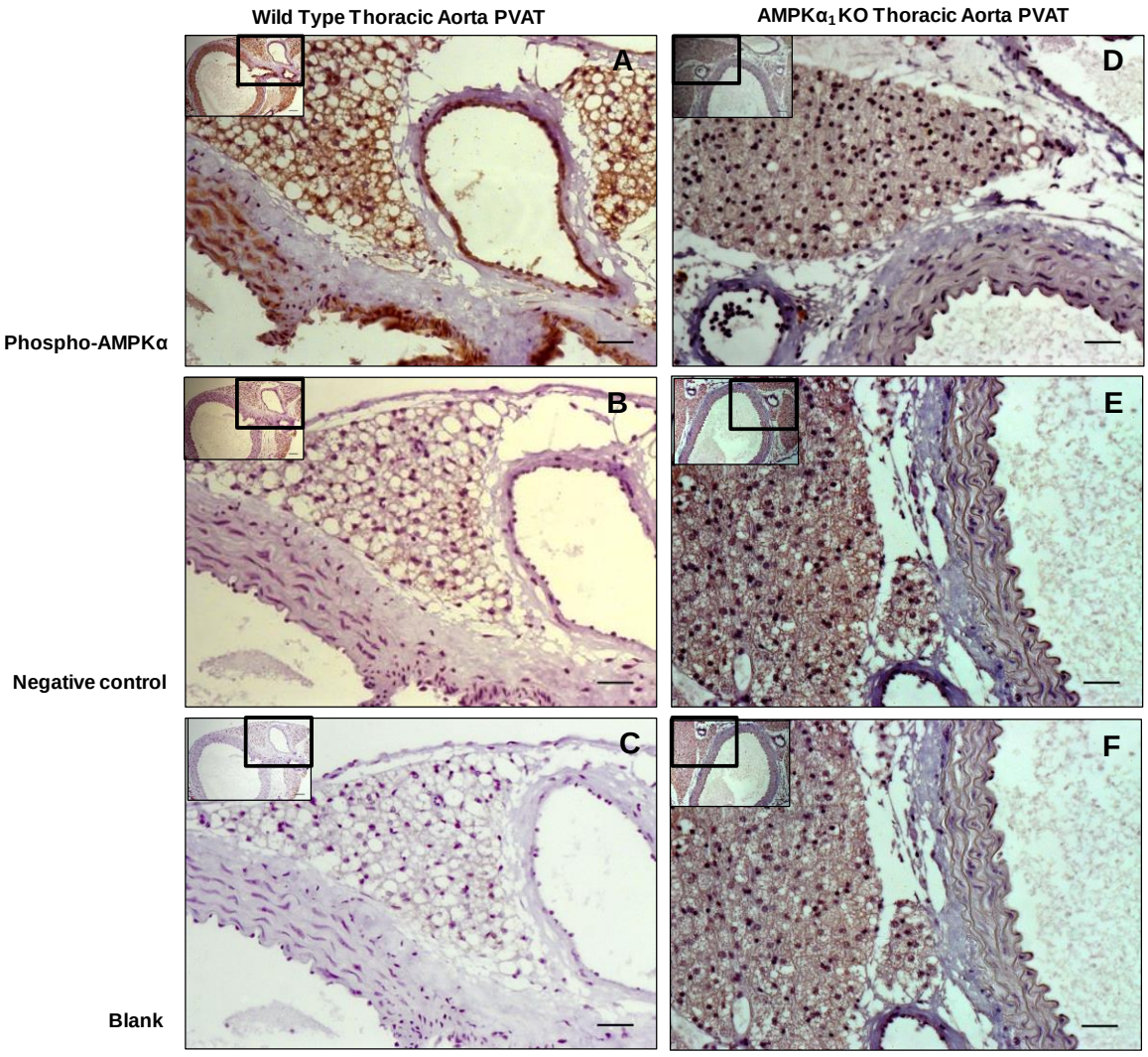

Figure 3-5 Phospho-AMPKα Thr172 levels in wild type and AMPKα1 knockout mouse thoracic aorta with intact PVAT.

Representative histological sections of thoracic aorta with intact PVAT from WT and KO mice stained with anti-Phospho AMPKα Thr172 antibodies and counterstained with haematoxylin. (A, D) Positive staining is indicated by brown colour. (B, E) Negative control represents aortic rings with anti-AMPKα primary antibodies only; (C, F) Blank (untreated) represents aortic rings without treatment Scale bar 20μm.

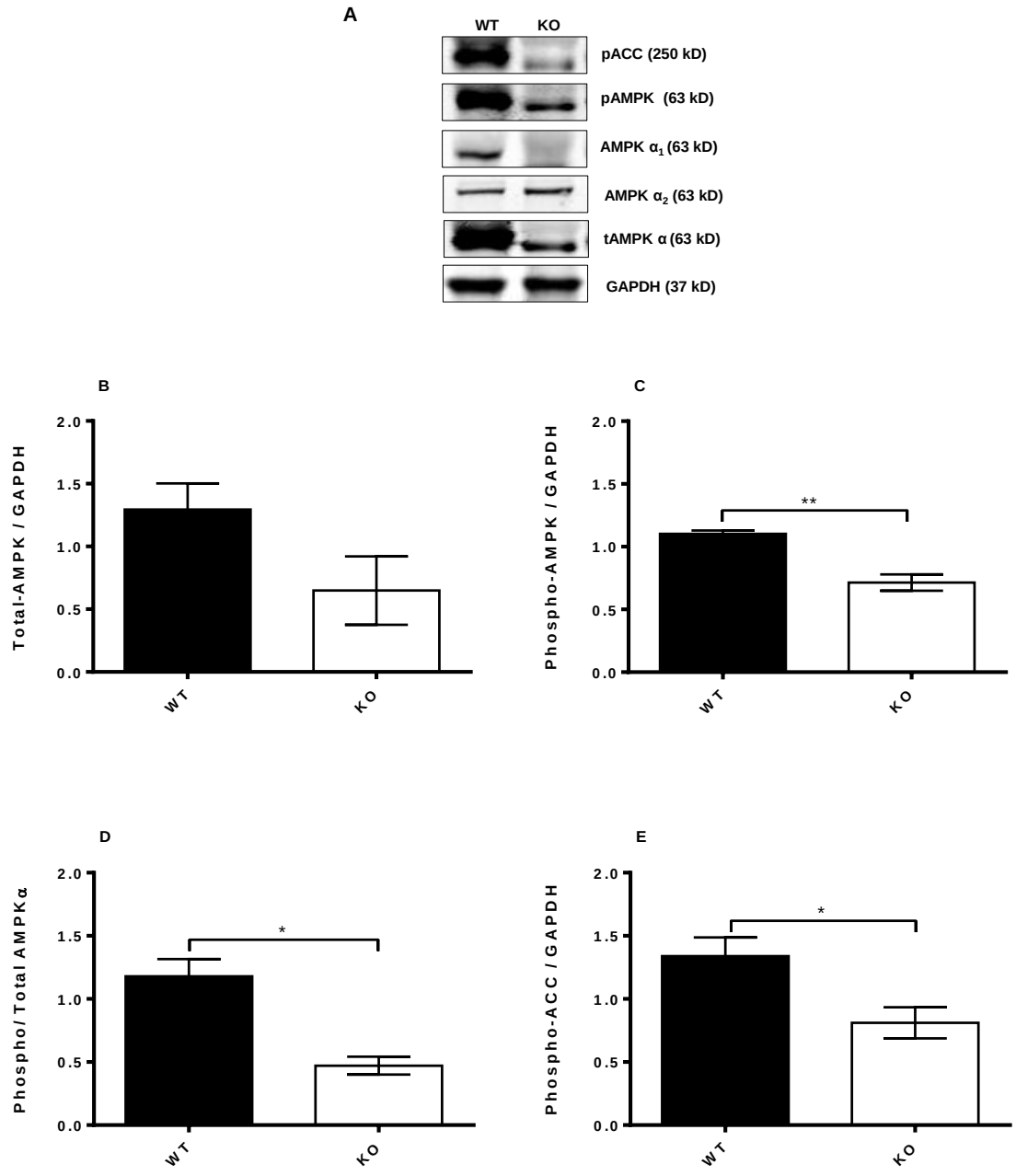

Figure 3-6 AMPK levels and activity in PVAT.

Lysates of thoracic PVAT from wild type and AMPKα1 knockout mice were immunoblotted with the indicated antibodies. A) Representative Immunoblots are shown. (B,C) Quantitative analysis of immunoblots, expressed as the ratio of the phosphorylated and total form of AMPKα divided by GAPDH (C). (D) Quantitative analysis of immunoblots, expressed as the ratio of the phosphorylated form of the enzyme divided by total AMPKα. (E) Quantitative analysis of immunoblots, expressed as the ratio of the phosphorylated form of ACC divided by GAPDH. **p<0.01 vs KO PVAT, n = 3; *p<0.05 vs KO PVAT, n = 3; *p<0.05 vs KO PVAT.

3.3.3 PVAT from AMPKα1 knockout mice enhances vascular contraction

To determine whether lack of AMPKα1 altered the contractile response of aortic rings in the presence or absence of associated PVAT, contractile responses to the thromboxane A_2 receptor agonist U46619 ($3x10^{-8}$M) was assessed (Figure 3-7). The presence and absence

of PVAT did not affect the maximal tension induced by U46619. These results showed that the presence of PVAT did not pose a constraint on the ability of the aorta to contract, and the procedure used to remove PVAT or endothelium neither damaged nor affected the contractility of the aorta in both WT and KO animals.

The magnitude of the U46619-induced vessel contraction was similar in the absence of PVAT in both mice strains (Figure 3-7). Wild type PVAT-free vessels contracted 1.49 ± 0.11 g (n = 29) versus 1.46 ± 0.11 g for AMPKα1 knockout vessels without PVAT (n = 31). The contraction in KO aortae devoid from PVAT was not significantly different from that with intact PVAT. The contraction of wild type aorta with intact PVAT was 1.15 ± .0.11 g (n = 28) which was significantly less than that reported in WT vessels without PVAT (1.49 ± 0.11 g = 26; $p<0.05$ vs WT intact PVAT arteries). In addition, the contraction of wild type aorta with intact PVAT was significantly less than that seen in PVAT-containing aorta from knockout mice; 1.62 ± 0.11 g (n = 32; $p<0.001$ vs WT vessels with PVAT), suggesting that WT PVAT has an anticontractile effect which is lost in KO mice.

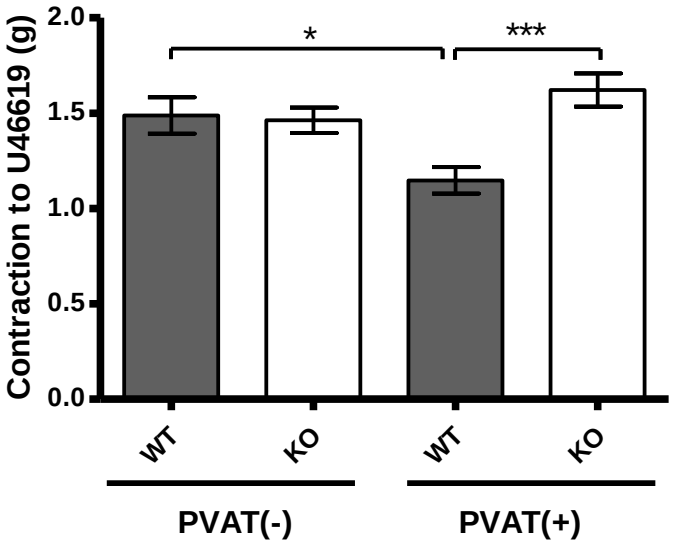

Figure 3-7 Effect of PVAT on thromboxane A_2 receptor agonist U46619 ($3x10^{-8}$ M) induced contraction.

Endothelium denuded, thoracic aortae with and without PVAT from WT and KO were stimulated with U46619 for approximately 30 min and contraction measured on a myograph. *p<0.05 vs WT aortic rings without PVAT, n = 31; ***p<0.001 vs WT vessels with intact PVAT, n =28-32.

3.3.4 PVAT enhances vascular relaxation to the AMPK activator AICAR

To test whether the presence of PVAT can augment relaxation, dose-response curves to a known vasodilator agent, the AMPK activating agent AICAR were constructed in endothelium-denuded thoracic aorta rings with (PVAT+) and without (PVAT-) associated PVAT as described in section 2.5. In wild type animals (Figure 3-8A), addition of AICAR to U46619-precontracted PVAT intact thoracic aortic rings resulted in a concentration-dependent, slowly developing relaxation, which reached a maximum (E_{max}) of 49.7 ± 2.6% (n = 6). This was significantly greater in comparison to vessels with PVAT removed (E_{max} 30.7 ± 0.3%, n = 6; $p<0.001$). AICAR also stimulated relaxation of U46619-precontracted AMPKα1 knockout thoracic aorta (n = 6), yet the presence of PVAT had no effect on the AICAR-induced relaxation (Figure 3-8 B). Addition of AICAR to PVAT intact thoracic rings resulted in a maximum relaxation response (E_{max}) of 29.3 ± 3.4% (n = 6), which was not different from that reported in aortic rings without PVAT (27.9 ± 4.9% (n = 6)).

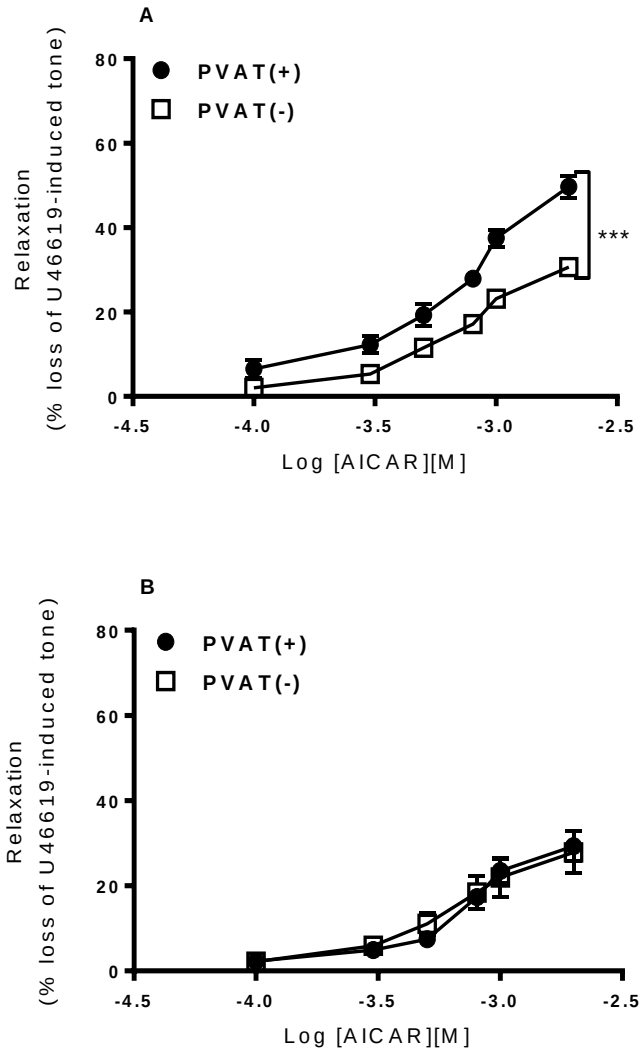

Figure 3-8 Effect of PVAT on AICAR induced relaxation in wild type and AMPKα1 knockout thoracic aorta.

Dose-response curves to AICAR were produced by wire myography in thoracic aortic rings with (+) and without (-) PVAT. All vessels were without endothelium. In wild type (A), PVAT significantly enhanced the relaxation to AICAR (n = 6, ***p<0.001 vs PVAT(-)). In AMPKα1 knockout mice (B), the presence of PVAT had no effect on vascular relaxation (n = 6, p =ns).

3.3.5 PVAT enhances vascular relaxation to cromakalim in wild type, but not AMPKα1 knockout aortic rings

To ensure that the anticontractile effect was due to the presence of PVAT and to rule out the possibility that activation of AMPK in vascular smooth muscle cells was responsible for the augmented relaxation to AICAR, we repeated the experiments using another vasodilator which does not activate AMPK (cromakalim). Cromakalim is a K^+ channel opener which induces vascular relaxation via hyperpolarisation of the vascular smooth muscle membrane. The results are summarised in Figure 3-9. The maximum response to 10^{-4}M cromakalim produced by aortic rings from WT with intact PVAT (59.0 ± 12.3%,

n=7; Figure 3-9 A) was significantly greater than that produced by aortic rings without PVAT (27.6 ± 2.8%, n=7; Figure 3-9 B). In KO, maximal responses to cromakalim were not significantly different between vessels with or without intact PVAT (21.6 ± 1.6% vs. 18.7 ± 4.0%; n=7; p=ns).

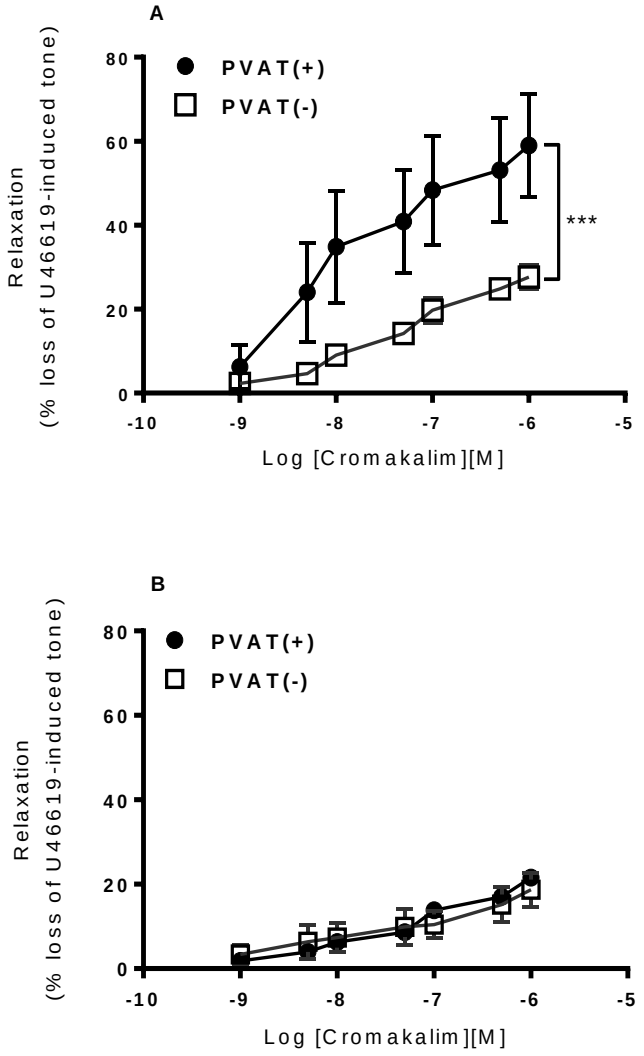

Figure 3-9 Effect of PVAT on cromakalim-induced relaxation in wild type and knockout thoracic aorta.

Dose-response curves induced by cromakalim in thoracic aortic rings with (+) and without (-) PVAT. In wild type (A), the presence of PVAT enhanced the response to cromakalim (n=7, ***p<0.001 vs. PVAT-). In AMPKα1 knockout (B), PVAT had no effect on vascular relaxation to cromakalim (n = 7, p =ns).

3.3.6 Effects of PVAT on AICAR and cromakalim- induced vascular relaxation in abdominal aortic rings

To confirm that the ability of PVAT to enhance vasorelaxation was not depot specific, the experiments with AICAR and cromakalim were repeated in abdominal thoracic aortic rings. As with the thoracic aorta, WT PVAT enhanced the relaxation caused by AICAR. (E_{max} 53.3 ± 5.2% in PVAT(+) vs. 24.5 ± 5.7% in PVAT(-), n = 6; $p<0.05$) (Figure 3-10A). In KO mouse abdominal aorta, PVAT had no effect on the AICAR-induced relaxation (E_{max} 33.3 ± 2.8% vs. 30.9 ± 5.1%, n = 5; p=ns) (Figure 3.10B).

The functional experiment in the abdominal aorta was repeated using cromakalim and the result showed the same pattern as with AICAR. In WT vessels with intact PVAT, maximum relaxation (E_{max}) was 50.9 ± 12.42%, (n = 6), significantly greater than abdominal aorta without PVAT (26.1 ± 8.3%, n = 6; $p<0.05$ vs. PVAT+) (Figure 3.11A). In KO animals (Figure 3.11 B), presence of PVAT had no effect on vascular relaxation induced by cromakalim (22.8 ± 5.8% vs. 17.4 ± 4.1%, n = 6).

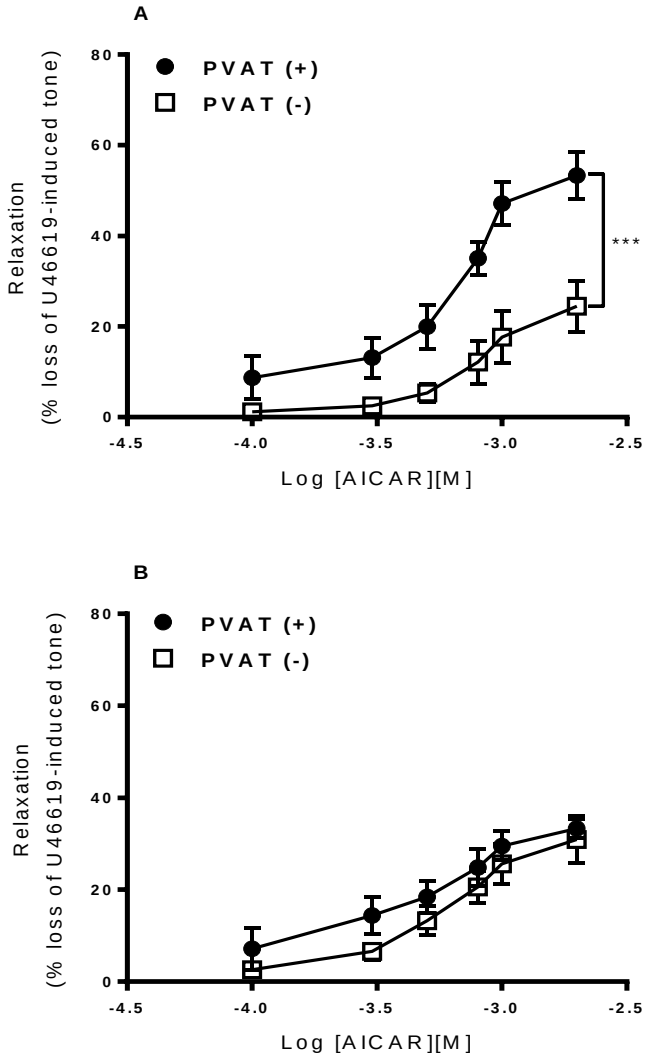

Figure 3-10 Effect of PVAT on AICAR-induced relaxation in wild type and knockout abdominal aorta.

Dose- response curves induced by AICAR in abdominal aortic rings with (+) and without (-) PVAT. In wild type (A), the presence of PVAT enhanced the response to AICAR (n=6, ***p<0.001). In AMPKα1 knockout (B), PVAT had no effect on vascular relaxation (n = 5, p =ns).

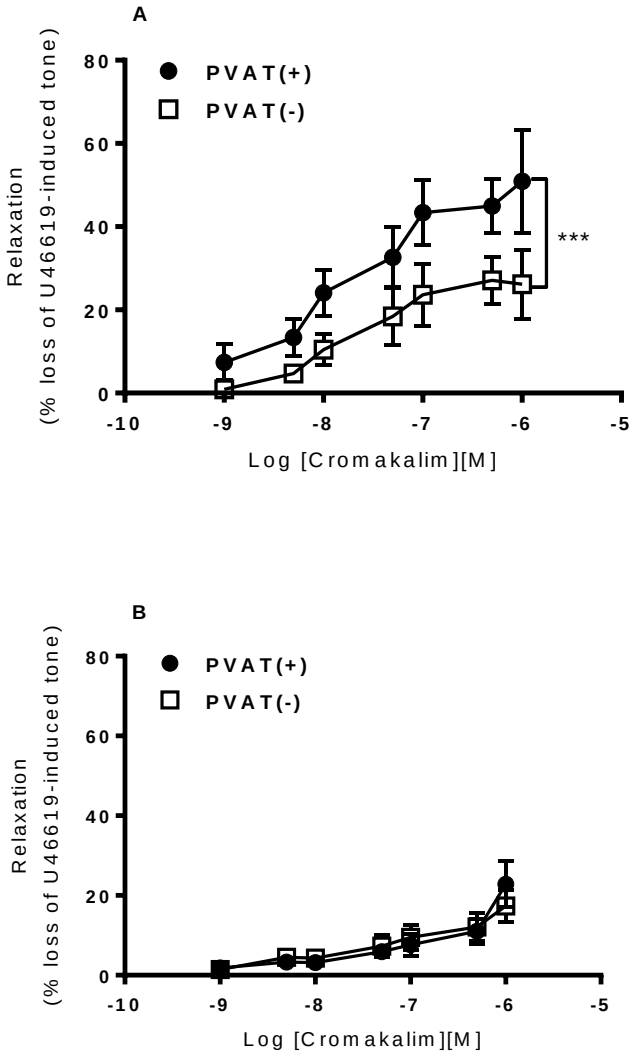

Figure 3-11 Effect of PVAT on cromakalim-induced relaxation in wild type and knockout abdominal aorta.

Dose- response curves induced by cromakalim in abdominal aortic rings with (+) and without (-) PVAT. In wild type (A), the presence of PVAT enhanced the response to cromakalim (n=6, ***p<0.001). In AMPKα1 knockout (B), PVAT had no effect on vascular relaxation (n = 6, p =ns).

3.3.7 Transfer studies

To study whether the PVAT had to be attached to the vessel in order to augment relaxation, thoracic arteries without PVAT were preconstricted with U46619 (3×10^{-8}M) and, once a stable constriction had developed, PVAT (unattached) was added to the myography bath and a dose-response curve to cromakalim was constructed. In wild-type vessels without PVAT (n = 5), addition of PVAT into the myography bath caused a significant increase in the relaxation (E_{max} 54.5± 8.3% vs. 15.9 ± 4.7%, Figure 3-12A). Contemporaneous control experiments with PVAT-intact WT arteries (n = 5) were performed which demonstrated that intact PVAT and added PVAT had a similar effect on augmenting relaxation to cromakalim (E_{max} 49.9 ± 6.7% vs. 30.1 ± 3.4%, Figure 3-12B).

When the transfer experiments were repeated in AMPKα1 knockout vessels it was found that KO PVAT, either attached or added to the myograph bath did not influence the relaxation induced by cromakalim (Figure 3-12 C&D).

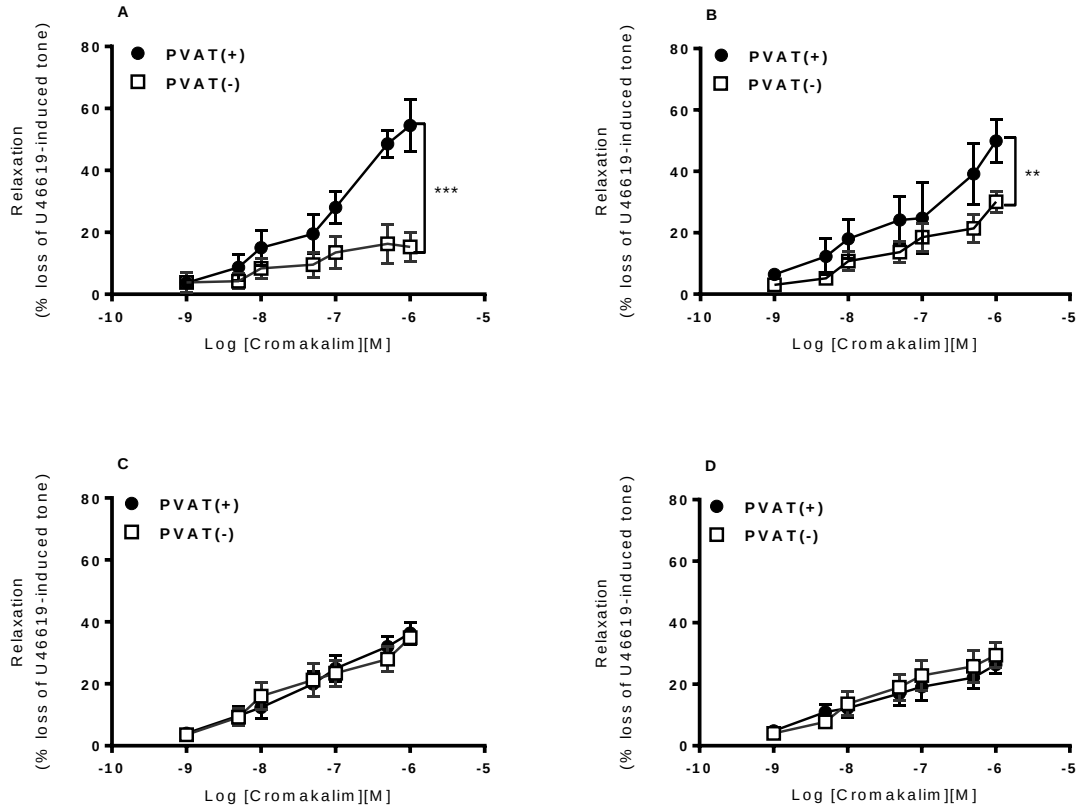

Figure 3-12 Effect of addition of PVAT on cromakalim-induced relaxation in wild type and AMPKα1 knockout thoracic aortae.

Dose- response curves induced by cromakalim in endothelium-denuded thoracic aortic rings with (+) and without (-) PVAT. Data are expressed as percentage loss of vascular tone induced by U46619. (A) Addition of unattached PVAT enhanced the response to cromakalim in wild type vessels without (-) PVAT (n=5, ***p<0.001 vs WT PVAT(-) vessels). (B) A contemporaneous control experiment comparing vessels with intact PVAT (+) and without PVAT (-) in wild type mice (n=5, **p<0.01 vs WT PVAT(-) vessels). (C) Addition of unattached PVAT did not enhance the response to cromakalim in AMPKα1 knockout mice aortic rings (n=5, p = ns vs KO PVAT(-) vessels). (D) A contemporaneous control experiment comparing vessels with intact PVAT (+) with those without PVAT in AMPKα1 knockout mice (n=5, p = ns vs KO PVAT(-) vessels).

3.3.8 Wild type PVAT enhances relaxation in AMPKα1 knockout vessels

To further investigate the function of the PVAT, and whether it is the PVAT or the medial smooth muscle cells which are compromised in KO mice, "cross over" studies were conducted. These experiments involved addition of unattached PVAT from WT mice to myography chambers containing aortic rings from AMPKα1 knockout and *vice versa.* After addition of the PVAT, thoracic arteries were preconstricted with U46619. Once a stable constriction had developed dose-response curves to AICAR and cromakalim were constructed.

It was found that WT PVAT significantly enhanced the AICAR-induced vasodilatation in KO arteries without PVAT ($p<0.001$, Figure 3-13A), and increased the E_{max} of AICAR from 27.7 ± 4.9 % to 52.7 ± 12.4% ($p<0.001$). In contrast, KO PVAT had no significant effect on AICAR-induced vasodilatation in wild type arteries without PVAT (p = ns, Figure 3-13B).

The same studies were repeated using cromakalim and the results were consistent with AICAR. Addition of WT PVAT (n = 6) significantly augmented relaxation in KO aortic rings to cromakalim. Wild type PVAT increased the E_{max} of cromakalim from 18.7 ± 4.0 % to 46.3 ± 12.4% ($p<0.001$, Figure 3-13C), whereas KO PVAT had no effect on the relaxation of WT thoracic aorta in which the PVAT was removed (Figure 3-13D).

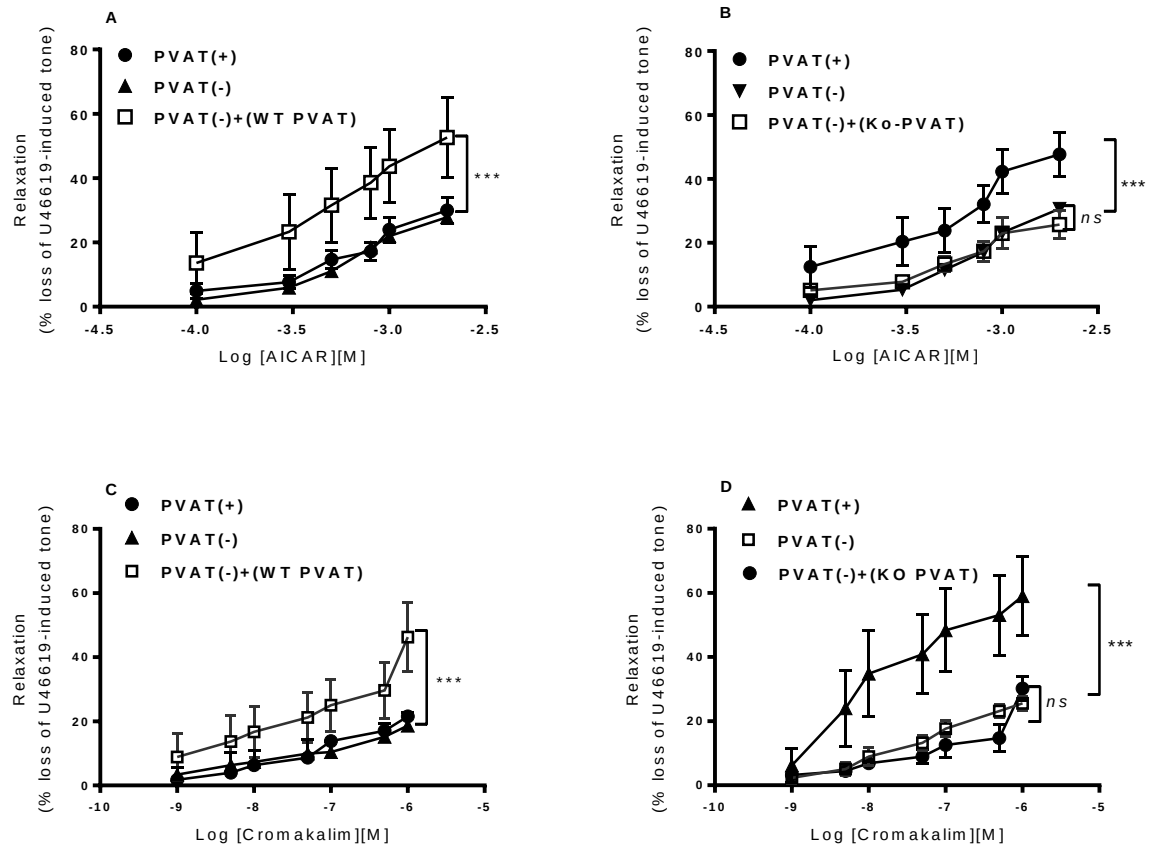

Figure 3-13 Effect of PVAT transfer on AICAR and cromakalim induced vasorelaxation.

Dose-response curves were constructed to AICAR and cromakalim in endothelium-denuded thoracic aortic rings. Data are expressed as percentage loss of U46619-induced contraction. (A) Addition of WT PVAT enhanced the response to AICAR in KO vessels without PVAT (n=5, ***p<0.001 vs KO PVAT(-) vessels). (B) KO PVAT did not affect AICAR induced relaxation in WT vessels without PVAT (n=5, p = ns). (C) Addition of WT PVAT enhanced the response to cromakalim in KO vessels without PVAT (n=6, ***p<0.001 vs KO PVAT(-) vessels). (D) KO PVAT did not affect cromakalim-induced relaxation in WT vessels without PVAT (n=6, p = ns).

3.3.9 Conditioned media from WT aortic PVAT reduces contractility in vessels without PVAT

To ascertain whether augmented relaxation caused by PVAT is due to release of a transmissible factor, solution transfer (conditioned media) studies were performed. Control experiments with intact PVAT from wild-type and knockout arteries were performed in parallel to determine whether the conditioned media is as effective as attached PVAT in augmenting aortic relaxation. Conditioned media was prepared by incubation of PVAT in Krebs' solution at 37℃ for 1 hour. In all experiments, conditioned media was added to the vessels without PVAT before pre-constriction to U46619 to ensure that the transferred solution would have the same effect as the attached (intact) PVAT vessels and also to determine whether there was any effect on U46619 induced contraction.

Conditioned media from WT PVAT significantly attenuated contraction induced by U46619 (Figure 3-14). Addition of WT conditioned media to WT aortic rings (n = 12) without PVAT reduced the maximum contraction from 1.19 ± 0.1 g to 0.86 ± 0.1 g ($p<0.05$). In contrast, conditioned media from KO PVAT had no effect on U46619-induced contraction of KO aortic rings (2.8 ± 1.4 *vs* 2.33 ± 1.3 PVAT (-), n =12, p = ns).

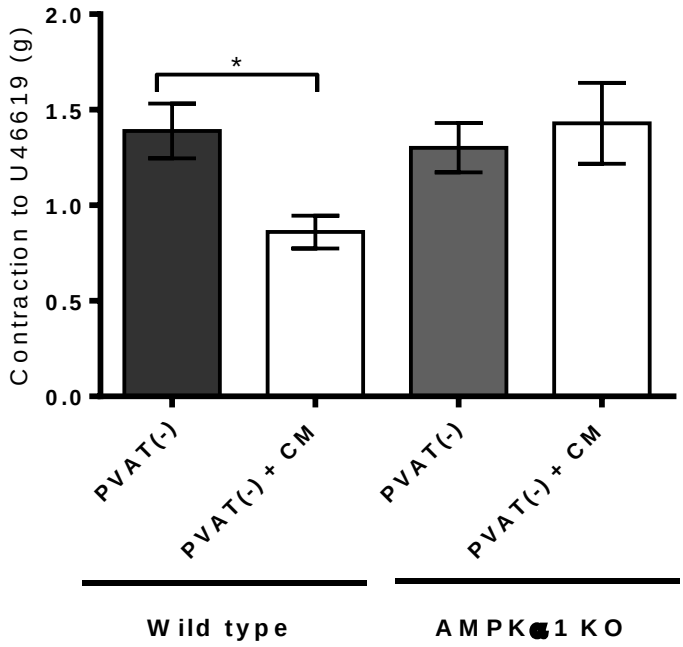

Figure 3-14 Effect of conditioned media on aortic ring contraction.

Conditioned media from WT and KO PVAT was added to endothelium-denuded thoracic aortic rings from WT and KO mice respectively in the absence of PVAT. Contraction to U46619 is expressed in g. *p<0.05 vs WT PVAT(-) vessels, n =12; p =ns vs KO PVAT(-) vessels, n =12.

3.3.10 Conditioned media from WT mice enhances AICAR and cromakalim induced relaxation

To investigate the ability of PVAT-secreted substances to modulate vasorelaxation, conditioned media from KO and WT PVAT were prepared and incubated with corresponding PVAT (-) vessels. To test the ability of conditioned media to enhance the relaxation to AICAR or cromakalim and that the enhanced relaxation was due to the conditioned media rather than decreased viability of the vessels over time, control experiments with intact PVAT were conducted concurrently. Prior to induction of contraction, vessels without PVAT from WT and KO mice were incubated with the conditioned media and once a stable constriction had developed in response to U46619, dose response curves for both AICAR and cromakalim were constructed.

Conditioned media from WT PVAT significantly increased the E_{max} of WT aortic rings without PVAT in response to AICAR (Figure 3-15A) and cromakalim (Figure 3-16A) from 38.9 ± 8.2% to 53.2 ± 8.2% (n=8) and 25.2 ± 2.2% to 52.4 ± 10.3% (n=6) respectively. Conditioned media derived from PVAT of AMPKα1 KO mice had no significant effect on the relaxation of WT aortic rings to either AICAR (Figure 3-17) or cromakalim (Figure 3-18), suggesting that dysfunction of the PVAT anticontractile response is related to AMPKα1 subunit deletion.

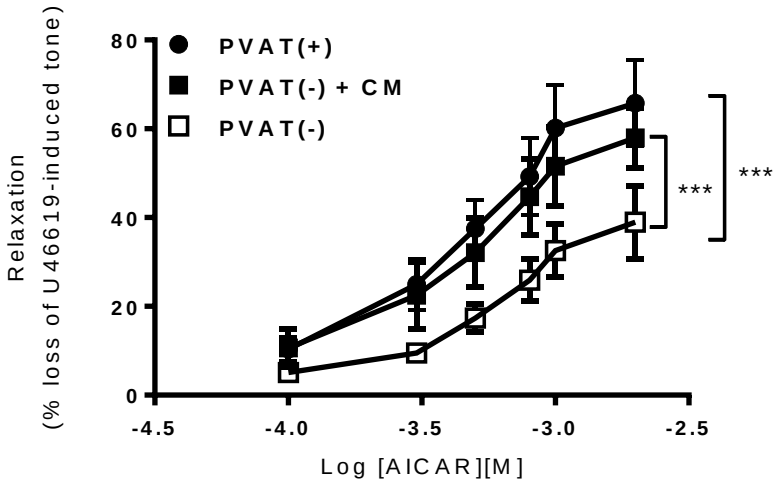

Figure 3-15 Effect of PVAT-derived conditioned media on AICAR induced vascular relaxation in WT aortic rings.

Dose-response curves were constructed to AICAR in endothelium-denuded WT thoracic aortic rings incubated with conditioned media from WT PVAT. Data are expressed as percentage of loss of U46619-induced tone. ***p<0.001 vs WT PVAT(-) vessels, n = 8 and ***p<0.001 vs WT PVAT(-) vessels.

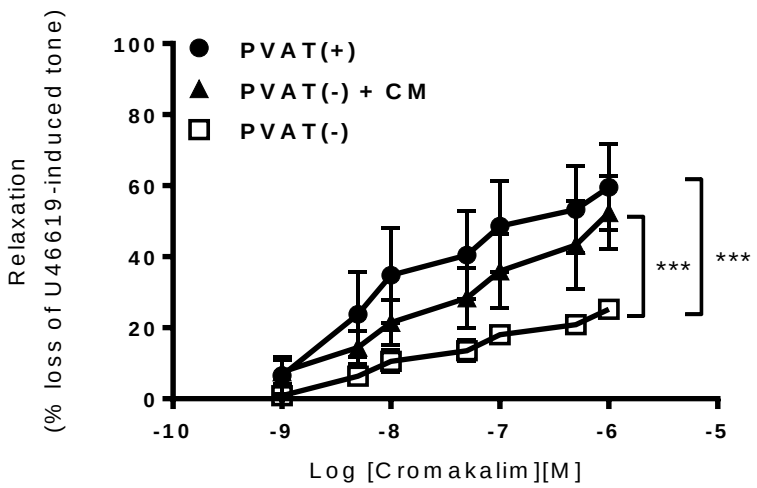

Figure 3-16 Effect of PVAT-derived conditioned media on cromakalim-induced vascular relaxation in wild type aortic rings.

Dose-response curves were constructed to AICAR in endothelium-denuded WT thoracic aortic rings incubated with conditioned media from WT PVAT. Data are expressed as percentage of loss of U46619-induced tone. ***p<0.001 vs WT PVAT(-) vessels and, n = 7 and ***p<0.001 vs WT PVAT(-) vessels, n =7.

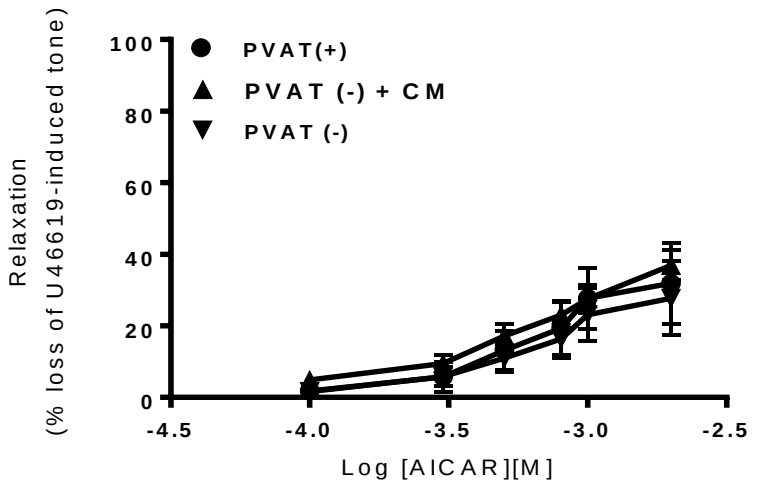

Figure 3-17 Effect of KO PVAT-derived conditioned media on AICAR-induced vascular relaxation in AMPKα1 knockout aortic rings.

Dose-response curves were constructed to AICAR in endothelium-denuded WT thoracic aorta incubated with conditioned media from PVAT of KO mice. Data are expressed as percentage loss of U46619-induced tone. p = ns vs KO PVAT(-) vessels and, n = 6 and p = ns vs KO PVAT(-) vessels, n =6.

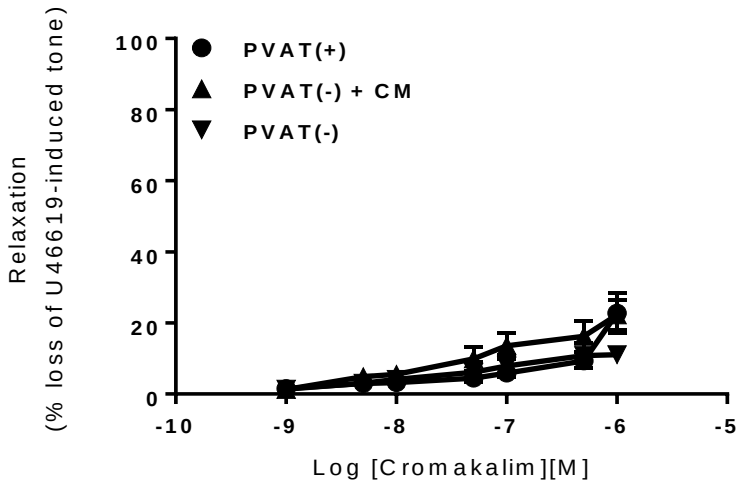

Figure 3-18 Effect of KO PVAT-conditioned media on cromakalim-induced vascular relaxation in AMPKα1 knockout aortic rings.

Dose-response curves were constructed to cromakalim in endothelium-denuded KO thoracic aorta incubated with conditioned media from PVAT of KO mice. Data are expressed as percentage loss of U46619-induced tone. Data shown are representative p = ns vs KO PVAT(-) vessels; n = 6 and p = 0.ns vs KO PVAT(-) vessels, n =6**.**

3.3.11 Cromakalim does not activate AMPK in vascular smooth muscle cells or 3T3-L1 adipocytes

To rule out the possibility that vasodilation to cromakalim is compromised in KO mice because chromakalim has AMPK-dependent actions, cultured rat vascular smooth muscle cells and 3T3-L1 adipocytes were incubated with AICAR (AMPK activator used as a positive control) or cromakalim. Western blotting (Figure 3-19A) demonstrated that cromakalim did not increase phosphorylation of AMPK in the vascular smooth muscle cells (n = 3, p=ns, Figure 3-19B*).* In addition, cromakalim had no effect on the phosphorylation of the AMPK substrate ACC (Figure 3.19C), a kinase downstream of AMPK. AICAR stimulated an increase in AMPK activity (n = 3, $p<0.05$) at a concentration of 10^{-3} M, as assessed by ACC phosphorylation but this was not observed with 10^{-2}M AICAR.

To examine whether cromakalim influenced adipocyte AMPK activity, the 3T3-L1 adipocyte cell line was utilised (Figure 3-20). Over a time course of 10 min and 30 min, adipocytes were incubated with AICAR (2mM) alone, AICAR (2mM) + cromakalim (200μM) and cromakalim (200μM) alone. In all experiments, neither AICAR nor cromakalim alone affected AMPK phosphorylation (n =3, p = ns) (Figure 3-20C&D). AICAR and cromakalim in combination also did not enhance the activity of AMPK in adipocytes as assessed by ACC phosphorylation (n =3, p = ns) (Figure3-20D&F). However, stimulation of 3T3-L1 adipocytes with AICAR alone did show a trend toward enhanced ACC phosphorylation, although this did not reach statistical significance.

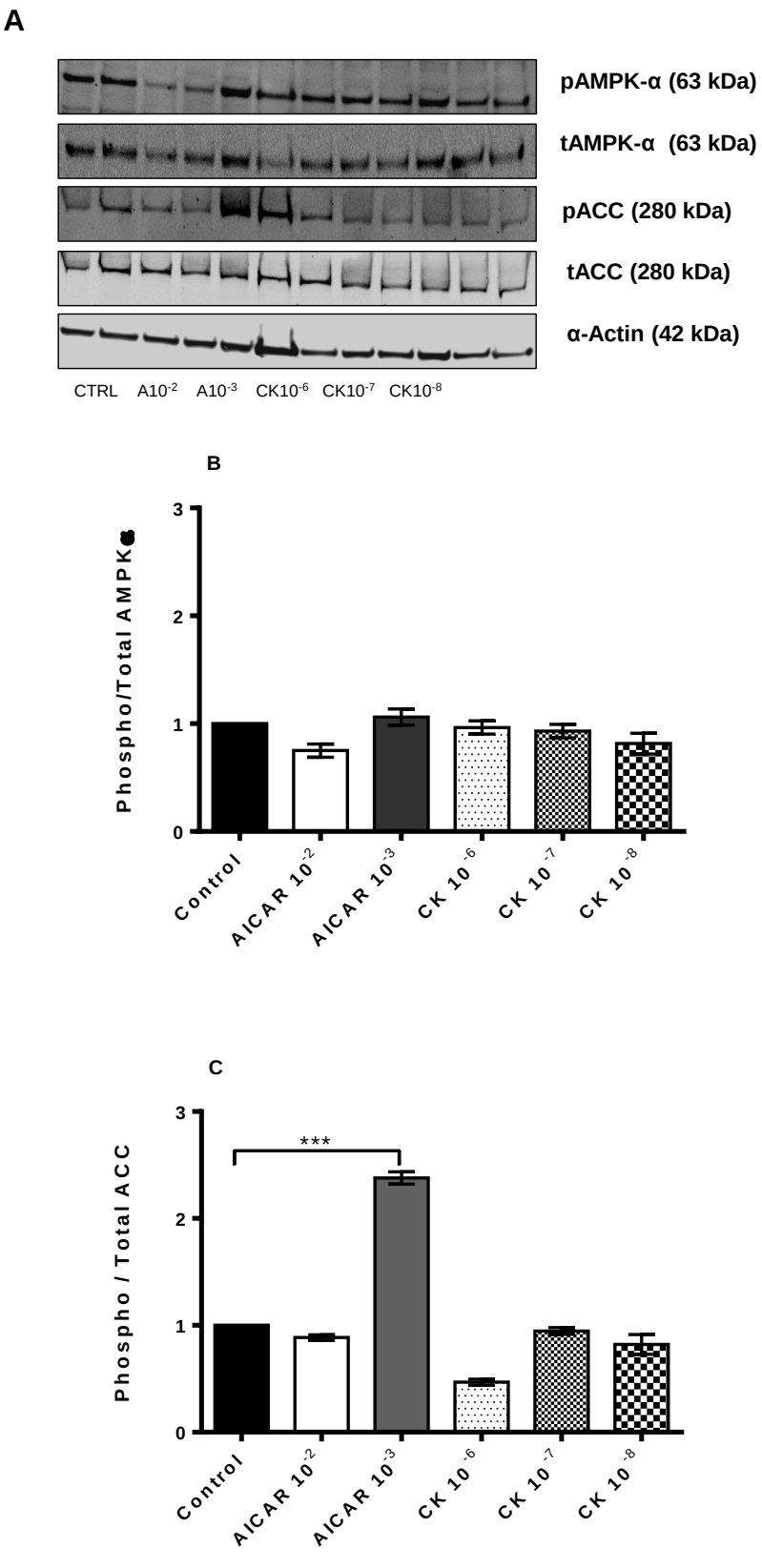

Figure 3-19 Effect of cromakalim on AMPK phosphorylation and activity in VSMCs.

Cultured rat VSMCs were stimulated with AICAR (A) or cromakalim (CK), lysates prepared and subjected to immunoblotting with the indicated antibodies. (A) representative immunoblots are shown). Quantification of (B) phospho-AMPKα Thr172 relative to total AMPKα levels or (C) phospho-ACC Ser79 relative to total ACC levels, normalised to control (vehicle-treated) cells. ***p<0.001 vs control (untreated). This data was generated in collaboration with Azizh Ugusman.

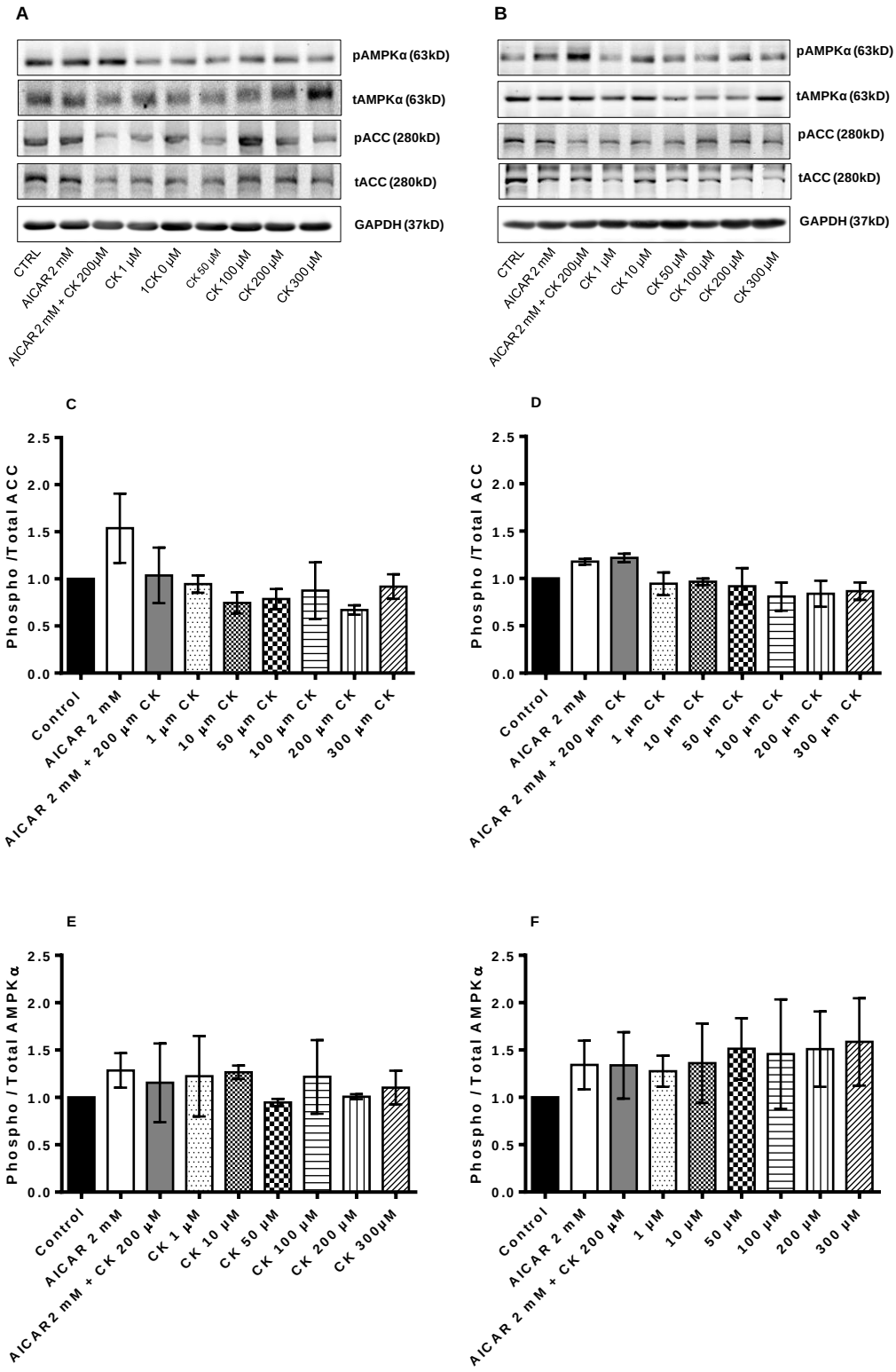

Figure 3-20 Effect of AICAR and cromakalim on AMPK activity following different incubation times in 3T3 adipocytes.

3T3 adipocytes were treated with AICAR, AICAR+ cromakalim and cromakalim alone over 10 min (Figs A, C, E) and 1 hour time interval (Figs B, D, F). Cells were then lysed and immunoblotting was performed. Graphs are expressed as the fold change of the phosphorylated form of each enzyme divided by the total AMPKα (C&D) and total ACC (E&F) to measure the activation of the enzyme. Blots shown are representative (A&B). p = ns vs control (untreated), n = 3. This data was generated in collaboration with PhD student Omer Katwan.

3.3.12 AMPKα1 knockout mouse PVAT has altered adipokine release

To assess the tissue levels and secretion of adipokines by PVAT of wild type and AMPKα1 knockout mice, homogenised PVAT and conditioned medium was assayed using a Proteome Profiler Adipokine array from R&D systems as screening test which detects 38 different adipocytokines. As shown in Figure 3.21 the comparative analysis of homogenised PVAT adipokine levels reveals that AMPKα1 knockout PVAT has reduced levels of adiponectin (Acrp30/AdipoQ), C-Reactive Protein (CRP), Dipeptidyl peptidase-4 (CD26/DPP4), ICAM-1 (CD54), Insulin-Like Growth Factor Binding Protein 2 (IGFBP-2), Insulin-Like Growth Factor Binding Protein 5 (IGFBP-5), Insulin-Like Growth Factor Binding Protein 6 (IGFBP-6), Lipocalin-2 (NGAL), Pentraxin 2 (PTX2/SAP), and Retinol binding protein 4 (RBP4), and higher levels of Fetuin A, Fibroblast Growth Factor 1 (FGF-1), Insulin-Like Growth Factor Binding Protein 3 (IGFBP-3), Pentraxin 2 (PTX2/SAP) and Resistin. Factors including Angiopoietin-like 3 (ANGPT-L3), Endocan (ESM-1), Insulin-like growth factor 2 (IGF-II), Insulin-Like Growth Factor Binding Protein 1 (IGFBP-1), and Receptor for Advanced Glycation Endproducts (RAGE) were below the detection limit of the Array in the AMPKα1 knockout in comparison with wild type PVAT.

In addition, to levels within homogenised PVAT, the same Proteome Profiler Adipokine array was used to detect adipokines in the conditioned medium derived from both wild type and AMPKα1 knockout PVAT. As can be seen in Figure 3.22, conditioned media derived from AMPKα1 knockout PVAT releases lower quantities of some adipokines in comparison with wild type PVAT. The release of factors including adiponectin, CRP, CD26/DPP4, Fetuin A, FGF-1, IGFBP-3, IGFBP-5, IGFBP-6, Lipocalin-2, Pentraxin 2, RBP4 and Resistin were reduced while higher levels of PAI-1 and VEGF-A were found in the KO conditioned media compared to that from wild type PVAT.

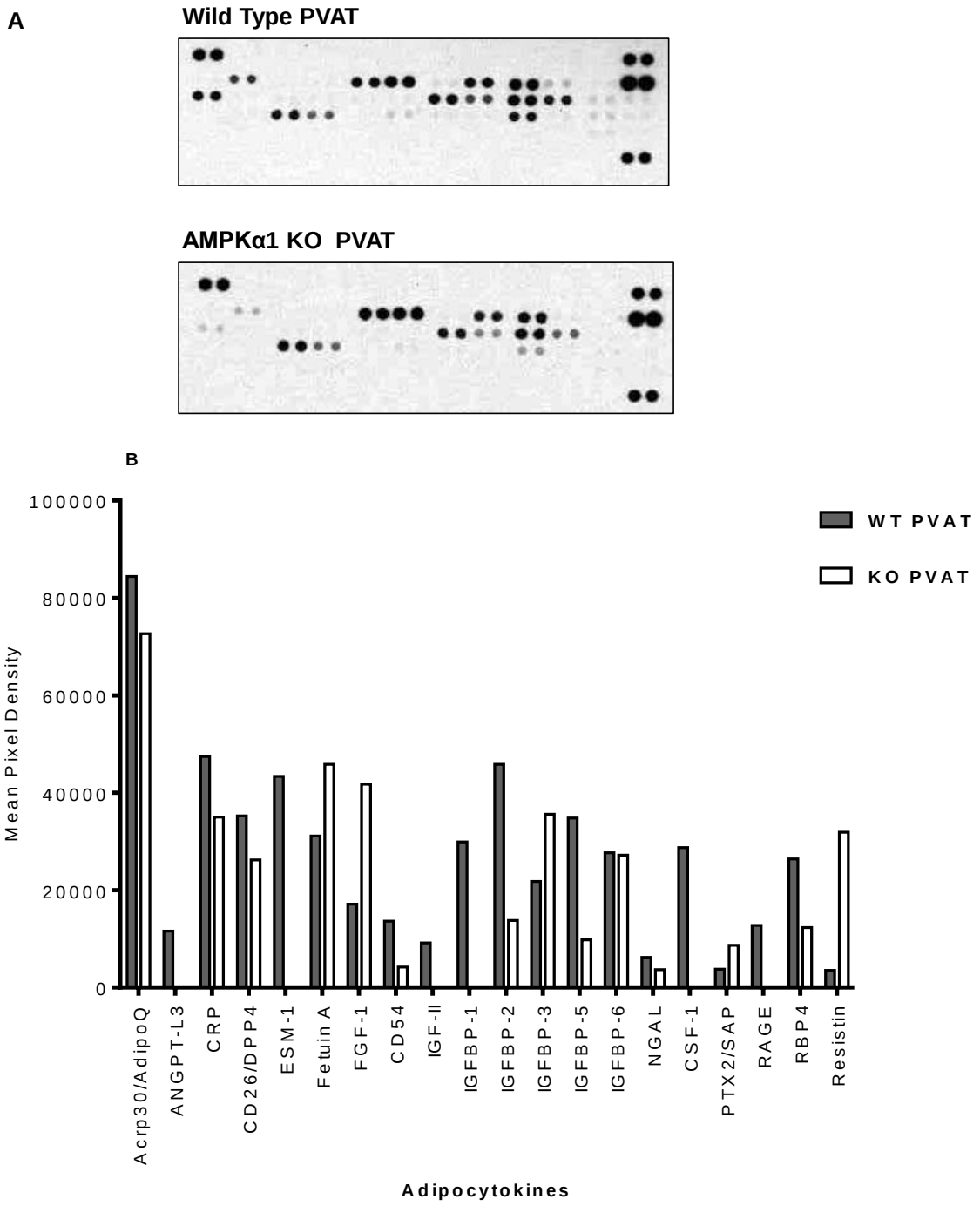

Figure 3-21 Adipocytokine levels in PVAT lysates of wild type and AMPKα1 knockout mice.

PVAT samples from both WT and KO were lysed and the array was performed. Chemiluminescent reaction spots on the adipokine profiler membranes represent various adipokines (A). The comparative expressions of adipokines corrected for protein content (in mean pixel density) obtained from densitometric analysis of the chemiluminescent reaction spots are presented in figure (B) (n=2).

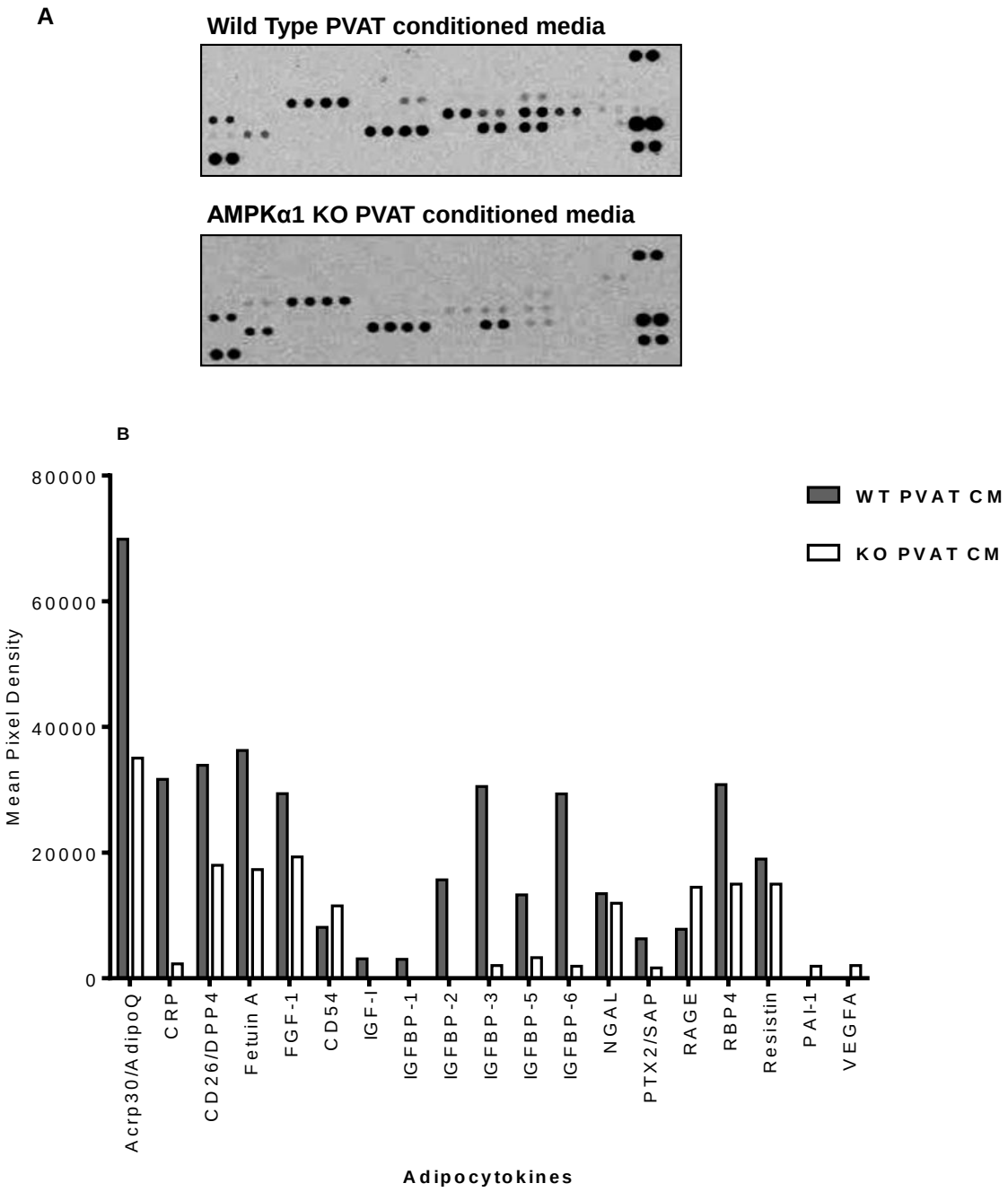

Figure 3-22 Adipocytokine levels in PVAT conditioned media of wild type and AMPKα1 KO mice.

PVAT from both WT and KO mice was incubated in Krebs' solution at 37℃ for 1 hour and conditioned medium collected. Adipokine levels in conditioned medium were assessed by array. (A) Representative array showing chemiluminescent reaction spots on the adipokine profiler membranes. (B) Comparative levels of adipokines corrected for protein content (in mean pixel density) obtained from densitometric analysis of the chemiluminescent reaction spots (n=2).

3.3.13 AMPKα1 knockout PVAT releases less adiponectin

Since the array data above indicated reduced adiponectin release by KO PVAT, an ELISA was used to quantify this. As can be seen in Figure 3-23, the concentration of adiponectin in KO conditioned media was significantly ($p<0.05$) lower than WT conditioned media (32.9 ± 3.3 ng/ml, n = 5 vs 47.5 ± 1.2 ng/ml, n = 5). These results are consistent with data from the adipokine array shown previously in Figure 3-22.

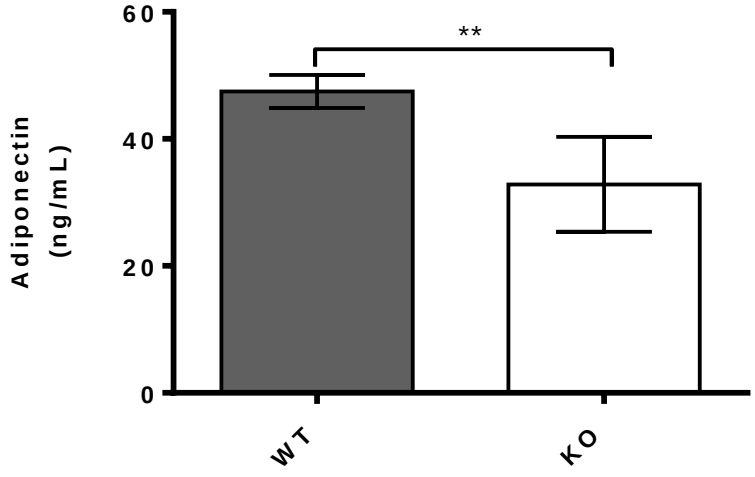

Figure 3-23 Content of adiponectin in conditioned media from PVAT.

Conditioned media samples were collected from WT and KO PVAT and an adiponectin ELISA performed. **p<0.01 vs KO CM, n = 5. CM; conditioned media.

3.3.14 Adiponectin is a potential PVAT derived vasodilator

To further investigate the role of adiponectin in PVAT-induced relaxation, endothelium-denuded thoracic aortic rings with and without PVAT from both wild type and AMPKα1 knockout mice were preconstricted with U46619 and incubated with an AdipoR1 receptor blocker peptide. Dose response curves were then constructed using AICAR and cromakalim. Application of AdipoR1 receptor blocker attenuated the relaxation induced by AICAR and cromakalim in wild type PVAT intact aortic rings but not in AMPKα1 knockout aortic rings with PVAT. In wild type aortic rings, adipoR1 blocking peptide reduced PVAT-induced relaxation to AICAR from 53.5 ± 2.8% to 30.1 ± 3.9% (n=6, $p<0.05$) (Figure 3-24A). The effect of PVAT on cromakalim-induced relaxation was also reduced by the adipoR1 blocking peptide (65.6 ± 14.2% to 39.9 ± 11.6%; n=6, $p<0.05$)

(Figure 3-24C). There was no obvious effect on aortic rings without PVAT when treated with AdipoR1 blocker prior to relaxation with AICAR or cromakalim (Figure 3-24B&D). In AMPKα1 KO aortic rings, addition of the AdipoR1 blocker to vessels without PVAT did not affect the relaxation induced by either AICAR or cromakalim (Figure 3-25 C&D). Additionally, Adiponectin receptor blocking peptide had no effect on the relaxation to AICAR or cromakalim in KO vessels with PVAT (37.8.2 ± 5.4% vs 32.5.8 ± 3.4%, n = 6, p = ns) and (29.6 ± 10.1% vs 19.2 ± 3.1%, n = 6, p = ns) respectively.

Addition of globular adiponectin to wild type and AMPKα1 knockout vessels did not affect the baseline contraction to U46619 as shown in Figure 3-26. In the presence of globular adiponectin, an enhanced relaxation to cromakalim was observed in endothelium-denuded wild type thoracic aortic rings without PVAT and in AMPKα1 knockout thoracic aortic rings in the presence and absence of PVAT (Figure 3-27). Aortic rings from wild type mice without PVAT (Figure 3-27A) (n = 5) dilated significantly from (33.6 ± 8.4%, n = 5) to (58.2 ± 9.9%) after addition of adiponectin in comparison with those with no added adiponectin (33.6 ± 8.4%, n = 5). Interestingly, addition of globular adiponectin caused relaxation in the presence and absence of PVAT in knockout aortic rings (Figure 3-27B). In thoracic aortic rings without PVAT, globular adiponectin increased the cromakalim-induced relaxation from 30.2 ± 4.7% to 58.6 ± 12.5%, n = 6, $p<0.05$ vs PVAT (-). Additionally, globular adiponectin caused an enhanced relaxation response to cromakalim in knockout aortic rings with intact PVAT (47.1 ± 14.4%, n =5) in comparison with intact PVAT aortic rings with no added adiponectin (20.1 ± 1.8%, n = 5; Figure 3-27C).

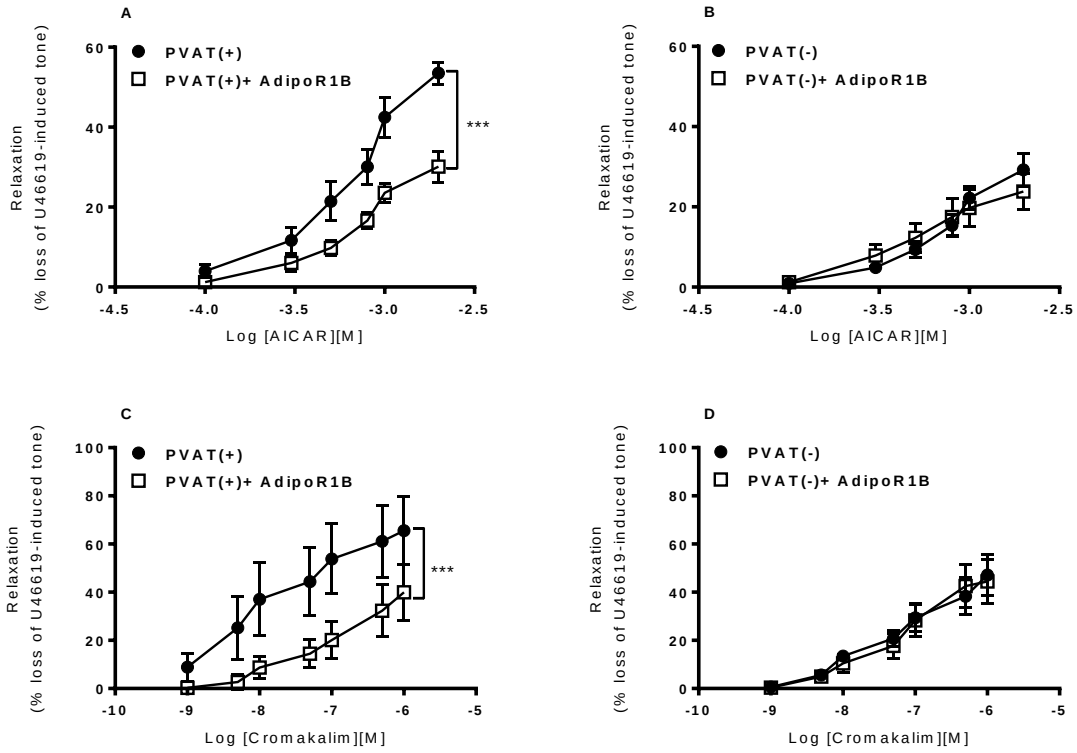

Figure 3-24 Effect of adiponectin receptor 1 (AdipoR1) blocking peptide on PVAT-enhanced relaxation in wild type mouse aorta.

Wild type aortic rings (A,C) with or (B,D) without PVAT were preconstricted with U46619, incubated with AdipoR1 blocking peptide and dose-response curves constructed to (A,B) AICAR or (C,D) cromakalim. Data are expressed as a percentage of loss of the U46619-induced tone. ***p<0.001 relative to absence of AdipoR1 blocking peptide, n = 6.

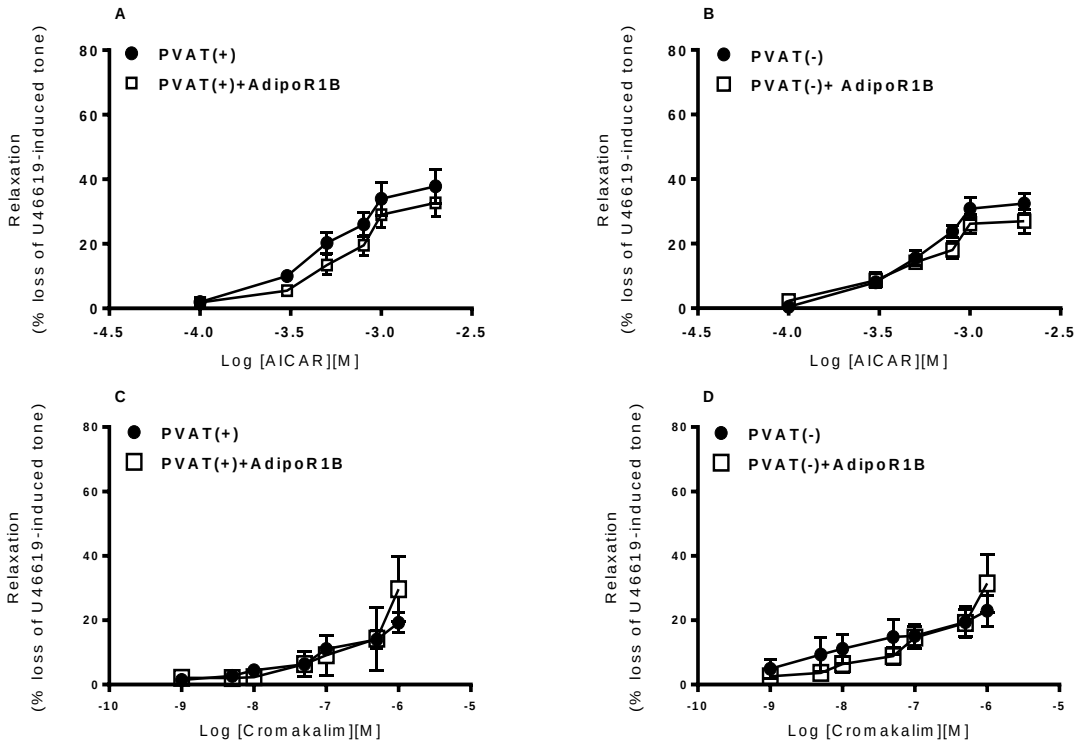

Figure 3-25 Effect of adiponectin receptor 1 (AdipoR1) blocking peptide on PVAT-enhanced relaxation in AMPKα1 KO mouse aorta.

KO aortic rings (A,C) with or (B,D) without PVAT were preconstricted with U46619, incubated with AdipoR1 blocking peptide and dose-response curves constructed to (A,B) AICAR or (C,D) cromakalim. Data are expressed as a percentage of loss of the U46619-induced tone. p = ns relative to absence of AdipoR1 blocking peptide, n = 6.

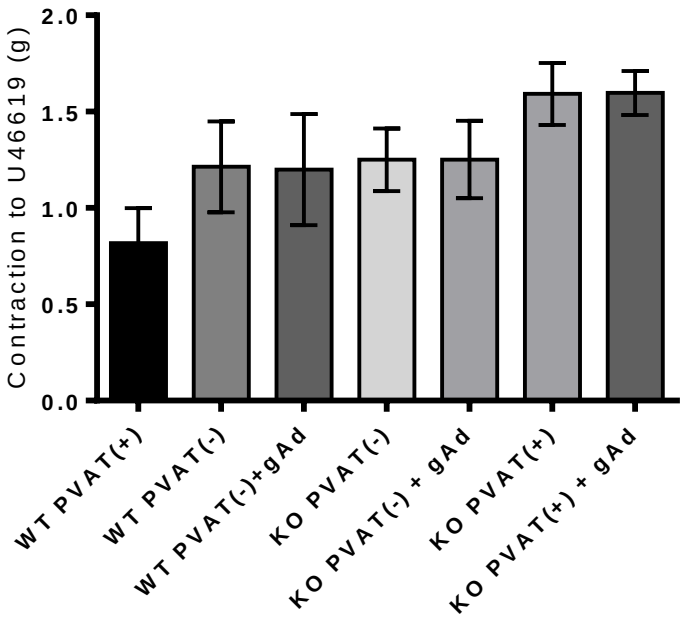

Figure 3-26 Effect of globular adiponectin (1µg/ml) on U46619-induced contraction.

WT and KO thoracic aortic rings with and without PVAT were contracted with U46619, washed and then incubated with globular adiponectin for 10 min. Rings were then contracted a second time with U46619. Data are expressed in g tension to U46619 before and after addition of globular adiponectin. n = 5.

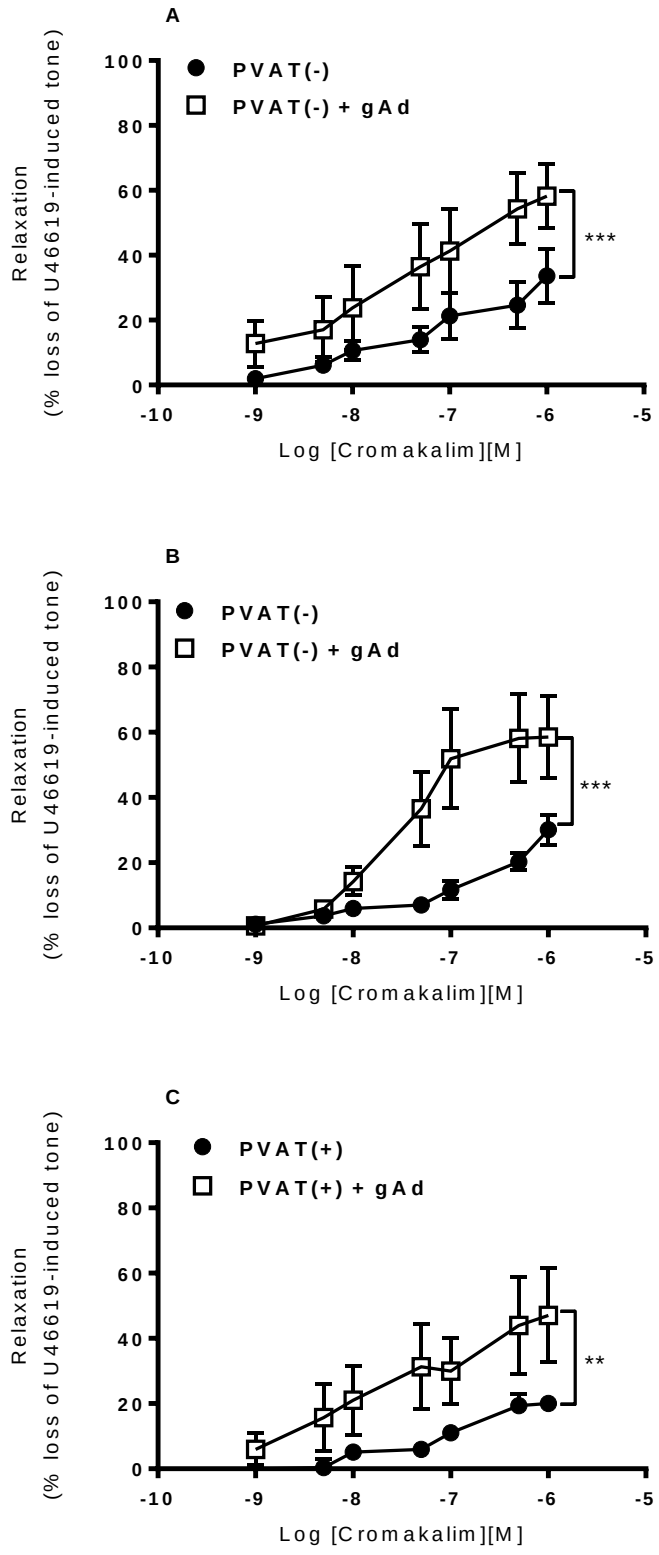

Figure 3-27 Effect of globular adiponectin on vascular relaxation induced by cromakalim.

Dose-response curves to cromakalim before and after addition of gAd to thoracic aorta from WT and KO mice. Data expressed as percentage of loss of U46619 induced tone. (A) Dose-response curve to cromakalim in WT vessels without PVAT ***p<0.001 vs WT PVAT(-) vessels, n = 5. (B) Dose-response curve to cromakalim in KO vessels without PVAT ***p<0.001 vs KO PVAT(-) vessels, n = 5. (C) Dose-response curve to cromakalim in KO vessels with intact PVAT ***p<0.001 vs KO PVAT(+) vessels, n = 5.

3.3.15 Effect of globular adiponectin and conditioned media on AMPK in VSMCs

To investigate whether adiponectin modulates vascular smooth muscle function through activation of AMPK, a VSMC cell line was utilised (Figure 3-28). Over a time course of 10 min and 1 hour, VSMCs were incubated with 1μg globular adiponectin, 100μg globular WT conditioned media and KO conditioned media. In all experiments, neither globular adiponectin nor conditioned media affected AMPK phosphorylation at 10 min (n =3, p = ns; Figure 3-12A) and 1 hour (n = 3, p = ns; Figure 3-28B).

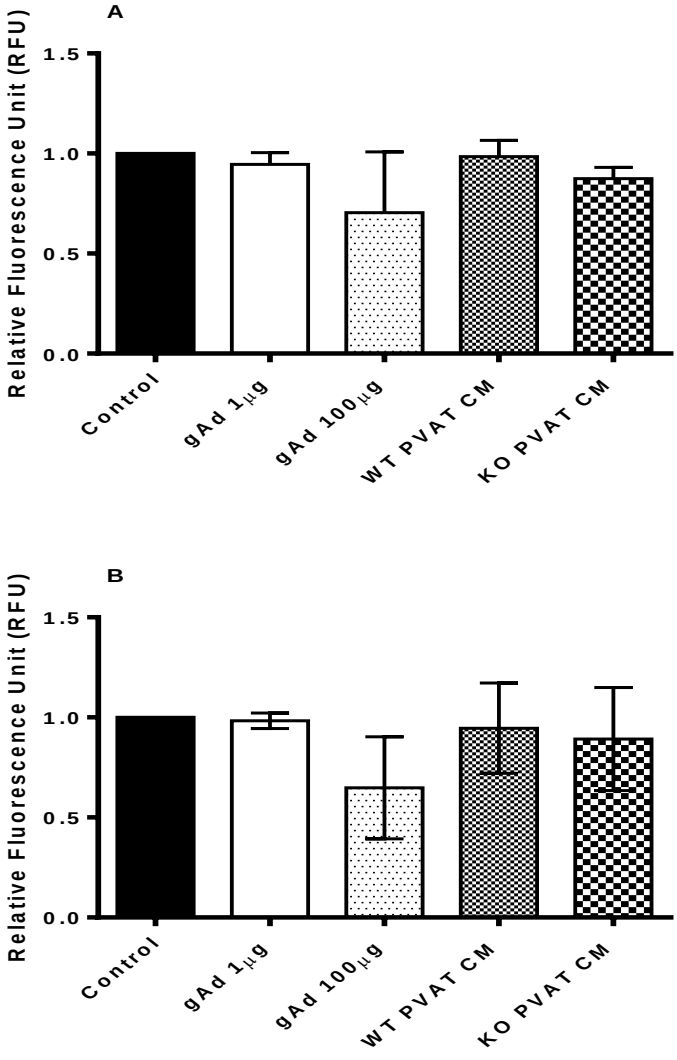

Figure 3-28 Effect of globular adiponectin (gAd) and conditioned media on AMPK in VSMCs.

Cultured rat VSMCs were incubated with globular adiponectin or conditioned media (CM) from WT and KO PVAT over 10 min and 30 min, lysates prepared and subjected to Western blotting with the anti phosphoAMPKα (thr172) antibody. Data are expressed as relative fluorescence units (RFU) to control (untreated). (A) Effect of globular adiponectin and CM on AMPKα phspohorylation at 10 min (n =3, p = ns). (B) Effect of globular adiponectin and CM on AMPKα phosphorylation at 1 hour (n =3, p = ns).

3.4 Discussion

The key observations in this chapter are that PVAT releases a substance(s) that can enhance the relaxation of preconstricted arteries and which appears to be mediated by the activation of K_{ATP} channel when using K^+ channel opener cromkalim. The effect was not dependent on the endothelium and may be mediated by stimulation of the AdipoR1 receptor. The results also showed that adiponectin augemted the relaxation respose to vasodiling agents.. The impaired anticontractile effect in the AMPKα1 knockout mice may be due to reduced adiponectin release by PVAT since the blunted vasodilation with KO PVAT was restored by globular adiponectin. These findings suggest that in KO PVAT, dysfunctional secretion may be related to lack of AMPKα1 in the PVAT.

3.4.1 Effect of AMPKα1 subunit deletion on PVAT phenotype

The first aim of this chapter was to study the effect of AMPKα1 ablation on morphological features of the PVAT by looking at phenotypic characteristics and comparing them with corresponding wild type littermates. This was performed by directly comparing the histological appearance of thoracic, abdominal and mesenteric PVAT to mouse interscapular BAT and epididymal WAT using H&E and UCP-1 as a marker for BAT. Examination of the tissue with standard histological staining (Figure 3-1) indicated structural similarity between thoracic aorta PVAT and brown (BAT) depots and between abdominal aorta PVAT and mesenteric PVAT and white (WAT) depots in both WT and KO. UCP-1 expression results (Figure 3-2 &3-3) showed that thoracic PVAT and BAT are virtually identical. This appears different from abdominal aorta PVAT, which showed an intermediate phenotype between white and brown adipose in histological appearance and analysis of BAT marker expression. Mesenteric PVAT is composed mainly of WAT as confirmed from the histological analysis and reduced UCP-1 expression. The results suggest that AMPKα1 catalytic subunit deletion had no effect on phenotypic features of the PVAT regardless of the PVAT depot type. Results from WT and KO mice are consistent with previous findings from other studies in Sv129 mice strain (Frontini and Cinti, 2010, Cinti, 2011) and also from other mice and rat strains (Cannon and Nedergaard, 2004, Fitzgibbons et al., 2011, Padilla et al., 2013) which reported that thoracic PVAT is composed mainly of a BAT like phenotype and that surrounding the abdominal aorta consists mainly of WAT. However, it is worth noting that these previous studies demonstrate that PVAT can have characteristics of both BAT and WAT but this largely depends on the anatomical context, animal strain and disease state.

Understanding the factors responsible for the difference in the PVAT phenotype throughout the arterial tree is an area of intense investigation. This is because phenotypic differences in PVAT depots may contribute to differences in disease risk in blood vessels. Several studies have reported a relationship between PVAT volume and the severity of vascular disease (Greif et al., 2009, Jeong et al., 2007). Studies have also indicated that PVAT can have a detrimental effect on vascular function and this effect is markedly exacerbated in disease such as obesity (Payne et al., 2010) which was also reported in the aortae (Ma et al., 2010) and mesenteric vessels (Ketonen et al., 2010) of obese rodents. In general, an increase in adipose tissue mass occurs due to adipocyte hyperplasia and/or an increase in triglyceride deposition in the preexisting adipocytes. It has been reported that lack or deficiency of AMPK activity may lead to development of obesity (Ruderman et al., 2003). Previous studies reported that lack of catalytic subunits of AMPK is associated with increased adipose tissue mass. For example, studies of AMPKα2-knockout mice fed a high-fat diet showed increased adipose tissue mass compared with wild-type mice, due to increased adipocyte size, with no change in cell number (Villena et al., 2004). The role of AMPK in the determination of PVAT phenotype was investigated in a study by Ma *et al* who demonstrated that high fat diet reduced activating Thr172 phosphorylation of AMPK in thoracic aortic PVAT, which was associated with not only increased intimal thickness but also increased adipocyte size (Ma et al., 2010). However, the adipocyte size changes reported in these previous studies may be due to reduced FA oxidation and a concomitant increase in lipogenesis resulting from ablation of AMPK in adipose tissue. In addition, the animal models utilized in these studies have a global knockout of AMPKα2 isoform, such that the observed effects may not be a direct effect of reduced AMPK activity in adipose or adipocytes alone.

Brown adipocytes contain high numbers of mitochondria and characteristically express UCP-1, which allows thermogenesis (Tam et al., 2012, Marzolla et al., 2012). AMPKα1 has been reported to be the dominant isoform of the catalytic α subunit of AMPK and is expressed in BAT more than other organs such as liver, suggesting a potential regulatory role for AMPK in BAT (Mulligan et al., 2007). AMPK activity in BAT is increased by cold exposure (Mulligan et al., 2007, Vucetic et al., 2011) and as a result of AICAR or β_3 adrenergic stimulation (Sakaue et al., 2003, Hutchinson et al., 2005, Pulinilkunnil et al., 2011) and this results in increased glucose transport and fatty acid oxidation. Furthermore, it has been reported that AMPK is involved in the regulation of brown adipocyte differentiation. In differentiating brown pre-adipocytes *in vitro*, AMPK activity increases

during differentiation after induction of adipogensis, and siRNA targeted to AMPK inhibited differentiation into mature brown adipocytes, accompanied by a reduction in UCP-1 expression. Additionally, continuous intra peritoneal AICAR administration in mice increased browning of WAT (Vila-Bedmar et al., 2010). This study suggests that AMPK may play a role in differentiation into FA-oxidizing BAT, leading to greater energy expenditure. However, in the current study there was no difference in the expression of UCP-1 between AMPKα1 deficient mice and wild type littermates which might be explained by a compensatory effect of the AMPKα2 subunit isoform, although there was no obvious enhanced expression of the α2 subunit or reduced AMPKα and ACC phosphorylation in KO PVAT. Indeed this has been suggested in other studies which reported that AMPKα1 deficient mice showed no alteration in cold tolerance or acute non-shivering thermogenesis, and that a compensatory increase in AMPKα2 expression may explain this lack of effect (Bauwens et al., 2011).

The absence of any difference in BAT markers between WT and KO PVAT may be related to a reduction of mitochondrial biogenesis PGC1α expression as a result of AMPK dysfunction. β_3-aderenoceptor stimulation in adipocytes results in increased phosphorylation of AMPK and ACC and induced expression of the transcriptional co-activator and master regulator of mitochondrial biogenesis PGC1α (Wan et al., 2014), which regulates UCP-1 transcription (Xue et al., 2005). These effects were reduced in epididymal adipose tissue from AMPKβ_1 KO mice which was also accompanied with a reduction in mitochondrial protein content, including a reduction of PGC1α (Wan et al., 2014). Taking these findings together, the absence of a difference in UCP-1 expression between WT and α_1 KO adipose tissue including PVAT and the findings from other studies suggest the possibility that AMPK's role in determining adipose tissue phenotype might depend on AMPK subunit type, animal strain, age and/or disease state.

3.4.2 Effect of AMPKα1 subunit ablation on AMPK activity

Another important question that was addressed in the present study was whether deletion of AMPKα1 subunit affects the activity of the AMPK in the PVAT, perhaps through compensation by another isoform of AMPK. Results showed reduced phosphorylated and total AMPK in PVAT (Figure 3-5) which correlated with data from immunoblots showing reduced phosphorylation of the downstream kinase ACC (Figure 3-6). There was no obvious compensatory upregulation in the AMPKα2 isoform. These data suggest the reduced activity of AMPK is due to the α_1 subunit deficiency and that the α_1 subunit might

be essential for regulation of AMPK function in adipose tissue. These results are in agreement with other studies demonstrating that the catalytic α1 subunit is the major catalytic subunit isoform expressed in adipose tissue and is also responsible for the major part of AMPK activity (Lihn et al., 2004, Daval et al., 2005).

3.4.3 Effect of AMPK AMPKα1 subunit ablation on anticontractile effect of PVAT

The current study investigated the effect of AMPKα1 subunit deficiency on the anticontractile effect of the PVAT. The studies have been carried out in thoracic and abdominal aortae from both wild-type mice and mice with a global AMPKα1 subunit knockout and using two relaxing agonists acting via different mechanisms. One of these agents is AICAR which known to activate AMPK. In the cytoplasm, AICAR is phosphorylated by adenosine kinase and converted to the active metabolite AICAribotide (ZMP), which mimics AMP and activates AMPK (Corton et al., 1995). AICAR is known to target both AMPKα1 and AMPKα2 and is able to induce aortic relaxation in mice in an endothelium and eNOS independent manner (Goirand et al., 2007). The other agonist used was cromakalim with has not previously been reported to have any effect on AMPK activity. Cromakalim acts via opening of ATP sensitive K^+ channels modulator (K^+_{ATP}) (Glavind-Kristensen et al., 2004) and hyperpolarising the VSMC membrane. In the current study, presence of PVAT augmented the relaxation induced by both agonists (Figure 3-8A &Figure 3-9A). Furthermore, the lack of AMPKα1 caused the PVAT to lose its anticontractile effect and its augmentation of relaxation to cromakalim and AICAR. These findings suggest the AMPKα1 isoform is likely involved in the anticontractile effect of PVAT. The difference in relaxation response between WT and KO is unlikely to be due to AMPK activation at the medial layer by AICAR and cromakalim as cromakalim had no effect on AMPK expression or phosphorylation in VSMCs (Figure 3-19) or cultured adipocytes (Figure 3-20). Furthermore, conditioned medium from WT PVAT was able to enhance relaxation of aortic rings from WT mice or KO mice with similar efficacy, suggesting the defect is at the level of the PVAT.

The present data support and add to the plethora of evidence that PVAT has an anticontractile effect in different vascular beds including human subcutaneous vessels, internal mammary artery, rat mesenteric, and rat aorta (Gao et al., 2005b, Greenstein et al., 2009) and also attenuates contraction to many agents including phenylephrine, 5-HT, angiotensin II and U46619 (Lohn et al., 2002, Verlohren et al., 2004, Gao et al., 2005a).

The mechanism for the attenuation of contraction by PVAT has been proposed as release of transferable relaxation factor(s) with unknown identity, termed adventitia-derived relaxation factor (ADRF) (Lohn et al., 2002). Results from the current study agree with this in that transfer of CM from WT mice augmented relaxation of aortic rings with PVAT. In addition, it was not necessary for the PVAT to be in contact with the vessel to exert an anticontractile effect. In the protocol CM was added prior to contraction of the vessel ring with U46619 and it was found that WT but not KO CM attenuated aortic contraction. This strongly suggests a transmissible factor is responsible for attenuating contraction and augmenting relaxation which is produced by aortic PVAT and in the KO mice this factor is reduced or absent and these findings are in agreement with many other studies (Lohn et al., 2002, Verlohren et al., 2004, Gao et al., 2005b, Malinowski et al., 2008, Greenstein et al., 2009).

3.4.4 AMPKα1 knockout PVAT is assochied with adipocytokines release dysfunction

PVAT is known to release many adipokines which can act in a paracrine fashion toward the blood vessels (Maenhaut and Van de Voorde, 2011). In 2002, Lohn and coworkers showed that the anticontractile effect of the PVAT is due to release of a transferable factor, termed ADRF (Lohn et al., 2002). Since then, many studies have revealed numerous adipokines that are involved in regulation of vascular tone (reviewed in Almabrouk et al., 2014). The adipokines with vasodilatory properties are adiponectin (Fesus et al., 2007), omentin (Yamawaki et al., 2010) and visfatin (Yamawaki et al., 2009). The contractile adipokines include Ang II (Soltis and Cassis, 1991) and resistin (Walcher et al., 2010). Adipokines with both contractile and anticontractile properties are reactive oxygen species (Fang et al., 2009, Gao et al., 2007), leptin (Nakagawa et al., 2002), TNF-α (Brian and Faraci, 1998) and apelin (Japp et al., 2008).

The release of the vasorelaxing factors (ADRF) has been reported to be dependent on Ca^{2+} and is regulated by intracellular signalling pathways involving tyrosine kinase and protein kinase A and independent of perivascular nerve endings (Dubrovska et al., 2004). This is in contrast to the study by Weston *et al*. which proposed that under basal, noncontracted conditions, β_3- stimulation in rat mesenteric PVAT induces release of an adipocyte-derived hyperpolarizing factor that is probably adiponectin (Weston et al., 2013). There are very few studies where the role of AMPK in release of ADRFs has been investigated. A study by Lihn *et al* indicated that the AMPK activator AICAR stimulated adipose tissue

AMPKα1 activity and adiponectin gene expression and reduced the release of TNF-α and IL-6 (Lihn et al., 2004). These cytokines have been shown to have inhibitory effects on adiponectin gene expression and release (Fasshauer et al., 2002, Maeda et al., 2002, Greenberg et al., 1991), such that activity of AMPK in the PVAT could regulate adiponectin expression (Lihn et al., 2004). Similarly, the PPARγ agonist troglitazone which also activates AMPK has a positive effect on adiponectin expression in mature adipocytes (Phillips et al., 2003, Sell et al., 2006). However, other studies using cultured 3T3-L1 adipocytes found that prolonged exposure to the AMPK activating agent metformin actually causes a significant reduction in adiponectin protein content of the adipocytes (Huypens et al., 2005). Another study reported that metformin had no effect on serum adiponectin concentration or adipocyte adiponectin content in type 2 diabetic patients (Phillips et al., 2003, Tiikkainen et al., 2004). In human adipose tissue, activation of AMPK by AICAR also reduces the expression and release of TNFα and interleukin-6 (IL-6) (Lihn et al., 2004, Sell et al., 2006). Furthermore, as it has been demonstrated that TNFα inhibits adiponectin expression (Kappes and Loffler, 2000), reduced TNFα expression results in up-regulation of adiponectin expression, such that the effects of AICAR on adiponectin may be indirect (Daval et al., 2006). To clarify how AMPKα1 KO affects the secretion of adipocytokines by aortic PVAT, an adipokine array was performed. Results showed that KO PVAT exhibits secretory dysfunction and the most striking difference was a reduction in adiponectin in KO PVAT and CM (Figure 3-21 &3-22). Quantitative studies using ELISA further confirmed a significant reduction in adiponectin in KO CM (Figure 3-23). Since adiponectin is a vasodilator (Fesus et al., 2007), it could account for the lack of an anticontractile effect in KO PVAT. These findings support previous indications that AMPK might be involved in regulation of adiponectin secretion (Lihn et al., 2004, Phillips et al., 2003), yet the mechanism of regulation needs further investigation.

3.4.5 Adiponectin is a candidate for ADRF

In the present study, the anticontractile effect of thoracic PVAT in wild type mice was abolished using a peptide blocking the effect of adiponectin (Figure 3-24), thereby suggesting that adiponectin might be responsible. This has also been demonstrated previously in human gluteal arteries (Fesus et al., 2007) and mice mesenteric arteries (Lynch et al., 2013). Furthermore, contractility studies conducted on AMPKα1 knockout mice demonstrated that PVAT was unable to attenuate contractility to U46619 as was observed with WT PVAT. It can therefore be proposed that impaired PVAT action is due

to the reduction in the release of adiponectin from the PVAT. The current study also demonstrated the ability of vessels to respond to exogenous globular adiponectin (Figure 3-27). The globular adiponectin used for this study is known to have a higher affinity for AdipoR1 and low affinity for AdipoR2 (Kadowaki et al., 2006, Ketonen et al., 2010, Lynch et al., 2013). Since all rings were denuded of endothelium, an effect of adiponectin on the endothelium or generation of endothelium-derived mediators can be ruled out and the action is likely mediated by the vessel media (Weston et al., 2013). Additionally, vascular relaxation was seen in both wild type and AMPKα1 knockout vessels suggesting that adiponectin can act directly on vascular smooth muscle cells through AdipoR1 and that the AMPK expressed in these vessels may not involved. In the array experiment, neither globular adiponectin nor conditioned media was able to phosphorylate AMPKα in cultured vascular smooth muscle cells which further suggests that adiponectin can induce effects in vascular smooth muscle cells directly (Figure 3-28). This is in contrast to the study by Lynch *et al* which demonstrated that adiponectin induces an anticontractile effect in an endothelium-independent manner which involves activation of AMPK in the vascular smooth muscle layer and subsequent BK_{Ca} channel activation (Lynch et al., 2013). Furthermore, adiponectin receptor antagonism and the AMPK inhibitor compound C have been reported to attenuate vascular relaxation, whereas globular adiponectin failed to induce vascular relaxation in AMPKα_2-deficient mice (Meijer et al., 2013). Such results, together with the findings from the current study, indicate that adiponectin may be the potential vasodilator molecule released by PVAT and that AMPK may regulate its release.

3.4.6 Role of K_{ATP} channels in anticontractile effect of PVAT

Two different vasodilators have been used in this study; AICAR which is a known AMPK activator and the K_{ATP} channel opener cromakalim. Indeed, PVAT enhanced the relaxation response induced by both agents. However, it is difficult to draw the conclusion that the observed AICAR-enhanced relaxation is due to PVAT as stimulation of VSMCs and 3T3-L1 adipocytes with AICAR increased AMPK activity. Therefore, the data with AICAR as a vasorelaxant should be treated with caution and need to be investigated further. As stated previously, PVAT also enhances the relaxation response to the K_{ATP} channel activator, cromakalim, which suggests the involvement of vascular smooth muscle K_{ATP} channels. The role of this channel in the endothelium-independent vascular relaxation induced by PVAT has been suggested in a previous study by Lohn *et al*. in which the PVAT transferable factor was not identified (Lohn et al., 2002). Vascular ATP-dependent K^+ channels are activated by a number of conditions such as ischaemia and hypoxia and the

mechanism may be mediated by a fall in the intracellular ATP concentration or by a rise in the intracellular ADP concentration. Opening of K_{ATP} channels results in cell membrane hyperpolarisation and subsequent inactivation of voltage gated Ca^{2+} channels. This will lead to a decrease in intracellular free Ca^{2+} of the smooth muscle cells and thus to a dilation of the artery. As these channels are accompanied by efflux of Ca^{2+} into VSMCs, it is logical to think that will result in activation of AMPK in the medial layer of the artery. To rule out this issue, studies conducted using VSMCs treated with cromakalim and AICAR showed that treatment with cromakalim was not associated with either increased phosphorylation or activity of AMPK in VSMCs. Hypoxic vasodilation in isolated, perfused guinea pig hearts can be prevented by glibenclamide, a blocker of adenosine triphosphate (ATP)-sensitive potassium channels, and can be mimicked by cromakalim, which opens ATP-sensitive potassium channels. (Daut et al., 1990). These channels have been found to be involved in regulation of basal vascular tone in a number of vascular bed including the coronary circulation (Samaha et al., 1992) and mesenteric vessels (Nelson and Quayle, 1995) and inhibition of this channel by glibenclamide has been found to attenuate coronary and cerebral autoregulation (Narishige et al., 1993, Hong et al., 1994). In the current study, PVAT enhanced the relaxation induced by cromakalim and that suggests PVAT can induce endothelium-independent relaxation which may involve the K_{ATP} channel or perhaps increasing the sensitivity of the channel. However, the role and the mechanism of activation needed to be further investigated.

3.5 Conclusion

This study has shown that PVAT has a profound anticontractile effect on mouse aortic rings. The effect may be due to release of adiponectin by the PVAT and this release is regulated by the activity of AMPKα1. In mouse aortic rings, adiponectin augments relaxation to cromakalim in an endothelium-independent manner although other effects of adiponectin on the endothelium cannot be ruled out. The study also demonstrated perivascular adventitial adipose tissue elaborates an adiponectin factor that acts at least in part by an effect on ATP-dependent K^+ channels. Clinically, there is evidence that PVAT becomes dysfunctional in obese humans and plasma adiponectin is reduced (Aghamohammadzadeh et al., 2015). Alterations in AMPK activity in the PVAT may be behind this effect.

Chapter 4

Role of AMPK in regulation of redox state of the PVAT and its effect on vascular function

4.1 Introduction

Many studies have demonstrated that PVAT or conditioned media can attenuate vessel contraction to various agonists including phenylephrine, 5-HT, angiotensin II and U46619 in the mouse aorta, rat mesenteric arteries and human internal thoracic arteries (Lohn et al., 2002, Verlohren et al., 2004, Gao et al., 2005b, Gao et al., 2005a). The mechanisms for the attenuation of contraction by PVAT are not fully understood, but the release of transferable relaxation factor(s) with unknown identity, termed adventitium-derived relaxation factor (ADRF), has been proposed. Several candidates have been suggested including adiponectin (Fesus et al., 2007), angiotensin-(1-7) (Lu et al., 2010), H_2O_2 (Gao et al., 2006), leptin (Galvez-Prieto et al., 2012), H_2S (Fang et al., 2009), methyl palmitate (Lee et al., 2011). Many of these transferable vasoactive factors induce an anti-contractile effect through increasing NO synthesis and release by the endothelium (Galvez-Prieto et al., 2012) and/or targeting K^+channels in vascular smooth muscle (Gao et al., 2007). It was also recently shown that PVAT from the thoracic aorta expresses the endothelial isoform of NO synthase (eNOS) (Araujo et al., 2015, Xia et al., 2016) and releases NO itself. PVAT-derived NO contributes to relaxation in both endothelium-intact and denuded thoracic aortic rings, indicating NO as a potential ADRF in this vessel (Xia et al., 2016).

On the other hand, a few studies have identified a procontractile effect of PVAT. Soltis and Cassis showed data indicating a contraction of PVAT-intact rat aorta in response to electrical field stimulation which was absent in tissues without PVAT (Soltis and Cassis, 1991). Similar findings were also reported in rat mesenteric arteries (Gao et al., 2006). This effect is thought to involve production of superoxide ($O_2^{\cdot-}$) by stimulation of NADPH oxidase in PVAT adipocytes (Gao et al., 2006). PVAT is a potential source of reactive oxygen species (Gao et al., 2006), which are by products of many reactions including cyclooxygenase-mediated production of prostanoids and uncoupling of eNOS from making NO (Mayr et al., 2005). There are two common ROS species that have been reported to affect vascular contractility; $O_2^{\cdot-}$ and H_2O_2. Apart from H_2O_2, which is a vasodilator (Gao et al., 2007), ROS can induce vasoconstriction via many mechanisms including: increasing the degradation of NO, formation of peroxynitrite, a strong cytosolic oxidant generated by the reaction of the $O_2^{\cdot-}$ with NO which inactivates PGI synthase and shifts the production of prostacyclin to that of other vasoconstrictor prostanoids or directly targeting the vascular smooth muscle layer by either induction of depolarisation or inhibition of ATP-sensitive potassium channels (K_{ATP}), voltage-activated potassium channels (K_v) and large conductance calcium-activated potassium channels (BK_{Ca}) (Wong and Vanhoutte, 2010).

The physiological significance of PVAT-derived O_2^- is still elusive, although there is some evidence suggesting that $O_2^{\cdot-}$ may affect vascular tone. It has been reported that $O_2^{\cdot-}$ released from mesenteric PVAT can potentiate the contraction of blood vessels to electric field stimulation (Gao et al., 2006). In denuded vessels, scavenging of O_2^- with exogenous superoxide dismutase (SOD) reduced contraction to phenylephrine in aortic arteries with intact PVAT but not those devoid of PVAT (Gao et al., 2007).

AMPK is a key regulator of cellular energy homeostasis and is activated in response to changes in energy status (Rubin et al., 2005, Adams et al., 2004). Activation of AMPK subsequently modifies the balance between energy generating and consuming metabolic pathways, enabling conservation of cellular energy status (Hardie and Carling, 1997). One of the vasculoprotective roles of AMPK is the control of vascular redox status. Oxidative stress and disturbed antioxidant defence is associated with endothelial dysfunction in vascular injury and atherosclerosis (Siersbaek et al., 2010, Sata et al., 2002). Increased production of oxidant species in the diseased vascular wall is associated with reduced NO production and further formation of damaging species such as peroxynitrite (Sata et al., 2000). The role of AMPK in alleviation of disturbed redox balance has been addressed in many studies. AMPK activation in HUVECs with AICAR was found to increase levels of superoxide dismutase (SOD), the enzyme responsible for removal of O_2^- (Kukidome et al., 2006). AICAR activation of AMPK in HUVECs also causes uncoupling of protein-2 expression which diminishes $O_2^{\cdot-}$ production and prostacyclin synthase nitration in diabetes (Serrano et al., 1997). In contrast, some studies have reported that AMPK is itself activated by ROS. Metformin has been proposed to activate AMPK via an increase in mitochondrial reactive nitrogen species (Zou et al., 2004). Additionally, Coi *et al* reported that statins induced ROS generation and that peroxynitrite was responsible for AMPK activation (Choi et al., 2008). Similarly, activation of AMPKα1 in HUVECs with low O_2 concentrations occurred as a result of mitochondrial ROS and was responsible for increased expression of antioxidant genes such as catalase and SOD (Colombo and Moncada, 2009). Furthermore, silencing of AMPKα1 was associated with enhanced oxidative stress, reduced expression of antioxidant defence genes such as catalase and SOD and diminished expression of NO generating enzyme eNOS (Colombo and Moncada, 2009).

Comparatively little is known about AMPK function in PVAT, although given its role in other tissues, AMPK signalling is likely to be integral to PVAT function (Almabrouk et al., 2014, Ewart and Kennedy, 2011). Loss of AMPK may increase PVAT inflammation and

shift its redox status towards a pro-oxidative environment. Together this could lead to increased PVAT ROS production, reduced NO availability and an impaired ability of PVAT to enhance relaxation. In support of this is the relationship between PVAT oxidative stress and PVAT dysfunction which has been demonstrated previously (Ketonen et al., 2010, Greenstein et al., 2009). Impaired anti-contractile properties of PVAT from obese mice was found to be restored by pre-incubation with free radical scavengers (Ketonen et al., 2010). In another study, PVAT obtained from obese humans had a compromised anti-contractile function which could be improved by treatment with SOD (Greenstein et al., 2009). Results from chapter 3 showed that PVAT from AMPKα1 KO mice exhibited reduced anti-contractile properties. The mechanisms underlying PVAT dysfunction in AMPKα1 KO mice are currently elusive. Therefore, the current hypothesis is that the anticontractile dysfunction may be related to the loss of protective AMPK in the PVAT which shifts the redox balance from NO production by eNOS to ROS production causing an increases in oxidative stress in the PVAT. Taken together, this chapter will investigate the role of AMPK in regulation of redox state of PVAT and how this affects its anticontractile function.

4.2 Aims of the study

- To characterise any differences in ROS and RNS expression between wild type and AMPKα1 KO PVAT

- To define the role of AMPK in the NO-dependent anticontractile effect of PVAT

4.3 Methods & Results

4.3.1 Expression of superoxide anion in wild type and AMPKα1 KO PVAT

To test whether AMPKα1 knockout resulted in enhanced production of $O_2^{\cdot-}$, immunofluorescence confocal microscopy was used. Briefly, thoracic aortic PVAT from WT and KO was dissected and rapidly placed into Krebs-Henseleit solution previously gassed. Segments were incubated with 10^{-5} M DHE for 30 minutes at 37°C in the dark and then washed (2 x 15 min) in KH at 37°C. Negative controls were incubated with 15 U/mL of SOD during exposure to dihydroethidium (DHE). Segments were fixed by immersion in acetic zinc formalin for 1 hour at room temperature, mounted on slides and visualised by confocal fluorescence microscopy. Representative images are shown in Figure 4-1. The

production of intracellular $O_2^{\cdot -}$ in adipocytes of PVAT was confirmed by the presence of dark red fluorescent staining. Upon visual appraisal (Figure 4-1), an enhanced fluorescence intensity seemed to be present in KO PVAT (B) in comparison with wild type (A). However, image analysis of the mean fluorescence intensity (MFI) showed only a non-significant trend toward increased MFI in KO PVAT (Figure 4-1E). The MFI in KO was 43.4 ± 12.6, n = 3 in comparison with 38.8 ± 5.6 n = 5 in WT, (p = ns). The production of $O_2^{\cdot -}$ was reduced by the scavenger enzyme SOD (15 U/mL) in both WT and KO PVAT; the reduction in intensity was more apparent in WT PVAT compared to KO PVAT although analysis of MFI showed that these differences were non-significant (Figure 4-1 C&D) with KO PVAT showing high variability in response to SOD (Figure 4-1E).

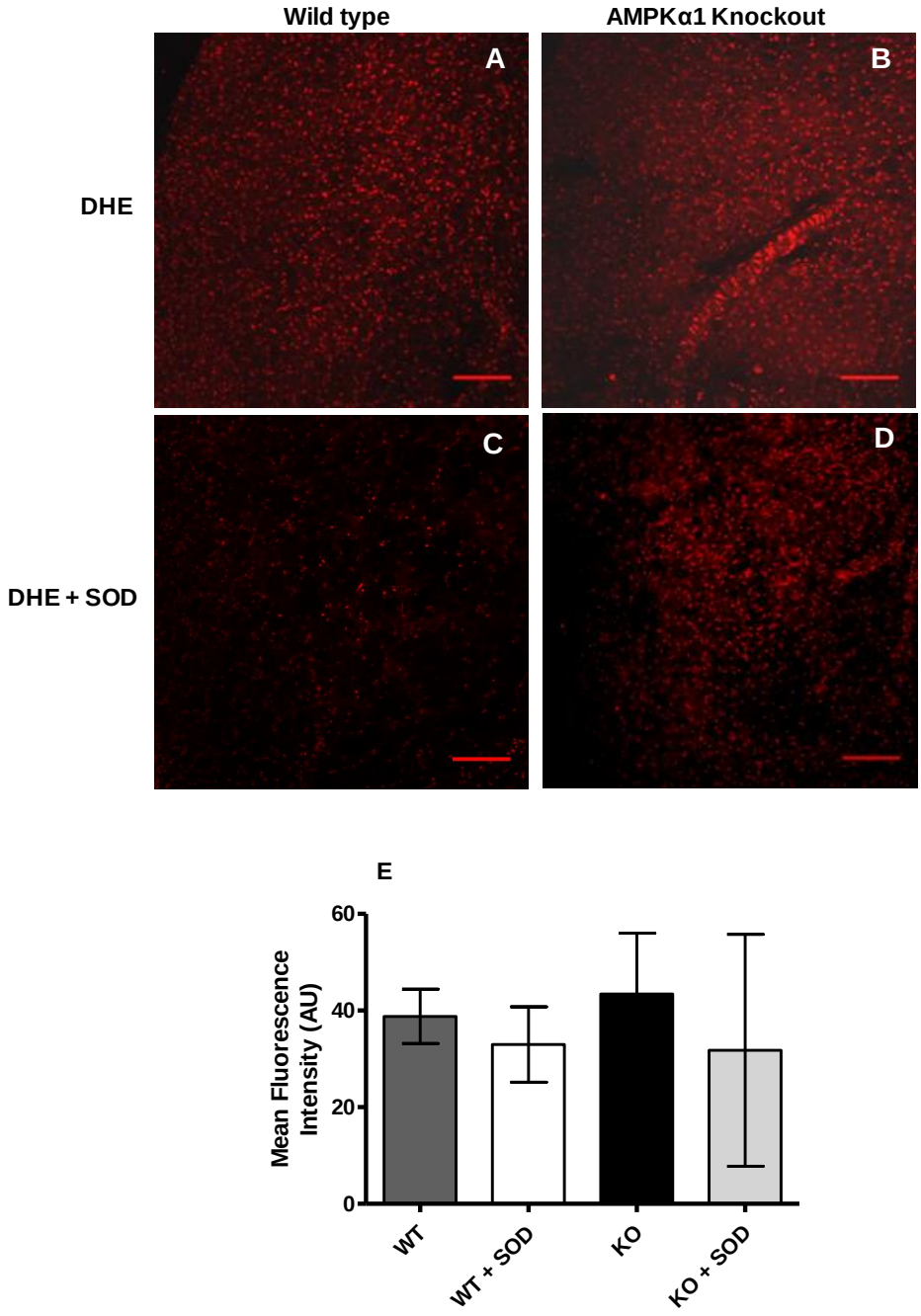

Figure 4-1 Representative Immunofluorescent images showing superoxide production by adipocytes in WT and KO thoracic PVAT, detected with dihydroethidium (DHE).

PVAT was labelled with DHE (10^{-5}M), which emits red fluorescence when oxidized by superoxide. Representative confocal images of WT and KO PVAT showing $O_2^{\cdot-}$ level (A,B) and the effect of treatment with SOD (C,D). (E) Quantitative fluorescence measurement of DHE in the presence and absence of SOD. Scale bar 20μm.

The production of $O_2^{\cdot-}$ by PVAT of each genotype was also evaluated by comparing the levels of nitrotyrosine using immunohistochemical staining with nitrotyrosine antibody. Aortic rings with attached PVAT were dissected from WT and KO and processed as detailed in Section 2.3.3. Briefly, WT and KO thoracic aortae were were excised

immediately after death and placed in 10% acetic zinc formalin overnight. Arteries were processed through a gradient of alcohols to Histoclear and embedded vertically in paraffin wax before being cut into 5 μm sections. Peroxynitrite reacts with protein tyrosine residues to form stable nitrotyrosine moieties which can be detected with specific antibodies and is used as a marker for peroxynitrite activity (Libby, 2002). Polymer-based immunohistochemistry was used to evaluate nitrotyrosine expression in PVAT from WT and KO mice. Figure 4-2 shows representative images of WT and KO aortic PVAT stained with nitrotyrosine antibody. Upon visual assessment, diffuse nitrotyrosine expression was apparent in the aortic PVAT of both strains. The intensity of antibody staining appeared greater in PVAT from AMPKα1 KO mice (n=3).

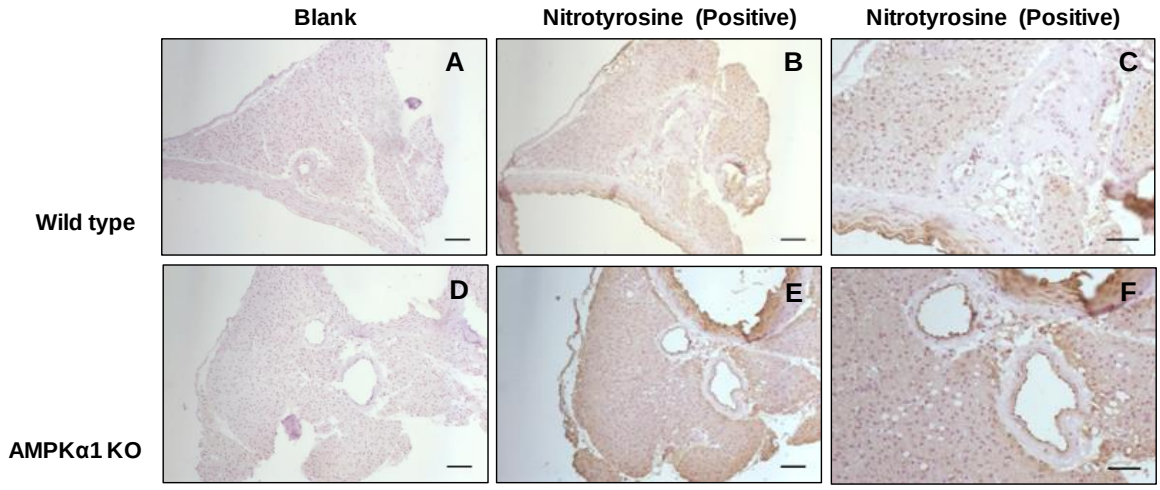

Figure 4-2 Nitrotyrosine expression in aortic PVAT from wild type and AMPKα1 knockout mice.

Representative histological sections of thoracic aorta with intact PVAT from WT and KO mice stained with anti-nitrotyrosine antibody and counterstained with haematoxylin. Positive staining is indicated by brown colour (B,C,E,F) and blank (untreated) is represented in A&D. Scale bar 20μm (A, B, D, E), 10μm (C,F).

4.3.2 eNOS and NO levels in WT and KO PVAT

To determine the effect of AMPKα1 deletion on NO production by PVAT, two approaches were used. Firstly, the effect of AMPKα1 ablation on the protein levels and phosphorylation state of eNOS in the PVAT was assessed. Expression of eNOS was measured by Western blot analysis as detailed in Section 2.7. Briefly, WT and KO PVAT samples were dissected free and lyastes were prepared. Protein content analysis from these

lysates was performed and protein was added at 10 μg per well. Immunoblotting was performed with antibodies against phospho-eNOS, total-eNOS and GAPDH which was used as a loading control. Membrane visualisation of immunolabelled bands was carried out using an Odyssey Sa Infrared Imaging System (LI-COR, USA) linked with Odyssey Sa Infrared Imaging System software (LI-COR, USA) (all antibody dilutions found in Table 2.5). Densitometric analysis of the blots demonstrated that the ratio of phosphorylation (p-eNOS)(ser1179) relative to total eNOS (t-eNOS), was significantly reduced in AMPK-α_1 knockout PVAT in comparison with wild type ($p<0.05$, n = 3) (Figure 4-3B). Similarly, total eNOS was also reduced in KO PVAT in comparison to WT PVAT ($p<0.01$, n = 3 vs KO PVAT) (Figure 4-3C)

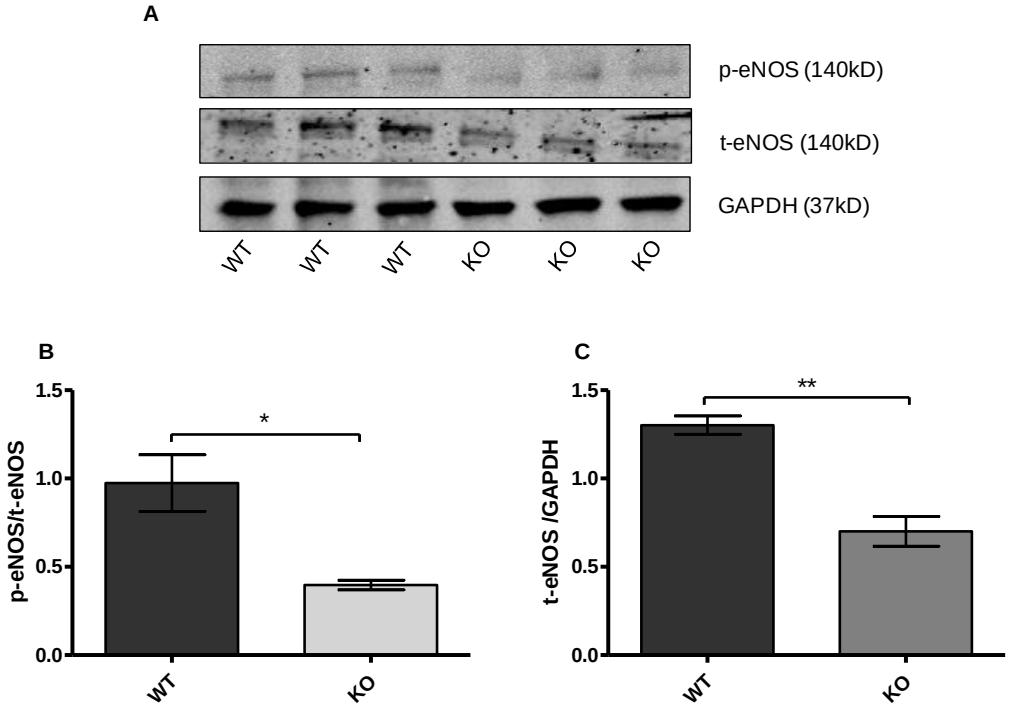

Figure 4-3 eNOS expression and activity in PVAT.

PVAT samples from wild type and AMPKα1 knockout were lysed and immunoblotting for total and phospho-eNOS (Ser1179) was performed. (A) Representative immunoblots are shown. (B) Densitometric analysis of immunoblots, presented as ratio of phosphorylated eNOS relative to total eNOS and ratio of total eNOS divided by by GAPDH (C). *p<0.05 vs KO PVAT, n = 3; **p<0.01 vs KO PVAT, n = 3.

The difference in the production of NO in aortic PVAT between WT and KO was also evaluated with the fluorescent dye DAF-2DA using immunofluorescence confocal microscopy. Preparation of PVAT samples was described in section 2.8.1. PVAT samples were incubated in 10 μM DAF-2DA for 30 minutes. 0.1 mM Nω-nitro-L-Arginine (L-NNA) and 15 U/L SOD were used as negative and positive controls respectively. After

fixation, samples were incubated in 1 μM SYTO 61 fluorescent nucleic acid stain (Thermo Fisher Scientific, UK) for 1 hour prior to mounting and confocal microscopy examination. Representative images of which are shown in Figure 4-4.

There was no difference in basal DAF-2DA fluorescence intensity between WT and KO (Figure 4-4 A, D). Incubation with the NOS inhibitor L-NNA visually reduced the fluorescence intensity in both genotypes (Figure 4-4B, E), yet this was not significant (Figure 4-4 G). In the presence of SOD, the fluorescence intensity was increased as assessed visually in both WT and KO (C, F). Statistical evaluation of the mean fluorescence intensity showed a non-significant trend toward increased enhanced production of NO in the presence of SOD (Figure 4-4 G).

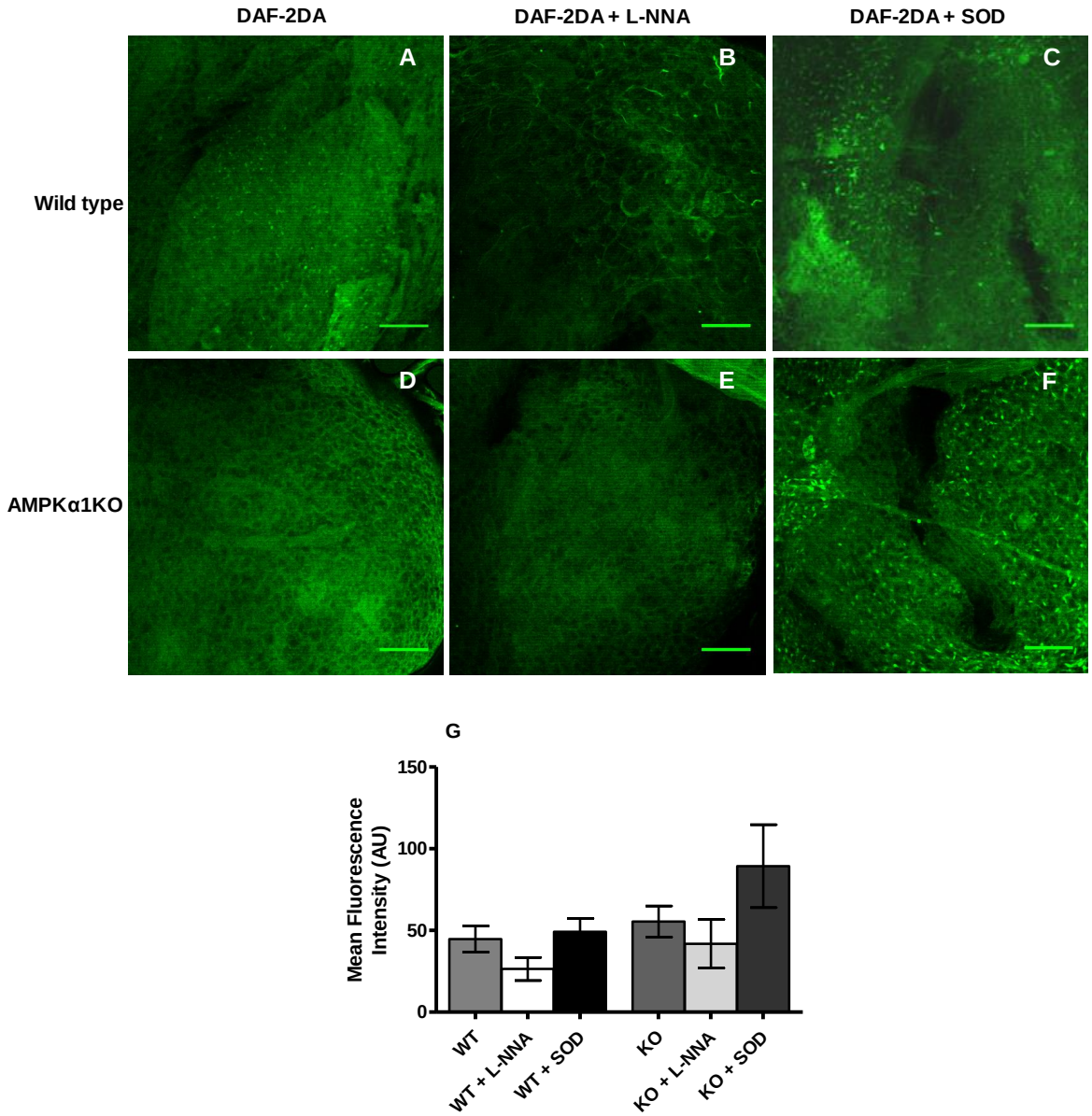

Figure 4-4 DAF-2 fluorescence in WT and KO thoracic PVAT.

PVAT was labelled with DAF-2DA (10 μM), which is hydrolysed to the impermeable 4,5 - diaminofluorescein (DAF-2) by cellular esterases. DAF-2 subsequently reacts with cellular NO to form the fluorescent triazolofluorescein. PVAT samples were then treated with either L-NNA (0.1 mM) or SOD (15 U/L). Representative confocal images of WT and KO PVAT showing NO production (A,D) and the effect of treatment with L-NNA (B,E) and SOD (C,F). (G) Quantification of DAF-2 mean fluorescence intensity in presence and absence of L-NNA or SOD. Scale bar 20μm.

4.3.3 Effect of PVAT on Sodium nitroprusside-induced relaxation

To determine the influence of AMPK in the PVAT on mediating relaxation of aortic rings to exogenous NO, concentration-response curves to the NO donor sodium nitroprusside were constructed. Denuded aortic rings with and without PVAT were dissected from WT and KO mice and cut into 2 mm segments and mounted on two 40 μm diameter wires in a small artery wire myograph as detailed in Section 2.4. Arterial rings were maintained in Krebs' solution at 37 °C and gassed continuously with 95 % O_2 and 5 % CO_2. Following a 30 minute equilibration period, the vessels were set to 1g optimal tension of. Viability of arterial rings was evaluated with 40 mM KCl. Following this, the artries were washed and pre-constricted with U46619 for a further 30 minutes. Cumulative dose-response curves to increasing concentrations nitric oxide donor sodium nitroprusside were constructed. Data were expressed as a percentage of loss in the vascular tone induced by U46619.

In rings from both WT and KO mice, the presence of thoracic PVAT had no effect on the relaxation induced by sodium nitroprusside (Figure 4-5 A&B). However, in wild type vessels without PVAT, sodium nitroprusside produced a maximum relaxation (E_{max}) of 36.2 ± 6.6%, (n = 6) which was approximately double the E_{max} observed in the KO (20.7 ± 5.5%, n = 9, $p < 0.05$) suggesting a dysfunctional vascular smooth muscle layer in AMPKα1 knockout mice (Figure 4-5C).

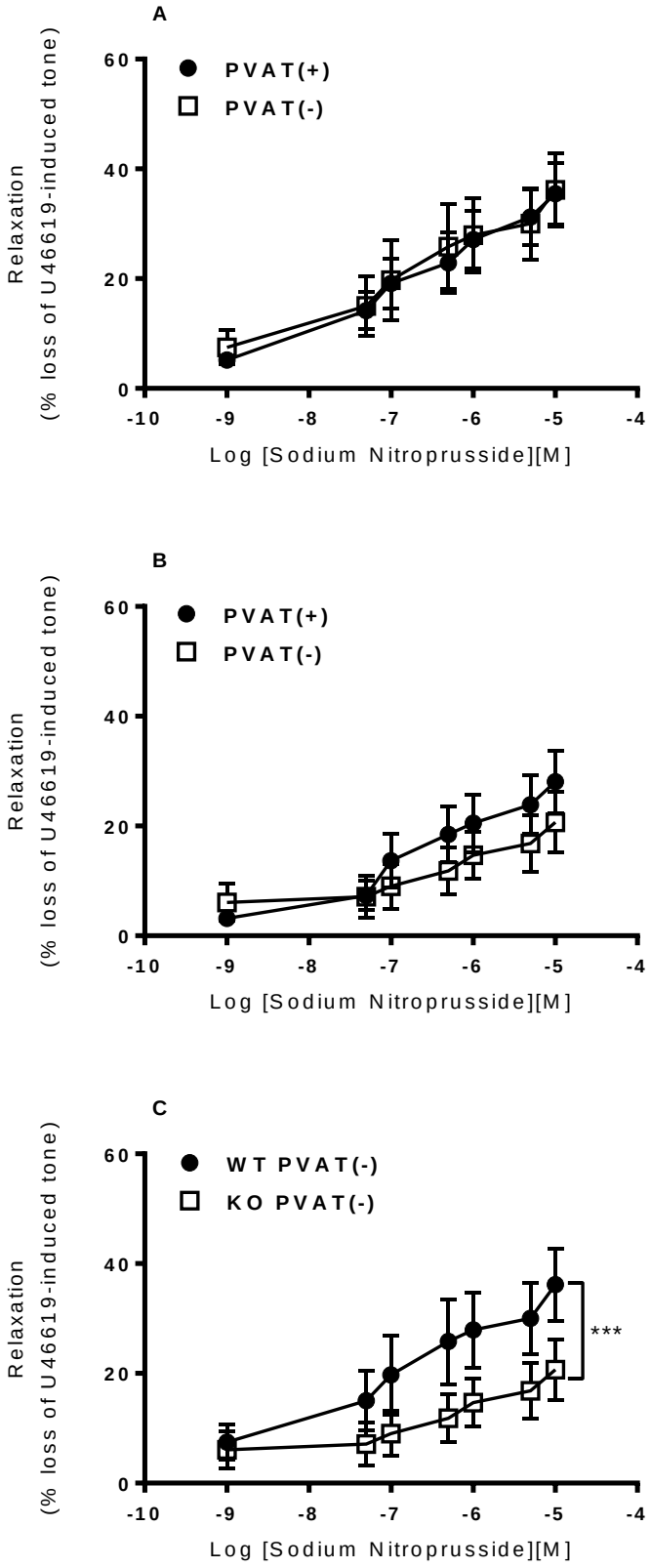

Figure 4-5 Effect of PVAT on Na nitroprusside-induced relaxation in wild type and knockout thoracic aorta.

Dose-response curves to Na nitroprusside (SNP) were produced by wire myography of thoracic aortic rings from (A) WT or (B) KO mice with (+) and without (-) PVAT. All vessels were without endothelium. (C) Comparison of effect of SNP in vessels from each genotype lacking PVAT. (n = 6, ***p<0.001).

4.4 Discussion

The aim of this chapter was to investigate the role of AMPK in regulation of the redox state in PVAT. The results presented show that (1) ROS production appears to be similar in both WT and KO PVAT, although the expression of nitrotyrosine, a marker for peroxynitrite appears higher in KO PVAT. (2) The level of NO appeared to be similar in both types of PVAT, although there was a significant reduction in the levels of phospho-eNOS and proportion of eNOS phosphorylated in KO PVAT when quantified by Western blotting. (3) There was a reduced relaxation to sodium nitroprusside in KO aortic rings, which indicates dysfunctional medial smooth muscle.

4.4.1 Role of AMPK in regulation of ROS release from PVAT

Many studies have now established that AMPK is a critical regulator of vascular redox balance. AMPK has been reported to abolish the formation of ROS by NADPH oxidase and induce NO production by eNOS (Fisslthaler and Fleming, 2009). Silencing of the AMPKα1 subunit isoform has also been reported to be associated with reduced expression of MnSOD, catalase, γ-glutamylcysteine synthase and thioredoxin, in endothelial cells (Colombo and Moncada, 2009). Conversely, activation of AMPK by AICAR or AMP can suppress the production of $O_2^{\cdot-}$ stimulated by phorbol esters or fMLP (Formyl-Methionyl-Leucyl-Phenylalanine) in neutrophils (Alba et al., 2004). Furthermore, activation of AMPK by rosiglitazone effectively attenuated the generation of ROS in HUVECs exposed to a high glucose concentration (Ceolotto et al., 2007). Not only this, AMPK can also influence the cellular redox balance via inhibition of prostacyclin synthase in endothelial cells by prevention of tyrosine nitration through upregulation of UCP-2 (Xie et al., 2008). As AMPK is expressed in all layers of the vascular wall including PVAT, it is plausible that AMPK is also involved in regulation of the redox state of the PVAT itself.

PVAT is known to release ROS such as $O_2^{\cdot-}$ (Ketonen et al., 2010). This chapter aimed firstly to investigate the role of AMPK in regulation of ROS production by looking at levels of $O_2^{\cdot-}$ and peroxynitrite. Using confocal microscopy, experiments using DHE fluorescence as a measurement of $O_2^{\cdot-}$ showed that there was no difference in the levels of $O_2^{\cdot-}$ between WT and KO PVAT (Figure 4-1). The absence of a difference may be attributed to the DHE which is known to produce multiple fluorescent products with overlapping emission spectra, only one of which is specific to $O_2^{\cdot-}$ (Fink et al., 2004, Zhao et al., 2003). DHE can be oxidized by oxidants other than $O_2^{\cdot-}$, such as H_2O_2 and

cytochrome C which can produce excitation emissions that are relatively near the excitation emission of DHE. Therefore, the detection system used in this study will have captured the composite spectra of non-specific DHE products and therefore the intensity values reported may reflect not just $O_2^{\cdot-}$ production by the PVAT but other radicals as well (Zhao et al., 2005). The issue of the DHE signal being nonspecific was investigated by incubating the PVAT with the superoxide scavenger SOD to enable $O_2^{\cdot-}$ specific fluorescence to be estimated. There was a reduction in the intensity in both WT and KO PVAT which was inconsistent and variable and which suggests perhaps a low production of extracellular $O_2^{\cdot-}$ that cannot be estimated by using unconjugated SOD. It has been reported that $O_2^{\cdot-}$ has a restricted ability to diffuse through cell membranes and so endogenous SOD is largely confined to intracellular compartments (Szabo et al., 2007). Application of unconjugated SOD which has a limited permeability makes the interpretation of the current data difficult as it may have been unable to access the site of $O_2^{\cdot-}$ generation. Alernatively, the current data suggest the need for more quantitative tools which are more specific for detecting $O_2^{\cdot-}$ and also using a more permeable form of SOD such as polyethylene glycolated SOD (Laurindo et al., 2008, Beckman et al., 1988).

Despite the findings that PVAT NO and $O_2^{\cdot-}$ levels were similar in both WT and KO PVAT, the content of peroxynitrite (detected as nitrotyrosine) was greater in the KO PVAT (Figure 4-2), suggesting an imbalance in the NO pathway. Peroxynitrite is a strong oxidant and nitrating compound formed from the extremely rapid reaction between $O_2^{\cdot-}$ and NO. The cellular source of NO is various NOS isoforms, whereas $O_2^{\cdot-}$ sources include the mitochondrial electron transport chain, NADPH oxidase and xanthine oxidase. Moreover, a deficiency in NO substrate (L-arginine) or cofactors (tetrahydrobiopterin) can lead to uncoupling of NOS and a shift towards generation of $O_2^{\cdot-}$ which will lead to oxidative stress (Liaudet et al., 2009). It is worth noting that the reaction of NO with O_2^{-} depends on the ratio of superoxide to NO which means that peroxynitrite production does not depend on enhanced NO or $O_2^{\cdot-}$ generation and that the generation of peroxynitrite under normal physiological conditions occurs when there are equal levels of both NO and $O_2^{\cdot-}$ (Pacher et al., 2007). More importantly, the rate of the formation of peroxynitrite is greater than the rate of superoxide decomposition by SOD (Liaudet et al., 2009). Therefore, any minimal changes in the rate of NO and $O_2^{\cdot-}$ generation can result in a substantially larger increase in the rate of peroxynitrite formation meaning that undetectable differences in NO and superoxide which were observed in this study, could manifest as significant differences in nitrotyrosine levels (Pacher et al., 2007).

In this study, nitrotyrosine levels were greater in aortic KO PVAT. A possible explanation of the difference is that mouse aortic PVAT has a similar morphology and gene expression profile to BAT, suggesting it performs similar functions (Frontini and Cinti, 2010, Fitzgibbons et al., 2011), which was also observed in chapter 3. In contrast to WAT, BAT is rich in mitochondria, reflected by the high metabolic activity and is a potent source of oxygen radicals (Cannon and Nedergaard, 2004, Lopez-Torres et al., 1991). Generation of oxygen radicals may contribute to an increased capacity to generate peroxynitrite (Radi et al., 2002). Deletion of AMPKα1 subunit in aortic PVAT was associated with increased nitrotyrosine expression, potentially due to augmented peroxynitrite production secondary to a disrupted metabolic and redox balance in the absence of AMPK.

4.4.2 Effect AMPKα1 deletion on eNOS and NO levels

Previous studies have demonstrated that eNOS is also expressed in white adipose tissue (Motoshima et al., 2004, Boyle et al., 2008). Another study using an immunohistochemical approach has reported eNOS staining within PVAT surrounding saphenous vein (Dashwood et al., 2007). The findings from the current study support previous data that PVAT (Figure 4-1A&B), and eNOS in the PVAT produce NO (Figure 4-4). The current study also showed that the levels of eNOS are downregulated in KO PVAT suggesting a potential link between AMPKα1 subunit and eNOS function in the PVAT. However, data from confocal analysis of DAF-2 fluorescence indicated no difference in the NO production between WT and KO PVAT. Furthermore, the production of NO by PVAT was supported using L-NNA which reduced NO-dependent fluorescence in both types of PVAT, albeit non-significantly and SOD, which caused a non-significant enhancement in NO-fluorescence (Figure 4-4). The absence of any difference in the NO fluorescence between WT and KO despite KO PVAT showing reduced levels of eNOS phosphorylation may be explained in two ways. Firstly, the NO fluorescence detected using DAF-2DA in the KO mouse may be a compensatory NO production from other NOS isoforms such as iNOS. Secondly, DAF-2DA is associated with high background fluorescence, believed to result from inherent fluorescent properties of the inactivated DAF-2 probe and its reaction products (Rodriguez et al., 2005). Low NO levels being produced in the PVAT may be obscured by background fluorescence and make the detection of any difference between KO and WT more difficult.

4.4.3 PVAT anticontractile effect in response to NO donor

As the AMPKα1 KO exhibited reduced expression of eNOS and enhanced expression of peroxynitrite, which suggests a redox status imbalance, this study further aimed to examine the functional properties of the PVAT by looking at the PVAT anticontractile effect. Dose response curves to sodium nitroprusside which is known to act via endothelium-independent generation of NO (Tesfamariam and Halpern, 1988) were constructed in WT and KO aortic rings with and without PVAT. In both WT and KO (Figure 4-5), the relaxation response to sodium nitroprusside was not altered by the presence of PVAT, as shown in another study (Gao et al., 2007). However, in vessels lacking PVAT, the maximum relaxation response to nitroprusside in WT aortic rings was significantly greater than that in KO aortic rings (Figure 4-5C). The explanation for this may be a dysfunctional vascular smooth muscle layer due to AMPKα1 subunit ablation and that AMPKα1 expression in VSMCs is essential for NO-mediated relaxation. Although this study reported reduced eNOS expression in the PVAT, the regulatory role of AMPK on eNOS activity and the magnitude of contribution of NO produced by eNOS in the PVAT to the endothelium independent anticontractile mechanism of the PVAT needs to be characterised further. Therefore, application of SOD and or L-NAME in functional studies such as myography would be a suitable approach to investigate this mechanism. Furthermore, as the response to SNP is very low, it is possible to test the effect of PVAT NO using another nitric oxide donor such as MAHMA NONOate (6-(2-Hydroxy-1-methyl-2-nitrosohydrazino)-N-methyl-1-hexanamine, NOC-9).

4.5 Conclusion

Comparison of PVAT from AMPKα1 KO and WT mice revealed no significant difference in $O_2^{\cdot-}$ or NO availability, although nitrotyrosine expression was higher and there was reduced eNOS phosphorylation in KO aortic PVAT. Although functional studies did not show any significant effect of PVAT on sodium nitroprusside induced relaxation, the contribution of PVAT-derived NO on vascular relaxation and the anticontractile effect of PVAT cannot be ruled out and needs further investigation.

Chapter 5

Effect of a high fat diet on perivascular adipose tissue function and the role of AMPK

5.1 Introduction

There is abundant evidence in the literature reported that obesity is a leading cause of insulin resistance, type 2 diabetes mellitus and increased blood pressure; all are major risk factors for cardiovascular disease (Gledhill et al., 2007). Generally, high-fat diet leads to adipocyte hypertrophy and the development of a low grade pro-inflammatory state (Jorgensen et al., 2004). As a result, there is increasing accumulation of macrophages and other leukocytes, particularly in obese adipose tissue (Weisberg et al., 2003). The function of adipocytes in storage of TAGs is also impaired, resulting in ectopic fat deposition in liver and skeletal muscle (Jorgensen et al., 2004). Furthermore, circulating adipose-derived pro-inflammatory cytokines, FAs and metabolites of this ectopic lipid are increased (Jorgensen et al., 2004). Excessive caloric intake is associated with increased secretion of proinflammatory adipokines such as TNF-α, leptin, IL-6, resistin, RBP4, lipocalin 2, IL-18, ANGPTL2 and reduced antinflammatory adipokines such as adiponectin and omentin (Nakamura et al., 2014). These changes reported in HFD may extend to PVAT and trigger both structural and functional changes which result in dysfunctional vasculature (Maenhaut and Van de Voorde, 2011).

Many studies have reported that the vasorelaxant function of PVAT is impaired in the presence of many pathophysiological conditions. Gao *et al* showed that the anticontractile effect of PVAT was reduced in spontaneously hypertensive rats (Lu et al., 2011a) and increased in streptozotocin-induced diabetic rats (Lee et al., 2009b). As obesity is associated with increased PVAT mass, it would be conceivable to expect an increased anticontractile effect of the PVAT due to enhanced PVAT-derived relaxing factors being released. However, it is now believed that obesity triggers structural and functional changes in PVAT which contribute to a loss or attenuation of the anticontractile effect. The loss of anticontractile effect has been reported in many studies. Chatterjee and co-workers reported that human coronary perivascular adipocytes exhibit a reduced state of adipocytic differentiation as compared with adipocytes derived from subcutaneous and visceral (perirenal) adipose depots. Secretion of adiponectin was significantly reduced, whereas that of proinflammatory cytokines interleukin-6, interleukin-8, and monocyte chemoattractant protein-1, was markedly increased in perivascular adipocytes (Chatterjee et al., 2009). It has been reported that the anticontractile effect of PVAT can be restored 6 months following bariatric surgery to encourage weight loss and that this corresponded to a significant reduction in TNF-α and macrophage infiltration in the PVAT.

It should be emphasized that not only obesity, but other pathological insults such as hypertension and balloon inflation during percutaneous intervention may trigger changes within the PVAT. It has been reported that PVAT generates complement 3 (C3) which stimulates fibroblast migration and differentiation via JNK activation (Ruan et al., 2010). This effect was thought to contribute to adventitial remodelling and increased vascular stiffness reported in the deoxycorticosterone acetate–salt hypertensive rat (Ruan et al., 2010). Furthermore, PVAT-released adipocytokines may enhance neointimal formation after vascular wire injury. In another study, transplantation of thoracic PVAT from donor mice fed a high-fat diet to the carotid arteries of recipient low-density lipoprotein receptor knockout mice also fed a high-fat diet was undertaken, followed by induction of intravascular wire injury after 2 weeks. The transplanted thoracic PVAT accelerated neointimal formation, adventitial angiogenesis, and macrophage infiltration (Manka et al., 2014). Furthermore, the same study reported that transplanted PVAT from MCP-1-deficient mice significantly reduced adventitial angiogenesis and neointimal hyperplasia with effects on macrophage infiltration (Manka et al., 2014). Indeed, PVAT inflammation induced by either HFD and/or intravascular wire injury contributes to vascular dysfunction including affecting the anticontractile activity of PVAT.

Although it is known that the anti-contractile properties of PVAT are lost in obese patients and animal models (Greenstein et al., 2009), the underlying mechanism of PVAT dysfunction remains elusive. AMPK maintains energy homoeostasis (Carling et al., 2011) and is involved in regulation of glucose, lipid and protein metabolism (Hardie, 2008). These basic functions are known to be dysregulated in obesity and metabolic syndrome in which the activity of AMPK is diminished (Ruderman et al., 2013). An impaired AMPK function associated with obesity has been reported with reduced eNOS activity and upregulation of mTOR which contributes to vascular remodelling and endothelial dysfunction (Ma et al., 2010). Furthermore, endothelial dysfunction in obesity can be reversed by AMPK activation, which increases phosphorylation of eNOS and enhances NO bioavailability; an effect which involved adiponectin (Deng et al., 2010). Another study demonstrated that PVAT-derived adiponectin can induce PVAT-dependent hyperpolarisation of vascular smooth muscle cells via AMPK (Weston et al., 2013), and thus reduced AMPK activation could also modify the PVAT effect on vascular contractility.

In spite of the fundamental role AMPK plays in regulation of cellular and whole-body energy demands, the effect of a HFD, a major cause of obesity and its complications (Hariri and Thibault, 2010, Woods et al., 2003b), on AMPK in the PVAT has not been comprehensively investigated. The effect of diet-induced obesity on AMPK has most frequently been studied in endothelium and VSMCs (Ma et al., 2010, Weston et al., 2013, Rubin et al., 2005, Nagata et al., 2004, Igata et al., 2005). These types of studies have yielded consistent results, showing that AMPK acts as a protective mechanism against diet-induced obesity and vascular injury. To date, no study has investigated the role of PVAT AMPK in the response to HFD and vascular injury. Therefore, we hypothesised that AMPK expressed in PVAT would act as a protective mechanism against diet-induced loss of anticontractile effect and wire-induced injury.

Aim of the study

- To determine whether high HFD could affect AMPK function and thus the anti-contractile properties of PVAT in mice aortae, and if so, to investigate the potential mechanisms involved.

- To determine the whether wire-induced injury could affect AMPK function in the PVAT and thus the antiprolefertive response in mice carotid artery.

5.2 Method and results

5.2.1 High fat diet increased the weight of both wild type and AMPKα1 knockout

Wild type (WT) (n =20) and AMPKα1 knockout (KO) (22) were divided into two groups and fed either a normal diet (ND) or a high fat diet (HFD) for 12 weeks starting at age 8 weeks. Body weight was measured at the start of the study and at the time of culling. At the start of the experiment, there was no difference in the weight between WT and KO mice for each group (Figure 5-1). After 12 weeks, there was a significant increase in the weight of WT mice on ND (16.9 ±2.9 g (n=10) compared to 33.2 ± 3.1 g (n=11)) in HFD group. Similarly, HFD increased the weight of KO mice to 33.4 ± 5.5 g (n=11) compared to 13.6 ± 2.3 g (n=10) in KO mice fed ND. Overall, both WT and KO HFD groups gained more than 50% weight in comparison with the respective ND groups. Figure 5-2 represents

the percentage of weight gain in the HFD group in comparison with normal diet (ND) group.

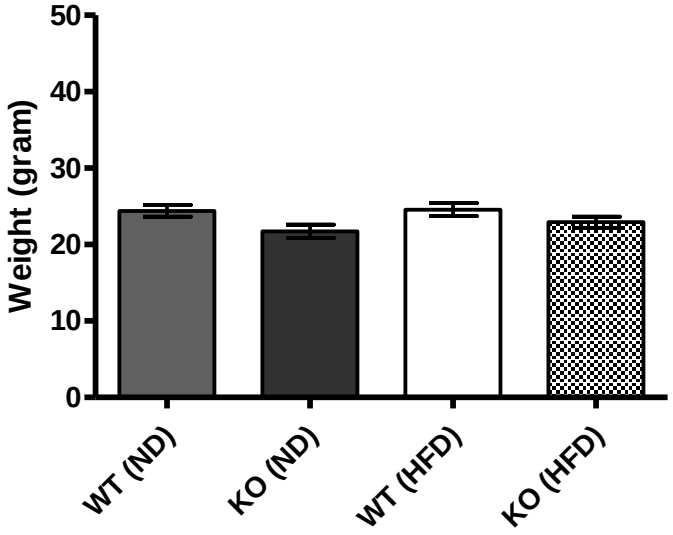

Figure 5-1 The average baseline weight of WT and KO mice before starting the HFD.

Wild type (WT) (n =20) and AMPKα1 knockout (KO) (n =22) were allocated randomly to ND and HFD groups and the weight of mice in each group was measured prior to starting ND or HFD.

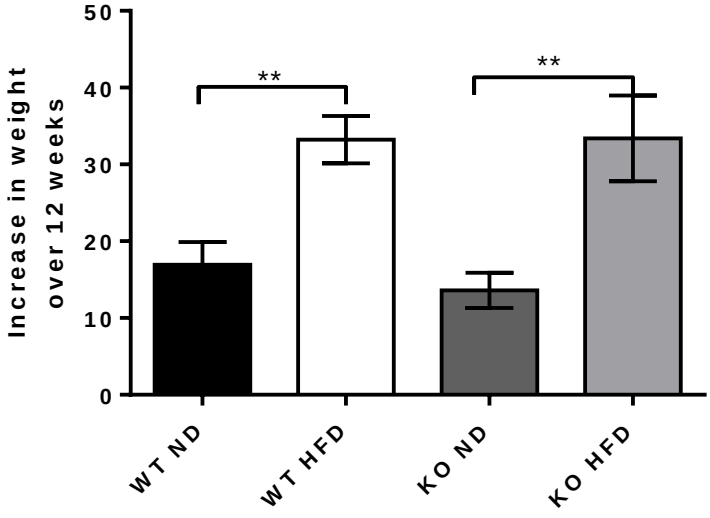

Figure 5-2 Weight gain in response to high-fat diet in wild type and AMPKα1 knockout mice.

Body weights were recorded at the beginning and at the end of the 12 wks of the study. Percentage weight gain was calculated for normal diet group and HFD group in both WT and KO. **p<0.01 vs WT HFD, n = 10-11, **p<0.01 vs KO HFD, n = 10-12.

5.2.2 Effect of high-fat diet on vascular contraction

The contractile response of thoracic aortic segments with or without attached PVAT from WT and KO mice on ND or HFD was measured in response to $3x10^{-8}$M of U46619 (Figure 5-3). Aortic segments with and without PVAT were dissected from WT and KO mice in ND and HFD groups, cut into 2 mm segments and mounted on two 40 μm diameter wires in a small artery wire myograph as described in Section 2.5. Arterial rings were maintained in Krebs' solution at 37 °C and gassed continuously with 95 % O_2 and 5 % CO_2. Following a 30 minute equilibration period, the arterial rings were exposed to 1 g tension for 30 min. Viability of arterial segments was measured with 40 mM KCl. Following this, the vessels were washed and then pre-constricted with U46619 for a further 30 minutes. Maximum contraction to U46619 was then recorded in grams and comapred between groups. The contraction of WT aorta without PVAT in ND group was 1.2 ± 0.3 g (n = 7) and was not significantly different from that reported in PVAT-free vessels from the HFD group (1.2 ± 0.2 g; n = 7). The contraction in WT aorta with intact PVAT from HFD group was (1.4 ± 0.3 g; n = 6) which was higher than that reported in the ND group (1.1 ± 0.1 g; n = 7) but did not reach statistical significance. There was no significant difference in contraction to U46619 in PVAT-free vessels from AMPKα1 KO mice in either the ND and HFD group (1.3 ± 0.2 g; n = 8 vs 1.4 ± 0.2 g; n = 6). Similarly, there was no statistical significance between vessels with intact PVAT in either the ND and HFD KO mice groups. The contraction in the ND group of KO mice with intact PVAT was 1.6 ± 0.2 g (n = 8) which was slightly higher than that in the KO HFD group (1.4 ± 0.2 g; n = 7; p = ns vs HFD intact PVAT arteries). Although the results did not show a significant difference between ND and HFD groups, the trend toward an enhanced contractile response in WT PVAT-intact vessels from mice fed a HFD was observed.

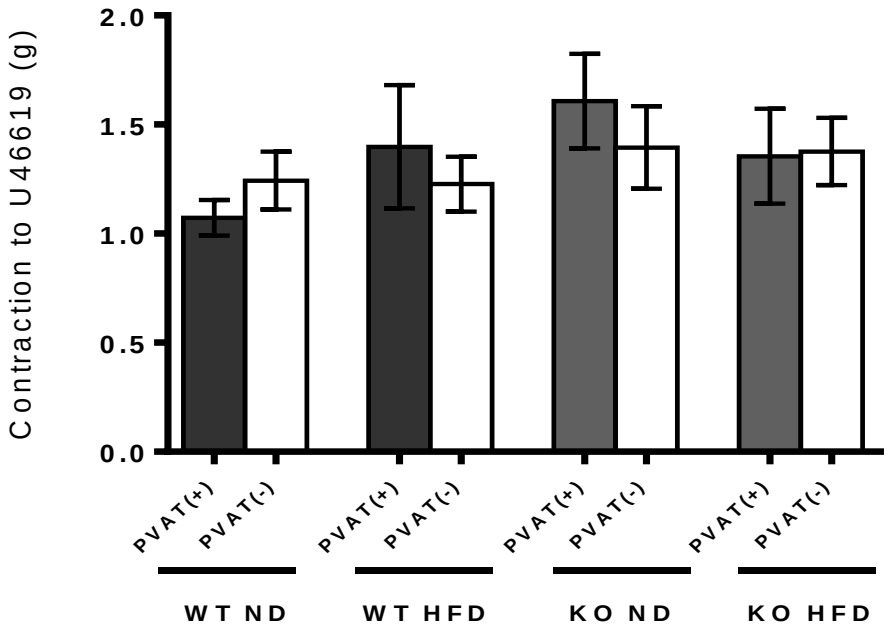

Figure 5-3 Effect of high-fat diet on thromboxane A_2 receptor agonist U46619 ($3x10^{-8}$ M) induced contraction.

Endothelium denuded, thoracic aortae with and without PVAT from WT and KO were dissected from ND and HFD groups and stimulated with U46619 for approximately 30 min and contraction measured on a myograph.

5.2.3 Effect of high-fat diet on the anticontractile effect of PVAT

At the end of the diet period, the anticontractile responses of the thoracic aorta to cromakalim were determined in WT and KO as described in section 2.5. Briefly, WT and KO thoracic aortae with and without PVAT from ND and HFD mice were preconstricted to U46619 and cumulative dose-response curves to increasing concentrations of cromakalim were constructed. In the ND group, the maximum relaxation to 10^{-4}M cromakalim produced by aortic rings from WT mice with intact PVAT (83.3 ± 3.6%, n=7; Figure 5-2A) was significantly greater than that produced by aortic rings without PVAT (27.6 ± 2.8%, n=7). At the end of 12 week of HFD, the maximal responses to cromakalim in intact PVAT aortic rings was 54.3 ± 3.5%; n = 7 in comparison with rings lacking PVAT from the same group (25.9 ± 4.6%; n = 7; Figure 5-2 B). Overall, in comparison with ND, HFD reduced the maximum response in aortic rings with intact PVAT by approximately 30%, while there was no effect in vessels without PVAT (Figure 5-2C), suggesting partial dysfunction of the PVAT caused by HFD which attenuates the anticontractile effect.

In the AMPKα1 KO mice, maximal responses to cromakalim were not significantly different between vessels with or without intact PVAT in both ND and HFD diet groups. The maximum responses were: 32.01 ± 4.02% vs. 21.7 ± 5.3%; n=7; p=ns with ND (Figure 5-3A) and 35.3 ± 4.4% vs. 33.5 ± 8.6%; n=7; p=ns with HFD (Figure 5-3B) respectively. Comparison between ND and HFD groups showed no significant difference (Figure 5-3C).

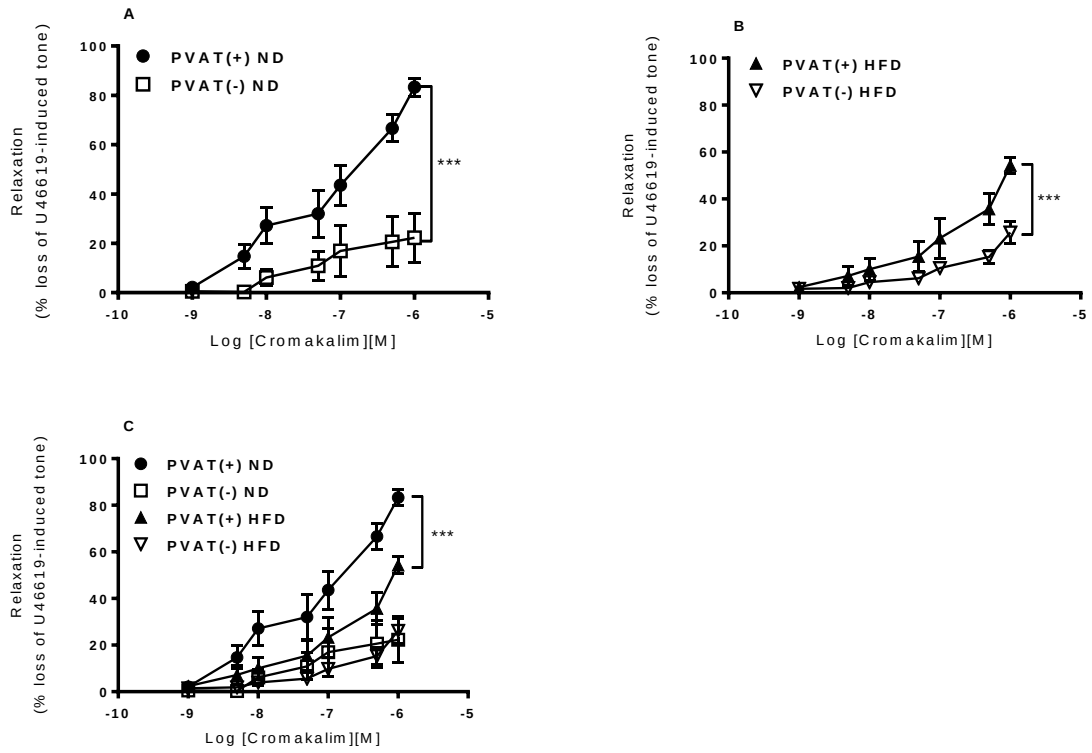

Figure 5-4 Effect of HFD on cromakalim-induced relaxation in WT thoracic aorta.

Dose-response curves to cromakalim were produced by wire myography in thoracic aortic rings with (+) and without (-) PVAT from WT mice fed ND or HFD. All vessels were without endothelium. (A) Dose-response curves to cromakalim in WT ND. (B) Dose-response curves to cromakalim in WT HFD. (C) Effect of HFD on cromakalim induced relaxation. ***p<0.001 vs ND PVAT(-), n = 6; ***p<0.01 vs HFD PVAT(-), n = 6; ***p<0.001 vs ND PVAT(+).

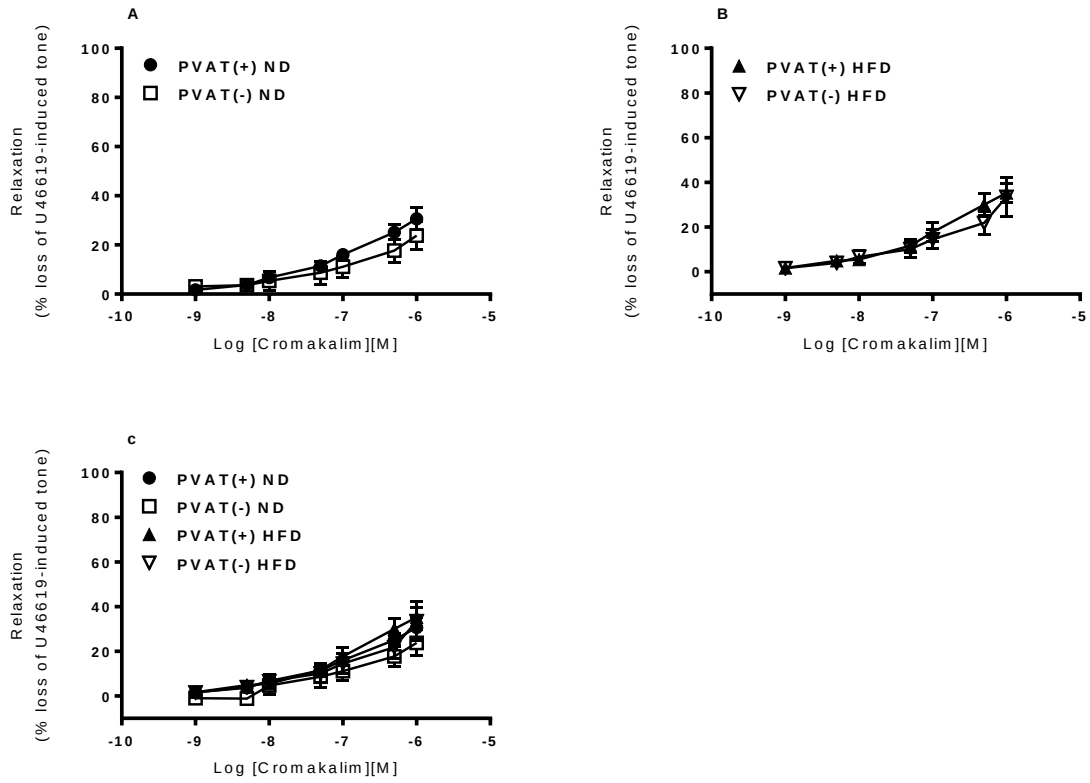

Figure 5-5 Effect of HFD on the cromakalim-induced relaxation in AMPKα1 KO thoracic aorta.

Dose-response curves to cromakalim were produced by wire myography in thoracic aortic rings with (+) and without (-) PVAT from KO mice fed ND (n = 6) or HFD (n = 6). All vessels were without endothelium. (A) Dose-response curves to cromakalim in KO ND. (B) Dose-response curves to cromakalim in KO HFD. (C) Effect of HFD on cromakalim induced relaxation.

5.2.4 Effect of high-fat diet on the morphology of PVAT

To determine the effect of HFD on PVAT phenotype, WT and KO thoracic aortic rings from ND and HFD were processed, cut and stained as detailed in Section 2.4. thoracic arteries with intact PVAT were excised immediately after death and placed in 10% zinc formalin overnight. Arteries were processed through a gradient of alcohols to Histoclear and embedded vertically in paraffin wax before being sectioned on a microtome at 5 µm. H&E staining was performed and sections visualised by light microscopy. The results shown in Figure 5-6 indicated that 12 weeks of HFD had obvious effects on adipocyte phenotypic features in both WT and KO PVAT. In both groups, aortic PVAT was composed of adipocytes with the morphological features of brown adipocytes with multiple lipid vacuoles and central nucleus. The WT and KO adipocytes from the HFD group were hypertrophied with some scattered WAT adipocytes present in the PVAT dissected from KO mice (Figure 5-6D).

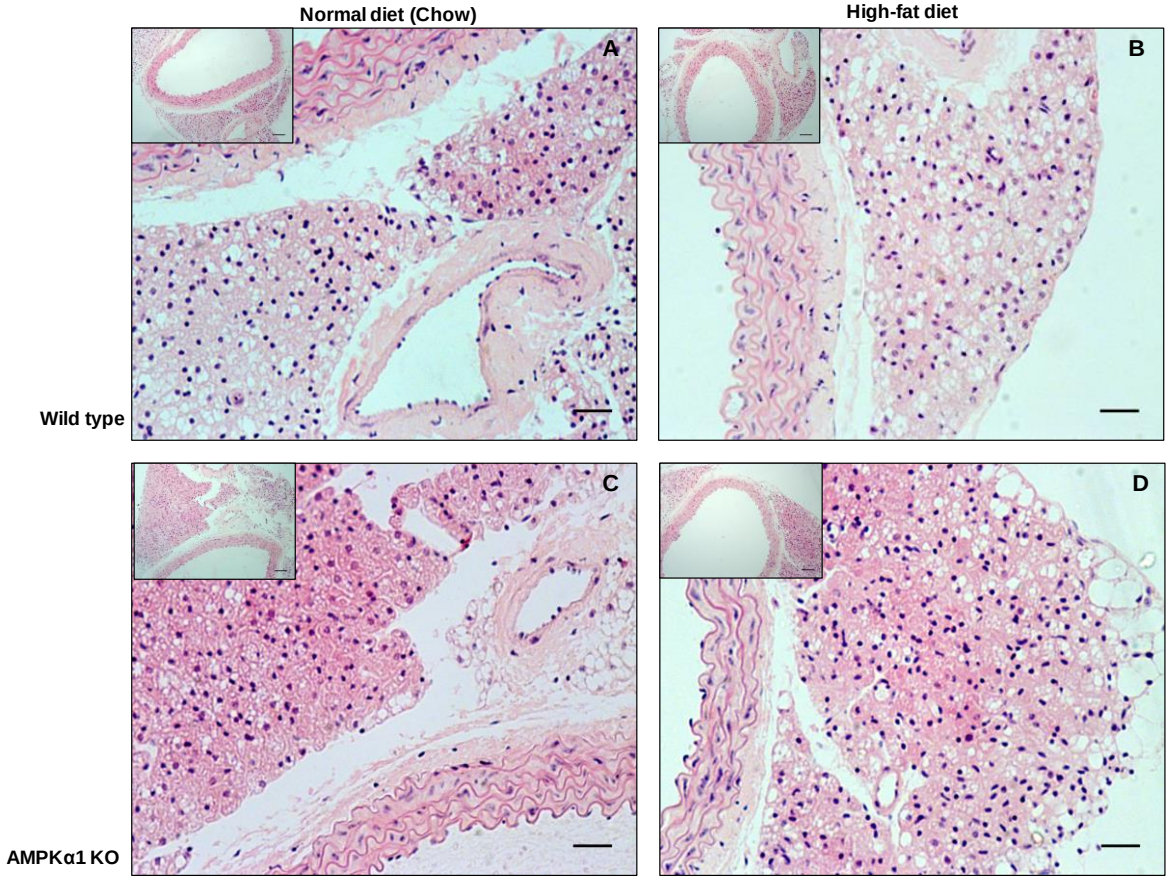

Figure 5-6 Effect of high-fat diet on thoracic PVAT phenotype from both WT and KO mice.

Sections of WT and KO thoracic aortic rings were harvested from mice fed normal diet (chow) or high fat diet and stained with H&E. Nuclei appear blue/purple whereas cytoplasm is stained pink. Scale bar; 20 µm. Representative micrographs are shown.

To further test the effect of HFD on the phenotype of the PVAT, quantitative analysis of levels of the brown adipose tissue marker UCP-1 was performed. Expression of UCP-1 was measured by Western blot analysis as detailed in Section 2.7. Briefly, WT and KO PVAT samples harvested from mice fed ND or HFD were dissected free and lyastes prepared. Protein estimation analysis from these lysates was performed and protein was added at 10 μg per well. Immunoblotting was performed with antibodies against UCP-1 and GAPDH which was used as a loading control. Membrane visualisation of immunolabelled bands was carried out using an Odyssey Sa Infrared Imaging System (LI-COR, USA) linked with Odyssey Sa Infrared Imaging System software (LI-COR, USA) (all antibody dilutions found in Table 2.5). The results showed that HFD increased the level of UCP-1 in both WT and KO PVAT in comparison with ND derived PVAT relative to GAPDH levels. In WT, HFD exhibited increased levels of UCP-1 (1.2 ± 0.03 vs 0.7 ± 0.1 in ND). Similarly, the level of UCP-1 was significantly elevated by HFD in KO PVAT (1.3 ± 0.1 vs 0.83 ± 0.1 in ND).

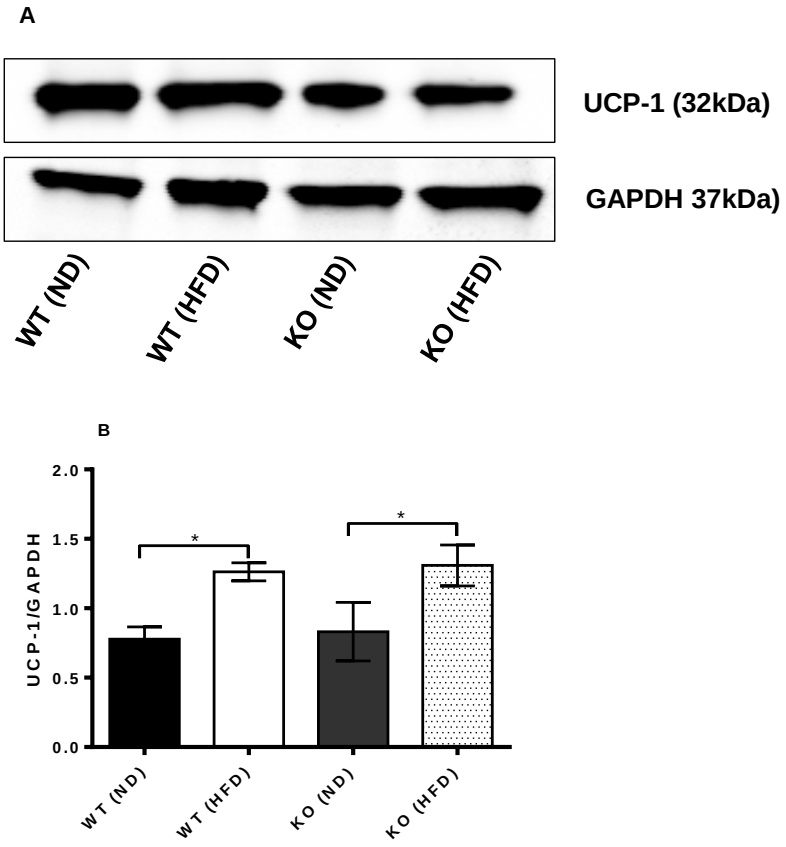

Figure 5-7 Effect of HFD on UCP-1 levels in PVAT.

Tissue lysates were prepared from thoracic aortic PVAT dissected from WT and KO mice fed ND or HFD and Western blotting was performed. UCP-1 level is presented as a ratio relative to the density of the GAPDH band to adjust for protein loading. The immunoblot shown is representative of (n= 4). *p<0.05 vs WT PVAT (ND); *p<0.05 vs KO PVAT (ND).

5.2.5 Effect of high-fat diet on AMPK level and activity

To examine the effect of HFD on AMPK level and activity, WT and KO thoracic aortic rings from both ND and HFD groups were analysed by immunohistochemistry for total and phospho-AMPKα (Thr172). Aortic rings dissected from WT and KO fed on ND or HFD were processed, cut and stained as detailed in Section 2.3.3. In brief, WT and KO thoracic aortae were excised immediately after death and placed in 10% acetic zinc formalin overnight. Arteries were processed through a gradient of alcohols to Histoclear and embedded vertically in paraffin wax before being cut into 5 μm sections. Polymer-based immunohistochemistry was used to evaluate expression of total and phospho-AMPKα in PVAT from WT and KO mice fed on ND or HFD. Figure 5-8 shows photomicrographs of total AMPKα in ND and HFD groups. Although there was an obvious reduction in staining intensity of total AMPKα and phospho-AMPKα in KO PVAT in comparsion with WT PVAT, there was no significant difference caused by HFD in either strain. Immunohistochemical staining of total AMPKα in both WT and KO aortic PVAT showed no difference in the staining intensity in WT (Figure 5-8A&D) and KO (Figure 5-8 G&J). Similarly, staining for phospho-AMPKα showed almost similar staining intensity in WT of the HFD group in comparison with WT of the ND group (Figure 5-9A&D). Thoracic aortic rings of KO mice of both ND and HFD group did not show any obvious difference in phospho-AMPKα level (Figure 5-9G&J).

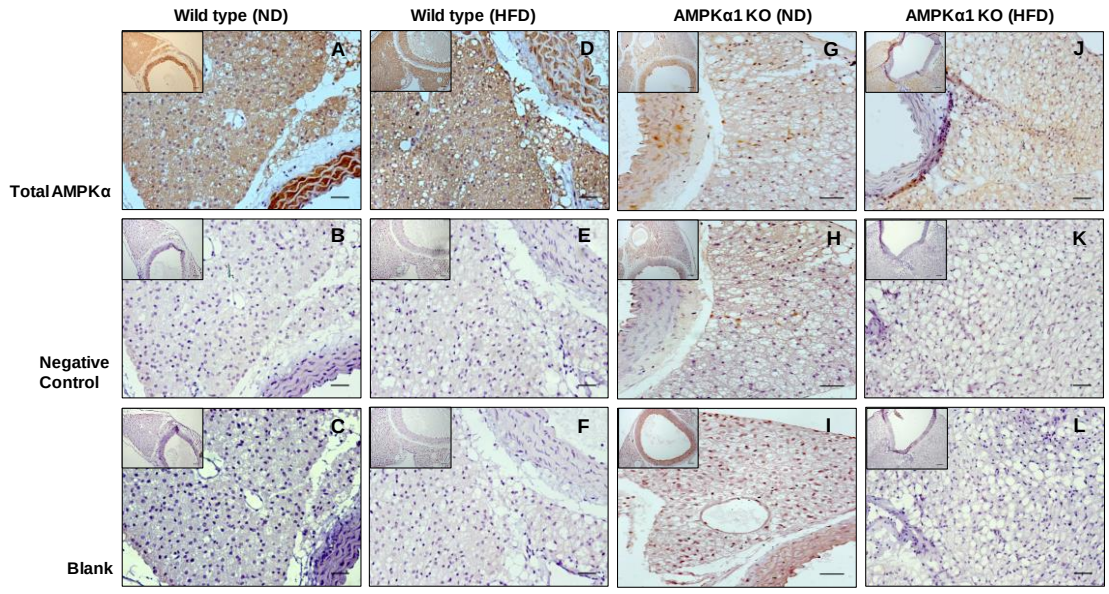

Figure 5-8 Effect of HFD on AMPKα levels in WT and KO PVAT.

Representative histological sections of WT and KO thoracic aorta with intact PVAT from normal diet (ND) and high fat diet (HFD) mice stained with anti-AMPKα antibodies and counterstained with haematoxylin. (A,D,G,J) Positive staining is indicated by brown colour. (B,E,H,K) Negative control represents aortic rings with anti-AMPKα primary antibodies only; (C,F,I,L) Blank (untreated) represents aortic section without treatment. Scale bar 20μm.

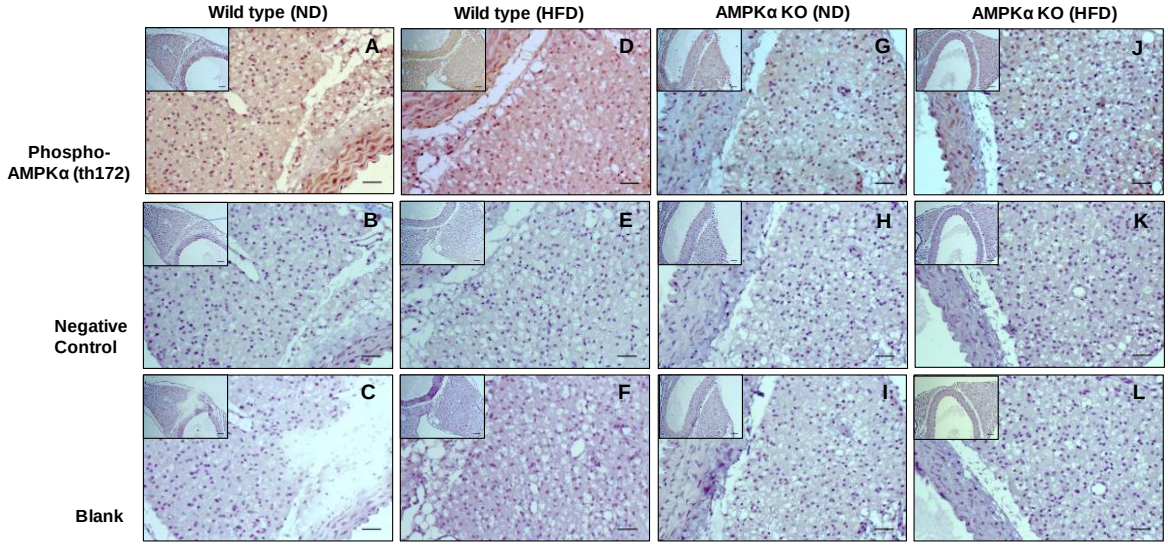

Figure 5-9 Effect of HFD on phospho-AMPKα levels in WT and KO PVAT.

Representative histological sections of WT and KO thoracic aorta with intact PVAT from normal diet (ND) and high fat diet (HFD) mice stained with anti-phospho-AMPKα (Thr172) antibodies and counterstained with haematoxylin. (A,D,G,J) Positive staining is indicated by brown colour. (B,E,H,K) Negative control represents aortic rings with anti-AMPKα primary antibodies only; (C,F,I,L) Blank (untreated) represents aortic section without treatment. Scale bar 20μm.

To further clarify the effect of HFD on AMPK level and activity, quantitative analysis of levels of total and phosphorylated form of AMPK was performed. Briefly, WT and KO PVAT samples harvested from mice fed ND or HFD were dissected free and lyastes was prepared. Protein estimation analysis from these lysates was performed and protein was added at 10 μg per well. Immunoblotting was performed with antibodies against total and phospho-AMPK, and total and phospho-ACC and GAPDH which was used as a loading control. Membrane visualisation of immunolabelled bands was carried out using an Odyssey Sa Infrared Imaging System (LI-COR, USA) linked with Odyssey Sa Infrared Imaging System software (LI-COR, USA). The results are illustrated in Figure 5-10. HFD significantly reduced the level of total AMPKα of WT PVAT (1.1 ± 0.24 vs 1.6 ± 0.2 in ND). Similar findings were observed in the level of phospho-AMPKα which was reduced significantly in HFD from 1.13 ± 01 down to to 0.9 ± 0.2. However, HFD had no effect on either total or phospho-AMPKα in KO mice (Figure 5-10 B&C). When measured as a ratio of phospho- to total-AMPKα and phospho-AMPK to total ACC, there were also significant reductions in response to HFD in WT but not KO mice (Figure 5-10 D&E).

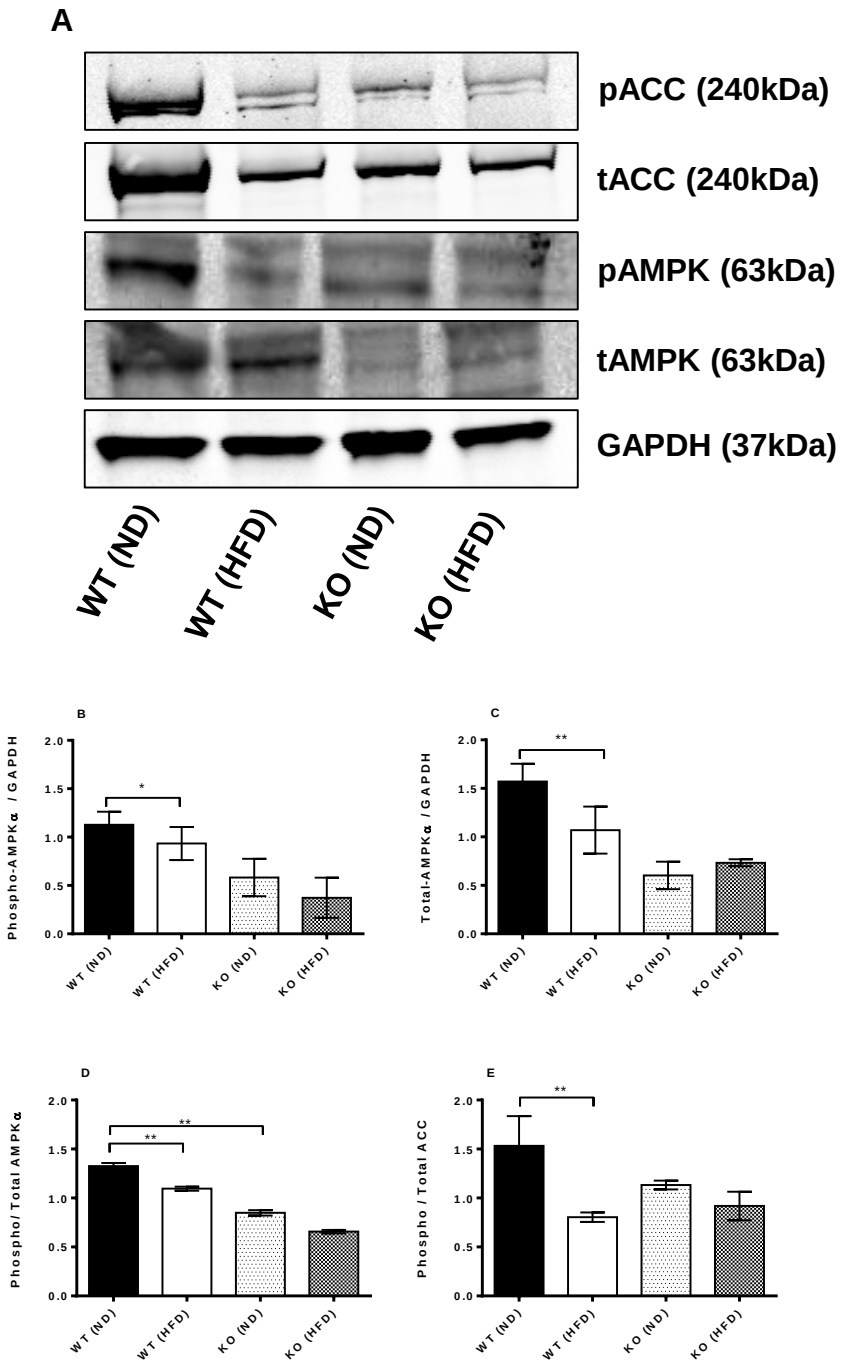

Figure 5-10 Effect of high-fat diet on phosphorylation and activity of the AMPK in the PVAT.

Lysates of PVAT from WT and KO mice fed ND and HFD were immunoblotted with the indicated antibodies. (A) Representative immunoblots are shown. (B,C) Quantitative analysis of immunoblots, expressed as the ratio of the phosphorylated (B) and total form of AMPKα divided by GAPDH (C). (D) Quantitative analysis of immunoblots, expressed as the ratio of the phosphorylated form of the enzyme divided by total AMPKα. (E) Quantitative analysis of immunoblots, expressed as the ratio of the phosphorylated form of ACC divided by total ACC. *p<0.05 vs WT PVAT (HFD), n = 3; **p<0.01 vs WT PVAT (HFD), n = 3; **p<0.01 vs KO PVAT (ND).

5.2.6 Effect of HFD on the inflammatory phenotype of PVAT

To test the effect of HFD on the inflammatory phenotype of the PVAT in both WT and KO mice, immunohistochemical staining with anti-MAC2 antibodies was performed. In brief, aortic rings from WT and KO mice fed ND or HFD and spleen were dissected and placed in 10% acetic zinc formalin overnight. Arteries were processed through a gradient of alcohols to Histoclear and embedded vertically in paraffin wax and cut into 5 μm sections. Sections of spleen were also prepared. Immunohistochemistry was used to evaluate the level MAC2 in PVAT from WT and KO mice fed on ND or HFD and spleen was used as a positive control. Histological analyses revealed considerable macrophage infiltrates in PVAT of KO mice compared to WT fed on ND (Figure 5-11 D&F). 12 weeks of HFD was accompanied by increased macrophage infiltration in WT PVAT compared to ND fed mice ($p = 6$, $p<0.05$; Figure 5-11 H). There was no significant difference in the intensity of MAC2 the staining in KO PVAT between the ND and HFD group (Figure 5-11 F&G).

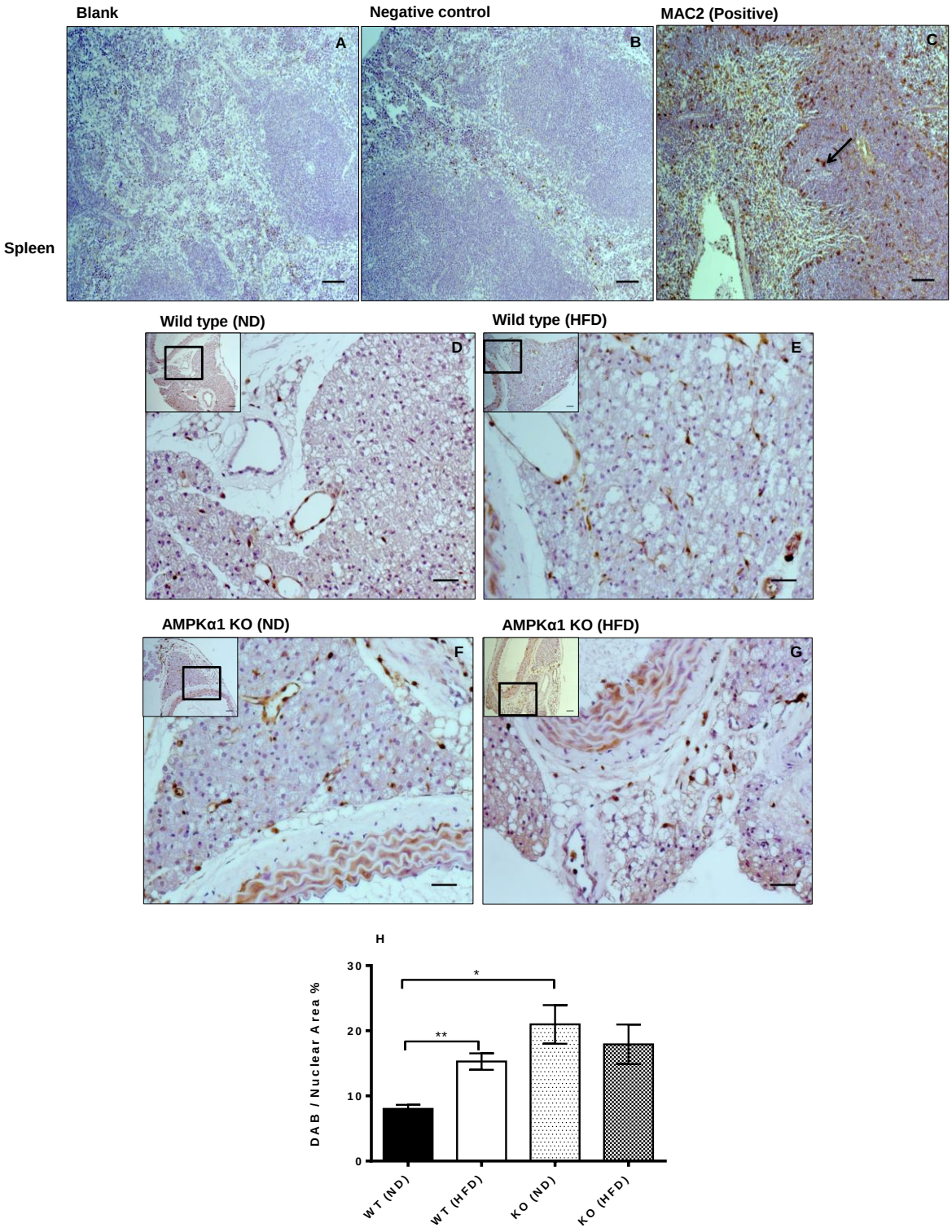

Figure 5-11 Effect of high-fat diet on inflammatory phenotype of WT and KO PVAT.

Representative histological sections of WT and KO thoracic aorta with intact PVAT from normal diet (ND) and high fat diet (HFD) mice stained with anti-MAC2 antibodies and counterstained with haematoxylin. Images shown are representative (A). (A,B,C) WT spleen anti-MAC2 antibody. (D) WT PVAT of ND mice; (E) WT PVAT of HFD; (F) KO PVAT from ND mice; (G) KO PVAT from HFD mice. Data were expressed as percentage of stained cells to total nuclear area in the section. **p <0.01 vs WT PVAT (ND); *p<0.05 vs WT PVAT (ND).

5.2.7 Effect of High-fat diet on adiponectin release

To examine the effect of HFD on adiponectin release from PVAT, adiponectin in conditioned media samples from WT and KO PVAT from ND and HFD groups were analysed by ELISA. PVAT samples were collected from WT and KO mice fed ND or HFD and incubated in Krebs solution for 1 hour at 37℃ and ELISA was performed as described in section 2.5. There was a significant reduction (approximately 70%) in the adiponectin in CM collected from WT PVAT of HFD mice compared to ND mice (n = 6, p<0.01; Figure 5-12). Similarly, there was a significant decrease in CM collected from KO mice fed ND in comparison with WT mice fed ND (n = 6, p<0.01; Figure 5-12). However, HFD had no effect on adiponectin secretion by PVAT of KO mice compared with ND (n = 6, p =ns).

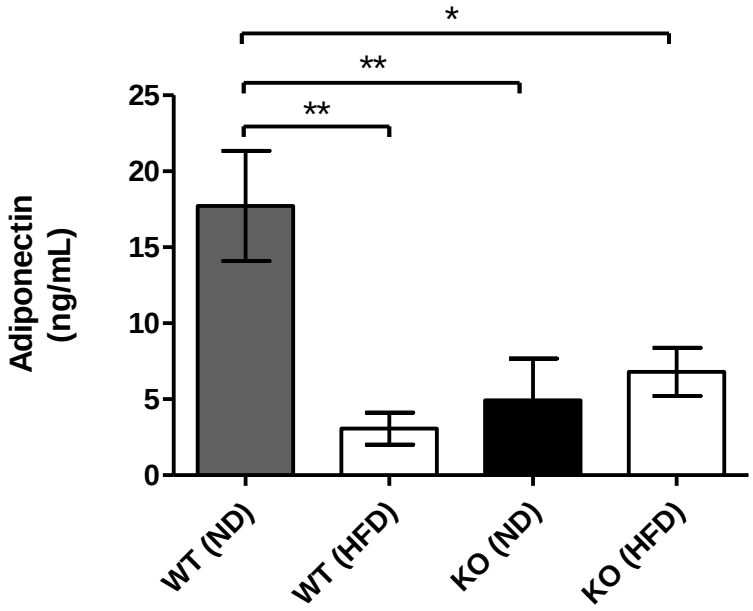

Figure 5-12 Effect of HFD on adiponectin release.

CM samples were collected from WT and KO PVAT from mice fed ND or HFD (n = 6) and adiponectin ELISA was performed. **p<0.01 vs WT ND CM, *p<0.05 vs WT CM.

5.2.8 Effect of vascular injury on the PVAT phenotype

To test the hypothesis that PVAT contributes to the vascular response to wire injury and investigate the role of AMPK in this response, right and left carotid arteries from WT and KO mice were utilised. The vessels utilised in this study were used in a previous study performed in our lab. This study involved induction of vascular injury using a wire inserted into the left carotid artery (LCA) in both WT and KO mice. Right carotid artery was not

injured and used as a control . After a week of wire injury, mice were sacrificed and carotid arteries with surrounding PVAT were dissected.

Firstly, the morphology of PVAT was evaluated using H&E which showed that in both WT and KO carotid arteries, the vessel was surrounded by BAT like adipocytes with the characteristic multiple lipid vacuoles and central nuclei (Figure 5-13). Although there was marked intimal thickening in both WT and KO LCAs and although the thickening was more pronounced in the KO derived LCAs, there was no phenotypic change in the surrounding adipocytes. The difference in the intimal thickening was not evaluated as it was not part of the current study.

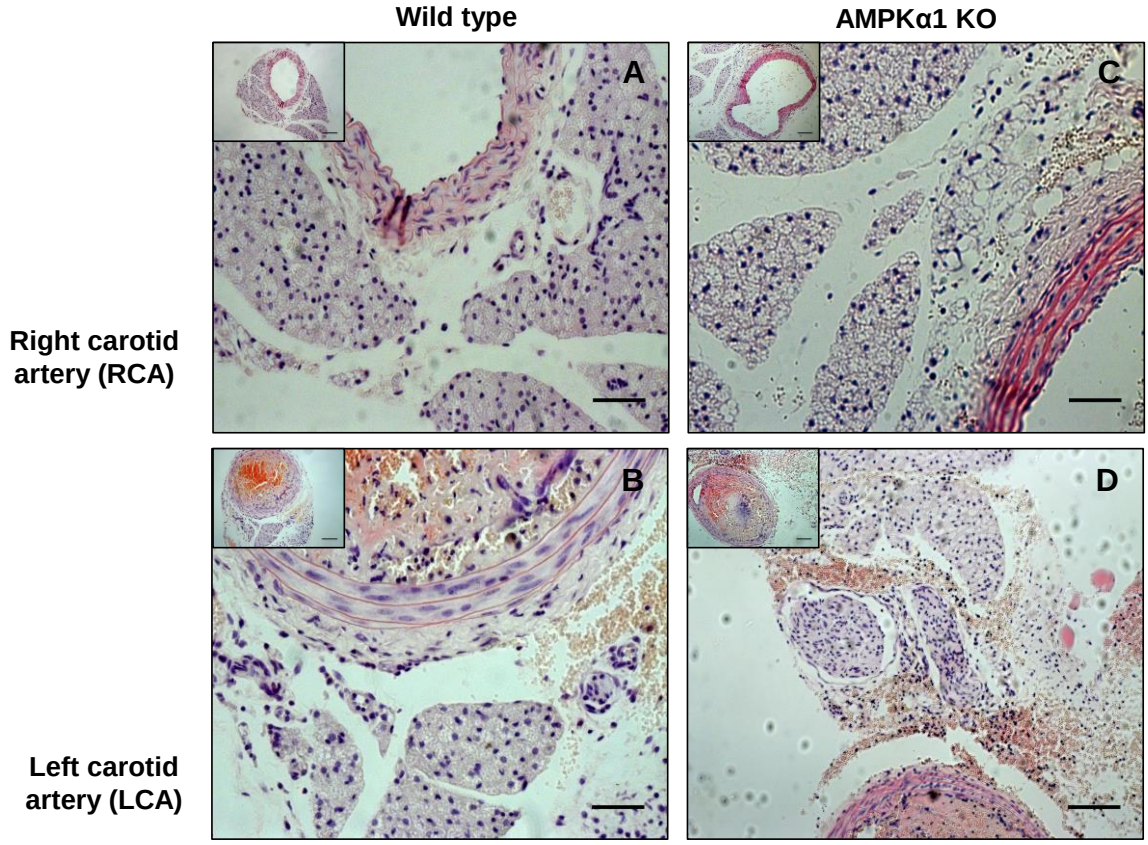

Figure 5-13 Effect of wire injury on carotid PVAT phenotype from both WT and KO mice.

Representative H&E stained sections harvested from WT and KO right carotid arteries (RCA) and left carotid arteries (LCA). Representative images are shown. Nuclei appear blue/purple whereas cytoplasm is stained pink. Scale bar; 20 μm.

5.2.9 Inflammatory response of WT and KO PVAT to vascular injury

To test the hypothesis that PVAT contributes to the vascular response to wire injury and to investigate the involvement of AMPK in regulation of this response, WT and KO carotid arteries with intact PVAT were utilised. As stated previously, wire injury was performed in LCA from both WT and KO and RCA was used as a control of the experiment in both types of mice. After a week of wire injury, mice were sacrificed and carotid arteries with surrounding PVAT were dissected. Immunohistochemistry using anti-MAC2 antibodies was performed to quantify PVAT macrophage infiltration.

LCAs from both WT and KO mice exhibited an obvious intimal thickening. In WT, vascular injury was associated with significant macrophage infiltration in LCA in comparison with control RCA (n = 4-5, **p<0.01; Figure 5-14 E). Although there was no significant difference in MAC2 between RCA and LCA of KO mice, there was a trend towards increased inflammatory infiltration (Figure 5-14 E; n = 3-4, p = ns).

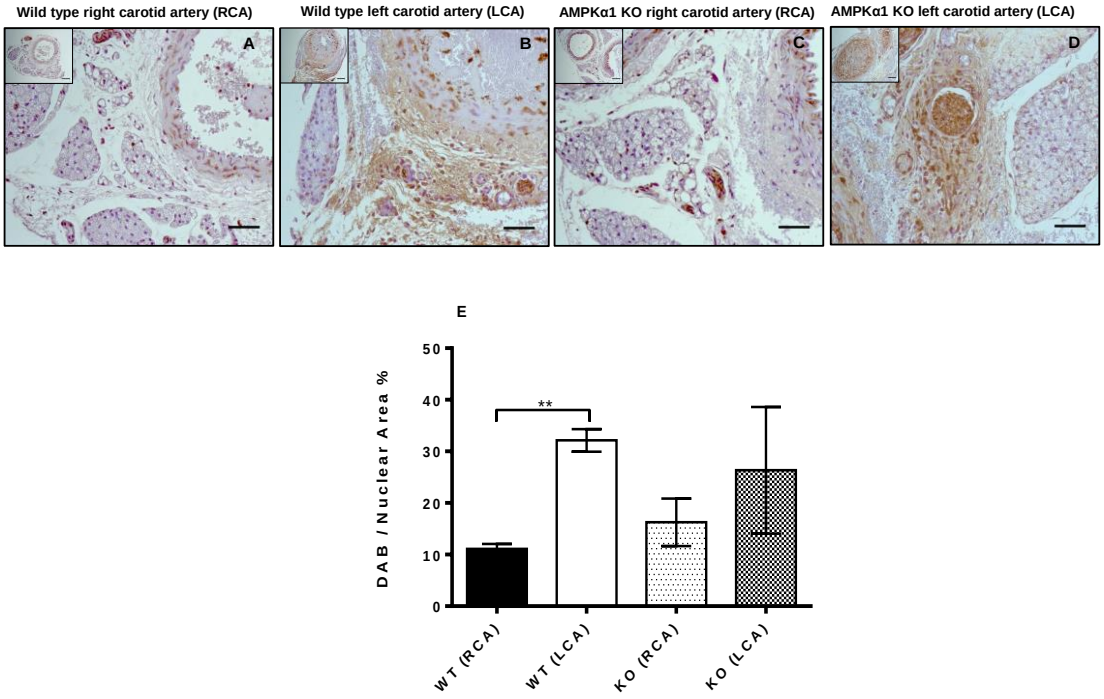

Figure 5-14 Inflammatory response of WT and KO PVAT to vascular injury.

Representative histological sections of WT and KO right and left carotid arteries with intact PVAT stained with anti- MAC2 antibody and counterstained with haematoxylin. Figures shown are representative (A). (A) Control WT RCA stained anti-MAC2 antibody. (B) 1 week post wire induced injury WT LCA. (C) Control KO RCA stained anti-MAC2 antibody. (D) 1 week post wire induced injury KO LCA .WT PVAT of HFD (F) KO PVAT from ND mice (G) KO PVAT from HFD mice. Data were expressed as percentage of stained cells to total nuclear area in the section. **p <0.001 vs WT RCA.

5.3 Discussion

This study investigated the effect of HFD on PVAT regulation of conduit artery tone in WT and AMPKα1 KO mice. The novel finding of the current research was that the anti-contractile effect of PVAT was significantly diminished in WT mice fed a HFD compared to those maintained on chow diet. The loss of anti-contractile function could be due in part to a reduction in PVAT-derived adiponectin release, due to AMPK dysfunction and/or inflammation of the PVAT.

5.3.1 Effect of HFD on anticontractile effect of PVAT

In the present study, thoracic aortae with intact PVAT and endothelium removed showed the greatest contractile response to U46619 in WT HFD group fed HFD in comparison with the ND group, although the difference was not statistically significant. The contractile response in vessels with intact PVAT in KO was similar in both control and HFD mice. Additionally, there was no difference in contraction in vessels with the PVAT removed across all groups. The endothelium-independent relaxation response to cromakalim was significantly reduced in HFD WT compared to ND arteries. The response of PVAT-free vessels was similar in both ND and HFD group. However, in KO mice there was no difference in relaxation between PVAT intact and removed vessels or in animals fed ND or HFD KO. Combination of both the U46619 and cromakalim experiments suggest that vascular dysfunction is at the level of the PVAT rather than medial layer and that AMPK might act as a protective mechanism as the anticontractile response was not completely lost in obese WT mice fed HFD.

The current results are consistent with previous studies reporting that PVAT-mediated anticontractile effect is impaired in HFD models (Fesus et al., 2007, Ma et al., 2010, Greenstein et al., 2009, Gao et al., 2005a, Owen et al., 2013, Nakagawa et al., 2002, Payne et al., 2010, Marchesi et al., 2009). Gao and co-workers reported that the anticontractile effect is lost in obese rats due to reduced release of relaxing factor despite the increased amount of PVAT around rat aorta (Gao et al., 2005a). A loss of the anticontractile effect of PVAT was also reported in obese New Zealand mice (NZO) model which was characterised by metabolic syndrome and larger amounts of PVAT. The lost function was suggested to be due to changes in the expression of PVAT-derived factors other than adiponectin (Fesus et al., 2007). In the Ossabaw swine model and using a proteomic profiler, there was an up-regulation of 186 PVAT-derived proteins which was associated

with increased coronary contractility and these included transforming protein RhoA and calpastatin (Owen et al., 2013).

5.3.2 Eeffect of HFD on PVAT phenotype

The mechanisms underlying the effect of AMPK in regulating adipose tissue mass are poorly characterised. Adipose tissue mass expansion occurs as a consequence of either an increase in adipocyte number as a result of enhanced adipogensis, an increase in cell size due to fat deposition in pre-existing cells, or a combination of both. It has been reported that the increase in adipose tissue mass in AMPKα2 knockout mice was due to an increased triglyceride accumulation in the preexisting adipocytes rather than an increase in cell number or differentiation as no changes in the expression of adipocyte transcription factors, PPARγ, C/EBPα, or the mature adipocyte markers, including aFABP/aP2, were reported (Villena et al., 2004). The model used in the current study is a global AMPKα1 knockout mouse and the findings indicate that adiponectin was reduced by HFD although no attempt was made to examine the transcription factor involved in regulation of cell differentiation such as PPARγ.

The study also looked at the effect of HFD on the brown adipose tissue marker UCP-1. As a general rule, prevention of the development of obesity is dependent on energy expenditure. The uncoupling of oxidative phosphorylation in BAT by UCP-1 plays a critical role in protecting the body from hypothermia or a hyperlipidaemic diet (Glavind-Kristensen et al., 2004, Cannon and Nedergaard, 2004). It was reported that increased expression of UCP-1 was associated with a decrease in the ATP/ADP and ATP/AMP ratios in the subcutaneous white fat of transgenic mice, increased activity of AMPK and enhanced oxidation of FA (Rossmeisl et al., 2004). Furthermore, it is well known that HFD increase UCP-1 mRNA and protein expression in BAT (Garcia-Ruiz et al., 2015). Therefore, it is plausible to think that HFD will result in an increased expression of UCP-1 in PVAT as a mechanism of dissipating energy and that this will be associated with increased AMPK activity in WT but not in AMPKα1 KO. Indeed, the results from the current study revealed an enhanced level of UCP-1 not only in WT but also KO in response to HFD (Figure 5-7) and was associated with reduced AMPK activity (Figure 5-10). The enhanced UCP-1 level in PVAT in both WT and KO in response to HFD can be explained by UCP-1 expression being regulated by many other mechanisms. It has been reported that the expression of UCP-1 can be increased in response to fatty acids (Cannon and Nedergaard, 2004). Another mechanism which can be proposed is involvement of

thyroid hormones (Guerra et al., 1996). Thyroid hormones (THs) are well known regulators of body energy expenditure (Klieverik et al., 2009). Treatment with THs has been reported to increase UCP-1 expression in BAT in rats as a result of binding to TH-responsive elements in the UCP1 promoter (Guerra et al., 1996). As thoracic PVAT exhibits BAT like features, it would be logical to think that the increased UCP-1 in both WT and KO occurs in response to circulating THs. Therefore, investigation of THs levels would be beneficial to assess the mechanism on UCP-1 elevation.

5.3.3 Effect of HFD on inflammatory phenotype of PVAT

Another question addressed in the current study was whether AMPK could affect the inflammatory phenotype of PVAT in response to HFD. The results showed increased macrophage infiltration indicated by increased MAC2 expression in HFD exposed WT mice. The increased MAC2 level in WT PVAT in the HFD group was associated with reduced AMPK activity in the PVAT (Figure 5-11). Therefore, it can be speculated that AMPK acts as a protective mechanism against inflammation and this effect is lost due to HFD-induced obesity. However, KO PVAT exhibit increased MAC2 expression under both ND and HFD conditions. These results further support the protective anti-inflammatory role of AMPK in the PVAT and that the absence of any difference between ND and HFD groups in the KO mice may be due to that fact the PVAT of ND KO mice is already maximally inflitrated or as a result of a compensation mechanism by AMPKα2 complexes preventing further inflammatory cell infiltration which needs further investigation. Indeed, these results support previous studies that demonstrated the loss of the anicontractile effect of PVAT in obesity (Marchesi et al., 2009, Rebolledo et al., 2010, Bailey-Downs et al., 2013, Chatterjee et al., 2009, Wang et al., 2012). HFD-induced obesity as discussed previously can impair PVAT anticontractile effect via promoting a marked proinflammatory shift in cytokines and chemokines which is associated with oxidative stress in the PVAT (Bailey-Downs et al., 2013). PVAT inflammation and oxidative stress can lead to endothelial dysfunction and decreased NO bioavailability and increased superoxide generation by uncoupled endothelial NO synthase in PVAT (Marchesi et al., 2009). Moreover, HFD induced PVAT dysfunction via increased macrophage accumulation in the PVAT and vascular oxidative stress (Wang et al., 2012). It has been reported that human coronary PVAT collected from organ donor candidates exhibits an enhanced release of IL-6, IL-8 and MCP-1 and reduced adipocyte differentiation (Chatterjee et al., 2009). These results indicate that inflammatory cytokines released by PVAT act as chemoattractants for macrophages and aggravating inflammation.

In contrast to the previous studies, Fitzgibbons and coworkers have shown that thoracic PVAT exhibits a very low grade of inflammation after 13 weeks of HFD. They proposed that the lack of effect was due to its similarities with BAT and because BAT-like adipose tissue is resistant to HFD-induced inflammatory changes (Fitzgibbons et al., 2011). When contrasting the Fitzgibbons findings to the current study, althought it used similar HFD period, it can be argued that Fitzgibbons *et al* study is conducted in a completely different mouse strain (C57BL6/J) and the low level of inflammation detected in this study may be related to the type of HFD used in the study.

Another important leading cause of PVAT anticontractile dysfunction is that HFD causes a rise in the inflammatory adipocytokine leptin and chemokine MIP1α concomitant with a decrease in the expression of adiponectin, PPARγ and FABP4 (Chatterjee et al., 2009). Although, the current study did not address adipokine leptin and inflammatory cytokines, the results showed reduced release of adiponectin from PVAT in WT and KO exposed to HFD. The findings from the current study support the previous evidence that 2 weeks HFD is associated with significant reduction of adiponectin expression (Chatterjee et al., 2009). In contrast to the Chatterjee study and the findings from the current study, Ketonen *et al* reported completely different results. They reported that 8 months of HFD in C57BL6/J mice had no effect on the adiponectin expression in the thoracic PVAT (Ketonen et al., 2010). Although both studies utilised the same mouse strain, the completely different results can be attributed to type of diet used and that the period of feeding used in Ketonen's study may lead to adiponectin being upregulated to overcome HFD induced PVAT dysfunction.

Several lines of evidence reported that AMPK activation is associated with increased secretion or expression of adiponectin by suppression of inflammatory cytokines such as TNF-α and IL-6 (Lihn et al., 2004, Sell et al., 2006, Tsuchida et al., 2005). Activation of AMPK with AICAR in human adipose tissue was associated with degradation of TNF-α and increase adiponectin gene expression (Lihn et al., 2004). TNF-α and IL-6 are known shown to have inhibitory effects on adiponectin gene expression and release (Fasshauer et al., 2002, Fasshauer et al., 2003). Moreover, TNF-α has been suggested to play a central role in regulating adiponectin levels (Greenberg et al., 1991). It can be speculated that the decrease in TNF-α protein may be involved in the up-regulation of adiponectin mRNA levels (Lihn et al., 2004). Sell *et al* reported activation of AMPK by AICAR and troglitazone was associated with reduction of IL-6, IL-8, MIP-1α/β, and MCP-1 and

upregulation of adiponectin expression (Sell et al., 2006). Similar findings demonstrate that the expression of inflammatory genes inculding TNF-α, MCP-1, and macrophage antigen-1 in WAT was reduced in response to PPARα agonist rosiglitazone (Tsuchida et al., 2005). The increase in the expression of macrophage markers reported in HFD and KO animals may be due to loss of AMPK antifilammatory activity leading to upregulation of inflammatory cytokines such as TNFα and IL-6 and downregulation of adiponectin. Therefore, investigation of cytokine expression in PVAT would be beneficial to further characterise the role of AMPK.

5.3.4 AMPK protects PVAT against endovascular injury

Obesity-induced inflammation in periadventitial adipose tissue is associated with upregulation of inflammatory adipocytokines and downregulation of the antiinflammatory adipocytokine adiponectin (Takaoka et al., 2009). These changes were associated with enhanced neointima formation after endovascular injury. Endothelial injury induces adhesion and migration of leukocytes, macrophages, and bone marrow–derived progenitor cells into the vessel wall (Beckman et al., 1990, Sata et al., 2000). Furthermore, pro-inflammatory cytokines have a fundamental role in mediating the initiation and progression of vascular lesion formation (Serrano et al., 1997, Libby, 2002, Beckmann et al., 1994, Xie et al., 2008).

Takaoka *et al* provide direct evidence that PVAT may protect against neointimal formation after angioplasty in lean status and that inflammatory changes in the periadventitial fat may have a direct role in the pathogenesis of vascular disease accelerated by obesity. They also suggested that adiponectin released from PVAT may play a protective role in neointima formation of the adjacent artery after vascular injury in lean mice (Takaoka et al., 2009). In this study, PVAT removal enhanced neointimal hyperplasia following endovascular injury in the femoral artery. Transplantation of subcutaneous fat from a normal mouse to surround the injured artery significantly reduced neointimal formation. These results demonstrate that PVAT may possess a protective role in neointimal hyperplasia (Takaoka et al., 2009).

In line with the previous findings, the protective effect of exogenous adipose tissue was lost when transplanted subcutaneous adipose tissue was derived from obese mice. This is likely related to phenotypic changes in adipose tissue associated with obesity. These changes include reduced production of anti-inflammatory adiponectin and increased pro-

inflammatory adipokines; IL-6, MCP-1, TNF-α and PAI-1 in subcutaneous adipose tissue-conditioned medium from obese mice compared with that from normal mice (Takaoka et al., 2010). In the same study, the conditioned medium derived from the subcutaneous adipose tissue of normal mice attenuated VSMC proliferation stimulated by platelet-derived growth factor (PDGF)-BB (Takaoka et al., 2010). On the other hand, the conditioned medium from obese mice increased VSMC proliferation, which was attenuated by pretreatment with anti-TNF-α antibodies. Furthermore, the conditioned medium of adiponectin-deficient subcutaneous adipose tissue enhanced VSMC proliferation. These findings reveal that TNF-α secreted from adipose tissue increased VSMC growth, and that adiponectin secreted from adipose tissue inhibited VSMC growth in response to PDGF-BB stimulation (Takaoka et al., 2010).

In the current study, the role of AMPK in regulation of PVAT inflammatory phenotype in response to intravascular wire injury was investigated. PVAT in both WT and KO carotid arteries composed of brown adipocytes with its multiple lipid vacuoles and central nuclus (Figure 5-13). These data support the findings reported by Cinti *et al* who reported that PVAT surrounding carotid artery possess the characteristic of BAT (Cinti, 2011). It also supported our view in chapter 3 that AMPK has no effect on the morphological feature of the PVAT. One week after wire injury induced in both WT and KO LCAs, there was an obvious intimal thickening in both strains and it was associated with increased macrophage infiltration in both intima and PVAT (Figure 5-14). It is worth noting that the thickening of the intima was visually more in the KO LCA in comparison with WT LCA, although no measurement was done. However, these data need further investigation. The results of current analysis show increased MAC2 expression in both WT and KO. The expression of MAC2 was more pounced in WT LCA in comparison with its control RCA. Additionally, there was a trend toward increased expression in KO LCA in contrast to RCA. The lack of statistical difference in KO derived vessels suggests that loss of AMPK is associated with increased inflammation of PVAT in KO of control and injured vessels and also that AMPK might act as protective mechanism against vascular intimal thickening associated with vascular injury. It is known that activation of AMPK in VSMCs reduced intimal hyperplasia by either inducing cell cycle arrest by upregulation of p53-p21 which inhibits VSMCs proliferation (Igata et al., 2005) or reducing protein synthesis mediated via inhibition of mTOR (Kim et al., 2014, Inoki et al., 2003). Furthermore, the implication of PVAT AMPK came from study by *Ma et al* who reported that PVAT can induce vascular dysfunction via dysregulation of the AMPK/mTOR signalling pathway in diet-induced

obese rat. They demonstarted that incubation of mesenteric arterial rings with periaortic fat from HFD rats caused attenuated endothelium-dependent relaxation and down-regulation of AMPK and eNOS in the aorta with a concurrent up-regulation of mTOR. This effect was absent in periaortic fat from rats on a chow diet. In the same study, co-culture of vascular SMCs with periaortic adipocytes from HFD animals also reduced AMPK phosphorylation and increased mTOR phosphorylation (Ma et al., 2010).

The findings from the current study revealed that adiponectin release was reduced in KO mice and this was associated with reduced expression of AMPK in PVAT (Figure 5-12). Therefore, it can be speculated that AMPKα1 deletion in PVAT leads to a reduction in the adiponectin release and loss of the protective function of the PVAT. The results in WT wire-injured LCA can be explained due to inflammation of the PVAT causedby vascular injury with increased macrophage infiltration and associated expression of inflammatory cytokines and reduction of antiinflammatory factors such as adiponectin. Current results support the evidence from other experiments that adiponectin suppresses cell proliferation induced by a low dose of oxidized low density lipoprotein (Motoshima et al., 2004). Exogenous adiponectin suppressed PDGF-BB-induced VSMC proliferation via AMPK activation (Igata et al., 2005). The AMPK pathway is also involved in the effect of adiponectin to inhibit the expression and activity of iNOS, secretion of adventitial antiinflammatory factors, division, proliferation and translation of adventitial fibroblasts, change of adventitial fibroblasts to myofibroblasts, and oxidative/nitrative stress which reduce atherosclerotic plaque area and stabilize atherosclerotic plaque (Cai et al., 2008). Thus, changes in adiponectin secretion by inflamed PVAT could also influence the reponse to vascular injury.

5.4 Conclusion

Taken together, HFD and wire injury are associated with increased macrophage infiltration and reduced AMPK activity in thoracic and carotid PVAT. Marked reduction in AMPK activity in WT PVAT, accompanied with the reduction in the release of adiponectin in HFD and KO animals may explain the impaired vascular function including loss of an anticontractile effect antiathergenic function. Further studies are needed to investigate the expression of different adipokines and cytokines released by PVAT exposed to HFD and intravascular injury.

Chapter 6

General Discussion

6.1 The hypothesis

The concept that adipose tissue is a functional endocrine organ involved in energy haemostasis was a huge step toward a greater understanding of the molecular basis of obesity and its co-morbidities. The link between obesity and CVD is further supported by Yudkin *et al* who speculated that PVAT might be the element that links obesity, insulin resistance and vascular disease due to its detrimental effects on blood vessels in obese people (Yudkin et al., 2005). PVAT is now considered a highly active endocrine organ that releases a variety of adipocytokines, and other factors which influence vascular tone in a paracrine manner. Under normal physiological conditions, PVAT can release adipocytokines which can attenuate contractility of the underlying vessel. The precise mechanism is still undefined, although some evidence suggests that PDRF may induce the anti-contractile effect via both endothelium-dependent and -independent mechanisms (Gao et al., 2007). Both mechanisms have been reported to involve AMPK, the cellular energy regulator. AMPK activation can induce vasodilation via phosphorylation and activation of endothelial NO synthase (eNOS) at Ser1179 (Morrow et al., 2003, Davis et al., 2006) and Ser663 (Chen et al., 2009) to increase NO production and vascular relaxation (Morrow et al., 2003, Davis et al., 2006). AMPK can also induce endothelium-independent relaxation via reduced sensitivity of myosin light-chain kinase (MLCK) to intracellular calcium (Horman et al., 2008). Although AMPK is expressed throughout the vessel wall, its role in the regulation of PVAT had not been investigated prior to this study. Therefore, the primary hypothesis was that AMPK is required for PVAT to function normally and that the α1 isoform is the most important isoform in mediating PVAT function. Therefore, the aim of this thesis was to investigate the role of AMPKα in the regulation of PVAT anti-contractile function using a mouse with a global AMPKα1 isoform knockout.

The data reported in this study demonstrate that PVAT has a profound anti-contractile effect on mouse thoracic aorta. The effect may be due to release of a transferable factor and that factor is likely to be adiponectin, release of which is regulated by the activity of AMPKα1. Furthermore, AMPK activity may regulate adiponectin secretion by either directly targeting its release from adipocytes and/or indirectly by its anti-inflammatory function which would limit the suppression of adiponectin expression. The studies in this thesis demonstrate that in mouse aortic rings, adiponectin augments relaxation to cromakalim in an endothelium-independent manner although other effects of adiponectin on the endothelium cannot be ruled out. Indeed, although aortic rings in this study were mechanically denuded, endothelial cells in vessels within the vasa vasorum will not be

affected and adiponectin could affect endothelial functiojn in these microvessels. The current research also reported that HFD-induced obesity is associated with a profound reduction in PVAT-mediated anti-contractile effects. Furthermore, HFD- induced obesity was associated with reduced AMPK activity, increased macrophage infiltration and a marked decrease in adiponectin release, all of which may contribute to dysfunctional PVAT.

6.2 The anticontractile effect of PVAT under basal conditions

Most blood vessels are surrounded by PVAT which may be predominantly WAT or a combination of BAT and WAT. The majority of the experiments in the thesis used conduit vessels, (thoracic aorta) which are surrounded by a mixture of WAT and BAT. The overall results suggest that brown PVAT can release adiponectin under the basal (unstimulated) state and that this may act as a PVAT-derived anticontractile factor (PDRF). Furthermore, AMPK regulates the secretion and/or function of this PVAT-derived adiponectin (Almabrouk et al., 2016).

6.3 U46619 as contractile agent

Like white PVAT, brown PVAT can also release factors and has anti-contractile effects on the surrounding vessels as reported in both rat (Lohn et al., 2002, Gao et al., 2007) and human internal thoracic aortas (Gao et al., 2005b). The anticontractile effect of the PVAT has been reported to different contractile agents including angiotensin II, 5-HT, phenylephrine (Lohn et al., 2002) and U46619 (Verlohren et al., 2004). These spasmogens are known to induce different types of contraction. Phenyephrine induces tonic contractions or initial vasoconstrictions followed by diameter oscillations (Inoki et al., 2003). Angiotensin II causes a biphasic contraction which rises rapidly and transiently and peaks in a few minutes, before declining to a lower steady level (Hardie, 2016). 5-HT induces a strong contraction which lasts for a long time in rat thoracic aorta (Ratz and Flaim, 1984). However, U46619 causes a tonic vascular contraction which is associated with a reduction in the diameter of the artery. In the case of U46619, the contraction induced is stable and the PVAT anticontractile effect is sub-maximal. Therefore, U46619 was utilised as contractile agent in this project to allow the effects of PVAT on relaxation to several vasodilators to be studied. Indeed, the use of U46619 only in the current thesis is a potential limitation as the effects of AMPK ablation may be specific to mechanisms after

U46619 -mediated contraction. Therefore, it would be beneficial to further test the hypothesis using different physiological constrictor agents to establish if PVAT from WT and KO animals had similar effects.

6.4 Endothelium-independent relaxation to AICAR and PVAT

The endothelium-independent relaxation to the AMPK activator AICAR has been documented in many animal models and vessels types, including mice aorta (Goirand et al., 2007), swine carotid artery (Rubin et al., 2005) and rat aorta (Majithiya and Balaraman, 2006). In these models, in addition to removal of endothelium, PVAT was also dissected during preparation of the vessels for functional studies. Removal of endothelium did not affect the relaxation response induced by AICAR. Indeed these observations indicate a direct effect of AMPK activation in VSMCs. While the findings in the current study confirm these previous observations, they also provide evidence that the presence of PVAT enhances the relaxation induced by AICAR in an endothelium-independent manner. Furthermore, the enhanced response is mediated by transferable factor(s) the action of which may involve AMPK as the effects were lost in KO mice (Figure 3-8) . As reported previously, AMPK is expressed in all layers of blood vessel including PVAT. Therefore, it is plausible that AICAR will also activate AMPK in the PVAT which makes delineating the contribution of AMPK in the PVAT more difficult as the markers of AMPK activation (phosphorylation at both AMPK activation site Thr172 and AMPK downstream target Ser79 on acetyl-CoA carboxylase) responded in the same dose-dependent manner to AICAR. Indeed, treatment of PVAT alone with AICAR can be a solution; however, the decision about the basal activity of AMPK becomes more difficult.

6.5 Relaxation to cromakalim and the role of K_{ATP} channels

The role of K_{ATP} channels in the anti-contractile effect of PVAT was first proposed by Lohn *et al* (Lohn et al., 2002). They proposed that PVAT releases a transferable factor that acts via tyrosine kinase-dependent activation of K_{ATP} channels in the medial layer and was blocked by glibenclamide (Lohn et al., 2002). In the current research, the primary aim was to investigate the role of AMPK in the PVAT. Therefore, cromakalim was used to examine the relaxing ability of PVAT. Cromakalim is known to induce vascular relaxation by activation of K_{ATP} and hyperpolarisation of vascular myocytes (Cook et al., 1988). In the

current experiments, PVAT enhanced the relaxation response to cromakalim in an endothelium-independent manner in WT mice (Figure 3-9A). These effects were lost in the KO mouse-derived arteries (Figure 3-9B). Indeed, the findings from this study indicated the involvement of K_{ATP} in the anticontractile effect of PVAT (Lohn et al., 2002), and further suggest a possible regulatory role of AMPK. In general, the contraction of vascular smooth muscle is closely related to the status of myocyte membrane potential. Depolarisation of the myocyte cell membrane leads to opening of L-type voltage-dependent Ca^{2+} channels causing Ca^{2+} influx into the cell and myocyte contraction. On the other hand, hyperpolarisation induced by opening of K^+ channels decreases L-type Ca^{2+} channel opening time and keeps the myocytes relaxed (Nelson and Quayle, 1995). Furthermore, K_{ATP} channels are activated in response to a reduction in intracellular ATP/ADP ratio, which help the myocytes to regulate the efflux of K^+ depending on their metabolic state (Nelson and Quayle, 1995). Indeed, these findings have made defining the role of AMPK in the PVAT more difficult as AMPK activation can occur in response to Ca^{2+} and a change in the ATP/ADP ratio as previously reported (reviewed in Hardie, 2008). Although, the role of K_{ATP} has been tested by examination of AMPK activity in cultured VSMCs treated with increasing concentrations of cromakalim, the role of AMPK activation in VSMCs cannot be completely excluded as there was a reduction in the relaxation response in KO vessels without PVAT in comparison with WT PVAT-free vessels. Additionally, it is known that tonic vascular myocytes have negative membrane potentials (Nelson and Quayle, 1995) that are close to the activation threshold of Kv channels. Opening of cell membrane K^+ channels allows K^+ efflux, keeping the myocyte hyperpolarised and preventing further influx of Ca^{2+} into the cells and that may control the activation of AMPK in VSMCs.

Taken together, these studies indicate that the activation of K_{ATP} in vascular myocytes, in addition to cromakalim, may be mediated by a transferable factor released from PVAT (adiponectin) and that AMPK is involved in this process by either controlling release of adiponectin and/or activation of K_{ATP} in vascular myocytes.

6.6 Adiponectin as ADRF?

In an attempt to determine the chemical nature of ADRF, the effects of adiponectin on whole vessels and cultured VSMCs were investigated. A previous study by Greenstein *et al* speculated that adiponectin was the PVAT-derived anticontractile factor in human vessels, since an adiponectin blocking peptide abolished the anticontractile effects of

PVAT. However, the mechanism proposed in their study involves activation of eNOS in the endothelium and subsequent release of NO (Greenstein et al., 2009). The role of adiponectin in endothelium-independent relaxation has been investigated in other studies which reported the involvement of both AMPK and BK_{Ca} (Weston et al., 2013, Lynch et al., 2013). In the current study, the importance of adiponectin to the anti-contractile effect of PVAT was illustrated as PVAT from AMPKα1 knockout mice had an impaired anti-contractile effect in functional studies and this corresponded with reduced adiponectin content and release. Application of globular adiponectin enhanced the vasorelaxant effect of both WT and KO thoracic aortae (Figure 3-27). Furthermore, by using a K_{ATP} channel opener in vessel tension experiments, the current study suggests that the attenuated relaxation in KO arteries may be attributed to the adiponectin deficiency in KO PVAT and that adiponectin-induced hyperpolarisation in WT occurs as a result of opening of K_{ATP} channels in the medial layer. The role of K_{ATP} channels could be confirmed using a selective blocker such as glibenclamide and/or measuring membrane potential in VSMCs treated with adiponectin. The role of K_{ATP} channels could also be studied using specific K_{ATP} channel knockout model animals. It is worth noting that a specific K_{ATP} channel KO has been reported by targeting Sur2 or Kir6.1 subunit (Nichols et al., 2013).

As application of globular adiponectin enhanced the cromakalim-induced relaxation in both wild type and AMPKα1-deficient vessels, four conclusions can be drawn. Firstly, the attenuated relaxation response in the KO occurred as result of dysfunctional adiponectin release from PVAT and that the downstream effectors in vascular smooth muscle are intact and still able to respond to adiponectin. Secondly, the expression of adiponectin receptors in the medial layer might be not affected by AMPKα1 deletion, although the expression of these receptors has not been investigated in the current study. Thirdly, adiponectin can activate K_{ATP} in the myocytes directly and induce hyperpolarisation and relaxation. The direct K_{ATP} activation by adiponectin has been reported previously in nerve cells (Hoyda and Ferguson, 2010). However, there are many different types of K_{ATP} channels with variable expression and tissue localisation (Ko et al., 2008). Furthermore, the role of K_{ATP} in the PVAT anti-contractile effect has been previously proposed by Lohn et al without defining the ADRF released by PVAT (Lohn et al., 2002). Finally, the enhanced relaxation in both WT and KO arteries in response to globular adiponectin suggests a possible direct action of adiponectin on vascular myocytes mediated by activation of MLCK which needs to be further clarified.

Together, these data indicate that non-stimulated PVAT releases adiponectin and that adiponectin (and perhaps other PVAT-derived factors) can activate K_{ATP} channels on the myocytes. It is likely in the mouse aorta that adiponectin is the ADRF. Hence, the anti-contractile effect of adiponectin is apparently via two different mechanisms: firstly, by activating the K_{ATP} channels on the myocytes to cause hyperpolarisation; secondly, it may also trigger inhibition of MLCK and/or activation of MLCP in VSMCs.

6.7 Proposed mechanism of relaxation

The release of ADRF has been reported to be dependent on Ca^{2+} and is regulated by intracellular signalling pathways involving tyrosine kinase and protein kinase A, independent of perivascular nerve endings (Dubrovska et al., 2004). There are very few studies where the role of AMPK in the release of ADRFs has been investigated. A study by Lihn et al indicated that the AMPK activator AICAR stimulated adipose tissue AMPKα1 activity and adiponectin gene expression and reduced the release of TNF-α and IL-6 (Lihn et al., 2004). These cytokines have been shown to have inhibitory effects on adiponectin gene expression and release (Fasshauer et al., 2002, Maeda et al., 2002, Greenberg et al., 1991), meaning that activity of AMPK in the PVAT could regulate adiponectin expression (Lihn et al., 2004). Similarly, the PPARγ agonist troglitazone which also activates AMPK has a positive effect on adiponectin expression in mature adipocytes (Phillips et al., 2003). The current study supports previous evidence as the KO PVAT exhibited a profound reduction in adiponectin release as confirmed by both array and ELISA (Figures 3-22 and 3-23). However, other studies using cultured 3T3-L1 adipocytes found that prolonged exposure to AMPK activating agents actually causes a significant reduction in adiponectin protein content of the adipocytes (Huypens et al., 2005). Therefore, it can be proposed that AMPK modulates adiponectin release by directly affecting its secretion by PVAT or indirectly via alleviating PVAT inflammation. Figure 6-1 illustrates the proposed mechanism by which PVAT AMPK modulates vascular function.

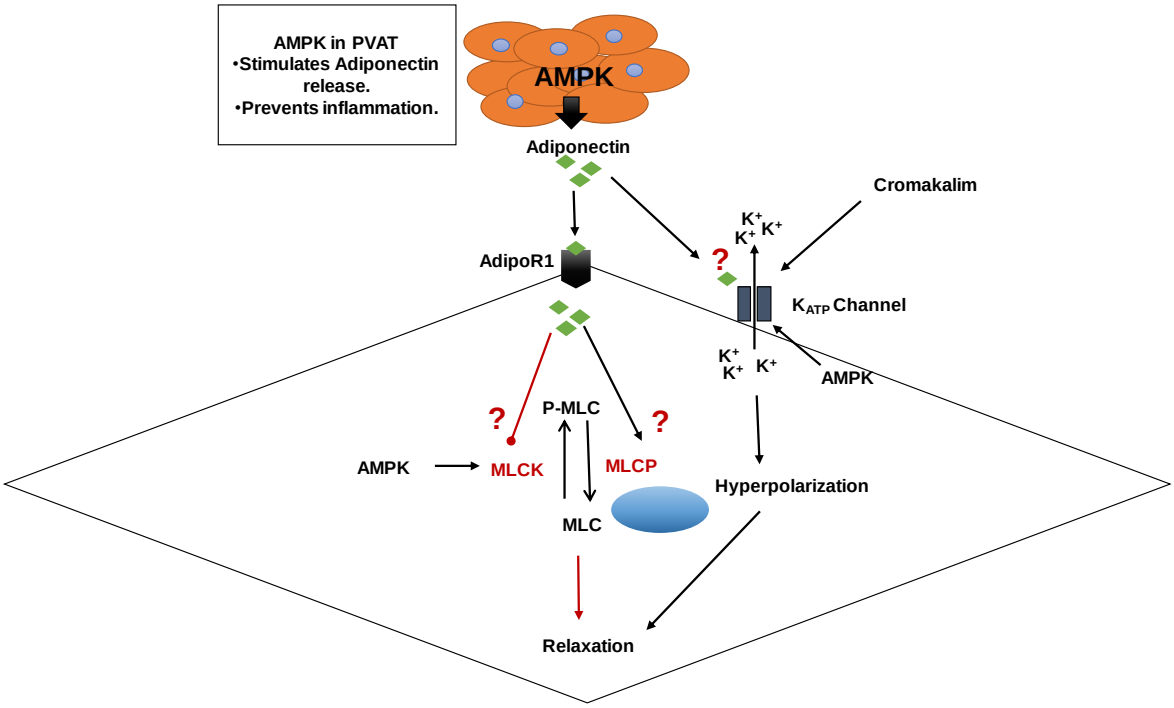

Figure 6-1 The proposed anticontractile mechanism of perivascular adipocytes on vascular myocytes.

AMPK: AMP-activated protein kinase; AdipoR1: Adiponectin receptor 1; K_{ATP}: ATP-sensitive potassium channel; MLCK: Myosin light chain Kinase; MLCP: Myosin light chain phosphatase.

6.8 Mechanism of PVAT dysfunction in obesity

In chapter 5, an investigation of the effects of obesity on PVAT function was examined, assessing the contribution of AMPK in more detail. The current investigation using ELISA showed that the levels of adiponectin were significantly lower in PVAT and CM from HFD-fed mice as compared with ND group (Figure 5-12). It has been reported previously that adiponectin released from PVAT has a profound vasorelaxant effect on nearby arteries (Greenstein et al., 2009), and that data presented in this thesis confirms that the PVAT anti-contractile effect is impaired in obese mice compared to healthy controls (Figure 5-4). The macrophage infiltration in the obese PVAT as reported in the current study (Figure 5-11) and previous reports (Aghamohammadzadeh et al., 2015) and the reduced activity of AMPK in obese and AMPKα1 knockout PVAT (Figure 5-10) suggests that higher levels of inflammatory mediators such as cytokines and superoxide in the PVAT may have adverse vasoactive effects on adjacent vasculature.

Obesity is associated with chronic low-grade inflammation in adipose tissue that can be extended to PVAT. HFD leads to an increase in adipose tissue mass that initially occurrs as

a result of cell hyperplasia mediated by the recruitment and proliferation of adipogenic progenitors such as IGF-I, IGF binding proteins, TNFα, angiotensin II, and MCSF(Hausman et al., 2001). Later, increased fatty acid deposition in adipocytes is associated with cell death. Cell death with the release of inflammatory cytokines leads to rerecruitment of inflammatory cells and to adipose tissue dysfunction (Cinti et al., 2005). Obesity causes major changes in cellular phenotype of adipose tissue that can be detected systemically or within local adipose tissue. HFD-induced obesity induces a shift in the PVAT secretory function profile from anti-inflammatory profile to pro-inflammatory profile by releasing cytokines and chemokines which are linked with oxidative stress in PVAT (Bailey-Downs et al., 2013). HFD-induced obesity is associated with enhanced production of proinflammatory adipokines, such as TNF-α, leptin, resistin and decreased production of anti-inflammatory adipokines, such as adiponectin (Chatterjee et al., 2009, Arita et al., 1999, Serne et al., 2007). In another study, HFD increased mesenteric PVAT macrophage content and vascular oxidative stress in mice (Wang et al., 2012). Human adipocytes show an increase in proinflammatory cytokines expression in obese states (IL-6, IL-8, and MCP-1) and reduced adipocytic differentiation (Chatterjee et al., 2009). These data suggest that inflammatory cytokine release by PVAT could attract macrophages to the depot further aggravating inflammation and PVAT dysfunction.

Several signalling pathways have been suggested in pro-inflammatory adipocytokine-induced adipose tissue inflammation. Cytokines such as TNF-α and IL-1β signalling pathway involves activation of pro-inflammatory transcription factors ERK, p38 and JNK MAP kinases and the NF-kB (Salt and Palmer, 2012). Factors such as leptin and IL-6 signalling involves JAK/STAT pathway (Richard and Stephens, 2014). In obesity, These signalling pathways result in upregulation of chemokines, including MCP-1 which stimulates macrophages infiltration to the site of inflammation (Gesta et al., 2007). Obesity-associated inflammation may also involve other chemokine receptors and ligands, including MIP-1, RANTES and MCP-2 (Kitade et al., 2012). Macrophage infiltration into adipose tissue also occures in response to adipocyte death as demonstrated by Cinti *et al* (Cinti et al., 2005) or in response to increased caloric intake (increased FA) (Nguyen et al., 2007). The recruitment of macrophages in response to FA occurs as a result of activation of TLR (Toll-like receptor) family which in turn trigger proinflammatory pathways and induces cytokine expression (Shi et al., 2006).

Adipose tissue macrophages in healthy mice have the genetic features of M2 macrophages with anti-inflammatory properties, which may protect adipocytes from inflammation. HFD-induced obesity causes a shift in the macrophage polarity to an M1 pro-inflammatory state that contributes to insulin resistance (Lumeng et al., 2007). It is worth noting that adiponectin induces anti-inflammatory function by polarisin adipose tissue macrophages into M2 macrophages with characteristic anti-inflammatory markers (Ohashi et al., 2010). Recruited macrophages can induce an inflammatory reaction via activation of NLRP3 inflammosome which results in maturation and release of cytokines IL-1β and IL-18 (Vandanmagsar et al., 2011).

There is much evidence demonstrating AMPK is anti-inflammatory and acts as a protective mechanism against inflammation (Salt and Palmer, 2012). Several mechanisms have been proposed. Activation of AMPK can abolish the production of pro-inflammatory cytokines such as TNF-α, IL-1β and IL-6 in macrophages (Galic et al., 2011, Yang et al., 2010, Jeong et al., 2009, Sag et al., 2008) and IL-6 and IL-8 in adipocytes (Lihn et al., 2008). AMPK activation was also shown to increase expression of anti-inflammatory cytokine IL-10 in macrophages (Galic et al., 2011, Sag et al., 2008). Activation of AMPK by AICAR in cultured adipocytes has been shown to promote adiponectin gene expression, while attenuating the release of TNF-α and IL-6 (Lihn et al., 2004). Similarly, activation of AMPK by berberine attenuates the expression of proinflammatory genes such as TNF-α, IL-1β, IL-6, MCP-1, iNOS, and COX-2 in adipose tissue (Jeong et al., 2009). Activation of NLRP3 inflammasome in myeloid cells by metformin has been reported to reduce release of IL-1β and IL-18 in monocyte-derived macrophages, an effect which may involve AMPK (Lee et al., 2013).

In addition, in healthy WT animals, there was preservation of PVAT anticontractile function after removal of the endothelium, thus supporting the data reported by Gao et al (Gao et al., 2007) that PVAT effect is not dependent on the presence of endothelium. In the HFD model, there was partial preservation of the anti-contractile capacity in WT but not KO mice in the absence of endothelium. These observations could be attributed to the protective mechanism of AMPK against inflammatory insults and/or contribution of other vasodilators released from PVAT such as H_2S.

Taken together, in obesity, increases in the amount of PVAT and in the expression pattern of adipokines and other PVAT-derived factors may shift the normal paracrine influence of PVAT from a net vasorelaxant role to an oxidative, pro-inflammatory, and contractile

status. This shift towards the dominance of vasoconstrictor and inflammatory factors, together with the lack of normal functioning AMPK in obesity could provide the link between obesity and the functional and structural changes observed in CVD.

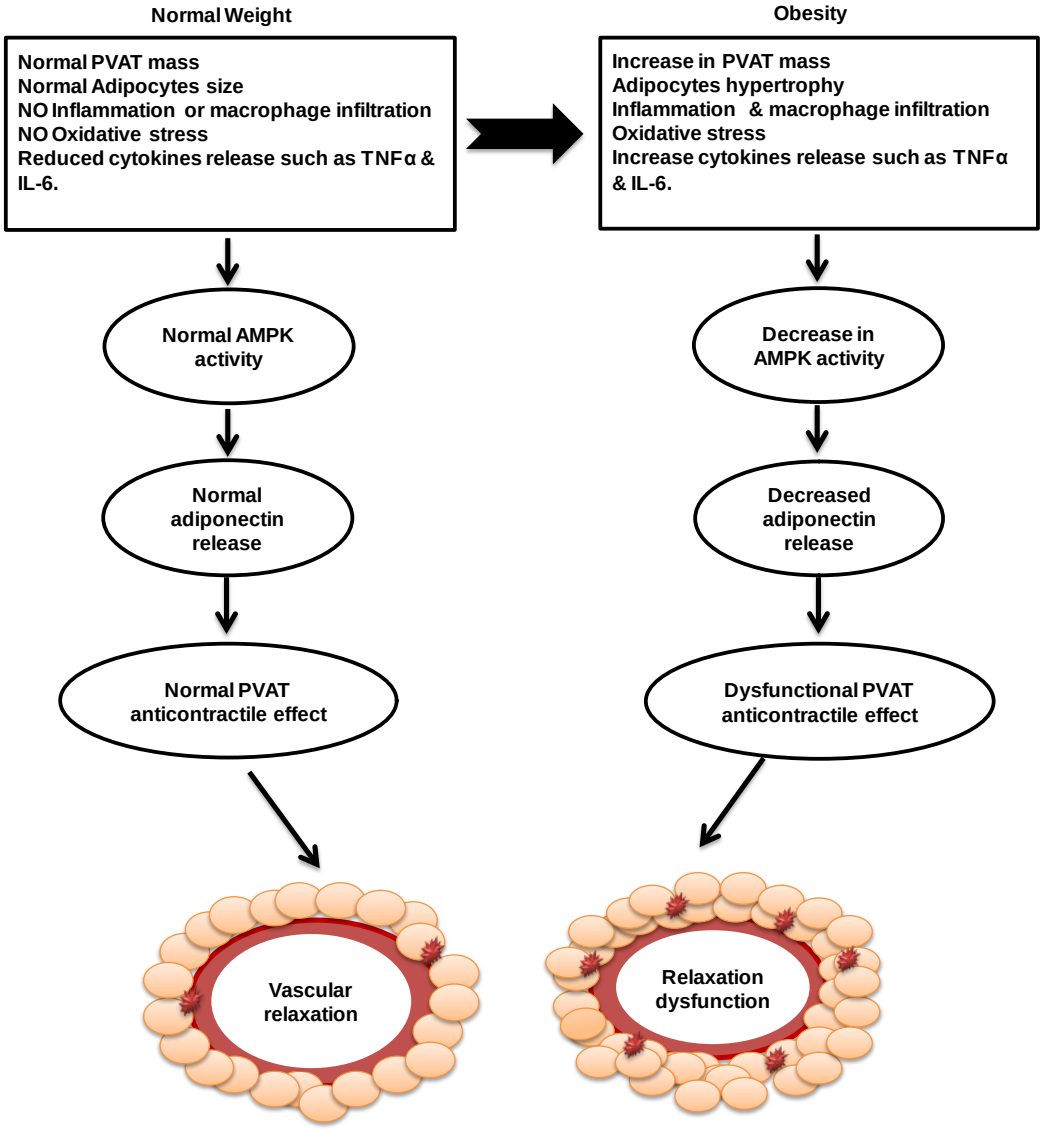

Figure 6-2 Hypothesis of the mechanism of PVAT dysfunction in obesity and the role of AMPK.

6.9 Potential physiological relevance and clinical implications

Findings generated in this thesis have physiological, pathophysiological and therapeutic implications. The results of the current thesis provide evidence that supports a potential role for PVAT in regulation of vascular contraction mediated via AMPK *in situ*, a vasoprotective function for AMPK in maintaining normal PVAT function in regulating

vasomotor responsiveness in healthy vasculature, and a potential therapeutic target for AMPK in treatment of vascular dysfunction associated with obesity and CVD.

6.9.1 Basal AMPK activity may act as vasculoprotective mechanism

The findings in this thesis indicate that basal AMPK activation is depressed in PVAT of both obese and KO mice relative to lean and WT animals, respectively (Figure 5-10). Since the reduction of AMPK in PVAT is associated with dysfunctional vasomotor function in obese and KO animals, it can be assumed that activation of AMPK at basal conditions will act as a protective mechanism against vascular insult, maintaining a healthy vascular function or perhaps help in alleviating the consequence of any pathological conditions that trigger vascular dysfunction.

The protective function of the AMPK has been reported before in endothelium and VSMCs. It has been reported that deletion of AMPKα2 subunit is associated with endothelial dysfunction (Wang et al., 2010b) and increased vascular smooth muscle contraction (Wang et al., 2011b). The study by Meijer *et al* investigated the effect of PVAT on the insulin-induced vasodilatation in muscular resistance arteries and showed that insulin causes dilation in AMPKα2 intact vessels while deletion of AMPKα2 caused insulin to induce vasoconstriction. Furthermore, the vasoralxant effect of PVAT was diminished in obese mice and that inhibition of JNK restored insulin-induced vasodilation in an adiponectin-dependent manner (Meijer et al., 2013). The current research reported different subunit contribution to the anti-contractile effect of PVAT. The difference in the findings may be related to the mice strain or to the type of vessels they utilise. Additionally, it might be related to the insulin signalling pathway which might be dependent of AMPKα2.

Another study reported that endothelial dysfunction was more pronounced in AMPK α1 deficient mice chronically treated with angiotensin II compared to WT mice and that the AMPK α1 in WT retain certain degree of endothelial function in mice treated with angiotensin II (Schuhmacher et al., 2011). Data from the current thesis suggest that AMPKα1 may partially preserve PVAT anticontractile effects in case of endothelial injury via modulation of adipocytokine production and release. These findings suggest that AMPK plays a vascular protective role under normal physiological conditions and protects against vascular tone dysfunction induced by cardiovascular pathologies.

However, the results using a global AMPK knockout model are not conclusive, as this model is also associated with other metabolic and physiological dysfunction that might lead to altered vasomotor impairment independently of the AMPK catalytic subunit ablation in the vessel or PVAT itself (Viollet et al., 2003, Jorgensen et al., 2004, Andreelli et al., 2006). Furthermore, it is difficult to determine the extent of α2 subunit compensation in the absence of the other alpha subunit. Indeed, the findings of the current research do appear to add to the previous evidence regarding the protective role for AMPK in maintaining normal vasomotor function, although continued investigation is mandatory to confirm the current data. If AMPK does play a role in regulating physiological responses to different stimuli in health, it is plausible to think that the depression of AMPK activity in blood vessels including PVAT in obesity contributes to the dysfunctional vascular phenotype in these animals.

6.9.2 Activation of AMPK in PVAT is a Potential therapeutic target

Currently, the only therapeutic strategy that has been reported to improve survival in obese patients is weight-reducing surgery. However, its higher cost makes it less efficient. Based on the current findings and evidence in literature, PVAT function is essential to maintain normal vascular haemostasis. If this is the case, any therapeutic strategy that can prevent inflammation and beneficially manipulate secretory function at the adipocyte level would be attractive.

Many studies have investigated the therapeutic benefit of AMPK-targeted compounds on the vascular tone in animal disease models. α-lipoic acid, a potent antioxidant used in treatment of diabetic neuropathy, has been found to alleviate endothelial dysfunction in obese rats (Lee et al., 2005). Another natural compound known as berberine was found to protect endothelial cells from hyperglycaemia and enhance vasodilation via AMPK activation (Wang et al., 2009c). Furthermore, *in vivo* administration of metformin has been found to enhance acetylcholine-induced relaxation and decrease endothelium-derived contracting factor (EDCF)-mediated contraction in OLEFT rat mesenteric rings (Matsumoto et al., 2008). Similarly, cultured SCAT derived from obese women and stimulated with AICAR showed enhanced adiponectin and GLUT4 expression and reduced TNF-α, IL-8 and IL-6 secretion (Lihn et al., 2004, Lihn et al., 2008).

Interestingly, a synthetic small-molecule adiponectin receptor agonist (adipoRon) has been synthesised and was found to have similar effects to adiponectin on muscle and liver.

AdipoRon alleviates obesity-associated insulin resistance and glucose intolerance in obese rodent model db/db mice, and prolonged the lifespan of db/db mice on a high-fat diet. This effect involves activation of AMPK and PPAR-α pathway (Okada-Iwabu et al., 2013). Perhaps most exciting is a recent report on adipoRon where it was found to induce vasodilation in rat cerebral and coronary arteries. However, the effect was endothelium-independent and also independent from AMPK, K^+ efflux and any decrease in intracellular Ca^{2+} (Hong et al., 2016). AdipoRon is a promising therapeutic approach for the treatment of obesity-related diseases such as type 2 diabetes.

The current evidence supports that PVAT have the capacity to act in a paracrine manner, on the circulation, the function of which it modulates via complex mechanisms which involves AMPK. The alterations in the anticontractile function of PVAT associated with obesity, metabolic syndrome, hypertension, or atherosclerosis are correlated with an imbalance in the secretion of adipokines such as adiponectin, inflammation and oxidative stress, resulted in vascular dysfunction. The sequence and the trigger of this phathophysiology are unclear, and the main events reported in this thesis, appear to be the PVAT infiltration by macrophage and reduced AMPK expression. A better understanding of PVAT physiology may allow for the design of therapies for vascular dysfunction and of strategies for directing these therapies to PVAT. Furthermore, the current findings provide meaningful data to justify follow-up in vivo studies to evaluate the role of AMPK activation in both physiological and pathophysiological state. Furthermore, more human studies are certainly needed in order to definitively define the role of PVAT AMPK in cardiovascular disease.

6.10 Limitations

Despite the research advances, AMPK remains a challenging system to study due to its multiple interactions with other molecules at both cellular and whole body level and its ubiquitous distribution. Furthermore, the lack of specific tools currently available to study this enzyme in adipose tissue including PVAT is one limitation that exists with this field of research. Although models of global AMPKα1 and α2 knockout have been generated, their application in identifying a specific role for PVAT AMPK in regulating vascular function is limited as these models are usually associated with metabolic and physiological dysfunction. Recently, adipose tissue-specific AMPKα1 and α2 knockout mouse models have been generated and used to investigate the role of AMPK in lipolysis and FA metabolism in adipose tissue under physiological conditions (Giordano et al., 2005). This

model may be more useful for providing insight regarding the vascular effects of PVAT AMPK, as these animals should exhibit major reductions in PVAT AMPK activity (AMPK α1 is the predominant isoform expressed in PVAT).

6.11 Concluding remarks

The results presented in this thesis have increased our understanding of signalling pathways involved in regulation of vascular contractility by providing insight on a novel mechanism and regulator of vascular tone in both health and disease state. Furthermore, the data presented in this thesis provides not only supporting evidence about the function of adiponectin as a potential physiological modulator of vascular tone but also helps the understanding of the molecular mechanisms behind the vasculoprotective effects of this adipokine and its interaction with AMPK.

It is, however, important to consider that the mechanisms proposed in this thesis and other research are *ex vivo/in vitro* studies and, thus, the physiological and clinical relevance of these results remains to be further investigated. Therefore, it is essential to continue to investigate the basic signalling mechanisms by which PVAT controls vascular haemostasis, as understanding the fundamental mechanism of AMPK vasomotor signalling pathways and their functional outcomes will broaden the understanding of regulation of vascular haemodynamic control. Furthermore, it will facilitate the development of potential novel therapeutic approaches that can be used to tackle vascular dysfunction associated with obesity and its complications.

Chapter 7

List of References

ADAMS, J., CHEN, Z. P., VAN DENDEREN, B. J., MORTON, C. J., PARKER, M. W., WITTERS, L. A., STAPLETON, D. & KEMP, B. E. 2004. Intrasteric control of AMPK via the gamma1 subunit AMP allosteric regulatory site. *Protein Sci,* 13**,** 155-65.

AGHAMOHAMMADZADEH, R., UNWIN, R. D., GREENSTEIN, A. S. & HEAGERTY, A. M. 2015. Effects of Obesity on Perivascular Adipose Tissue Vasorelaxant Function: Nitric Oxide, Inflammation and Elevated Systemic Blood Pressure. *J Vasc Res,* 52**,** 299-305.

ALBA, G., EL BEKAY, R., ALVAREZ-MAQUEDA, M., CHACON, P., VEGA, A., MONTESEIRIN, J., SANTA MARIA, C., PINTADO, E., BEDOYA, F. J., BARTRONS, R. & SOBRINO, F. 2004. Stimulators of AMP-activated protein kinase inhibit the respiratory burst in human neutrophils. *FEBS Lett,* 573**,** 219-25.

ALMABROUK, T. A., EWART, M. A., SALT, I. P. & KENNEDY, S. 2014. Perivascular fat, AMP-activated protein kinase and vascular diseases. *Br J Pharmacol,* 171**,** 595-617.

ALMABROUK, T. A., UGUSMAN, A. B., KATWAN, O. J., SALT, I. P. & KENNEDY, S. 2016. Deletion of AMPKalpha1 attenuates the anticontractile effect of perivascular adipose tissue (PVAT) and reduces adiponectin release. *Br J Pharmacol*.

ANDERSON, K. A., RIBAR, T. J., LIN, F., NOELDNER, P. K., GREEN, M. F., MUEHLBAUER, M. J., WITTERS, L. A., KEMP, B. E. & MEANS, A. R. 2008. Hypothalamic CaMKK2 contributes to the regulation of energy balance. *Cell Metab,* 7**,** 377-88.

ANDREELLI, F., FORETZ, M., KNAUF, C., CANI, P. D., PERRIN, C., IGLESIAS, M. A., PILLOT, B., BADO, A., TRONCHE, F., MITHIEUX, G., VAULONT, S., BURCELIN, R. & VIOLLET, B. 2006. Liver adenosine monophosphate-activated kinase-alpha2 catalytic subunit is a key target for the control of hepatic glucose production by adiponectin and leptin but not insulin. *Endocrinology,* 147**,** 2432-41.

ANTIPATIS, V. J. & GILL, T. P. 2001. *International Textbook of Obesity,* Chichester, John Wiley & Sons, Ltd.

ANTONIADES, C., ANTONOPOULOS, A. S., TOUSOULIS, D. & STEFANADIS, C. 2009. Adiponectin: from obesity to cardiovascular disease. *Obes Rev,* 10**,** 269-79.

ARAUJO, H. N., VALGAS DA SILVA, C. P., SPONTON, A. C., CLERICI, S. P., DAVEL, A. P., ANTUNES, E., ZANESCO, A. & DELBIN, M. A. 2015. Perivascular adipose tissue and vascular responses in healthy trained rats. *Life Sci,* 125**,** 79-87.

ARITA, Y., KIHARA, S., OUCHI, N., MAEDA, K., KURIYAMA, H., OKAMOTO, Y., KUMADA, M., HOTTA, K., NISHIDA, M., TAKAHASHI, M., NAKAMURA, T., SHIMOMURA, I., MURAGUCHI, M., OHMOTO, Y., FUNAHASHI, T. &

MATSUZAWA, Y. 2002. Adipocyte-derived plasma protein adiponectin acts as a platelet-derived growth factor-BB-binding protein and regulates growth factor-induced common postreceptor signal in vascular smooth muscle cell. *Circulation,* 105**,** 2893-8.

ARITA, Y., KIHARA, S., OUCHI, N., TAKAHASHI, M., MAEDA, K., MIYAGAWA, J., HOTTA, K., SHIMOMURA, I., NAKAMURA, T., MIYAOKA, K., KURIYAMA, H., NISHIDA, M., YAMASHITA, S., OKUBO, K., MATSUBARA, K., MURAGUCHI, M., OHMOTO, Y., FUNAHASHI, T. & MATSUZAWA, Y. 1999. Paradoxical decrease of an adipose-specific protein, adiponectin, in obesity. *Biochem Biophys Res Commun,* 257**,** 79-83.

ASANO, K., CHEE, C. B., GASTON, B., LILLY, C. M., GERARD, C., DRAZEN, J. M. & STAMLER, J. S. 1994. Constitutive and inducible nitric oxide synthase gene expression, regulation, and activity in human lung epithelial cells. *Proc Natl Acad Sci U S A,* 91**,** 10089-93.

AZIMOVA, K., SAN JUAN, Z. & MUKHERJEE, D. 2014. Cardiovascular safety profile of currently available diabetic drugs. *Ochsner J,* 14**,** 616-32.

BAHRING, R., MILLIGAN, C. J., VARDANYAN, V., ENGELAND, B., YOUNG, B. A., DANNENBERG, J., WALDSCHUTZ, R., EDWARDS, J. P., WRAY, D. & PONGS, O. 2001. Coupling of voltage-dependent potassium channel inactivation and oxidoreductase active site of Kvbeta subunits. *J Biol Chem,* 276**,** 22923-9.

BAILEY-DOWNS, L. C., TUCSEK, Z., TOTH, P., SOSNOWSKA, D., GAUTAM, T., SONNTAG, W. E., CSISZAR, A. & UNGVARI, Z. 2013. Aging exacerbates obesity-induced oxidative stress and inflammation in perivascular adipose tissue in mice: a paracrine mechanism contributing to vascular redox dysregulation and inflammation. *J Gerontol A Biol Sci Med Sci,* 68**,** 780-92.

BAUMANN, P., MANDL-WEBER, S., EMMERICH, B., STRAKA, C. & SCHMIDMAIER, R. 2007. Activation of adenosine monophosphate activated protein kinase inhibits growth of multiple myeloma cells. *Exp Cell Res,* 313**,** 3592-603.

BAUWENS, J. D., SCHMUCK, E. G., LINDHOLM, C. R., ERTEL, R. L., MULLIGAN, J. D., HOVIS, I., VIOLLET, B. & SAUPE, K. W. 2011. Cold tolerance, cold-induced hyperphagia, and nonshivering thermogenesis are normal in alpha(1)-AMPK-/- mice. *Am J Physiol Regul Integr Comp Physiol,* 301**,** R473-83.

BECKMAN, J. S., BECKMAN, T. W., CHEN, J., MARSHALL, P. A. & FREEMAN, B. A. 1990. Apparent hydroxyl radical production by peroxynitrite: implications for endothelial injury from nitric oxide and superoxide. *Proc Natl Acad Sci U S A,* 87**,** 1620-4.

BECKMAN, J. S., MINOR, R. L., JR., WHITE, C. W., REPINE, J. E., ROSEN, G. M. & FREEMAN, B. A. 1988. Superoxide dismutase and catalase conjugated to polyethylene

glycol increases endothelial enzyme activity and oxidant resistance. *J Biol Chem,* 263**,** 6884-92.

BECKMANN, J. S., YE, Y. Z., ANDERSON, P. G., CHEN, J., ACCAVITTI, M. A., TARPEY, M. M. & WHITE, C. R. 1994. Extensive nitration of protein tyrosines in human atherosclerosis detected by immunohistochemistry. *Biol Chem Hoppe Seyler,* 375**,** 81-8.

BILODEAU-GOESEELS, S., PANICH, P. L. & KASTELIC, J. P. 2011. Activation of AMP-activated protein kinase may not be involved in AICAR- and metformin-mediated meiotic arrest in bovine denuded and cumulus-enclosed oocytes in vitro. *Zygote,* 19**,** 97-106.

BOLTON, T. B. & IMAIZUMI, Y. 1996. Spontaneous transient outward currents in smooth muscle cells. *Cell Calcium,* 20**,** 141-52.

BOYLE, J. G., LOGAN, P. J., EWART, M.-A., REIHILL, J. A., RITCHIE, S. A., CONNELL, J. M. C., CLELAND, S. J. & SALT, I. P. 2008. Rosiglitazone Stimulates Nitric Oxide Synthesis in Human Aortic Endothelial Cells via AMP-activated Protein Kinase. *Journal of Biological Chemistry,* 283**,** 11210-11217.

BRADLEY, E. A., ERINGA, E. C., STEHOUWER, C. D., KORSTJENS, I., VAN NIEUW AMERONGEN, G. P., MUSTERS, R., SIPKEMA, P., CLARK, M. G. & RATTIGAN, S. 2010. Activation of AMP-activated protein kinase by 5-aminoimidazole-4-carboxamide-1-beta-D-ribofuranoside in the muscle microcirculation increases nitric oxide synthesis and microvascular perfusion. *Arterioscler Thromb Vasc Biol,* 30**,** 1137-42.

BRIAN, J. E., JR. & FARACI, F. M. 1998. Tumor necrosis factor-alpha-induced dilatation of cerebral arterioles. *Stroke,* 29**,** 509-15.

BROILLET, M., RANDIN, O. & CHATTON, J. 2001. Photoactivation and calcium sensitivity of the fluorescent NO indicator 4,5-diaminofluorescein (DAF-2): implications for cellular NO imaging. *FEBS Lett,* 491**,** 227-32.

BROWN, N. K., ZHOU, Z., ZHANG, J., ZENG, R., WU, J., EITZMAN, D. T., CHEN, Y. E. & CHANG, L. 2014. Perivascular Adipose Tissue in Vascular Function and Disease: A Review of Current Research and Animal Models. *Arteriosclerosis, Thrombosis, and Vascular Biology,* 34**,** 1621-1630.

BRUEGGEMANN, L. I., MORAN, C. J., BARAKAT, J. A., YEH, J. Z., CRIBBS, L. L. & BYRON, K. L. 2007. Vasopressin stimulates action potential firing by protein kinase C-dependent inhibition of KCNQ5 in A7r5 rat aortic smooth muscle cells. *Am J Physiol Heart Circ Physiol,* 292**,** H1352-63.

BRUNMAIR, B., STANIEK, K., GRAS, F., SCHARF, N., ALTHAYM, A., CLARA, R., RODEN, M., GNAIGER, E., NOHL, H., WALDHAUSL, W. & FURNSINN, C. 2004.

Thiazolidinediones, like metformin, inhibit respiratory complex I: a common mechanism contributing to their antidiabetic actions? *Diabetes,* 53**,** 1052-9.

BUHL, E. S., JESSEN, N., POLD, R., LEDET, T., FLYVBJERG, A., PEDERSEN, S. B., PEDERSEN, O., SCHMITZ, O. & LUND, S. 2002. Long-term AICAR administration reduces metabolic disturbances and lowers blood pressure in rats displaying features of the insulin resistance syndrome. *Diabetes,* 51**,** 2199-206.

BURNS, K. A. & VANDEN HEUVEL, J. P. 2007. Modulation of PPAR activity via phosphorylation. *Biochim Biophys Acta,* 1771**,** 952-60.

CAHOON, W. D., JR. & CROUCH, M. A. 2007. Preprocedural statin therapy in percutaneous coronary intervention. *Ann Pharmacother,* 41**,** 1687-93.

CAI, X. J., CHEN, L., LI, L., FENG, M., LI, X., ZHANG, K., RONG, Y. Y., HU, X. B., ZHANG, M. X., ZHANG, Y. & ZHANG, M. 2010. Adiponectin inhibits lipopolysaccharide-induced adventitial fibroblast migration and transition to myofibroblasts via AdipoR1-AMPK-iNOS pathway. *Mol Endocrinol,* 24**,** 218-28.

CAI, X. J., LI, C. J., CHEN, L., RONG, Y. Y., ZHANG, Y. & ZHANG, M. 2008. A hypothesis: adiponectin mediates anti-atherosclerosis via adventitia-AMPK-iNOS pathway. *Med Hypotheses,* 70**,** 1044-7.

CALABRESE, M. F., RAJAMOHAN, F., HARRIS, M. S., CASPERS, N. L., MAGYAR, R., WITHKA, J. M., WANG, H., BORZILLERI, K. A., SAHASRABUDHE, P. V., HOTH, L. R., GEOGHEGAN, K. F., HAN, S., BROWN, J., SUBASHI, T. A., REYES, A. R., FRISBIE, R. K., WARD, J., MILLER, R. A., LANDRO, J. A., LONDREGAN, A. T., CARPINO, P. A., CABRAL, S., SMITH, A. C., CONN, E. L., CAMERON, K. O., QIU, X. & KURUMBAIL, R. G. 2014. Structural basis for AMPK activation: natural and synthetic ligands regulate kinase activity from opposite poles by different molecular mechanisms. *Structure,* 22**,** 1161-72.

CALVERT, J. W., GUNDEWAR, S., JHA, S., GREER, J. J., BESTERMANN, W. H., TIAN, R. & LEFER, D. J. 2008. Acute metformin therapy confers cardioprotection against myocardial infarction via AMPK-eNOS-mediated signaling. *Diabetes,* 57**,** 696-705.

CANNON, B. & NEDERGAARD, J. 2004. Brown adipose tissue: function and physiological significance. *Physiol Rev,* 84**,** 277-359.

CAO, X., LI, H., TAO, H., WU, N., YU, L., ZHANG, D., LU, X., ZHU, J., LU, Z. & ZHU, Q. 2013. Metformin inhibits vascular calcification in female rat aortic smooth muscle cells via the AMPK-eNOS-NO pathway. *Endocrinology,* 154**,** 3680-9.

CARLING, D., MAYER, F. V., SANDERS, M. J. & GAMBLIN, S. J. 2011. AMP-activated protein kinase: nature's energy sensor. *Nat Chem Biol,* 7**,** 512-8.

CATERSON, I. D., HUBBARD, V., BRAY, G. A., GRUNSTEIN, R., HANSEN, B. C., HONG, Y., LABARTHE, D., SEIDELL, J. C. & SMITH, S. C., JR. 2004. Prevention Conference VII: Obesity, a worldwide epidemic related to heart disease and stroke: Group III: worldwide comorbidities of obesity. *Circulation,* 110**,** e476-83.

CENTENO-BAEZ, C., DALLAIRE, P. & MARETTE, A. 2011. Resveratrol inhibition of inducible nitric oxide synthase in skeletal muscle involves AMPK but not SIRT1. *Am J Physiol Endocrinol Metab,* 301**,** E922-30.

CEOLOTTO, G., GALLO, A., PAPPARELLA, I., FRANCO, L., MURPHY, E., IORI, E., PAGNIN, E., FADINI, G. P., ALBIERO, M., SEMPLICINI, A. & AVOGARO, A. 2007. Rosiglitazone reduces glucose-induced oxidative stress mediated by NAD(P)H oxidase via AMPK-dependent mechanism. *Arterioscler Thromb Vasc Biol,* 27**,** 2627-33.

CHA, H. N., CHOI, J. H., KIM, Y. W., KIM, J. Y., AHN, M. W. & PARK, S. Y. 2010. Metformin Inhibits Isoproterenol-induced Cardiac Hypertrophy in Mice. *Korean J Physiol Pharmacol,* 14**,** 377-84.

CHANG, L., VILLACORTA, L., LI, R., HAMBLIN, M., XU, W., DOU, C., ZHANG, J., WU, J., ZENG, R. & CHEN, Y. E. 2012. Loss of perivascular adipose tissue on peroxisome proliferator-activated receptor-gamma deletion in smooth muscle cells impairs intravascular thermoregulation and enhances atherosclerosis. *Circulation,* 126**,** 1067-78.

CHATTERJEE, T. K., STOLL, L. L., DENNING, G. M., HARRELSON, A., BLOMKALNS, A. L., IDELMAN, G., ROTHENBERG, F. G., NELTNER, B., ROMIG-MARTIN, S. A., DICKSON, E. W., RUDICH, S. & WEINTRAUB, N. L. 2009. Proinflammatory phenotype of perivascular adipocytes: influence of high-fat feeding. *Circ Res,* 104**,** 541-9.

CHEN, H., MONTAGNANI, M., FUNAHASHI, T., SHIMOMURA, I. & QUON, M. J. 2003. Adiponectin Stimulates Production of Nitric Oxide in Vascular Endothelial Cells. *Journal of Biological Chemistry,* 278**,** 45021-45026.

CHEN, Z., PENG, I. C., SUN, W., SU, M. I., HSU, P. H., FU, Y., ZHU, Y., DEFEA, K., PAN, S., TSAI, M. D. & SHYY, J. Y. 2009. AMP-activated protein kinase functionally phosphorylates endothelial nitric oxide synthase Ser633. *Circ Res,* 104**,** 496-505.

CHEN, Z. P., MITCHELHILL, K. I., MICHELL, B. J., STAPLETON, D., RODRIGUEZ-CRESPO, I., WITTERS, L. A., POWER, D. A., ORTIZ DE MONTELLANO, P. R. & KEMP, B. E. 1999. AMP-activated protein kinase phosphorylation of endothelial NO synthase. *FEBS Lett,* 443**,** 285-9.

CHENG, K. H., CHU, C. S., LEE, K. T., LIN, T. H., HSIEH, C. C., CHIU, C. C., VOON, W. C., SHEU, S. H. & LAI, W. T. 2008. Adipocytokines and proinflammatory mediators

from abdominal and epicardial adipose tissue in patients with coronary artery disease. *Int J Obes (Lond),* 32**,** 268-74.

CHENG, K. K., LAM, K. S., WANG, Y., HUANG, Y., CARLING, D., WU, D., WONG, C. & XU, A. 2007. Adiponectin-induced endothelial nitric oxide synthase activation and nitric oxide production are mediated by APPL1 in endothelial cells. *Diabetes,* 56**,** 1387-94.

CHOI, H. C., SONG, P., XIE, Z., WU, Y., XU, J., ZHANG, M., DONG, Y., WANG, S., LAU, K. & ZOU, M. H. 2008. Reactive nitrogen species is required for the activation of the AMP-activated protein kinase by statin in vivo. *J Biol Chem,* 283**,** 20186-97.

CHOW, W. S., CHEUNG, B. M., TSO, A. W., XU, A., WAT, N. M., FONG, C. H., ONG, L. H., TAM, S., TAN, K. C., JANUS, E. D., LAM, T. H. & LAM, K. S. 2007. Hypoadiponectinemia as a predictor for the development of hypertension: a 5-year prospective study. *Hypertension,* 49**,** 1455-61.

CINTI, S. 2005. The adipose organ. *Prostaglandins Leukot Essent Fatty Acids,* 73**,** 9-15.

CINTI, S. 2011. Between brown and white: novel aspects of adipocyte differentiation. *Ann Med,* 43**,** 104-15.

CINTI, S., MITCHELL, G., BARBATELLI, G., MURANO, I., CERESI, E., FALOIA, E., WANG, S., FORTIER, M., GREENBERG, A. S. & OBIN, M. S. 2005. Adipocyte death defines macrophage localization and function in adipose tissue of obese mice and humans. *Journal of Lipid Research,* 46**,** 2347-2355.

COLE, W. C. & CLÉMENT-CHOMIENNE, O. 2003. ATP-Sensitive K+ Channels of Vascular Smooth Muscle Cells. *Journal of Cardiovascular Electrophysiology,* 14**,** 94-103.

COLEMAN, H. A., TARE, M. & PARKINGTON, H. C. 2004. Endothelial potassium channels, endothelium-dependent hyperpolarization and the regulation of vascular tone in health and disease. *Clin Exp Pharmacol Physiol,* 31**,** 641-9.

COLOMBO, S. L. & MONCADA, S. 2009. AMPKalpha1 regulates the antioxidant status of vascular endothelial cells. *Biochem J,* 421**,** 163-9.

COMBS, T. P., BERG, A. H., RAJALA, M. W., KLEBANOV, S., IYENGAR, P., JIMENEZ-CHILLARON, J. C., PATTI, M. E., KLEIN, S. L., WEINSTEIN, R. S. & SCHERER, P. E. 2003. Sexual differentiation, pregnancy, calorie restriction, and aging affect the adipocyte-specific secretory protein adiponectin. *Diabetes,* 52**,** 268-76.

COOK, N. S., WEIR, S. W. & DANZEISEN, M. C. 1988. Anti-vasoconstrictor effects of the K+ channel opener cromakalim on the rabbit aorta--comparison with the calcium antagonist isradipine. *Br J Pharmacol,* 95**,** 741-52.

COOKE, J. P. & OKA, R. K. 2002. Does leptin cause vascular disease? *Circulation,* 106**,** 1904-5.

COOL, B., ZINKER, B., CHIOU, W., KIFLE, L., CAO, N., PERHAM, M., DICKINSON, R., ADLER, A., GAGNE, G., IYENGAR, R., ZHAO, G., MARSH, K., KYM, P., JUNG, P., CAMP, H. S. & FREVERT, E. 2006. Identification and characterization of a small molecule AMPK activator that treats key components of type 2 diabetes and the metabolic syndrome. *Cell Metab,* 3**,** 403-16.

CORTON, J. M., GILLESPIE, J. G., HAWLEY, S. A. & HARDIE, D. G. 1995. 5-aminoimidazole-4-carboxamide ribonucleoside. A specific method for activating AMP-activated protein kinase in intact cells? *Eur J Biochem,* 229**,** 558-65.

CUTHBERTSON, D. J., BABRAJ, J. A., MUSTARD, K. J., TOWLER, M. C., GREEN, K. A., WACKERHAGE, H., LEESE, G. P., BAAR, K., THOMASON-HUGHES, M., SUTHERLAND, C., HARDIE, D. G. & RENNIE, M. J. 2007. 5-aminoimidazole-4-carboxamide 1-beta-D-ribofuranoside acutely stimulates skeletal muscle 2-deoxyglucose uptake in healthy men. *Diabetes,* 56**,** 2078-84.

DASHWOOD, M. R., DOOLEY, A., SHI-WEN, X., ABRAHAM, D. J. & SOUZA, D. S. 2007. Does periadventitial fat-derived nitric oxide play a role in improved saphenous vein graft patency in patients undergoing coronary artery bypass surgery? *J Vasc Res,* 44**,** 175-81.

DAUT, J., MAIER-RUDOLPH, W., VON BECKERATH, N., MEHRKE, G., GUNTHER, K. & GOEDEL-MEINEN, L. 1990. Hypoxic dilation of coronary arteries is mediated by ATP-sensitive potassium channels. *Science,* 247**,** 1341-1344.

DAVAL, M., DIOT-DUPUY, F., BAZIN, R., HAINAULT, I., VIOLLET, B., VAULONT, S., HAJDUCH, E., FERRE, P. & FOUFELLE, F. 2005. Anti-lipolytic action of AMP-activated protein kinase in rodent adipocytes. *J Biol Chem,* 280**,** 25250-7.

DAVAL, M., FOUFELLE, F. & FERRE, P. 2006. Functions of AMP-activated protein kinase in adipose tissue. *J Physiol,* 574**,** 55-62.

DAVIGNON, J. & GANZ, P. 2004. Role of endothelial dysfunction in atherosclerosis. *Circulation,* 109**,** III27-32.

DAVIS, B. J., XIE, Z., VIOLLET, B. & ZOU, M.-H. 2006. Activation of the AMP-Activated Kinase by Antidiabetes Drug Metformin Stimulates Nitric Oxide Synthesis In Vivo by Promoting the Association of Heat Shock Protein 90 and Endothelial Nitric Oxide Synthase. *Diabetes,* 55**,** 496-505.

DAVIS, K. E. & SCHERER, P. E. 2008. Adiponectin: no longer the lone soul in the fight against insulin resistance? *Biochem J,* 416**,** e7-9.

DEANFIELD, J. E., HALCOX, J. P. & RABELINK, T. J. 2007. Endothelial function and dysfunction: testing and clinical relevance. *Circulation,* 115**,** 1285-95.

DENG, G., LONG, Y., YU, Y. R. & LI, M. R. 2010. Adiponectin directly improves endothelial dysfunction in obese rats through the AMPK-eNOS Pathway. *Int J Obes (Lond),* 34**,** 165-71.

DENZEL, M. S., SCIMIA, M. C., ZUMSTEIN, P. M., WALSH, K., RUIZ-LOZANO, P. & RANSCHT, B. 2010. T-cadherin is critical for adiponectin-mediated cardioprotection in mice. *J Clin Invest,* 120**,** 4342-52.

DERAVE, W., AI, H., IHLEMANN, J., WITTERS, L. A., KRISTIANSEN, S., RICHTER, E. A. & PLOUG, T. 2000. Dissociation of AMP-activated protein kinase activation and glucose transport in contracting slow-twitch muscle. *Diabetes,* 49**,** 1281-7.

DIGBY, J. E., MCNEILL, E., DYAR, O. J., LAM, V., GREAVES, D. R. & CHOUDHURY, R. P. 2010. Anti-inflammatory effects of nicotinic acid in adipocytes demonstrated by suppression of fractalkine, RANTES, and MCP-1 and upregulation of adiponectin. *Atherosclerosis,* 209**,** 89-95.

DONG, Y., ZHANG, M., LIANG, B., XIE, Z., ZHAO, Z., ASFA, S., CHOI, H. C. & ZOU, M. H. 2010. Reduction of AMP-activated protein kinase alpha2 increases endoplasmic reticulum stress and atherosclerosis in vivo. *Circulation,* 121**,** 792-803.

DOWLING, R. J., ZAKIKHANI, M., FANTUS, I. G., POLLAK, M. & SONENBERG, N. 2007. Metformin inhibits mammalian target of rapamycin-dependent translation initiation in breast cancer cells. *Cancer Res,* 67**,** 10804-12.

DUBROVSKA, G., VERLOHREN, S., LUFT, F. C. & GOLLASCH, M. 2004. Mechanisms of ADRF release from rat aortic adventitial adipose tissue. *Am J Physiol Heart Circ Physiol,* 286**,** H1107-13.

EID, H. M., LYBERG, T., ARNESEN, H. & SELJEFLOT, I. 2007. Insulin and adiponectin inhibit the TNFalpha-induced ADMA accumulation in human endothelial cells: the role of DDAH. *Atherosclerosis,* 194**,** e1-8.

ENGELI, S. 2005. Is there a pathophysiological role for perivascular adipocytes? *Am J Physiol Heart Circ Physiol,* 289**,** H1794-5.

EVANS, A. M., MUSTARD, K. J., WYATT, C. N., PEERS, C., DIPP, M., KUMAR, P., KINNEAR, N. P. & HARDIE, D. G. 2005. Does AMP-activated protein kinase couple inhibition of mitochondrial oxidative phosphorylation by hypoxia to calcium signaling in O2-sensing cells? *J Biol Chem,* 280**,** 41504-11.

EWART, M. A. & KENNEDY, S. 2011. AMPK and vasculoprotection. *Pharmacol Ther,* 131**,** 242-53.

EWART, M. A., KOHLHAAS, C. F. & SALT, I. P. 2008. Inhibition of tumor necrosis factor alpha-stimulated monocyte adhesion to human aortic endothelial cells by AMP-activated protein kinase. *Arterioscler Thromb Vasc Biol,* 28**,** 2255-7.

FANG, L., ZHAO, J., CHEN, Y., MA, T., XU, G., TANG, C., LIU, X. & GENG, B. 2009. Hydrogen sulfide derived from periadventitial adipose tissue is a vasodilator. *J Hypertens,* 27**,** 2174-85.

FANGER, C. M., GHANSHANI, S., LOGSDON, N. J., RAUER, H., KALMAN, K., ZHOU, J., BECKINGHAM, K., CHANDY, K. G., CAHALAN, M. D. & AIYAR, J. 1999. Calmodulin Mediates Calcium-dependent Activation of the Intermediate Conductance KCa Channel,IKCa1. *Journal of Biological Chemistry,* 274**,** 5746-5754.

FASSHAUER, M., KLEIN, J., NEUMANN, S., ESZLINGER, M. & PASCHKE, R. 2002. Hormonal regulation of adiponectin gene expression in 3T3-L1 adipocytes. *Biochem Biophys Res Commun,* 290**,** 1084-9.

FASSHAUER, M., KRALISCH, S., KLIER, M., LOSSNER, U., BLUHER, M., KLEIN, J. & PASCHKE, R. 2003. Adiponectin gene expression and secretion is inhibited by interleukin-6 in 3T3-L1 adipocytes. *Biochemical and Biophysical Research Communications,* 301**,** 1045-1050.

FERRARA, N., GERBER, H. P. & LECOUTER, J. 2003. The biology of VEGF and its receptors. *Nat Med,* 9**,** 669-76.

FERRER, A., CAELLES, C., MASSOT, N. & HEGARDT, F. G. 1985. Activation of rat liver cytosolic 3-hydroxy-3-methylglutaryl coenzyme A reductase kinase by adenosine 5'-monophosphate. *Biochem Biophys Res Commun,* 132**,** 497-504.

FESUS, G., DUBROVSKA, G., GORZELNIAK, K., KLUGE, R., HUANG, Y., LUFT, F. C. & GOLLASCH, M. 2007. Adiponectin is a novel humoral vasodilator. *Cardiovasc Res,* 75**,** 719-27.

FINK, B., LAUDE, K., MCCANN, L., DOUGHAN, A., HARRISON, D. G. & DIKALOV, S. 2004. Detection of intracellular superoxide formation in endothelial cells and intact tissues using dihydroethidium and an HPLC-based assay. *Am J Physiol Cell Physiol,* 287**,** C895-902.

FINKEL, D., JAMES, A., BRUMBAUGH, K., DHAWAN, S., GOETZ, C., BONNEVIER, J. & WEGNER, G. 2014. Profiling secreted cytokines from human Th2 and Th17 cells using antibody arrays (TECH1P.845). *The Journal of Immunology,* 192**,** 69.13.

FISSLTHALER, B., DIMMELER, S., HERMANN, C., BUSSE, R. & FLEMING, I. 2000. Phosphorylation and activation of the endothelial nitric oxide synthase by fluid shear stress. *Acta Physiol Scand,* 168**,** 81-8.

FISSLTHALER, B. & FLEMING, I. 2009. Activation and signaling by the AMP-activated protein kinase in endothelial cells. *Circ Res,* 105**,** 114-27.

FITZGIBBONS, T. P., KOGAN, S., AOUADI, M., HENDRICKS, G. M., STRAUBHAAR, J. & CZECH, M. P. 2011. Similarity of mouse perivascular and brown adipose tissues and their resistance to diet-induced inflammation. *American Journal of Physiology-Heart and Circulatory Physiology,* 301**,** H1425-H1437.

FLEMING, I., FISSLTHALER, B., DIXIT, M. & BUSSE, R. 2005. Role of PECAM-1 in the shear-stress-induced activation of Akt and the endothelial nitric oxide synthase (eNOS) in endothelial cells. *J Cell Sci,* 118**,** 4103-11.

FOGARTY, S. & HARDIE, D. G. 2009. C-terminal phosphorylation of LKB1 is not required for regulation of AMP-activated protein kinase, BRSK1, BRSK2, or cell cycle arrest. *J Biol Chem,* 284**,** 77-84.

FORD, R. J., TESCHKE, S. R., REID, E. B., DURHAM, K. K., KROETSCH, J. T. & RUSH, J. W. 2012. AMP-activated protein kinase activator AICAR acutely lowers blood pressure and relaxes isolated resistance arteries of hypertensive rats. *J Hypertens,* 30**,** 725-33.

FORETZ, M., HEBRARD, S., LECLERC, J., ZARRINPASHNEH, E., SOTY, M., MITHIEUX, G., SAKAMOTO, K., ANDREELLI, F. & VIOLLET, B. 2010. Metformin inhibits hepatic gluconeogenesis in mice independently of the LKB1/AMPK pathway via a decrease in hepatic energy state. *J Clin Invest,* 120**,** 2355-69.

FORSTERMANN, U., BOISSEL, J. P. & KLEINERT, H. 1998. Expressional control of the 'constitutive' isoforms of nitric oxide synthase (NOS I and NOS III). *FASEB J,* 12**,** 773-90.

FORSTERMANN, U. & SESSA, W. C. 2012. Nitric oxide synthases: regulation and function. *Eur Heart J,* 33**,** 829-37, 837a-837d.

FOX, C. S., MASSARO, J. M., HOFFMANN, U., POU, K. M., MAUROVICH-HORVAT, P., LIU, C. Y., VASAN, R. S., MURABITO, J. M., MEIGS, J. B., CUPPLES, L. A., D'AGOSTINO, R. B., SR. & O'DONNELL, C. J. 2007. Abdominal visceral and subcutaneous adipose tissue compartments: association with metabolic risk factors in the Framingham Heart Study. *Circulation,* 116**,** 39-48.

FRONTINI, A. & CINTI, S. 2010. Distribution and development of brown adipocytes in the murine and human adipose organ. *Cell Metab,* 11**,** 253-6.

FRYER, L. G., FOUFELLE, F., BARNES, K., BALDWIN, S. A., WOODS, A. & CARLING, D. 2002. Characterization of the role of the AMP-activated protein kinase in the stimulation of glucose transport in skeletal muscle cells. *Biochem J,* 363**,** 167-74.

FU, Y. N., XIAO, H., MA, X. W., JIANG, S. Y., XU, M. & ZHANG, Y. Y. 2011. Metformin attenuates pressure overload-induced cardiac hypertrophy via AMPK activation. *Acta Pharmacol Sin,* 32**,** 879-87.

FUJITA, Y., HOSOKAWA, M., FUJIMOTO, S., MUKAI, E., ABUDUKADIER, A., OBARA, A., OGURA, M., NAKAMURA, Y., TOYODA, K., NAGASHIMA, K., SEINO, Y. & INAGAKI, N. 2010. Metformin suppresses hepatic gluconeogenesis and lowers fasting blood glucose levels through reactive nitrogen species in mice. *Diabetologia,* 53**,** 1472-81.

FUKUHARA, A., MATSUDA, M., NISHIZAWA, M., SEGAWA, K., TANAKA, M., KISHIMOTO, K., MATSUKI, Y., MURAKAMI, M., ICHISAKA, T., MURAKAMI, H., WATANABE, E., TAKAGI, T., AKIYOSHI, M., OHTSUBO, T., KIHARA, S., YAMASHITA, S., MAKISHIMA, M., FUNAHASHI, T., YAMANAKA, S., HIRAMATSU, R., MATSUZAWA, Y. & SHIMOMURA, I. 2005. Visfatin: a protein secreted by visceral fat that mimics the effects of insulin. *Science,* 307**,** 426-30.

FURCHGOTT, R. F. & ZAWADZKI, J. V. 1980. The obligatory role of endothelial cells in the relaxation of arterial smooth muscle by acetylcholine. *Nature,* 288**,** 373-6.

GALIC, S., FULLERTON, M. D., SCHERTZER, J. D., SIKKEMA, S., MARCINKO, K., WALKLEY, C. R., IZON, D., HONEYMAN, J., CHEN, Z. P., VAN DENDEREN, B. J., KEMP, B. E. & STEINBERG, G. R. 2011. Hematopoietic AMPK beta1 reduces mouse adipose tissue macrophage inflammation and insulin resistance in obesity. *J Clin Invest,* 121**,** 4903-15.

GALVEZ-PRIETO, B., BOLBRINKER, J., STUCCHI, P., DE LAS HERAS, A. I., MERINO, B., ARRIBAS, S., RUIZ-GAYO, M., HUBER, M., WEHLAND, M., KREUTZ, R. & FERNANDEZ-ALFONSO, M. S. 2008. Comparative expression analysis of the renin-angiotensin system components between white and brown perivascular adipose tissue. *J Endocrinol,* 197**,** 55-64.

GALVEZ-PRIETO, B., SOMOZA, B., GIL-ORTEGA, M., GARCIA-PRIETO, C. F., DE LAS HERAS, A. I., GONZALEZ, M. C., ARRIBAS, S., ARANGUEZ, I., BOLBRINKER, J., KREUTZ, R., RUIZ-GAYO, M. & FERNANDEZ-ALFONSO, M. S. 2012. Anticontractile Effect of Perivascular Adipose Tissue and Leptin are Reduced in Hypertension. *Front Pharmacol,* 3**,** 103.

GALVEZ, B., DE CASTRO, J., HEROLD, D., DUBROVSKA, G., ARRIBAS, S., GONZALEZ, M. C., ARANGUEZ, I., LUFT, F. C., RAMOS, M. P., GOLLASCH, M. & FERNANDEZ ALFONSO, M. S. 2006. Perivascular adipose tissue and mesenteric

vascular function in spontaneously hypertensive rats. *Arterioscler Thromb Vasc Biol,* 26**,** 1297-302.

GAO, Y. J. 2007. Dual modulation of vascular function by perivascular adipose tissue and its potential correlation with adiposity/lipoatrophy-related vascular dysfunction. *Curr Pharm Des,* 13**,** 2185-92.

GAO, Y. J., HIROTA, S., ZHANG, D. W., JANSSEN, L. J. & LEE, R. M. 2003. Mechanisms of hydrogen-peroxide-induced biphasic response in rat mesenteric artery. *Br J Pharmacol,* 138**,** 1085-92.

GAO, Y. J., HOLLOWAY, A. C., ZENG, Z. H., LIM, G. E., PETRIK, J. J., FOSTER, W. G. & LEE, R. M. 2005a. Prenatal exposure to nicotine causes postnatal obesity and altered perivascular adipose tissue function. *Obes Res,* 13**,** 687-92.

GAO, Y. J., LU, C., SU, L. Y., SHARMA, A. M. & LEE, R. M. 2007. Modulation of vascular function by perivascular adipose tissue: the role of endothelium and hydrogen peroxide. *Br J Pharmacol,* 151**,** 323-31.

GAO, Y. J., TAKEMORI, K., SU, L. Y., AN, W. S., LU, C., SHARMA, A. M. & LEE, R. M. 2006. Perivascular adipose tissue promotes vasoconstriction: the role of superoxide anion. *Cardiovasc Res,* 71**,** 363-73.

GAO, Y. J., ZENG, Z. H., TEOH, K., SHARMA, A. M., ABOUZAHR, L., CYBULSKY, I., LAMY, A., SEMELHAGO, L. & LEE, R. M. 2005b. Perivascular adipose tissue modulates vascular function in the human internal thoracic artery. *J Thorac Cardiovasc Surg,* 130**,** 1130-6.

GARCIA-RUIZ, E., REYNES, B., DIAZ-RUA, R., CERESI, E., OLIVER, P. & PALOU, A. 2015. The intake of high-fat diets induces the acquisition of brown adipocyte gene expression features in white adipose tissue. *Int J Obes (Lond),* 39**,** 1619-29.

GASKIN, F. S., KAMADA, K., YUSOF, M. & KORTHUIS, R. J. 2007. 5'-AMP-activated protein kinase activation prevents postischemic leukocyte-endothelial cell adhesive interactions. *Am J Physiol Heart Circ Physiol,* 292**,** H326-32.

GAVRILOVA, O., HALUZIK, M., MATSUSUE, K., CUTSON, J. J., JOHNSON, L., DIETZ, K. R., NICOL, C. J., VINSON, C., GONZALEZ, F. J. & REITMAN, M. L. 2003. Liver peroxisome proliferator-activated receptor gamma contributes to hepatic steatosis, triglyceride clearance, and regulation of body fat mass. *J Biol Chem,* 278**,** 34268-76.

GESTA, S., TSENG, Y. H. & KAHN, C. R. 2007. Developmental origin of fat: tracking obesity to its source. *Cell,* 131**,** 242-56.

GIL-ORTEGA, M., STUCCHI, P., GUZMAN-RUIZ, R., CANO, V., ARRIBAS, S., GONZALEZ, M. C., RUIZ-GAYO, M., FERNANDEZ-ALFONSO, M. S. & SOMOZA, B. 2010. Adaptative nitric oxide overproduction in perivascular adipose tissue during early diet-induced obesity. *Endocrinology,* 151**,** 3299-306.

GIORDANO, A., FRONTINI, A., CASTELLUCCI, M. & CINTI, S. 2004. Presence and distribution of cholinergic nerves in rat mediastinal brown adipose tissue. *J Histochem Cytochem,* 52**,** 923-30.

GIORDANO, A., FRONTINI, A., MURANO, I., TONELLO, C., MARINO, M. A., CARRUBA, M. O., NISOLI, E. & CINTI, S. 2005. Regional-dependent increase of sympathetic innervation in rat white adipose tissue during prolonged fasting. *J Histochem Cytochem,* 53**,** 679-87.

GIORDANO, A., SONG, C. K., BOWERS, R. R., EHLEN, J. C., FRONTINI, A., CINTI, S. & BARTNESS, T. J. 2006. White adipose tissue lacks significant vagal innervation and immunohistochemical evidence of parasympathetic innervation. *Am J Physiol Regul Integr Comp Physiol,* 291**,** R1243-55.

GLAVIND-KRISTENSEN, M., MATCHKOV, V., HANSEN, V. B., FORMAN, A., NILSSON, H. & AALKJAER, C. 2004. KATP-channel-induced vasodilation is modulated by the Na,K-pump activity in rabbit coronary small arteries. *Br J Pharmacol,* 143**,** 872-80.

GLEDHILL, J. R., MONTGOMERY, M. G., LESLIE, A. G. & WALKER, J. E. 2007. Mechanism of inhibition of bovine F1-ATPase by resveratrol and related polyphenols. *Proc Natl Acad Sci U S A,* 104**,** 13632-7.

GOIRAND, F., SOLAR, M., ATHEA, Y., VIOLLET, B., MATEO, P., FORTIN, D., LECLERC, J., HOERTER, J., VENTURA-CLAPIER, R. & GARNIER, A. 2007. Activation of AMP kinase alpha1 subunit induces aortic vasorelaxation in mice. *J Physiol,* 581**,** 1163-71.

GORANSSON, O., MCBRIDE, A., HAWLEY, S. A., ROSS, F. A., SHPIRO, N., FORETZ, M., VIOLLET, B., HARDIE, D. G. & SAKAMOTO, K. 2007. Mechanism of action of A-769662, a valuable tool for activation of AMP-activated protein kinase. *J Biol Chem,* 282**,** 32549-60.

GRAHAME HARDIE, D. 2016. Regulation of AMP-activated protein kinase by natural and synthetic activators. *Acta Pharmaceutica Sinica B,* 6**,** 1-19.

GRASSIA, G., MADDALUNO, M., MUSILLI, C., DE STEFANO, D., CARNUCCIO, R., DI LAURO, M. V., PARRATT, C. A., KENNEDY, S., DI MEGLIO, P., IANARO, A., MAFFIA, P., PARENTI, A. & IALENTI, A. 2010. The I{kappa}B kinase inhibitor nuclear factor-{kappa}B essential modulator-binding domain peptide for inhibition of injury-induced neointimal formation. *Arterioscler Thromb Vasc Biol,* 30**,** 2458-66.

GREENBERG, A. S., EGAN, J. J., WEK, S. A., GARTY, N. B., BLANCHETTE-MACKIE, E. J. & LONDOS, C. 1991. Perilipin, a major hormonally regulated adipocyte-specific phosphoprotein associated with the periphery of lipid storage droplets. *J Biol Chem,* 266**,** 11341-6.

GREENSTEIN, A. S., KHAVANDI, K., WITHERS, S. B., SONOYAMA, K., CLANCY, O., JEZIORSKA, M., LAING, I., YATES, A. P., PEMBERTON, P. W., MALIK, R. A. & HEAGERTY, A. M. 2009. Local inflammation and hypoxia abolish the protective anticontractile properties of perivascular fat in obese patients. *Circulation,* 119**,** 1661-70.

GREIF, M., BECKER, A., VON ZIEGLER, F., LEBHERZ, C., LEHRKE, M., BROEDL, U. C., TITTUS, J., PARHOFER, K., BECKER, C., REISER, M., KNEZ, A. & LEBER, A. W. 2009. Pericardial Adipose Tissue Determined by Dual Source CT Is a Risk Factor for Coronary Atherosclerosis. *Arteriosclerosis, Thrombosis, and Vascular Biology,* 29**,** 781-786.

GUERRA, C., RONCERO, C., PORRAS, A., FERNANDEZ, M. & BENITO, M. 1996. Triiodothyronine induces the transcription of the uncoupling protein gene and stabilizes its mRNA in fetal rat brown adipocyte primary cultures. *J Biol Chem,* 271**,** 2076-81.

GUH, J. H., CHANG, W. L., YANG, J., LEE, S. L., WEI, S., WANG, D., KULP, S. K. & CHEN, C. S. 2010. Development of novel adenosine monophosphate-activated protein kinase activators. *J Med Chem,* 53**,** 2552-61.

GUTMAN, G. A., CHANDY, K. G., GRISSMER, S., LAZDUNSKI, M., MCKINNON, D., PARDO, L. A., ROBERTSON, G. A., RUDY, B., SANGUINETTI, M. C., STÜHMER, W. & WANG, X. 2005. International Union of Pharmacology. LIII. Nomenclature and Molecular Relationships of Voltage-Gated Potassium Channels. *Pharmacological Reviews,* 57**,** 473-508.

HALBERG, N., SCHRAW, T. D., WANG, Z. V., KIM, J. Y., YI, J., HAMILTON, M. P., LUBY-PHELPS, K. & SCHERER, P. E. 2009. Systemic fate of the adipocyte-derived factor adiponectin. *Diabetes,* 58**,** 1961-70.

HANNAN, R. E., DAVIS, E. A. & WIDDOP, R. E. 2003. Functional role of angiotensin II AT2 receptor in modulation of AT1 receptor-mediated contraction in rat uterine artery: involvement of bradykinin and nitric oxide. *Br J Pharmacol,* 140**,** 987-95.

HANNER, M., SCHMALHOFER, W. A., MUNUJOS, P., KNAUS, H.-G., KACZOROWSKI, G. J. & GARCIA, M. L. 1997. The β subunit of the high-conductance calcium-activated potassium channel contributes to the high-affinity receptor for charybdotoxin. *Proceedings of the National Academy of Sciences of the United States of America,* 94**,** 2853-2858.

HARDIE, D. G. 1999. Roles of the AMP-activated/SNF1 protein kinase family in the response to cellular stress. *Biochem Soc Symp,* 64**,** 13-27.

HARDIE, D. G. 2005. New roles for the LKB1-->AMPK pathway. *Curr Opin Cell Biol,* 17**,** 167-73.

HARDIE, D. G. 2007. AMP-activated/SNF1 protein kinases: conserved guardians of cellular energy. *Nat Rev Mol Cell Biol,* 8**,** 774-85.

HARDIE, D. G. 2008. AMPK: a key regulator of energy balance in the single cell and the whole organism. *Int J Obes (Lond),* 32 Suppl 4**,** S7-12.

HARDIE, D. G. 2011. AMP-activated protein kinase: an energy sensor that regulates all aspects of cell function. *Genes Dev,* 25**,** 1895-908.

HARDIE, D. G. 2016. Regulation of AMP-activated protein kinase by natural and synthetic activators. *Acta Pharmaceutica Sinica B,* 6**,** 1-19.

HARDIE, D. G. & CARLING, D. 1997. The AMP-activated protein kinase--fuel gauge of the mammalian cell? *Eur J Biochem,* 246**,** 259-73.

HARDIE, D. G., CARLING, D. & GAMBLIN, S. J. 2011. AMP-activated protein kinase: also regulated by ADP? *Trends Biochem Sci,* 36**,** 470-7.

HARDIE, D. G., SCOTT, J. W., PAN, D. A. & HUDSON, E. R. 2003. Management of cellular energy by the AMP-activated protein kinase system. *FEBS Lett,* 546**,** 113-20.

HARIRI, N. & THIBAULT, L. 2010. High-fat diet-induced obesity in animal models. *Nutr Res Rev,* 23**,** 270-99.

HATTORI, T., KAJIKURI, J., KATSUYA, H. & ITOH, T. 2003. Effects of H2O2 on membrane potential of smooth muscle cells in rabbit mesenteric resistance artery. *Eur J Pharmacol,* 464**,** 101-9.

HATTORI, Y., NAKANO, Y., HATTORI, S., TOMIZAWA, A., INUKAI, K. & KASAI, K. 2008. High molecular weight adiponectin activates AMPK and suppresses cytokine-induced NF-kappaB activation in vascular endothelial cells. *FEBS Lett,* 582**,** 1719-24.

HAUSMAN, D. B., DIGIROLAMO, M., BARTNESS, T. J., HAUSMAN, G. J. & MARTIN, R. J. 2001. The biology of white adipocyte proliferation. *Obes Rev,* 2**,** 239-54.

HAWLEY, S. A., BOUDEAU, J., REID, J. L., MUSTARD, K. J., UDD, L., MAKELA, T. P., ALESSI, D. R. & HARDIE, D. G. 2003. Complexes between the LKB1 tumor suppressor, STRAD alpha/beta and MO25 alpha/beta are upstream kinases in the AMP-activated protein kinase cascade. *J Biol,* 2**,** 28.

HAWLEY, S. A., PAN, D. A., MUSTARD, K. J., ROSS, L., BAIN, J., EDELMAN, A. M., FRENGUELLI, B. G. & HARDIE, D. G. 2005. Calmodulin-dependent protein kinase kinase-beta is an alternative upstream kinase for AMP-activated protein kinase. *Cell Metab,* 2**,** 9-19.

HAWLEY, S. A., ROSS, F. A., CHEVTZOFF, C., GREEN, K. A., EVANS, A., FOGARTY, S., TOWLER, M. C., BROWN, L. J., OGUNBAYO, O. A., EVANS, A. M. & HARDIE, D. G. 2010. Use of cells expressing gamma subunit variants to identify diverse mechanisms of AMPK activation. *Cell Metab,* 11**,** 554-65.

HAWLEY, S. A., SELBERT, M. A., GOLDSTEIN, E. G., EDELMAN, A. M., CARLING, D. & HARDIE, D. G. 1995. 5'-AMP activates the AMP-activated protein kinase cascade, and Ca2+/calmodulin activates the calmodulin-dependent protein kinase I cascade, via three independent mechanisms. *J Biol Chem,* 270**,** 27186-91.

HEMMINKI, A., MARKIE, D., TOMLINSON, I., AVIZIENYTE, E., ROTH, S., LOUKOLA, A., BIGNELL, G., WARREN, W., AMINOFF, M., HOGLUND, P., JARVINEN, H., KRISTO, P., PELIN, K., RIDANPAA, M., SALOVAARA, R., TORO, T., BODMER, W., OLSCHWANG, S., OLSEN, A. S., STRATTON, M. R., DE LA CHAPELLE, A. & AALTONEN, L. A. 1998. A serine/threonine kinase gene defective in Peutz-Jeghers syndrome. *Nature,* 391**,** 184-7.

HENRICHOT, E., JUGE-AUBRY, C. E., PERNIN, A., PACHE, J. C., VELEBIT, V., DAYER, J. M., MEDA, P., CHIZZOLINI, C. & MEIER, C. A. 2005. Production of chemokines by perivascular adipose tissue: a role in the pathogenesis of atherosclerosis? *Arterioscler Thromb Vasc Biol,* 25**,** 2594-9.

HEVENER, A. L., HE, W., BARAK, Y., LE, J., BANDYOPADHYAY, G., OLSON, P., WILKES, J., EVANS, R. M. & OLEFSKY, J. 2003. Muscle-specific Pparg deletion causes insulin resistance. *Nat Med,* 9**,** 1491-7.

HILL, J. O., WYATT, H. R., REED, G. W. & PETERS, J. C. 2003. Obesity and the environment: where do we go from here? *Science,* 299**,** 853-5.

HOLMES, B. F., KURTH-KRACZEK, E. J. & WINDER, W. W. 1999. Chronic activation of 5'-AMP-activated protein kinase increases GLUT-4, hexokinase, and glycogen in muscle. *J Appl Physiol (1985),* 87**,** 1990-5.

HONG, K., LEE, S., LI, R., YANG, Y., TANNER, M. A., WU, J. & HILL, M. A. 2016. Adiponectin Receptor Agonist, AdipoRon, Causes Vasorelaxation Predominantly Via a Direct Smooth Muscle Action. *Microcirculation,* 23**,** 207-20.

HONG, K. W., PYO, K. M., LEE, W. S., YU, S. S. & RHIM, B. Y. 1994. Pharmacological evidence that calcitonin gene-related peptide is implicated in cerebral autoregulation. *American Journal of Physiology - Heart and Circulatory Physiology,* 266**,** H11-H16.

HORMAN, S., MOREL, N., VERTOMMEN, D., HUSSAIN, N., NEUMANN, D., BEAULOYE, C., EL NAJJAR, N., FORCET, C., VIOLLET, B., WALSH, M. P., HUE, L. & RIDER, M. H. 2008. AMP-activated protein kinase phosphorylates and desensitizes smooth muscle myosin light chain kinase. *J Biol Chem,* 283**,** 18505-12.

HOYDA, T. D. & FERGUSON, A. V. 2010. Adiponectin modulates excitability of rat paraventricular nucleus neurons by differential modulation of potassium currents. *Endocrinology,* 151**,** 3154-62.

HUANG, F., XIONG, X. F., WANG, H. B., YOU, S. & ZENG, H. S. 2010. Leptin-induced vascular smooth muscle cell proliferation via regulating cell cycle, activating ERK1/2 and NF-kappa B. *Acta Biochimica Et Biophysica Sinica,* 42**,** 325-331.

HUG, C., WANG, J., AHMAD, N. S., BOGAN, J. S., TSAO, T. S. & LODISH, H. F. 2004. T-cadherin is a receptor for hexameric and high-molecular-weight forms of Acrp30/adiponectin. *Proc Natl Acad Sci U S A,* 101**,** 10308-13.

HUND, T. J. & MOHLER, P. J. 2011. Differential roles for SUR subunits in K(ATP) channel membrane targeting and regulation. *American Journal of Physiology - Heart and Circulatory Physiology,* 300**,** H33-H35.

HUTCHINSON, D. S., CHERNOGUBOVA, E., DALLNER, O. S., CANNON, B. & BENGTSSON, T. 2005. Beta-adrenoceptors, but not alpha-adrenoceptors, stimulate AMP-activated protein kinase in brown adipocytes independently of uncoupling protein-1. *Diabetologia,* 48**,** 2386-95.

HUYPENS, P., QUARTIER, E., PIPELEERS, D. & VAN DE CASTEELE, M. 2005. Metformin reduces adiponectin protein expression and release in 3T3-L1 adipocytes involving activation of AMP activated protein kinase. *European Journal of Pharmacology,* 518**,** 90-95.

HWANG, J. T., KWON, D. Y. & YOON, S. H. 2009. AMP-activated protein kinase: a potential target for the diseases prevention by natural occurring polyphenols. *N Biotechnol,* 26**,** 17-22.

IGATA, M., MOTOSHIMA, H., TSURUZOE, K., KOJIMA, K., MATSUMURA, T., KONDO, T., TAGUCHI, T., NAKAMARU, K., YANO, M., KUKIDOME, D., MATSUMOTO, K., TOYONAGA, T., ASANO, T., NISHIKAWA, T. & ARAKI, E. 2005. Adenosine monophosphate-activated protein kinase suppresses vascular smooth muscle cell proliferation through the inhibition of cell cycle progression. *Circ Res,* 97**,** 837-44.

IGLESIAS, M. A., YE, J. M., FRANGIOUDAKIS, G., SAHA, A. K., TOMAS, E., RUDERMAN, N. B., COONEY, G. J. & KRAEGEN, E. W. 2002. AICAR administration

causes an apparent enhancement of muscle and liver insulin action in insulin-resistant high-fat-fed rats. *Diabetes,* 51**,** 2886-94.

IGNARRO, L. J., BUGA, G. M., WOOD, K. S., BYRNS, R. E. & CHAUDHURI, G. 1987. Endothelium-derived relaxing factor produced and released from artery and vein is nitric oxide. *Proc Natl Acad Sci U S A,* 84**,** 9265-9.

IIDA, Y. & KATUSIC, Z. S. 2000. Mechanisms of cerebral arterial relaxations to hydrogen peroxide. *Stroke,* 31**,** 2224-30.

INOKI, K., ZHU, T. & GUAN, K. L. 2003. TSC2 mediates cellular energy response to control cell growth and survival. *Cell,* 115**,** 577-90.

ISAKOVIC, A., HARHAJI, L., STEVANOVIC, D., MARKOVIC, Z., SUMARAC-DUMANOVIC, M., STARCEVIC, V., MICIC, D. & TRAJKOVIC, V. 2007. Dual antiglioma action of metformin: cell cycle arrest and mitochondria-dependent apoptosis. *Cell Mol Life Sci,* 64**,** 1290-302.

JAMALUDDIN, M. S., WEAKLEY, S. M., YAO, Q. & CHEN, C. 2012. Resistin: functional roles and therapeutic considerations for cardiovascular disease. *Br J Pharmacol,* 165**,** 622-32.

JAPP, A. G., CRUDEN, N. L., AMER, D. A., LI, V. K., GOUDIE, E. B., JOHNSTON, N. R., SHARMA, S., NEILSON, I., WEBB, D. J., MEGSON, I. L., FLAPAN, A. D. & NEWBY, D. E. 2008. Vascular effects of apelin in vivo in man. *J Am Coll Cardiol,* 52**,** 908-13.

JEONG, H. W., HSU, K. C., LEE, J. W., HAM, M., HUH, J. Y., SHIN, H. J., KIM, W. S. & KIM, J. B. 2009. Berberine suppresses proinflammatory responses through AMPK activation in macrophages. *Am J Physiol Endocrinol Metab,* 296**,** E955-64.

JEONG, J. W., JEONG, M. H., YUN, K. H., OH, S. K., PARK, E. M., KIM, Y. K., RHEE, S. J., LEE, E. M., LEE, J., YOO, N. J., KIM, N. H. & PARK, J. C. 2007. Echocardiographic epicardial fat thickness and coronary artery disease. *Circ J,* 71**,** 536-9.

JIN, R. C. & LOSCALZO, J. 2010. Vascular Nitric Oxide: Formation and Function. *J Blood Med,* 2010**,** 147-162.

JORGENSEN, S. B., VIOLLET, B., ANDREELLI, F., FROSIG, C., BIRK, J. B., SCHJERLING, P., VAULONT, S., RICHTER, E. A. & WOJTASZEWSKI, J. F. 2004. Knockout of the alpha2 but not alpha1 5'-AMP-activated protein kinase isoform abolishes 5-aminoimidazole-4-carboxamide-1-beta-4-ribofuranosidebut not contraction-induced glucose uptake in skeletal muscle. *J Biol Chem,* 279**,** 1070-9.

KADOWAKI, T. & YAMAUCHI, T. 2005. Adiponectin and adiponectin receptors. *Endocr Rev,* 26**,** 439-51.

KADOWAKI, T., YAMAUCHI, T., KUBOTA, N., HARA, K., UEKI, K. & TOBE, K. 2006. Adiponectin and adiponectin receptors in insulin resistance, diabetes, and the metabolic syndrome. *J Clin Invest,* 116**,** 1784-92.

KAHN, B. B., ALQUIER, T., CARLING, D. & HARDIE, D. G. 2005. AMP-activated protein kinase: ancient energy gauge provides clues to modern understanding of metabolism. *Cell Metab,* 1**,** 15-25.

KAPPES, A. & LOFFLER, G. 2000. Influences of ionomycin, dibutyryl-cycloAMP and tumour necrosis factor-alpha on intracellular amount and secretion of apM1 in differentiating primary human preadipocytes. *Horm Metab Res,* 32**,** 548-54.

KEMP, B. E., STAPLETON, D., CAMPBELL, D. J., CHEN, Z. P., MURTHY, S., WALTER, M., GUPTA, A., ADAMS, J. J., KATSIS, F., VAN DENDEREN, B., JENNINGS, I. G., ISELI, T., MICHELL, B. J. & WITTERS, L. A. 2003. AMP-activated protein kinase, super metabolic regulator. *Biochem Soc Trans,* 31**,** 162-8.

KERN, P. A., RANGANATHAN, S., LI, C., WOOD, L. & RANGANATHAN, G. 2001. Adipose tissue tumor necrosis factor and interleukin-6 expression in human obesity and insulin resistance. *Am J Physiol Endocrinol Metab,* 280**,** E745-51.

KETONEN, J., SHI, J., MARTONEN, E. & MERVAALA, E. 2010. Periadventitial adipose tissue promotes endothelial dysfunction via oxidative stress in diet-induced obese C57Bl/6 mice. *Circ J,* 74**,** 1479-87.

KIM, E. J., CHOI, Y. K., HAN, Y. H., KIM, H. J., LEE, I. K. & LEE, M. O. 2014. RORalpha suppresses proliferation of vascular smooth muscle cells through activation of AMP-activated protein kinase. *Int J Cardiol,* 175**,** 515-21.

KIM, M. S., PARK, J. Y., NAMKOONG, C., JANG, P. G., RYU, J. W., SONG, H. S., YUN, J. Y., NAMGOONG, I. S., HA, J., PARK, I. S., LEE, I. K., VIOLLET, B., YOUN, J. H., LEE, H. K. & LEE, K. U. 2004. Anti-obesity effects of alpha-lipoic acid mediated by suppression of hypothalamic AMP-activated protein kinase. *Nat Med,* 10**,** 727-33.

KIM, S. A. & CHOI, H. C. 2012. Metformin inhibits inflammatory response via AMPK-PTEN pathway in vascular smooth muscle cells. *Biochem Biophys Res Commun,* 425**,** 866-72.

KIRPICHNIKOV, D., MCFARLANE, S. I. & SOWERS, J. R. 2002. Metformin: an update. *Ann Intern Med,* 137**,** 25-33.

KITADE, H., SAWAMOTO, K., NAGASHIMADA, M., INOUE, H., YAMAMOTO, Y., SAI, Y., TAKAMURA, T., YAMAMOTO, H., MIYAMOTO, K.-I., GINSBERG, H. N., MUKAIDA, N., KANEKO, S. & OTA, T. 2012. CCR5 Plays a Critical Role in Obesity-Induced Adipose Tissue Inflammation and Insulin Resistance by Regulating Both Macrophage Recruitment and M1/M2 Status. *Diabetes,* 61**,** 1680-1690.

KLIEVERIK, L. P., COOMANS, C. P., ENDERT, E., SAUERWEIN, H. P., HAVEKES, L. M., VOSHOL, P. J., RENSEN, P. C., ROMIJN, J. A., KALSBEEK, A. & FLIERS, E. 2009. Thyroid hormone effects on whole-body energy homeostasis and tissue-specific fatty acid uptake in vivo. *Endocrinology,* 150**,** 5639-48.

KO, E. A., HAN, J., JUNG, I. D. & PARK, W. S. 2008. Physiological roles of K+ channels in vascular smooth muscle cells. *J Smooth Muscle Res,* 44**,** 65-81.

KOH, S. D., BRADLEY, K. K., RAE, M. G., KEEF, K. D., HOROWITZ, B. & SANDERS, K. M. 1998. Basal activation of ATP-sensitive potassium channels in murine colonic smooth muscle cell. *Biophysical Journal,* 75**,** 1793-1800.

KOROVKINA, V. P. & ENGLAND, S. K. 2002. Molecular diversity of vascular potassium channel isoforms. *Clin Exp Pharmacol Physiol,* 29**,** 317-23.

KRISHAN, S., RICHARDSON, D. R. & SAHNI, S. 2015. Adenosine monophosphate-activated kinase and its key role in catabolism: structure, regulation, biological activity, and pharmacological activation. *Mol Pharmacol,* 87**,** 363-77.

KUBOTA, N., YANO, W., KUBOTA, T., YAMAUCHI, T., ITOH, S., KUMAGAI, H., KOZONO, H., TAKAMOTO, I., OKAMOTO, S., SHIUCHI, T., SUZUKI, R., SATOH, H., TSUCHIDA, A., MOROI, M., SUGI, K., NODA, T., EBINUMA, H., UETA, Y., KONDO, T., ARAKI, E., EZAKI, O., NAGAI, R., TOBE, K., TERAUCHI, Y., UEKI, K., MINOKOSHI, Y. & KADOWAKI, T. 2007. Adiponectin stimulates AMP-activated protein kinase in the hypothalamus and increases food intake. *Cell Metab,* 6**,** 55-68.

KUKIDOME, D., NISHIKAWA, T., SONODA, K., IMOTO, K., FUJISAWA, K., YANO, M., MOTOSHIMA, H., TAGUCHI, T., MATSUMURA, T. & ARAKI, E. 2006. Activation of AMP-activated protein kinase reduces hyperglycemia-induced mitochondrial reactive oxygen species production and promotes mitochondrial biogenesis in human umbilical vein endothelial cells. *Diabetes,* 55**,** 120-7.

KUMADA, M., KIHARA, S., SUMITSUJI, S., KAWAMOTO, T., MATSUMOTO, S., OUCHI, N., ARITA, Y., OKAMOTO, Y., SHIMOMURA, I., HIRAOKA, H., NAKAMURA, T., FUNAHASHI, T. & MATSUZAWA, Y. 2003. Association of hypoadiponectinemia with coronary artery disease in men. *Arterioscler Thromb Vasc Biol,* 23**,** 85-9.

LAMERS, D., SCHLICH, R., GREULICH, S., SASSON, S., SELL, H. & ECKEL, J. 2011. Oleic acid and adipokines synergize in inducing proliferation and inflammatory signalling in human vascular smooth muscle cells. *J Cell Mol Med,* 15**,** 1177-88.

LAUFS, U., GERTZ, K., DIRNAGL, U., BOHM, M., NICKENIG, G. & ENDRES, M. 2002. Rosuvastatin, a new HMG-CoA reductase inhibitor, upregulates endothelial nitric oxide synthase and protects from ischemic stroke in mice. *Brain Res,* 942**,** 23-30.

LAUFS, U., GERTZ, K., HUANG, P., NICKENIG, G., BOHM, M., DIRNAGL, U. & ENDRES, M. 2000. Atorvastatin upregulates type III nitric oxide synthase in thrombocytes, decreases platelet activation, and protects from cerebral ischemia in normocholesterolemic mice. *Stroke,* 31**,** 2442-9.

LAURINDO, F. R., FERNANDES, D. C. & SANTOS, C. X. 2008. Assessment of superoxide production and NADPH oxidase activity by HPLC analysis of dihydroethidium oxidation products. *Methods Enzymol,* 441**,** 237-60.

LEBRASSEUR, N. K., KELLY, M., TSAO, T. S., FARMER, S. R., SAHA, A. K., RUDERMAN, N. B. & TOMAS, E. 2006. Thiazolidinediones can rapidly activate AMP-activated protein kinase in mammalian tissues. *Am J Physiol Endocrinol Metab,* 291**,** E175-81.

LEE, H. M., KIM, J. J., KIM, H. J., SHONG, M., KU, B. J. & JO, E. K. 2013. Upregulated NLRP3 inflammasome activation in patients with type 2 diabetes. *Diabetes,* 62**,** 194-204.

LEE, K. Y. & CHOI, H. C. 2013. Acetylcholine-induced AMP-activated protein kinase activation attenuates vasoconstriction through an LKB1-dependent mechanism in rat aorta. *Vascul Pharmacol,* 59**,** 96-102.

LEE, R. M., LU, C., SU, L. Y. & GAO, Y. J. 2009a. Endothelium-dependent relaxation factor released by perivascular adipose tissue. *J Hypertens,* 27**,** 782-90.

LEE, R. M., LU, C., SU, L. Y., WERSTUCK, G. & GAO, Y. J. 2009b. Effects of hyperglycemia on the modulation of vascular function by perivascular adipose tissue. *J Hypertens,* 27**,** 118-31.

LEE, W. J., LEE, I. K., KIM, H. S., KIM, Y. M., KOH, E. H., WON, J. C., HAN, S. M., KIM, M. S., JO, I., OH, G. T., PARK, I. S., YOUN, J. H., PARK, S. W., LEE, K. U. & PARK, J. Y. 2005. Alpha-lipoic acid prevents endothelial dysfunction in obese rats via activation of AMP-activated protein kinase. *Arterioscler Thromb Vasc Biol,* 25**,** 2488-94.

LEE, Y. C., CHANG, H. H., CHIANG, C. L., LIU, C. H., YEH, J. I., CHEN, M. F., CHEN, P. Y., KUO, J. S. & LEE, T. J. 2011. Role of perivascular adipose tissue-derived methyl palmitate in vascular tone regulation and pathogenesis of hypertension. *Circulation,* 124**,** 1160-71.

LERMAN, A. & ZEIHER, A. M. 2005. Endothelial function: cardiac events. *Circulation,* 111**,** 363-8.

LEVINE, Y. C., LI, G. K. & MICHEL, T. 2007. Agonist-modulated regulation of AMP-activated protein kinase (AMPK) in endothelial cells. Evidence for an AMPK -> Rac1 -> Akt -> endothelial nitric-oxide synthase pathway. *J Biol Chem,* 282**,** 20351-64.

LIAUDET, L., VASSALLI, G. & PACHER, P. 2009. Role of peroxynitrite in the redox regulation of cell signal transduction pathways. *Frontiers in bioscience : a journal and virtual library,* 14**,** 4809-4814.

LIBBY, P. 2002. Inflammation in atherosclerosis. *Nature,* 420**,** 868-74.

LIHN, A. S., JESSEN, N., PEDERSEN, S. B., LUND, S. & RICHELSEN, B. 2004. AICAR stimulates adiponectin and inhibits cytokines in adipose tissue. *Biochem Biophys Res Commun,* 316**,** 853-8.

LIHN, A. S., PEDERSEN, S. B., LUND, S. & RICHELSEN, B. 2008. The anti-diabetic AMPK activator AICAR reduces IL-6 and IL-8 in human adipose tissue and skeletal muscle cells. *Mol Cell Endocrinol,* 292**,** 36-41.

LIN, Y. C., HUNG, C. M., TSAI, J. C., LEE, J. C., CHEN, Y. L., WEI, C. W., KAO, J. Y. & WAY, T. D. 2010. Hispidulin potently inhibits human glioblastoma multiforme cells through activation of AMP-activated protein kinase (AMPK). *J Agric Food Chem,* 58**,** 9511-7.

LIU, C., LIANG, B., WANG, Q., WU, J. & ZOU, M. H. 2010. Activation of AMP-activated protein kinase alpha1 alleviates endothelial cell apoptosis by increasing the expression of anti-apoptotic proteins Bcl-2 and survivin. *J Biol Chem,* 285**,** 15346-55.

LIU, V. W. & HUANG, P. L. 2008. Cardiovascular roles of nitric oxide: a review of insights from nitric oxide synthase gene disrupted mice. *Cardiovasc Res,* 77**,** 19-29.

LIZCANO, J. M., GORANSSON, O., TOTH, R., DEAK, M., MORRICE, N. A., BOUDEAU, J., HAWLEY, S. A., UDD, L., MAKELA, T. P., HARDIE, D. G. & ALESSI, D. R. 2004. LKB1 is a master kinase that activates 13 kinases of the AMPK subfamily, including MARK/PAR-1. *EMBO J,* 23**,** 833-43.

LOCHHEAD, P. A., SALT, I. P., WALKER, K. S., HARDIE, D. G. & SUTHERLAND, C. 2000. 5-aminoimidazole-4-carboxamide riboside mimics the effects of insulin on the expression of the 2 key gluconeogenic genes PEPCK and glucose-6-phosphatase. *Diabetes,* 49**,** 896-903.

LOHN, M., DUBROVSKA, G., LAUTERBACH, B., LUFT, F. C., GOLLASCH, M. & SHARMA, A. M. 2002. Periadventitial fat releases a vascular relaxing factor. *FASEB J,* 16**,** 1057-63.

LOPEZ-TORRES, M., PEREZ-CAMPO, R. & BARJA DE QUIROGA, G. 1991. Aging in brown fat: antioxidant defenses and oxidative stress. *Mech Ageing Dev,* 59**,** 129-37.

LU, C., SU, L. Y., LEE, R. M. & GAO, Y. J. 2010. Mechanisms for perivascular adipose tissue-mediated potentiation of vascular contraction to perivascular neuronal stimulation: the role of adipocyte-derived angiotensin II. *Eur J Pharmacol,* 634**,** 107-12.

LU, C., SU, L. Y., LEE, R. M. & GAO, Y. J. 2011a. Alterations in perivascular adipose tissue structure and function in hypertension. *Eur J Pharmacol,* 656**,** 68-73.

LU, C., ZHAO, A. X., GAO, Y. J. & LEE, R. M. 2011b. Modulation of vein function by perivascular adipose tissue. *Eur J Pharmacol,* 657**,** 111-6.

LUMENG, C. N., BODZIN, J. L. & SALTIEL, A. R. 2007. Obesity induces a phenotypic switch in adipose tissue macrophage polarization. *J Clin Invest,* 117**,** 175-84.

LYNCH, F. M., WITHERS, S. B., YAO, Z., WERNER, M. E., EDWARDS, G., WESTON, A. H. & HEAGERTY, A. M. 2013. Perivascular adipose tissue-derived adiponectin activates BK(Ca) channels to induce anticontractile responses. *Am J Physiol Heart Circ Physiol,* 304**,** H786-95.

MA, L., MA, S., HE, H., YANG, D., CHEN, X., LUO, Z., LIU, D. & ZHU, Z. 2010. Perivascular fat-mediated vascular dysfunction and remodeling through the AMPK/mTOR pathway in high-fat diet-induced obese rats. *Hypertens Res,* 33**,** 446-53.

MACKIE, A. R., BRUEGGEMANN, L. I., HENDERSON, K. K., SHIELS, A. J., CRIBBS, L. L., SCROGIN, K. E. & BYRON, K. L. 2008. Vascular KCNQ potassium channels as novel targets for the control of mesenteric artery constriction by vasopressin, based on studies in single cells, pressurized arteries, and in vivo measurements of mesenteric vascular resistance. *J Pharmacol Exp Ther,* 325**,** 475-83.

MAEDA, N., SHIMOMURA, I., KISHIDA, K., NISHIZAWA, H., MATSUDA, M., NAGARETANI, H., FURUYAMA, N., KONDO, H., TAKAHASHI, M., ARITA, Y., KOMURO, R., OUCHI, N., KIHARA, S., TOCHINO, Y., OKUTOMI, K., HORIE, M., TAKEDA, S., AOYAMA, T., FUNAHASHI, T. & MATSUZAWA, Y. 2002. Diet-induced insulin resistance in mice lacking adiponectin/ACRP30. *Nat Med,* 8**,** 731-737.

MAENHAUT, N. & VAN DE VOORDE, J. 2011. Regulation of vascular tone by adipocytes. *BMC Med,* 9**,** 25.

MAIELLARO, K. & TAYLOR, W. R. 2007. The role of the adventitia in vascular inflammation. *Cardiovasc Res,* 75**,** 640-8.

MAJITHIYA, J. B. & BALARAMAN, R. 2006. Metformin reduces blood pressure and restores endothelial function in aorta of streptozotocin-induced diabetic rats. *Life Sci,* 78**,** 2615-24.

MALINOWSKI, M., DEJA, M. A., GOLBA, K. S., ROLEDER, T., BIERNAT, J. & WOS, S. 2008. Perivascular tissue of internal thoracic artery releases potent nitric oxide and prostacyclin-independent anticontractile factor. *Eur J Cardiothorac Surg,* 33**,** 225-31.

MANGANO, D. T. 1997. Effects of acadesine on myocardial infarction, stroke, and death following surgery. A meta-analysis of the 5 international randomized trials. The Multicenter Study of Perioperative Ischemia (McSPI) Research Group. *JAMA,* 277**,** 325-32.

MANKA, D., CHATTERJEE, T. K., STOLL, L. L., BASFORD, J. E., KONANIAH, E. S., SRINIVASAN, R., BOGDANOV, V. Y., TANG, Y., BLOMKALNS, A. L., HUI, D. Y. & WEINTRAUB, N. L. 2014. Transplanted perivascular adipose tissue accelerates injury-induced neointimal hyperplasia: role of monocyte chemoattractant protein-1. *Arterioscler Thromb Vasc Biol,* 34**,** 1723-30.

MARCHESI, C., EBRAHIMIAN, T., ANGULO, O., PARADIS, P. & SCHIFFRIN, E. L. 2009. Endothelial nitric oxide synthase uncoupling and perivascular adipose oxidative stress and inflammation contribute to vascular dysfunction in a rodent model of metabolic syndrome. *Hypertension,* 54**,** 1384-92.

MARIMAN, E. C. & WANG, P. 2010. Adipocyte extracellular matrix composition, dynamics and role in obesity. *Cell Mol Life Sci,* 67**,** 1277-92.

MARZOLLA, V., ARMANI, A., ZENNARO, M.-C., CINTI, F., MAMMI, C., FABBRI, A., ROSANO, G. M. C. & CAPRIO, M. 2012. The role of the mineralocorticoid receptor in adipocyte biology and fat metabolism. *Molecular and Cellular Endocrinology,* 350**,** 281-288.

MATSUMOTO, T., NOGUCHI, E., ISHIDA, K., KOBAYASHI, T., YAMADA, N. & KAMATA, K. 2008. Metformin normalizes endothelial function by suppressing vasoconstrictor prostanoids in mesenteric arteries from OLETF rats, a model of type 2 diabetes. *Am J Physiol Heart Circ Physiol,* 295**,** H1165-H1176.

MAYR, M., CHUNG, Y. L., MAYR, U., YIN, X., LY, L., TROY, H., FREDERICKS, S., HU, Y., GRIFFITHS, J. R. & XU, Q. 2005. Proteomic and metabolomic analyses of atherosclerotic vessels from apolipoprotein E-deficient mice reveal alterations in inflammation, oxidative stress, and energy metabolism. *Arterioscler Thromb Vasc Biol,* 25**,** 2135-42.

MCKEOWN, L., SWANTON, L., ROBINSON, P. & JONES, O. T. 2008. Surface expression and distribution of voltage-gated potassium channels in neurons (Review). *Mol Membr Biol,* 25**,** 332-43.

MEERA, P., WALLNER, M., JIANG, Z. & TORO, L. 1996. A calcium switch for the functional coupling between alpha (hslo) and beta subunits (KV,Ca beta) of maxi K channels. *FEBS Lett,* 382**,** 84-8.

MEIJER, R. I., BAKKER, W., ALTA, C. L., SIPKEMA, P., YUDKIN, J. S., VIOLLET, B., RICHTER, E. A., SMULDERS, Y. M., VAN HINSBERGH, V. W., SERNE, E. H. & ERINGA, E. C. 2013. Perivascular adipose tissue control of insulin-induced vasoreactivity in muscle is impaired in db/db mice. *Diabetes,* 62**,** 590-8.

MERRILL, G. F., KURTH, E. J., HARDIE, D. G. & WINDER, W. W. 1997. AICA riboside increases AMP-activated protein kinase, fatty acid oxidation, and glucose uptake in rat muscle. *Am J Physiol,* 273**,** E1107-12.

MINOKOSHI, Y., ALQUIER, T., FURUKAWA, N., KIM, Y. B., LEE, A., XUE, B., MU, J., FOUFELLE, F., FERRE, P., BIRNBAUM, M. J., STUCK, B. J. & KAHN, B. B. 2004. AMP-kinase regulates food intake by responding to hormonal and nutrient signals in the hypothalamus. *Nature,* 428**,** 569-74.

MOMCILOVIC, M., HONG, S. P. & CARLSON, M. 2006. Mammalian TAK1 activates Snf1 protein kinase in yeast and phosphorylates AMP-activated protein kinase in vitro. *J Biol Chem,* 281**,** 25336-43.

MORROW, V. A., FOUFELLE, F., CONNELL, J. M., PETRIE, J. R., GOULD, G. W. & SALT, I. P. 2003. Direct activation of AMP-activated protein kinase stimulates nitric-oxide synthesis in human aortic endothelial cells. *J Biol Chem,* 278**,** 31629-39.

MOTOSHIMA, H., GOLDSTEIN, B. J., IGATA, M. & ARAKI, E. 2006. AMPK and cell proliferation--AMPK as a therapeutic target for atherosclerosis and cancer. *J Physiol,* 574**,** 63-71.

MOTOSHIMA, H., WU, X., MAHADEV, K. & GOLDSTEIN, B. J. 2004. Adiponectin suppresses proliferation and superoxide generation and enhances eNOS activity in endothelial cells treated with oxidized LDL. *Biochem Biophys Res Commun,* 315**,** 264-71.

MULLIGAN, J. D., GONZALEZ, A. A., STEWART, A. M., CAREY, H. V. & SAUPE, K. W. 2007. Upregulation of AMPK during cold exposure occurs via distinct mechanisms in brown and white adipose tissue of the mouse. *J Physiol,* 580**,** 677-84.

MUSI, N. & GOODYEAR, L. J. 2002. Targeting the AMP-activated protein kinase for the treatment of type 2 diabetes. *Curr Drug Targets Immune Endocr Metabol Disord,* 2**,** 119-27.

NAGATA, D., MOGI, M. & WALSH, K. 2003. AMP-activated protein kinase (AMPK) signaling in endothelial cells is essential for angiogenesis in response to hypoxic stress. *J Biol Chem,* 278**,** 31000-6.

NAGATA, D., TAKEDA, R., SATA, M., SATONAKA, H., SUZUKI, E., NAGANO, T. & HIRATA, Y. 2004. AMP-activated protein kinase inhibits angiotensin II-stimulated vascular smooth muscle cell proliferation. *Circulation,* 110**,** 444-51.

NAKAGAWA, K., HIGASHI, Y., SASAKI, S., OSHIMA, T., MATSUURA, H. & CHAYAMA, K. 2002. Leptin causes vasodilation in humans. *Hypertens Res,* 25**,** 161-5.

NAKAMURA, K., FUSTER, J. J. & WALSH, K. 2014. Adipokines: a link between obesity and cardiovascular disease. *J Cardiol,* 63**,** 250-9.

NAKANE, M., SCHMIDT, H. H., POLLOCK, J. S., FORSTERMANN, U. & MURAD, F. 1993. Cloned human brain nitric oxide synthase is highly expressed in skeletal muscle. *FEBS Lett,* 316**,** 175-80.

NARISHIGE, T., EGASHIRA, K., AKATSUKA, Y., KATSUDA, Y., NUMAGUCHI, K., SAKATA, M. & TAKESHITA, A. 1993. Glibenclamide, a putative ATP-sensitive K+ channel blocker, inhibits coronary autoregulation in anesthetized dogs. *Circ Res,* 73**,** 771-6.

NELSON, M. T. & QUAYLE, J. M. 1995. Physiological roles and properties of potassium channels in arterial smooth muscle. *Am J Physiol,* 268**,** C799-822.

NGUYEN, M. T. A., FAVELYUKIS, S., NGUYEN, A.-K., REICHART, D., SCOTT, P. A., JENN, A., LIU-BRYAN, R., GLASS, C. K., NEELS, J. G. & OLEFSKY, J. M. 2007. A Subpopulation of Macrophages Infiltrates Hypertrophic Adipose Tissue and Is Activated by Free Fatty Acids via Toll-like Receptors 2 and 4 and JNK-dependent Pathways. *Journal of Biological Chemistry,* 282**,** 35279-35292.

NICHOLS, C. G. 2006. KATP channels as molecular sensors of cellular metabolism. *Nature,* 440**,** 470-6.

NICHOLS, C. G., SINGH, G. K. & GRANGE, D. K. 2013. K(ATP) channels and cardiovascular disease: Suddenly a syndrome. *Circulation research,* 112**,** 1059-1072.

NING, J. & CLEMMONS, D. R. 2010. AMP-activated protein kinase inhibits IGF-I signaling and protein synthesis in vascular smooth muscle cells via stimulation of insulin receptor substrate 1 S794 and tuberous sclerosis 2 S1345 phosphorylation. *Mol Endocrinol,* 24**,** 1218-29.

NISSEN, S. E., TUZCU, E. M., SCHOENHAGEN, P., CROWE, T., SASIELA, W. J., TSAI, J., ORAZEM, J., MAGORIEN, R. D., O'SHAUGHNESSY, C. & GANZ, P. 2005.

Statin therapy, LDL cholesterol, C-reactive protein, and coronary artery disease. *N Engl J Med,* 352**,** 29-38.

OAKHILL, J. S., CHEN, Z. P., SCOTT, J. W., STEEL, R., CASTELLI, L. A., LING, N., MACAULAY, S. L. & KEMP, B. E. 2010. beta-Subunit myristoylation is the gatekeeper for initiating metabolic stress sensing by AMP-activated protein kinase (AMPK). *Proc Natl Acad Sci U S A,* 107**,** 19237-41.

OAKHILL, J. S., SCOTT, J. W. & KEMP, B. E. 2009. Structure and function of AMP-activated protein kinase. *Acta Physiol (Oxf),* 196**,** 3-14.

OAKHILL, J. S., STEEL, R., CHEN, Z. P., SCOTT, J. W., LING, N., TAM, S. & KEMP, B. E. 2011. AMPK is a direct adenylate charge-regulated protein kinase. *Science,* 332**,** 1433-5.

ODA, A., TANIGUCHI, T. & YOKOYAMA, M. 2001. Leptin stimulates rat aortic smooth muscle cell proliferation and migration. *Kobe J Med Sci,* 47**,** 141-50.

OHASHI, K., PARKER, J. L., OUCHI, N., HIGUCHI, A., VITA, J. A., GOKCE, N., PEDERSEN, A. A., KALTHOFF, C., TULLIN, S., SAMS, A., SUMMER, R. & WALSH, K. 2010. Adiponectin Promotes Macrophage Polarization toward an Anti-inflammatory Phenotype. *The Journal of Biological Chemistry,* 285**,** 6153-6160.

OHMAN, M. K., LUO, W., WANG, H., GUO, C., ABDALLAH, W., RUSSO, H. M. & EITZMAN, D. T. 2011. Perivascular visceral adipose tissue induces atherosclerosis in apolipoprotein E deficient mice. *Atherosclerosis,* 219**,** 33-9.

OKADA-IWABU, M., YAMAUCHI, T., IWABU, M., HONMA, T., HAMAGAMI, K., MATSUDA, K., YAMAGUCHI, M., TANABE, H., KIMURA-SOMEYA, T., SHIROUZU, M., OGATA, H., TOKUYAMA, K., UEKI, K., NAGANO, T., TANAKA, A., YOKOYAMA, S. & KADOWAKI, T. 2013. A small-molecule AdipoR agonist for type 2 diabetes and short life in obesity. *Nature,* 503**,** 493-9.

OKAMOTO, E., COUSE, T., DE LEON, H., VINTEN-JOHANSEN, J., GOODMAN, R. B., SCOTT, N. A. & WILCOX, J. N. 2001. Perivascular inflammation after balloon angioplasty of porcine coronary arteries. *Circulation,* 104**,** 2228-35.

OKAMOTO, Y., KIHARA, S., FUNAHASHI, T., MATSUZAWA, Y. & LIBBY, P. 2006. Adiponectin: a key adipocytokine in metabolic syndrome. *Clinical Science,* 110**,** 267-278.

ORIOWO, M. A. 2015. Perivascular adipose tissue, vascular reactivity and hypertension. *Med Princ Pract,* 24 Suppl 1**,** 29-37.

OUCHI, N., OHISHI, M., KIHARA, S., FUNAHASHI, T., NAKAMURA, T., NAGARETANI, H., KUMADA, M., OHASHI, K., OKAMOTO, Y., NISHIZAWA, H.,

KISHIDA, K., MAEDA, N., NAGASAWA, A., KOBAYASHI, H., HIRAOKA, H., KOMAI, N., KAIBE, M., RAKUGI, H., OGIHARA, T. & MATSUZAWA, Y. 2003. Association of hypoadiponectinemia with impaired vasoreactivity. *Hypertension,* 42**,** 231-4.

OUCHI, N., SHIBATA, R. & WALSH, K. 2006. Cardioprotection by adiponectin. *Trends Cardiovasc Med,* 16**,** 141-6.

OWEN, M. K., WITZMANN, F. A., MCKENNEY, M. L., LAI, X., BERWICK, Z. C., MOBERLY, S. P., ALLOOSH, M., STUREK, M. & TUNE, J. D. 2013. Perivascular adipose tissue potentiates contraction of coronary vascular smooth muscle: influence of obesity. *Circulation,* 128**,** 9-18.

PACHER, P., BECKMAN, J. S. & LIAUDET, L. 2007. Nitric oxide and peroxynitrite in health and disease. *Physiol Rev,* 87**,** 315-424.

PADILLA, J., JENKINS, N. T., VIEIRA-POTTER, V. J. & LAUGHLIN, M. H. 2013. Divergent phenotype of rat thoracic and abdominal perivascular adipose tissues. *Am J Physiol Regul Integr Comp Physiol,* 304**,** R543-52.

PALMER, R. M., ASHTON, D. S. & MONCADA, S. 1988. Vascular endothelial cells synthesize nitric oxide from L-arginine. *Nature,* 333**,** 664-6.

PALMER, R. M., FERRIGE, A. G. & MONCADA, S. 1987. Nitric oxide release accounts for the biological activity of endothelium-derived relaxing factor. *Nature,* 327**,** 524-6.

PAYNE, G. A., BORBOUSE, L., KUMAR, S., NEEB, Z., ALLOOSH, M., STUREK, M. & TUNE, J. D. 2010. Epicardial perivascular adipose-derived leptin exacerbates coronary endothelial dysfunction in metabolic syndrome via a protein kinase C-beta pathway. *Arterioscler Thromb Vasc Biol,* 30**,** 1711-7.

PERRIN, C., KNAUF, C. & BURCELIN, R. 2004. Intracerebroventricular infusion of glucose, insulin, and the adenosine monophosphate-activated kinase activator, 5-aminoimidazole-4-carboxamide-1-beta-D-ribofuranoside, controls muscle glycogen synthesis. *Endocrinology,* 145**,** 4025-33.

PHILLIPS, S. A., CIARALDI, T. P., KONG, A. P., BANDUKWALA, R., ARODA, V., CARTER, L., BAXI, S., MUDALIAR, S. R. & HENRY, R. R. 2003. Modulation of circulating and adipose tissue adiponectin levels by antidiabetic therapy. *Diabetes,* 52**,** 667-74.

PILON, G., DALLAIRE, P. & MARETTE, A. 2004. Inhibition of inducible nitric-oxide synthase by activators of AMP-activated protein kinase: a new mechanism of action of insulin-sensitizing drugs. *J Biol Chem,* 279**,** 20767-74.

PISCHON, T., HOTAMISLIGIL, G. S. & RIMM, E. B. 2003. Adiponectin: stability in plasma over 36 hours and within-person variation over 1 year. *Clin Chem,* 49**,** 650-2.

POLIKANDRIOTIS, J. A., MAZZELLA, L. J., RUPNOW, H. L. & HART, C. M. 2005. Peroxisome proliferator-activated receptor gamma ligands stimulate endothelial nitric oxide production through distinct peroxisome proliferator-activated receptor gamma-dependent mechanisms. *Arterioscler Thromb Vasc Biol,* 25**,** 1810-6.

PULINILKUNNIL, T., HE, H., KONG, D., ASAKURA, K., PERONI, O. D., LEE, A. & KAHN, B. B. 2011. Adrenergic regulation of AMP-activated protein kinase in brown adipose tissue in vivo. *J Biol Chem,* 286**,** 8798-809.

QUAYLE, J. M., NELSON, M. T. & STANDEN, N. B. 1997. ATP-sensitive and inwardly rectifying potassium channels in smooth muscle. *Physiol Rev,* 77**,** 1165-232.

RADI, R., CASSINA, A., HODARA, R., QUIJANO, C. & CASTRO, L. 2002. Peroxynitrite reactions and formation in mitochondria. *Free Radic Biol Med,* 33**,** 1451-64.

RAJSHEKER, S., MANKA, D., BLOMKALNS, A. L., CHATTERJEE, T. K., STOLL, L. L. & WEINTRAUB, N. L. 2010. Crosstalk between perivascular adipose tissue and blood vessels. *Curr Opin Pharmacol,* 10**,** 191-6.

RATZ, P. H. & FLAIM, S. F. 1984. Mechanism of 5-HT contraction in isolated bovine ventricular coronary arteries. Evidence for transient receptor-operated calcium influx channels. *Circ Res,* 54**,** 135-43.

REBOLLEDO, A., REBOLLEDO, O. R., MARRA, C. A., GARCIA, M. E., ROLDAN PALOMO, A. R., RIMORINI, L. & GAGLIARDINO, J. J. 2010. Early alterations in vascular contractility associated to changes in fatty acid composition and oxidative stress markers in perivascular adipose tissue. *Cardiovasc Diabetol,* 9**,** 65.

REIHILL, J. A., EWART, M. A., HARDIE, D. G. & SALT, I. P. 2007. AMP-activated protein kinase mediates VEGF-stimulated endothelial NO production. *Biochem Biophys Res Commun,* 354**,** 1084-8.

REIHILL, J. A., EWART, M. A. & SALT, I. P. 2011. The role of AMP-activated protein kinase in the functional effects of vascular endothelial growth factor-A and -B in human aortic endothelial cells. *Vasc Cell,* 3**,** 9.

RICHARD, A. J. & STEPHENS, J. M. 2014. The role of JAK-STAT signaling in adipose tissue function. *Biochim Biophys Acta,* 1842**,** 431-9.

RODRIGUEZ, J., SPECIAN, V., MALONEY, R., JOURD'HEUIL, D. & FEELISCH, M. 2005. Performance of diamino fluorophores for the localization of sources and targets of nitric oxide. *Free Radic Biol Med,* 38**,** 356-68.

ROMACHO, T., AZCUTIA, V., VAZQUEZ-BELLA, M., MATESANZ, N., CERCAS, E., NEVADO, J., CARRARO, R., RODRIGUEZ-MANAS, L., SANCHEZ-FERRER, C. F. & PEIRO, C. 2009. Extracellular PBEF/NAMPT/visfatin activates pro-inflammatory signalling in human vascular smooth muscle cells through nicotinamide phosphoribosyltransferase activity. *Diabetologia,* 52**,** 2455-63.

ROSS, R. 1999. Atherosclerosis--an inflammatory disease. *N Engl J Med,* 340**,** 115-26.

ROSSMEISL, M., FLACHS, P., BRAUNER, P., SPONAROVA, J., MATEJKOVA, O., PRAZAK, T., RUZICKOVA, J., BARDOVA, K., KUDA, O. & KOPECKY, J. 2004. Role of energy charge and AMP-activated protein kinase in adipocytes in the control of body fat stores. *Int J Obes Relat Metab Disord,* 28 Suppl 4**,** S38-44.

RUAN, C. C., ZHU, D. L., CHEN, Q. Z., CHEN, J., GUO, S. J., LI, X. D. & GAO, P. J. 2010. Perivascular adipose tissue-derived complement 3 is required for adventitial fibroblast functions and adventitial remodeling in deoxycorticosterone acetate-salt hypertensive rats. *Arterioscler Thromb Vasc Biol,* 30**,** 2568-74.

RUBIN, L. J., MAGLIOLA, L., FENG, X., JONES, A. W. & HALE, C. C. 2005. Metabolic activation of AMP kinase in vascular smooth muscle. *J Appl Physiol (1985),* 98**,** 296-306.

RUDERMAN, N. B., CARLING, D., PRENTKI, M. & CACICEDO, J. M. 2013. AMPK, insulin resistance, and the metabolic syndrome. *J Clin Invest,* 123**,** 2764-72.

RUDERMAN, N. B., SAHA, A. K. & KRAEGEN, E. W. 2003. Minireview: malonyl CoA, AMP-activated protein kinase, and adiposity. *Endocrinology,* 144**,** 5166-71.

RUDIJANTO, A. 2007. The role of vascular smooth muscle cells on the pathogenesis of atherosclerosis. *Acta Med Indones,* 39**,** 86-93.

SAG, D., CARLING, D., STOUT, R. D. & SUTTLES, J. 2008. Adenosine 5'-monophosphate-activated protein kinase promotes macrophage polarization to an anti-inflammatory functional phenotype. *J Immunol,* 181**,** 8633-41.

SAKAUE, H., NISHIZAWA, A., OGAWA, W., TESHIGAWARA, K., MORI, T., TAKASHIMA, Y., NODA, T. & KASUGA, M. 2003. Requirement for 3-phosphoinositide-kependent dinase-1 (PDK-1) in insulin-induced glucose uptake in immortalized brown adipocytes. *J Biol Chem,* 278**,** 38870-4.

SALCEDO, A., GARIJO, J., MONGE, L., FERNANDEZ, N., LUIS GARCIA-VILLALON, A., SANCHEZ TURRION, V., CUERVAS-MONS, V. & DIEGUEZ, G. 2007. Apelin effects in human splanchnic arteries. Role of nitric oxide and prostanoids. *Regul Pept,* 144**,** 50-5.

SALMENNIEMI, U., RUOTSALAINEN, E., PIHLAJAMAKI, J., VAUHKONEN, I., KAINULAINEN, S., PUNNONEN, K., VANNINEN, E. & LAAKSO, M. 2004. Multiple abnormalities in glucose and energy metabolism and coordinated changes in levels of adiponectin, cytokines, and adhesion molecules in subjects with metabolic syndrome. *Circulation,* 110**,** 3842-8.

SALT, I., CELLER, J. W., HAWLEY, S. A., PRESCOTT, A., WOODS, A., CARLING, D. & HARDIE, D. G. 1998. AMP-activated protein kinase: greater AMP dependence, and preferential nuclear localization, of complexes containing the alpha2 isoform. *Biochem J,* 334 (Pt 1)**,** 177-87.

SALT, I. P. & PALMER, T. M. 2012. Exploiting the anti-inflammatory effects of AMP-activated protein kinase activation. *Expert Opin Investig Drugs,* 21**,** 1155-67.

SAMAHA, F. F., HEINEMAN, F. W., INCE, C., FLEMING, J. & BALABAN, R. S. 1992. ATP-sensitive potassium channel is essential to maintain basal coronary vascular tone in vivo. *American Journal of Physiology - Cell Physiology,* 262**,** C1220-C1227.

SANDERS, M. J., ALI, Z. S., HEGARTY, B. D., HEATH, R., SNOWDEN, M. A. & CARLING, D. 2007. Defining the mechanism of activation of AMP-activated protein kinase by the small molecule A-769662, a member of the thienopyridone family. *J Biol Chem,* 282**,** 32539-48.

SARTORE, S., CHIAVEGATO, A., FAGGIN, E., FRANCH, R., PUATO, M., AUSONI, S. & PAULETTO, P. 2001. Contribution of adventitial fibroblasts to neointima formation and vascular remodeling: from innocent bystander to active participant. *Circ Res,* 89**,** 1111-21.

SATA, M., MAEJIMA, Y., ADACHI, F., FUKINO, K., SAIURA, A., SUGIURA, S., AOYAGI, T., IMAI, Y., KURIHARA, H., KIMURA, K., OMATA, M., MAKUUCHI, M., HIRATA, Y. & NAGAI, R. 2000. A mouse model of vascular injury that induces rapid onset of medial cell apoptosis followed by reproducible neointimal hyperplasia. *J Mol Cell Cardiol,* 32**,** 2097-104.

SATA, M., SAIURA, A., KUNISATO, A., TOJO, A., OKADA, S., TOKUHISA, T., HIRAI, H., MAKUUCHI, M., HIRATA, Y. & NAGAI, R. 2002. Hematopoietic stem cells differentiate into vascular cells that participate in the pathogenesis of atherosclerosis. *Nat Med,* 8**,** 403-9.

SCHERER, P. E., WILLIAMS, S., FOGLIANO, M., BALDINI, G. & LODISH, H. F. 1995. A novel serum protein similar to C1q, produced exclusively in adipocytes. *J Biol Chem,* 270**,** 26746-9.

SCHLEIFENBAUM, J., KOHN, C., VOBLOVA, N., DUBROVSKA, G., ZAVARIRSKAYA, O., GLOE, T., CREAN, C. S., LUFT, F. C., HUANG, Y.,

SCHUBERT, R. & GOLLASCH, M. 2010. Systemic peripheral artery relaxation by KCNQ channel openers and hydrogen sulfide. *J Hypertens,* 28**,** 1875-82.

SCHRAW, T., WANG, Z. V., HALBERG, N., HAWKINS, M. & SCHERER, P. E. 2008. Plasma adiponectin complexes have distinct biochemical characteristics. *Endocrinology,* 149**,** 2270-82.

SCHUBERT, R. & MULVANY, M. J. 1999. The myogenic response: established facts and attractive hypotheses. *Clin Sci (Lond),* 96**,** 313-26.

SCHUHMACHER, S., FORETZ, M., KNORR, M., JANSEN, T., HORTMANN, M., WENZEL, P., OELZE, M., KLESCHYOV, A. L., DAIBER, A., KEANEY, J. F., JR., WEGENER, G., LACKNER, K., MUNZEL, T., VIOLLET, B. & SCHULZ, E. 2011. alpha1AMP-activated protein kinase preserves endothelial function during chronic angiotensin II treatment by limiting Nox2 upregulation. *Arterioscler Thromb Vasc Biol,* 31**,** 560-6.

SCHULTZ, K.-D., SCHULTZ, K. & SCHULTZ, G. 1977. Sodium nitroprusside and other smooth muscle-relaxants increase cyclic GMP levels in rat ductus deferens. *Nature,* 265**,** 750-751.

SCOTT, J. W., VAN DENDEREN, B. J., JORGENSEN, S. B., HONEYMAN, J. E., STEINBERG, G. R., OAKHILL, J. S., ISELI, T. J., KOAY, A., GOOLEY, P. R., STAPLETON, D. & KEMP, B. E. 2008. Thienopyridone drugs are selective activators of AMP-activated protein kinase beta1-containing complexes. *Chem Biol,* 15**,** 1220-30.

SCOTT, N. A., CIPOLLA, G. D., ROSS, C. E., DUNN, B., MARTIN, F. H., SIMONET, L. & WILCOX, J. N. 1996. Identification of a potential role for the adventitia in vascular lesion formation after balloon overstretch injury of porcine coronary arteries. *Circulation,* 93**,** 2178-87.

SELL, H., DIETZE-SCHROEDER, D., ECKARDT, K. & ECKEL, J. 2006. Cytokine secretion by human adipocytes is differentially regulated by adiponectin, AICAR, and troglitazone. *Biochem Biophys Res Commun,* 343**,** 700-6.

SEMPLE, R. K., CHATTERJEE, V. K. & O'RAHILLY, S. 2006. PPAR gamma and human metabolic disease. *J Clin Invest,* 116**,** 581-9.

SERNE, E. H., DE JONGH, R. T., ERINGA, E. C., RG, I. J. & STEHOUWER, C. D. 2007. Microvascular dysfunction: a potential pathophysiological role in the metabolic syndrome. *Hypertension,* 50**,** 204-11.

SERRANO, C. V., JR., RAMIRES, J. A., VENTURINELLI, M., ARIE, S., D'AMICO, E., ZWEIER, J. L., PILEGGI, F. & DA LUZ, P. L. 1997. Coronary angioplasty results in

leukocyte and platelet activation with adhesion molecule expression. Evidence of inflammatory responses in coronary angioplasty. *J Am Coll Cardiol,* 29**,** 1276-83.

SHAN, J., NGUYEN, T. B., TOTARY-JAIN, H., DANSKY, H., MARX, S. O. & MARKS, A. R. 2008. Leptin-enhanced neointimal hyperplasia is reduced by mTOR and PI3K inhibitors. *Proc Natl Acad Sci U S A,* 105**,** 19006-11.

SHI, H., KOKOEVA, M. V., INOUYE, K., TZAMELI, I., YIN, H. & FLIER, J. S. 2006. TLR4 links innate immunity and fatty acid-induced insulin resistance. *J Clin Invest,* 116**,** 3015-25.

SHIBATA, R., OUCHI, N. & MUROHARA, T. 2009. Adiponectin and cardiovascular disease. *Circ J,* 73**,** 608-14.

SHU, Y., SHEARDOWN, S. A., BROWN, C., OWEN, R. P., ZHANG, S., CASTRO, R. A., IANCULESCU, A. G., YUE, L., LO, J. C., BURCHARD, E. G., BRETT, C. M. & GIACOMINI, K. M. 2007. Effect of genetic variation in the organic cation transporter 1 (OCT1) on metformin action. *J Clin Invest,* 117**,** 1422-31.

SIERSBAEK, R., NIELSEN, R. & MANDRUP, S. 2010. PPARgamma in adipocyte differentiation and metabolism--novel insights from genome-wide studies. *FEBS Lett,* 584**,** 3242-9.

SNELL-BERGEON, J. K., BUDOFF, M. J. & HOKANSON, J. E. 2013. Vascular calcification in diabetes: mechanisms and implications. *Curr Diab Rep,* 13**,** 391-402.

SOBEY, C. G. 2001. Potassium channel function in vascular disease. *Arterioscler Thromb Vasc Biol,* 21**,** 28-38.

SOLTIS, E. E. & CASSIS, L. A. 1991. Influence of perivascular adipose tissue on rat aortic smooth muscle responsiveness. *Clin Exp Hypertens A,* 13**,** 277-96.

SPIROGLOU, S. G., KOSTOPOULOS, C. G., VARAKIS, J. N. & PAPADAKI, H. H. 2010. Adipokines in periaortic and epicardial adipose tissue: differential expression and relation to atherosclerosis. *J Atheroscler Thromb,* 17**,** 115-30.

STAHMANN, N., WOODS, A., CARLING, D. & HELLER, R. 2006. Thrombin activates AMP-activated protein kinase in endothelial cells via a pathway involving Ca2+/calmodulin-dependent protein kinase kinase beta. *Mol Cell Biol,* 26**,** 5933-45.

STASTNY, J., BIENERTOVA-VASKU, J. & VASKU, A. 2012. Visfatin and its role in obesity development. *Diabetes Metab Syndr,* 6**,** 120-4.

STOCKER, D. J., TAYLOR, A. J., LANGLEY, R. W., JEZIOR, M. R. & VIGERSKY, R. A. 2007. A randomized trial of the effects of rosiglitazone and metformin on inflammation and subclinical atherosclerosis in patients with type 2 diabetes. *Am Heart J,* 153**,** 445 e1-6.

SUN, W., LEE, T. S., ZHU, M., GU, C., WANG, Y., ZHU, Y. & SHYY, J. Y. 2006. Statins activate AMP-activated protein kinase in vitro and in vivo. *Circulation,* 114**,** 2655-62.

SUZUKI, K., UCHIDA, K., NAKANISHI, N. & HATTORI, Y. 2008. Cilostazol activates AMP-activated protein kinase and restores endothelial function in diabetes. *Am J Hypertens,* 21**,** 451-7.

SZABO, C., ISCHIROPOULOS, H. & RADI, R. 2007. Peroxynitrite: biochemistry, pathophysiology and development of therapeutics. *Nat Rev Drug Discov,* 6**,** 662-680.

SZASZ, T., BOMFIM, G. F. & WEBB, R. C. 2013. The influence of perivascular adipose tissue on vascular homeostasis. *Vasc Health Risk Manag,* 9**,** 105-16.

SZASZ, T. & WEBB, R. C. 2012. Perivascular adipose tissue: more than just structural support. *Clin Sci (Lond),* 122**,** 1-12.

TAKAOKA, M., NAGATA, D., KIHARA, S., SHIMOMURA, I., KIMURA, Y., TABATA, Y., SAITO, Y., NAGAI, R. & SATA, M. 2009. Periadventitial adipose tissue plays a critical role in vascular remodeling. *Circ Res,* 105**,** 906-11.

TAKAOKA, M., SUZUKI, H., SHIODA, S., SEKIKAWA, K., SAITO, Y., NAGAI, R. & SATA, M. 2010. Endovascular injury induces rapid phenotypic changes in perivascular adipose tissue. *Arterioscler Thromb Vasc Biol,* 30**,** 1576-82.

TAM, C. S., LECOULTRE, V. & RAVUSSIN, E. 2012. Brown Adipose Tissue. *Mechanisms and Potential Therapeutic Targets,* 125**,** 2782-2791.

TAMAS, P., HAWLEY, S. A., CLARKE, R. G., MUSTARD, K. J., GREEN, K., HARDIE, D. G. & CANTRELL, D. A. 2006. Regulation of the energy sensor AMP-activated protein kinase by antigen receptor and Ca2+ in T lymphocytes. *J Exp Med,* 203**,** 1665-70.

TANAKA, Y., MEERA, P., SONG, M., KNAUS, H. G. & TORO, L. 1997. Molecular constituents of maxi KCa channels in human coronary smooth muscle: predominant alpha + beta subunit complexes. *The Journal of Physiology,* 502**,** 545-557.

TERADA, S., GOTO, M., KATO, M., KAWANAKA, K., SHIMOKAWA, T. & TABATA, I. 2002. Effects of low-intensity prolonged exercise on PGC-1 mRNA expression in rat epitrochlearis muscle. *Biochem Biophys Res Commun,* 296**,** 350-4.

TERAMOTO, N., TOMODA, T., YUNOKI, T. & ITO, Y. 2006. Different glibenclamide-sensitivity of ATP-sensitive K+ currents using different patch-clamp recording methods. *Eur J Pharmacol,* 531**,** 34-40.

TESFAMARIAM, B. & HALPERN, W. 1988. Endothelium-dependent and endothelium-independent vasodilation in resistance arteries from hypertensive rats. *Hypertension,* 11**,** 440-4.

THALMANN, S. & MEIER, C. A. 2007. Local adipose tissue depots as cardiovascular risk factors. *Cardiovasc Res,* 75**,** 690-701.

THEANDER-CARRILLO, C., WIEDMER, P., CETTOUR-ROSE, P., NOGUEIRAS, R., PEREZ-TILVE, D., PFLUGER, P., CASTANEDA, T. R., MUZZIN, P., SCHURMANN, A., SZANTO, I., TSCHOP, M. H. & ROHNER-JEANRENAUD, F. 2006. Ghrelin action in the brain controls adipocyte metabolism. *J Clin Invest,* 116**,** 1983-93.

THENGCHAISRI, N. & KUO, L. 2003. Hydrogen peroxide induces endothelium-dependent and -independent coronary arteriolar dilation: role of cyclooxygenase and potassium channels. *Am J Physiol Heart Circ Physiol,* 285**,** H2255-63.

THORS, B., HALLDORSSON, H. & THORGEIRSSON, G. 2004. Thrombin and histamine stimulate endothelial nitric-oxide synthase phosphorylation at Ser1177 via an AMPK mediated pathway independent of PI3K-Akt. *FEBS Lett,* 573**,** 175-80.

TIIKKAINEN, M., HAKKINEN, A. M., KORSHENINNIKOVA, E., NYMAN, T., MAKIMATTILA, S. & YKI-JARVINEN, H. 2004. Effects of rosiglitazone and metformin on liver fat content, hepatic insulin resistance, insulin clearance, and gene expression in adipose tissue in patients with type 2 diabetes. *Diabetes,* 53**,** 2169-76.

TRAYHURN, P. 2005. Endocrine and signalling role of adipose tissue: new perspectives on fat. *Acta Physiol Scand,* 184**,** 285-93.

TRAYHURN, P. & WOOD, I. S. 2004. Adipokines: inflammation and the pleiotropic role of white adipose tissue. *Br J Nutr,* 92**,** 347-55.

TSUCHIDA, A., YAMAUCHI, T., TAKEKAWA, S., HADA, Y., ITO, Y., MAKI, T. & KADOWAKI, T. 2005. Peroxisome Proliferator–Activated Receptor (PPAR)α Activation Increases Adiponectin Receptors and Reduces Obesity-Related Inflammation in Adipose Tissue. *Comparison of Activation of PPARα, PPARγ, and Their Combination,* 54**,** 3358-3370.

TURER, A. T. & SCHERER, P. E. 2012. Adiponectin: mechanistic insights and clinical implications. *Diabetologia,* 55**,** 2319-26.

TURNER, N., LI, J. Y., GOSBY, A., TO, S. W., CHENG, Z., MIYOSHI, H., TAKETO, M. M., COONEY, G. J., KRAEGEN, E. W., JAMES, D. E., HU, L. H., LI, J. & YE, J. M. 2008. Berberine and its more biologically available derivative, dihydroberberine, inhibit mitochondrial respiratory complex I: a mechanism for the action of berberine to activate AMP-activated protein kinase and improve insulin action. *Diabetes,* 57**,** 1414-8.

UEMURA, Y., SHIBATA, R., OHASHI, K., ENOMOTO, T., KAMBARA, T., YAMAMOTO, T., OGURA, Y., YUASA, D., JOKI, Y., MATSUO, K., MIYABE, M., KATAOKA, Y., MUROHARA, T. & OUCHI, N. 2013. Adipose-derived factor CTRP9 attenuates vascular smooth muscle cell proliferation and neointimal formation. *FASEB J,* 27**,** 25-33.

VAN VEELEN, W., KORSSE, S. E., VAN DE LAAR, L. & PEPPELENBOSCH, M. P. 2011. The long and winding road to rational treatment of cancer associated with LKB1/AMPK/TSC/mTORC1 signaling. *Oncogene,* 30**,** 2289-303.

VANDANMAGSAR, B., YOUM, Y.-H., RAVUSSIN, A., GALGANI, J. E., STADLER, K., MYNATT, R. L., RAVUSSIN, E., STEPHENS, J. M. & DIXIT, V. D. 2011. The NLRP3 inflammasome instigates obesity-induced inflammation and insulin resistance. *Nat Med,* 17**,** 179-188.

VECCHIONE, C., MAFFEI, A., COLELLA, S., ARETINI, A., POULET, R., FRATI, G., GENTILE, M. T., FRATTA, L., TRIMARCO, V., TRIMARCO, B. & LEMBO, G. 2002. Leptin effect on endothelial nitric oxide is mediated through Akt-endothelial nitric oxide synthase phosphorylation pathway. *Diabetes,* 51**,** 168-73.

VERLOHREN, S., DUBROVSKA, G., TSANG, S. Y., ESSIN, K., LUFT, F. C., HUANG, Y. & GOLLASCH, M. 2004. Visceral periadventitial adipose tissue regulates arterial tone of mesenteric arteries. *Hypertension,* 44**,** 271-6.

VILA-BEDMAR, R., LORENZO, M. & FERNANDEZ-VELEDO, S. 2010. Adenosine 5'-monophosphate-activated protein kinase-mammalian target of rapamycin cross talk regulates brown adipocyte differentiation. *Endocrinology,* 151**,** 980-92.

VILLENA, J. A., VIOLLET, B., ANDREELLI, F., KAHN, A., VAULONT, S. & SUL, H. S. 2004. Induced adiposity and adipocyte hypertrophy in mice lacking the AMP-activated protein kinase-alpha2 subunit. *Diabetes,* 53**,** 2242-9.

VIOLLET, B., ANDREELLI, F., JORGENSEN, S. B., PERRIN, C., GELOEN, A., FLAMEZ, D., MU, J., LENZNER, C., BAUD, O., BENNOUN, M., GOMAS, E., NICOLAS, G., WOJTASZEWSKI, J. F., KAHN, A., CARLING, D., SCHUIT, F. C., BIRNBAUM, M. J., RICHTER, E. A., BURCELIN, R. & VAULONT, S. 2003. The AMP-activated protein kinase alpha2 catalytic subunit controls whole-body insulin sensitivity. *J Clin Invest,* 111**,** 91-8.

VIOLLET, B., HORMAN, S., LECLERC, J., LANTIER, L., FORETZ, M., BILLAUD, M., GIRI, S. & ANDREELLI, F. 2010. AMPK inhibition in health and disease. *Crit Rev Biochem Mol Biol,* 45**,** 276-95.

VUCETIC, M., OTASEVIC, V., KORAC, A., STANCIC, A., JANKOVIC, A., MARKELIC, M., GOLIC, I., VELICKOVIC, K., BUZADZIC, B. & KORAC, B. 2011. Interscapular brown adipose tissue metabolic reprogramming during cold acclimation: Interplay of HIF-1alpha and AMPKalpha. *Biochim Biophys Acta,* 1810**,** 1252-61.

WALCHER, D., HESS, K., BERGER, R., ALEKSIC, M., HEINZ, P., BACH, H., DURST, R., HAUSAUER, A., HOMBACH, V. & MARX, N. 2010. Resistin: a newly identified chemokine for human CD4-positive lymphocytes. *Cardiovascular Research,* 85**,** 167-174.

WALLERATH, T., GATH, I., AULITZKY, W. E., POLLOCK, J. S., KLEINERT, H. & FORSTERMANN, U. 1997. Identification of the NO synthase isoforms expressed in human neutrophil granulocytes, megakaryocytes and platelets. *Thromb Haemost,* 77**,** 163-7.

WAN, Z., ROOT-MCCAIG, J., CASTELLANI, L., KEMP, B. E., STEINBERG, G. R. & WRIGHT, D. C. 2014. Evidence for the role of AMPK in regulating PGC-1 alpha expression and mitochondrial proteins in mouse epididymal adipose tissue. *Obesity (Silver Spring),* 22**,** 730-8.

WANG, H., LUO, W., WANG, J., GUO, C., WANG, X., WOLFFE, S. L., BODARY, P. F. & EITZMAN, D. T. 2012. Obesity-induced endothelial dysfunction is prevented by deficiency of P-selectin glycoprotein ligand-1. *Diabetes,* 61**,** 3219-27.

WANG, P., BAI, C., XU, Q. Y., XU, T. Y., SU, D. F., SASSARD, J. & MIAO, C. Y. 2010a. Visfatin is associated with lipid metabolic abnormalities in Lyon hypertensive rats. *Clin Exp Pharmacol Physiol,* 37**,** 894-9.

WANG, P., XU, T. Y., GUAN, Y. F., SU, D. F., FAN, G. R. & MIAO, C. Y. 2009a. Perivascular adipose tissue-derived visfatin is a vascular smooth muscle cell growth factor: role of nicotinamide mononucleotide. *Cardiovasc Res,* 81**,** 370-80.

WANG, P., XU, T. Y., GUAN, Y. F., TIAN, W. W., VIOLLET, B., RUI, Y. C., ZHAI, Q. W., SU, D. F. & MIAO, C. Y. 2011a. Nicotinamide phosphoribosyltransferase protects against ischemic stroke through SIRT1-dependent adenosine monophosphate-activated kinase pathway. *Ann Neurol,* 69**,** 360-74.

WANG, S., LIANG, B., VIOLLET, B. & ZOU, M. H. 2011b. Inhibition of the AMP-activated protein kinase-alpha2 accentuates agonist-induced vascular smooth muscle contraction and high blood pressure in mice. *Hypertension,* 57**,** 1010-7.

WANG, S., XU, J., SONG, P., VIOLLET, B. & ZOU, M. H. 2009b. In vivo activation of AMP-activated protein kinase attenuates diabetes-enhanced degradation of GTP cyclohydrolase I. *Diabetes,* 58**,** 1893-901.

WANG, S., ZHANG, M., LIANG, B., XU, J., XIE, Z., LIU, C., VIOLLET, B., YAN, D. & ZOU, M. H. 2010b. AMPKalpha2 deletion causes aberrant expression and activation of NAD(P)H oxidase and consequent endothelial dysfunction in vivo: role of 26S proteasomes. *Circ Res,* 106**,** 1117-28.

WANG, Y., HUANG, Y., LAM, K. S., LI, Y., WONG, W. T., YE, H., LAU, C. W., VANHOUTTE, P. M. & XU, A. 2009c. Berberine prevents hyperglycemia-induced endothelial injury and enhances vasodilatation via adenosine monophosphate-activated protein kinase and endothelial nitric oxide synthase. *Cardiovasc Res,* 82**,** 484-92.

WARD, N. C., CHEN, K., LI, C., CROFT, K. D. & KEANEY, J. F. 2011. Chronic AMPK activation prevents 20-HETE induced endothelial dysfunction. *Clinical and experimental pharmacology & physiology,* 38**,** 328-333.

WEBB, R. C. 2003. SMOOTH MUSCLE CONTRACTION AND RELAXATION. *Advances in Physiology Education,* 27**,** 201-206.

WEI, A., SOLARO, C., LINGLE, C. & SALKOFF, L. 1994. Calcium sensitivity of BK-type KCa channels determined by a separable domain. *Neuron,* 13**,** 671-81.

WEISBERG, S. P., MCCANN, D., DESAI, M., ROSENBAUM, M., LEIBEL, R. L. & FERRANTE, A. W., JR. 2003. Obesity is associated with macrophage accumulation in adipose tissue. *J Clin Invest,* 112**,** 1796-808.

WESTON, A. H., EGNER, I., DONG, Y., PORTER, E. L., HEAGERTY, A. M. & EDWARDS, G. 2013. Stimulated release of a hyperpolarizing factor (ADHF) from mesenteric artery perivascular adipose tissue: involvement of myocyte BKCa channels and adiponectin. *Br J Pharmacol,* 169**,** 1500-9.

WILCOX, J. N. & SCOTT, N. A. 1996. Potential role of the adventitia in arteritis and atherosclerosis. *Int J Cardiol,* 54 Suppl**,** S21-35.

WOJTASZEWSKI, J. F., JORGENSEN, S. B., HELLSTEN, Y., HARDIE, D. G. & RICHTER, E. A. 2002. Glycogen-dependent effects of 5-aminoimidazole-4-carboxamide (AICA)-riboside on AMP-activated protein kinase and glycogen synthase activities in rat skeletal muscle. *Diabetes,* 51**,** 284-92.

WONG, M. S. & VANHOUTTE, P. M. 2010. COX-mediated endothelium-dependent contractions: from the past to recent discoveries. *Acta Pharmacol Sin,* 31**,** 1095-102.

WOODS, A., CHEUNG, P. C., SMITH, F. C., DAVISON, M. D., SCOTT, J., BERI, R. K. & CARLING, D. 1996. Characterization of AMP-activated protein kinase beta and gamma subunits. Assembly of the heterotrimeric complex in vitro. *J Biol Chem,* 271**,** 10282-90.

WOODS, A., DICKERSON, K., HEATH, R., HONG, S. P., MOMCILOVIC, M., JOHNSTONE, S. R., CARLSON, M. & CARLING, D. 2005. Ca2+/calmodulin-dependent protein kinase kinase-beta acts upstream of AMP-activated protein kinase in mammalian cells. *Cell Metab,* 2**,** 21-33.

WOODS, A., JOHNSTONE, S. R., DICKERSON, K., LEIPER, F. C., FRYER, L. G., NEUMANN, D., SCHLATTNER, U., WALLIMANN, T., CARLSON, M. & CARLING, D. 2003a. LKB1 is the upstream kinase in the AMP-activated protein kinase cascade. *Curr Biol,* 13**,** 2004-8.

WOODS, S. C., SEELEY, R. J., RUSHING, P. A., D'ALESSIO, D. & TSO, P. 2003b. A controlled high-fat diet induces an obese syndrome in rats. *J Nutr,* 133**,** 1081-7.

WORLD HEALTH ORGANISATION. 2014. *Obesity and overweight* [Online]. Available: http://www.who.int/mediacentre/factsheets/fs311/en/ [Accessed 13 March 2016].

WRIGHT, D. C., GEIGER, P. C., HOLLOSZY, J. O. & HAN, D. H. 2005. Contraction- and hypoxia-stimulated glucose transport is mediated by a Ca2+-dependent mechanism in slow-twitch rat soleus muscle. *Am J Physiol Endocrinol Metab,* 288**,** E1062-6.

XENOS, E. S., STEVENS, S. L., FREEMAN, M. B., CASSADA, D. C. & GOLDMAN, M. H. 2005. Nitric oxide mediates the effect of fluvastatin on intercellular adhesion molecule-1 and platelet endothelial cell adhesion molecule-1 expression on human endothelial cells. *Ann Vasc Surg,* 19**,** 386-92.

XI, W., SATOH, H., KASE, H., SUZUKI, K. & HATTORI, Y. 2005. Stimulated HSP90 binding to eNOS and activation of the PI3-Akt pathway contribute to globular adiponectin-induced NO production: vasorelaxation in response to globular adiponectin. *Biochem Biophys Res Commun,* 332**,** 200-5.

XIA, N., HORKE, S., HABERMEIER, A., CLOSS, E. I., REIFENBERG, G., GERICKE, A., MIKHED, Y., MUNZEL, T., DAIBER, A., FORSTERMANN, U. & LI, H. 2016. Uncoupling of Endothelial Nitric Oxide Synthase in Perivascular Adipose Tissue of Diet-Induced Obese Mice. *Arterioscler Thromb Vasc Biol,* 36**,** 78-85.

XIA, X. M., FAKLER, B., RIVARD, A., WAYMAN, G., JOHNSON-PAIS, T., KEEN, J. E., ISHII, T., HIRSCHBERG, B., BOND, C. T., LUTSENKO, S., MAYLIE, J. & ADELMAN, J. P. 1998. Mechanism of calcium gating in small-conductance calcium-activated potassium channels. *Nature,* 395**,** 503-507.

XIE, M., ZHANG, D., DYCK, J. R., LI, Y., ZHANG, H., MORISHIMA, M., MANN, D. L., TAFFET, G. E., BALDINI, A., KHOURY, D. S. & SCHNEIDER, M. D. 2006. A pivotal role for endogenous TGF-beta-activated kinase-1 in the LKB1/AMP-activated protein kinase energy-sensor pathway. *Proc Natl Acad Sci U S A,* 103**,** 17378-83.

XIE, Z., ZHANG, J., WU, J., VIOLLET, B. & ZOU, M. H. 2008. Upregulation of mitochondrial uncoupling protein-2 by the AMP-activated protein kinase in endothelial cells attenuates oxidative stress in diabetes. *Diabetes,* 57**,** 3222-30.

XIONG, Q., SUN, H., ZHANG, Y., NAN, F. & LI, M. 2008. Combinatorial augmentation of voltage-gated KCNQ potassium channels by chemical openers. *Proc Natl Acad Sci U S A,* 105**,** 3128-33.

XUE, B., COULTER, A., RIM, J. S., KOZA, R. A. & KOZAK, L. P. 2005. Transcriptional Synergy and the Regulation of Ucp1 during Brown Adipocyte Induction in White Fat Depots. *Molecular and Cellular Biology,* 25**,** 8311-8322.

YAMAMOTO, S., MATSUSHITA, Y., NAKAGAWA, T., HAYASHI, T., NODA, M. & MIZOUE, T. 2014. Circulating adiponectin levels and risk of type 2 diabetes in the Japanese. *Nutrition & Diabetes,* 4**,** e130.

YAMAUCHI, T., KAMON, J., ITO, Y., TSUCHIDA, A., YOKOMIZO, T., KITA, S., SUGIYAMA, T., MIYAGISHI, M., HARA, K., TSUNODA, M., MURAKAMI, K., OHTEKI, T., UCHIDA, S., TAKEKAWA, S., WAKI, H., TSUNO, N. H., SHIBATA, Y., TERAUCHI, Y., FROGUEL, P., TOBE, K., KOYASU, S., TAIRA, K., KITAMURA, T., SHIMIZU, T., NAGAI, R. & KADOWAKI, T. 2003. Cloning of adiponectin receptors that mediate antidiabetic metabolic effects. *Nature,* 423**,** 762-9.

YAMAUCHI, T., KAMON, J., MINOKOSHI, Y., ITO, Y., WAKI, H., UCHIDA, S., YAMASHITA, S., NODA, M., KITA, S., UEKI, K., ETO, K., AKANUMA, Y., FROGUEL, P., FOUFELLE, F., FERRE, P., CARLING, D., KIMURA, S., NAGAI, R., KAHN, B. B. & KADOWAKI, T. 2002. Adiponectin stimulates glucose utilization and fatty-acid oxidation by activating AMP-activated protein kinase. *Nat Med,* 8**,** 1288-95.

YAMAUCHI, T., KAMON, J., WAKI, H., TERAUCHI, Y., KUBOTA, N., HARA, K., MORI, Y., IDE, T., MURAKAMI, K., TSUBOYAMA-KASAOKA, N., EZAKI, O., AKANUMA, Y., GAVRILOVA, O., VINSON, C., REITMAN, M. L., KAGECHIKA, H., SHUDO, K., YODA, M., NAKANO, Y., TOBE, K., NAGAI, R., KIMURA, S., TOMITA, M., FROGUEL, P. & KADOWAKI, T. 2001. The fat-derived hormone adiponectin reverses insulin resistance associated with both lipoatrophy and obesity. *Nat Med,* 7**,** 941-6.

YAMAWAKI, H., HARA, N., OKADA, M. & HARA, Y. 2009. Visfatin causes endothelium-dependent relaxation in isolated blood vessels. *Biochem Biophys Res Commun,* 383**,** 503-8.

YAMAWAKI, H., TSUBAKI, N., MUKOHDA, M., OKADA, M. & HARA, Y. 2010. Omentin, a novel adipokine, induces vasodilation in rat isolated blood vessels. *Biochem Biophys Res Commun,* 393**,** 668-72.

YANG, Z., KAHN, B. B., SHI, H. & XUE, B. Z. 2010. Macrophage alpha1 AMP-activated protein kinase (alpha1AMPK) antagonizes fatty acid-induced inflammation through SIRT1. *J Biol Chem,* 285**,** 19051-9.

YEH, L. A., LEE, K. H. & KIM, K. H. 1980. Regulation of rat liver acetyl-CoA carboxylase. Regulation of phosphorylation and inactivation of acetyl-CoA carboxylase by the adenylate energy charge. *Journal of Biological Chemistry,* 255**,** 2308-2314.

YOUNG, L. H., LI, J., BARON, S. J. & RUSSELL, R. R. 2005. AMP-activated protein kinase: a key stress signaling pathway in the heart. *Trends Cardiovasc Med,* 15**,** 110-8.

YUDKIN, J. S., ERINGA, E. & STEHOUWER, C. D. 2005. "Vasocrine" signalling from perivascular fat: a mechanism linking insulin resistance to vascular disease. *Lancet,* 365**,** 1817-20.

ZHAN, J. K., WANG, Y. J., WANG, Y., TANG, Z. Y., TAN, P., HUANG, W. & LIU, Y. S. 2014. Adiponectin attenuates the osteoblastic differentiation of vascular smooth muscle cells through the AMPK/mTOR pathway. *Exp Cell Res,* 323**,** 352-8.

ZHANG, C. X., PAN, S. N., MENG, R. S., PENG, C. Q., XIONG, Z. J., CHEN, B. L., CHEN, G. Q., YAO, F. J., CHEN, Y. L., MA, Y. D. & DONG, Y. G. 2011. Metformin attenuates ventricular hypertrophy by activating the AMP-activated protein kinase-endothelial nitric oxide synthase pathway in rats. *Clin Exp Pharmacol Physiol,* 38**,** 55-62.

ZHAO, H., JOSEPH, J., FALES, H. M., SOKOLOSKI, E. A., LEVINE, R. L., VASQUEZ-VIVAR, J. & KALYANARAMAN, B. 2005. Detection and characterization of the product of hydroethidine and intracellular superoxide by HPLC and limitations of fluorescence. *Proc Natl Acad Sci U S A,* 102**,** 5727-32.

ZHAO, H., KALIVENDI, S., ZHANG, H., JOSEPH, J., NITHIPATIKOM, K., VÁSQUEZ-VIVAR, J. & KALYANARAMAN, B. 2003. Superoxide reacts with hydroethidine but forms a fluorescent product that is distinctly different from ethidium: potential implications in intracellular fluorescence detection of superoxide. *Free Radical Biology and Medicine,* 34**,** 1359-1368.

ZHAO, W. & WANG, R. 2002. H(2)S-induced vasorelaxation and underlying cellular and molecular mechanisms. *Am J Physiol Heart Circ Physiol,* 283**,** H474-80.

ZHAO, W., ZHANG, J., LU, Y. & WANG, R. 2001. The vasorelaxant effect of H(2)S as a novel endogenous gaseous K(ATP) channel opener. *EMBO J,* 20**,** 6008-16.

ZINGARETTI, M. C., CROSTA, F., VITALI, A., GUERRIERI, M., FRONTINI, A., CANNON, B., NEDERGAARD, J. & CINTI, S. 2009. The presence of UCP1 demonstrates that metabolically active adipose tissue in the neck of adult humans truly represents brown adipose tissue. *FASEB J,* 23**,** 3113-20.

ZOU, M. H., KIRKPATRICK, S. S., DAVIS, B. J., NELSON, J. S., WILES, W. G. T., SCHLATTNER, U., NEUMANN, D., BROWNLEE, M., FREEMAN, M. B. & GOLDMAN, M. H. 2004. Activation of the AMP-activated protein kinase by the anti-diabetic drug metformin in vivo. Role of mitochondrial reactive nitrogen species. *J Biol Chem,* 279**,** 43940-51.

Appendices

Appendix 1:

T.A. Almabrouk, M.A. Ewart, I.P. Salt and S. Kennedy (2014) Perivascular fat, AMP-activated protein kinase and vascular diseases. *Br J Pharmacol,* 171**,** 595-617.

Appendix 2:

T.A.M. Almabrouk, A.B. Ugusman, O. Katwan, I.P. Salt and S. Kennedy (2016) Deletion of AMPKα1 Attenuates the Anticontractile Effect of Perivascular Adipose Tissue (PVAT) and Reduces Adiponectin Release. *Br J Pharmacol,*DOI:10.1111/bph.13633.